Screening, Isolation and Characterisation of Antibodies That Block Aggrecanase Activity of ADAMTS-5

Salvatore Santamaria

A thesis submitted for the degree of Doctor of Philosophy to
Imperial College London

September 2013

Department of Matrix Biology
The Kennedy Institute of Rheumatology Division
Faculty of Medicine
Imperial College London

Abstract

A Disintegrin and Metalloproteinase with ThromboSpondin Motif (ADAMTS)-5 is considered to play a key role in degradation of aggrecan during the progression of osteoarthritis (OA). Thus, ADAMTS-5 inhibitors are emerging as potential disease-modifying OA drugs. The generation of small molecule inhibitors of metalloproteinases has not achieved successful outcomes primarily due to the lack of selectivity. On the other hand, monoclonal antibodies were proved potent and selective binders of many biologically relevant targets. We therefore aimed to isolate inhibitory antibodies against ADAMTS-5.

A human naïve single-chain variable fragment library was used to select and isolate anti-ADAMTS-5 antibodies. Among the isolated antibodies, clones 2D3 and 2D5 inhibited ADAMTS-5 cleavage both of a peptide substrate ($K_{i\ app}$ values of 2 nM and 18 nM, respectively) and bovine aggrecan ($K_{i\ app}$ values of 30 nM and 300 nM, respectively). Antibody 2B9 did not inhibit ADAMTS-5 activity against the peptide substrate, but it inhibited the cleavage of aggrecan ($K_{i\ app}$: 300 nM). Surface plasmon resonance studies with a series of deletion mutants of ADAMTS-5 indicated that 2D3 and 2D5 bind to the catalytic/disintegrin domain (K_D values of 3 nM and 55 nM, respectively), whereas 2B9 binds to the spacer domain of this enzyme (K_D value of 6 nM), thus being an exosite inhibitor. Kinetic studies indicated that the anti-ADAMTS-5 antibodies described here do not act through a zinc-chelating mechanism of inhibition. Moreover, inhibition and co-immunoprecipitation data suggested that for some antibodies, such as 2D5, the binding site is different from that of TIMP-3.

The efficacy of ADAMTS-5-blocking antibodies was investigated using model systems of aggrecan degradation (IL-1α/oncostatin M-stimulated porcine and human articular cartilage explants). The results indicated that antibodies 2D3 and 2B9 effectively inhibited aggrecanase activity in these systems. These antibodies may therefore be useful as chondroprotectant agents in OA.

TABLE OF CONTENTS

CHAPTER 2: MATERIALS AND METHODS

LIST OF FIGURES

LIST OF TABLES

Chapter 6

Declaration of originality

This PhD thesis is a result of my own work. All collaborations have been acknowledged in the appropriate place within the text.

Salvatore Santamaria
London, 27th September 2013

Copyright Declaration

ACKNOWLEDGEMENTS

I wish to express my grateful thanks to my supervisors Prof. Hideaki Nagase and Prof. Gillian Murphy for all their support, advice and ideas, as well as their lessons on science, science writing and…life. They laid the foundations for this field and I hope to add a clay tile on the roof. It has been an honour working with somebody whose works introduced me to the scientific world.

This was a complex project and I needed three labs to achieve my objectives. Thanks to all the people in Matrix biology lab, Kennedy Institute: Anna Piccinini, Han Lim, Kazu Yamamoto, Yazu Shitomi, Leandro Lo Cascio, Linda Troeberg, Rob Visse, Simone Scilabra and Szymon Manka. In particular, Rob kindly provided aligned structures and 3D models for Figures 5.27 and 5.28 and Kazu's help was essential for my cartilage experiments. I would also like to extend my gratitude to Marta Zaionc for her work with mouse ADAMTS-5 cell lines, the former KIR secretary Christine Greig for all her help with my bumf and bureaucracy, and Ewa Paleolog for sorting out all the small problems that occurred during my PhD.

Thanks to all the people in the Oncology Department, Cancer Research Institute, Cambridge: Chris Tape, Magda Rapti, and Kenneth Botkjaer. In particular, Chris was the first one to guide me through the phage display world and Kenneth helped me a lot with SPR experiments.

Thanks to all the McCafferty Lab for their support with the phage display and screening: Alicia Martin, Aneesh Karatt Vellatt, Kotai Parthiban, Mike Dyson, Peter Slavny and Tony Pope. The amount of things I learned from them was crazy. It has been great talking and planning experiments with John, whenever I meet him I tell myself: "I'm working with the guy that published the first paper on antibody phage display!". Without his library, today I could not talk about anti-ADAMTS-5 antibodies.

I wish to thank Prof. Armando Rossello, Medicinal Chemistry Department, Università di Pisa; without him all this could have not been possible. Finally, I wish to thank Prof. Giovanni Cercignani and Mario Cappiello, Università di Pisa, who introduced me to the fantastic biochemistry world.

Endless thanks to my family for their encouragements and support.

Finally, 2165 thanks to my girlfriend Enrica, for her infinite patience and understanding: I think that putting up with me is something that only extraordinary people can do and you are extraordinary indeed.

ABBREVIATIONS

α2M α2 macroglobulin

AD Alzheimer's disease

ADAM A Disintegrin And Metalloproteinase

ADAMTS A Disintegrin And Metalloproteinase with ThromboSpondin motif

ADAMTSL ADAMTS-Like protein

ALK activin receptor-like kinase

AP alkaline phosphatase

BSA bovine serum albumin

Cat catalytic domain

CBB Coomassie Brilliant Blue

CFU colony-forming units

CDR complementarity determining region

COMP cartilage oligomeric matrix protein

CUB complement C1r/C1s Uegf (EGF-related sea urchin protein) and BMP-1 (bone morphogenic protein-1)

CS chondroitin sulphate

CysR cysteine-rich domain

dAb domain antibody

DELFIA dissociation-enhanced lanthanide fluorescence immunoassay

dH_2O distilled water

Dis disintegrin domain

DMM destabilisation of medial meniscus

DMMB Dimethylmethylene blue

DOL degree of labelling

ECM extracellular matrix

ELISA Enzyme-Linked Immunosorbent Assay

ERK extracellular-signal-regulated kinase

Fab antigen-binding fragment

FCS fetal calf serum

FGF fibroblast growth factor

FRET Förster resonance energy transfer

GAG glycosaminoglycan

HA hyaluronan

HEK293-EBNA cell Human embryonic kidney 293-Epstein Barr nuclear antigen cell

hcAbs heavy chain antibodies

IGD interglobular domain of aggrecan

IgG immunoglobulin G

IL-1 interleukin-1

IMAC immobilised metal chromatography

IPTG isopropyl β-D-1 thiogalactopyranoside

KS keratan sulphate

LDL low-density lipoprotein

LRP low-density lipoprotein receptor-related protein

mAb monoclonal antibody

miRNA microRNA

mRNA messenger RNA

MMP matrix metalloproteinases

MSS musculoskeletal syndrome

Ni-NTA Nickel-nitrilotriacetic

NHS *N*-hydroxysuccinimide

OA osteoarthritis

OD optical density

OSM oncostatin M

PACE paired-basic amino acid converting enzyme

PAGE polyacrylamide gel electrophoresis

PC proprotein convertase

PCR polymerase chain reaction

PEI polyethyleneimine

PLAC protease and lacunine motif

PBS phosphate-buffered saline

PPS pentosan polysulphate

QF quenched fluorescent

RA rheumatoid arthritis

RFU raw fluorescent units

RT room temperature

RUNX runt-related transcription factor

scFv single chain variable fragment

SDS sodium dodecyl sulphate

SF synovial fluid

siRNA short interfering RNA

Sp spacer domain

SPR surface plasmon resonance

TBS Tris-buffered saline

TCA trichloroacetic acid

TGF transforming growth factor

TIMP tissue inhibitor of metalloproteinases

TNF tumour necrosis factor

TS thrombospondin type-I motif

TTP thrombotic thrombocytopenic purpura

TTR TGF-β1 injection and enforced uphill treadmill running

TY trypton yeast extract

uPA urokinase plasminogen activator

VEGF vascular endothelial growth factor

V_H heavy chain variable domain

V_L light chain variable domain

VSMC vascular smooth muscle cells

vWF von Willebrand Factor

Chapter 1
Introduction

1.1. Protease-mediated degradation of articular cartilage

Osteoarthritis (OA) and rheumatoid arthritis (RA) are the two most common joint disorders, affecting a significant proportion of the human population. In particular, symptomatic knee OA occurs in 10% men and 13% women aged 60 years or older (Zhang and Jordan, 2010) and pain related to this pathology is the leading cause of impaired mobility in the elderly population in the USA (Helmick et al., 2008). Twenty-seven million individuals have been diagnosed with OA in the USA alone (Lawrence et al., 2008) and this number is expected to rise to 67 million by 2030 (Hootman and Helmick, 2006). Although they differ in aetiology, both OA and RA are characterised by destruction of articular cartilage, which ultimately leads to pain and disability.

Articular cartilage is composed of chondrocytes embedded in an extracellular matrix (ECM) which bestows the biomechanical properties (elasticity and compressibility) that are essential for movement. The two major ECM components are type II collagen fibrils and aggrecan proteoglycans; other less abundant macromolecules are fibromodulin, decorin, biglycan, cartilage oligomeric matrix protein (COMP), fibronectin, hyaluronan (HA), link protein, type VI, IX, and XI collagens and cell surface proteoglycans (**Figure 1.1**). Collagen is the main structural component of cartilage and provides tensile strength to the tissue; aggrecan provides flexibility, elasticity and compressibility and these functions are mediated by the negatively-charged glycosaminoglycans (GAG) chains attached to its core which ultimately are responsible for the high osmotic pressure in cartilage (Vertel and Ratcliffe, 2000). Multiple aggrecan molecules associate with a single HA filament (an unsulphated GAG), and each interaction is further stabilised by link protein. Proteoglycans and collagens interact with each other: perlecan proteoglycan enhances fibril formation (Kvist et al., 2006) and collagen VI microfibrils connect to collagen II and aggrecan via complexes of matrilin-1 and biglycan or decorin (Wiberg et al., 2002).

The development of OA is related to genetic and environmental factors, metabolic disorders, and biochemical and/or biomechanical abnormalities. Under physiological conditions, cartilage homeostasis is maintained by a balance between the synthesis and degradation of aggrecan and collagen, but in OA and other joint disorders this equilibrium shifts towards catabolism. Enzymes involved in catabolism of collagens and proteoglycans are produced primarily by chondrocytes after inductive stimuli such as mechanical stress, injury, oxidative stress, etc.

Loss of aggrecan is an early event in the onset of cartilage destruction, occurring initially at the joint surface and progressing to deeper zones (Pond and Nuki, 1973; Pratta et al., 2003). It has been hypothesised that aggrecan protects the collagen fibrillar network from proteolytic attack by collagenases due to steric and charge hindrance by its GAG chains (Pratta et al., 2003). In fact, no detectable levels of collagen release in interleukin-1 (IL-1)-stimulated bovine articular cartilage

explants have been noted until after 14 days of culture, when most of the aggrecan had been depleted from the ECM (Billinghurst et al., 2000).

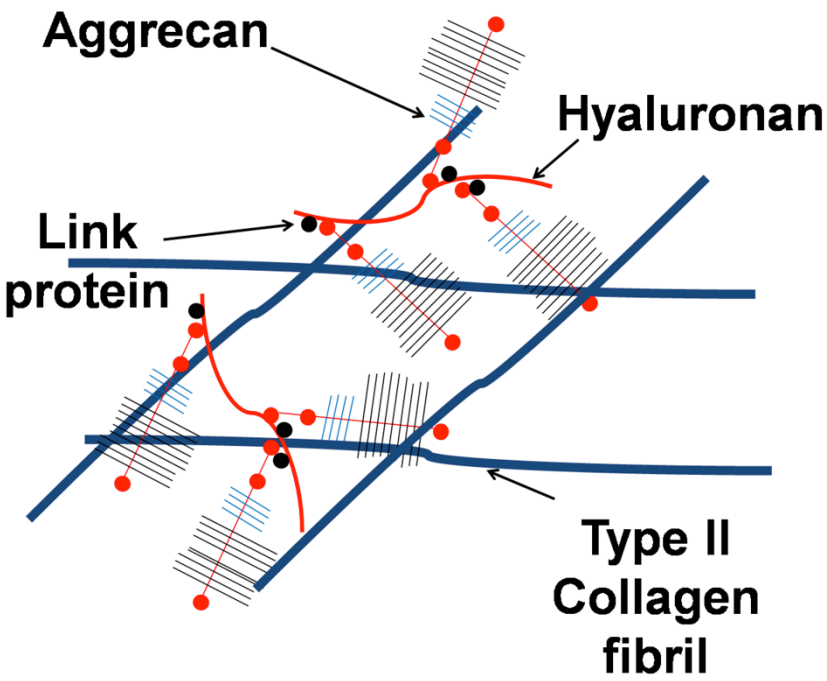

Figure 1.1. Schematic representation of articular cartilage ECM.

Aggrecan breakdown which occurs at the earlier stages of OA is compensated by new synthesis (Lorenzo et al., 2004) and represents a reversible stage of cartilage degradation (Karsdal et al., 2008). Once collagen breakdown begins, OA becomes irreversible (Karsdal et al., 2008). It is noteworthy that a collagenase selective inhibitor (Ro-32-3555, Trocade, Cipemastat), developed by Roche, did not prevent progression of joint damage in patients with RA (Close, 2001) despite the favourable preclinical data (Lewis et al., 1997) and pharmacokinetics (Brewster et al., 1998).

The term "aggrecanase" was coined to define operationally the enzymatic ability to cleave aggrecan at the $Glu^{392}\downarrow^{393}Ala$ bond (Sandy et al., 1991). Cleavage at this site represents a primary event in the proteolysis of aggrecan since fragments with the ^{393}Ala N-terminus are the major products in catabolism of aggrecan by both chondrosarcoma cells and primary bovine chondrocytes (Lark et al., 1995). In 1999, aggrecanases have been identified as two members of A Disintegrin and Metalloproteinase with Thrombospondin Motifs (ADAMTS) family of metalloproteinases, aggrecanase-1 (ADAMTS-4) and aggrecanase-2 (ADAMTS-5, which was originally coined ADAMTS-11) (Tortorella et al., 1999; Abbaszade et al., 1999).

1.2. ADAMTSs

1.2.1. The ADAMTS family

The ADAMTS proteases belong to family M12 in clan MA of the metallopeptidases according to the MEROPS database (Rawlings et al., 2004). Other peptidases in family M12 include astacins, the adamalysin peptidases (ADAMs) and the snake venom metallopeptidases (reprolysins). To date, 19 distinct ADAMTS gene products have been identified in humans (http://degradome.uniovi.es/met.html), as well as 7 ADAMTS-like (ADAMTSL) proteins lacking the catalytic domain (**Figure 1.2**).

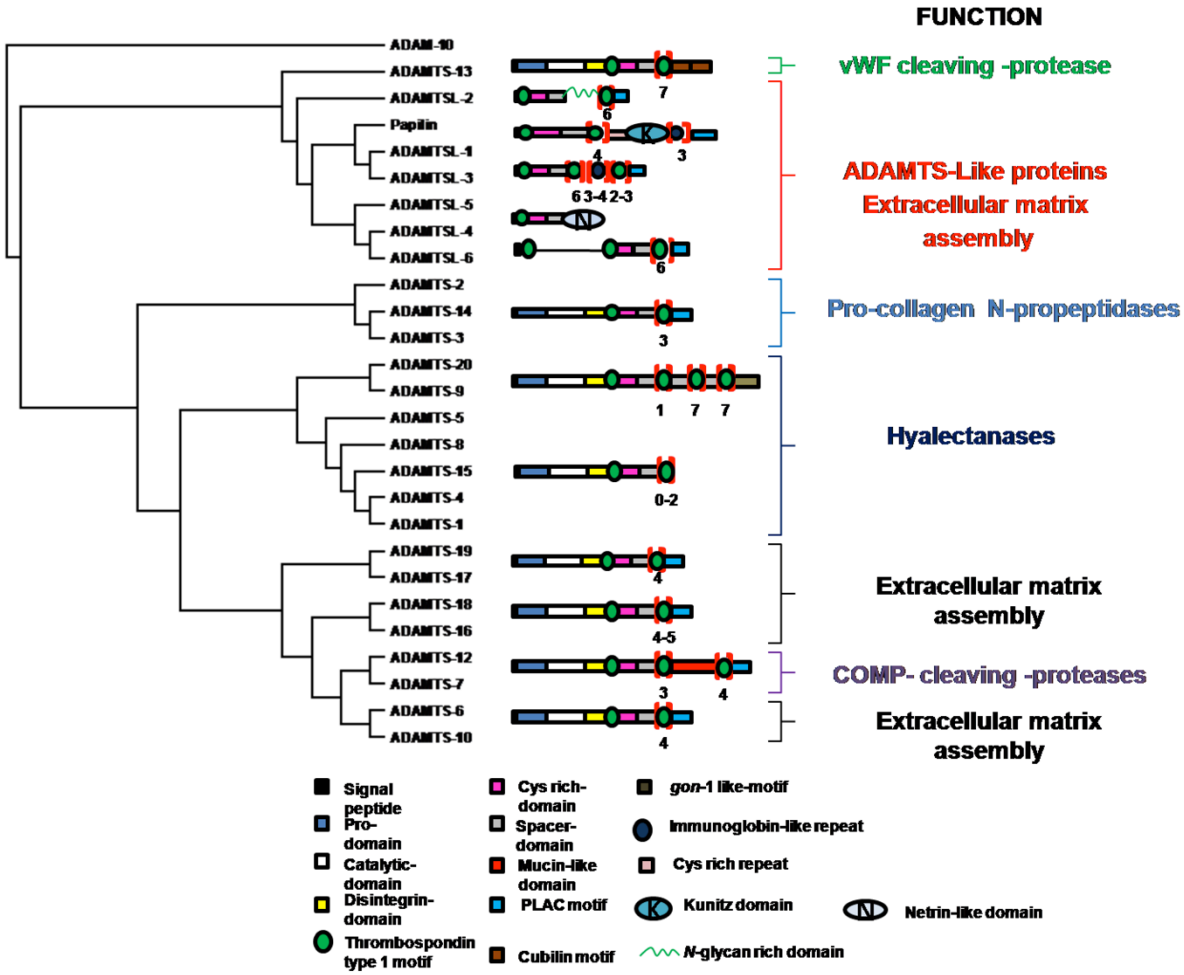

Figure 1.2: Schematic representation of the structural and evolutionary relationship of human ADAMTS and ADAMTSL gene products. 19 ADAMTS and 7 ADAMTSL protein sequences (from UniProt) were aligned with ClustalW 1.83 (Aiyar, 2000) and the resulting dendrogram was visualised with TreeView 1.6.6. Where applicable, the long form of splice variant is shown. There is no ADAMTS-11 because early reports of ADAMTS-11 (Abbaszade et al., 1999) were later found to describe ADAMTS-5. ADAMTSL-4 presents a large insertion in the first thrombospondin- type 1 domain. vWF, von Willebrand Factor, COMP, cartilage oligomeric matrix protein. ADAM-10 is reported as out-group. Note that domains are not to scale. For details about the creation of the phylogram see Section 2.2.8.

On the basis of the sequence homology and substrate specificity, ADAMTSs can be grouped into 7 subdivisions: 1) ADAMTS-1, -4, -5, -8 and -15; 2) ADAMTS-2, -3 and 14; 3) ADAMTS-9 and -20; 4) ADAMTS-6, -7, -10 and -12; 5) ADAMTS-16 and -18; 6) ADAMTS-17 and -19; 7) ADAMTS-13 (Nicholson et al., 2005). Under a broad ClustalW analysis, ADAMTSL proteins fall in the same cluster as ADAMTS-13 (**Figure 1.2**) (Brocker et al., 2009).

1.2.2. Biological role of ADAMTSs

The (patho)physiological roles of the ADAMTSs have been defined for only few members. Members of the subgroup comprising ADAMTS-1, -4, -5, -8, -15, are also called "aggrecanases" or, more broadly, "hyalectanases", to indicate their ability to cleave a family of large-aggregating proteoglycans ("hyalectans", namely aggrecan, versican, brevican and neurocan) (Gao et al., 2002). Further studies have demonstrated that this activity is shared with ADAMTS-9, -16, and -20 (Somerville et al., 2004; Zeng et al., 2006).

Versican is the main proteoglycan in many tissues where it provides a loose and highly hydrated ECM and plays a role in cell adhesion, proliferation, migration and ECM assembly (Wight, 2002). Hyalectanases are able to cleave versican *in vivo* and are therein involved in several developmental processes where versican cleavage has been proved pivotal: ovulation (Russell et al., 2003; Brown et al., 2006; 2010) and urogenital system development (ADAMTS-1) (Mittaz et al., 2004); interdigital web regression (ADAMTS-5, -9 and -20) (McCulloch et al., 2009a); endocardial cushion remodelling during valve development (ADAMTS-5, -9) and myocardial compaction (Kern et al., 2010; Dupuis et al., 2011; Stankunas et al., 2008); myoblast fusion (ADAMTS-1, -9) (Stupka et al., 2013); palatogenesis (ADAMTS-9, 20) (Enomoto et al., 2010); melanoblast colonisation of skin (ADAMTS-20) (Silver et al., 2008).

McCulloch et al. (2009a) showed an operational model in which several ADAMTSs (ADAMTS-5, -20, and -9, with a pivotal role exerted by ADAMTS-5) work cooperatively to influence apoptosis during the regression of the interdigital webs in mammalian limb morphogenesis through the production of pro-apoptotic versican fragments. *Adamts-5*$^{-/-}$/*Adamts-20*$^{-/-}$ double knock-out mice exhibit soft tissue syndactyly since the interdigital webs have reduced apoptosis and decreased cleavage of versican (McCulloch et al., 2009a). Cooperation by ADAMTS-9 and ADAMTS-20 in versican cleavage plays a role also in palatogenesis, since *Adamts-9*$^{+/-}$/*Adamts-20*$^{-/-}$ mice show cleft palate as a result of decrease of cell proliferation (Enomoto et al., 2010). Also, mutations in *Adamts-20* gene have been found to cause the belted white-spotting mutation in mice, resulting from a defect in melanocyte development or migration during embryogenesis (Rao et al., 2003).

ADAMTS-5 and -15 contribute to the formation of multinucleated myotubes during myogenesis by remodelling a versican-rich pericellular matrix and facilitating the myoblast fusion (Stupka et al., 2013). The universal importance of versican cleavage by hyalectanases during development has been shown by GON-1, an orthologue of ADAMTS-9 and -20 in *Caenorhabditis elegans*, which is required for migration of distal tip cells during gonadal morphogenesis (Blelloch et al., 1999). Versican is the primary proteoglycan in vasculature (Salter et al., 2010) and can form a complex with multiple Low-Density Lipoprotein (LDL) molecules. Positively-charged lipoproteins interact with sulphated negatively-charged GAG chains of versican and other proteoglycans and this complex can increase lipoprotein uptake in both vascular smooth muscle cells (VSMCs) and macrophages (Hurt-Camejo et al., 1992; Llorente-Cortés et al., 2002). Both biglycan and versican accumulate in atherosclerosis-prone arteries, where they trap LDL molecules (Skalén et al., 2002); LDL lipoproteins then aggregate and elicit an inflammatory response, involving alterations of VSMCs and remodelling of ECM (Chait and Wight, 2002).

ADAMTS-4 and -8 have been implicated in the formation of atherosclerotic plaques and atherosclerotic disease (Wågsäter et al., 2008). ADAMTS-1, -4, -5 and -8 are present within human carotid lesions and advanced coronary atherosclerotic plaques (Wågsäter et al., 2008; Jönsson-Rylander et al., 2005). In particular, ADAMTS-4, -5 and -8 are localised in macrophages, whereas ADAMTS-1 is localised in endothelial and VSMCs (Wågsäter et al., 2008; Jönsson-Rylander et al., 2005). Cleavage of versican by ADAMTS-1 may promote VSMC migration (Jönsson-Rylander et al., 2005). On the other hand, ADAMTS-5 activity is needed for proteoglycan-mediated lipoprotein retention (Didangelos et al., 2012) **(See Section 1.3.5)**.

Other than versican, another main substrate of hyalectanases is aggrecan, one major component of articular cartilage. Studies with *Adamts-5*-null mice showed that the lack of ADAMTS-5 is sufficient to protect from cartilage destruction when OA (Glasson et al., 2005) or inflammatory arthritis (Stanton et al., 2005) was induced **(See Section 1.3.5.).** ADAMTS-4 and ADAMTS-5 play a role in the form of arthritis occurring in Lyme disease (Behera et al., 2006). Products formed by cleavage at $Glu^{392}\downarrow^{393}Ala$ of aggrecan are detected in synovial fluid (SF) from patients affected by this form of arthritis (Hu et al., 2001). Active ADAMTS-4 levels are also increased in SF from these patients and human chondrocytes infected with *Borrelia burgdorferi*, the etiologic agent of Lyme disease, show highly induced levels of ADAMTS-4 but not ADAMTS-5 (Behera et al., 2006). *ADAMTS-5* expression is associated with herniated disc and cervical disc degeneration pathology, suggesting a role in intervertebral disc degeneration (Zhao et al., 2011). In this case, IL-1β-induced expression of *ADAMTS-5* is mediated by nitric oxide through induction of inducible nitric oxidase (Stradner et al., 2008; Zhao et al., 2011).

Adamts-4 is transcriptionally induced in rat astrocytes treated with β-amyloid, suggesting it may be involved in Alzheimer's disease (AD), possibly through cleavage of brevican, a proteoglycan specific to the central nervous system (Satoh, 2000). Proteoglycans such as brevican, neurocan and phosphacan inhibit neural plasticity under physiological and pathological conditions and this is mainly due to their GAG groups (Silver and Miller, 2004). ADAMTS-4 can reverse inhibition of neurite outgrowth by cleaving these proteoglycans *in vitro* and administration of exogenous ADAMTS-4 promotes motor function recovery after spinal cord injury in rats (Tauchi et al., 2012). However, inactive ADAMTS-4 promotes neurite outgrowth extension through activation of extracellular-signal-regulated kinase (ERK), thus catalytic activity is not strictly required (Hamel et al., 2008). Activation of ERK kinases is possibly mediated by binding to heparan-sulphate-containing proteins such as syndecans on the cell surface (Gao et al., 2004). Thus ADAMTSs promote neurite extension by two mechanisms: 1) they cleave proteoglycans which inhibit neurite outgrowth; 2) they enhance neurite outgrowth directly by activating ERK cascade (Hamel et al., 2008). To support a role in neural regeneration, expression of both *Adamts-4* and *Adamts-1* is up-regulated following neuronal injuries (Yuan et al., 2002; Cross et al., 2006).

Reelin is a secreted glycoprotein that is mainly expressed in the brain where it is essential for proper neurodevelopment and synaptic plasticity (Hisanaga et al., 2012). Reelin binds to apolipoprotein E receptor 2 and very low-density lipoprotein receptor, and then activates intracellular signalling events that eventually regulate normal development and function of the central nervous system (Honda et al., 2011). Proteolytic processing of Reelin decreases its signalling activity and promotes its aggregation *in vitro*; dysfunction of this processing is involved in AD and schizophrenia (Kohno et al., 2009). Cleavage of Reelin produces one N-terminal and one C-terminal fragment (Lambert de Rouvroit et al., 1999). The N-terminal cleavage fragment is prone to aggregate (Utsunomiya-Tate et al., 2000). ADAMTS-4 and ADAMTS-5 (but not ADAMTS-1 nor ADAMTS-8) can cleave *in vitro* Reelin, but only ADAMTS-5 is able to degrade the N-terminal fragment (Hisanaga et al., 2012; Krstic et al., 2012) (see **Section 1.3.5**). AD mice show decreased expression of *Adamts-5* in the hippocampus, therefore decreased processing of the N-terminal fragment by ADAMTS-5 may be responsible for accelerated Reelin aggregation in the hippocampus of AD mice (Krstic et al., 2012).

ADAMTS-2, -3, and -14 have been characterised as procollagen N-propeptidases. These enzymes cleave the N-terminal propeptides of type I, II, and III procollagens and mutations in the human *ADAMTS-2* gene cause Ehlers-Danlos Syndrome type VII C (EDS-VIIC), a recessively-inherited disorder characterised by the presence in the skin of procollagen incompletely processed at the N-terminus, and dermatosparaxis in bovine (Colige et al., 1999). *Adamts-2* is specifically co-

expressed with collagen III in the lung and aorta and *Adamts-2*$^{-/-}$ mice had abnormal lungs with decreased parenchymal density (Le Goff et al., 2006).

Null mutations in *ADAMTS-10* have been associated with a recessive form of Weill-Marchesani syndrome (Dagoneau et al., 2004; Morales et al., 2009) and primary open angle glaucoma in dogs (Kuchtey et al., 2011), and mutations in *ADAMTS-17* have been identified in patients affected by a "Weill-Marchesani-like" syndrome (Morales et al., 2009). ADAMTS-10 promotes fibrillin-1 deposition in ECM of cultured fibroblasts, supporting a role for this enzyme in microfibril biogenesis (Kutz et al., 2011). On the other hand, fibrillin-1 *(FBN1)* mutations can cause dominant Weill-Marchesani syndrome and associated ectopia lentis (dislocation of ocular lens), a condition caused by disruption of the zonular fibres supporting the lens (Faivre et al., 2003).

ADAMTS-18 has been found mutated in patients affected by Knobloch syndrome, a developmental disorder characterised by eye abnormalities including high myopia, cataracts, dislocated lens, vitreoretinal degeneration and retinal detachments, and occipital skull defects (Aldahmesh et al. 2011).

ADAMTSL proteins, devoid of a catalytic domain, appear to exert regulatory roles in ECM. A homozygous mutation in *ADAMTSL-4* was identified in autosomal recessive ectopia lentis et pupillae (Ahram et al., 2009; Christensen et al., 2010). In summary, these observations suggest that ADAMTSL-4, ADAMTS-10 and ADAMTS-17 play a critical role in crystalline lens zonule and connective tissue formation.

ADAMTSL-2 is involved in geleophysic dysplasia (GD), an autosomal recessive disorder characterised by short stature, brachydactyly, thick skin and cardiac valvular anomalies (Le Goff et al., 2008). The presence of very high levels of active transforming growth factor (TGF)-β in GD strongly suggests that this protein is important in sequestering TGF-β in ECM (Le Goff et al., 2008). ADAMTSL2 interacts with latent TGF-β-binding protein 1 and fibrillin-1 and is expressed in heart, skin and pulmonary arteries, as well as in chondrocyte columns in the hypertrophic and reserve zones of the proximal femoral growth plate (Le Goff et al., 2008). An *ADAMTSL-2* mutation causes Musladin-Lueke syndrome, a fibrotic disorder in beagle dogs (Bader et al., 2010).

ADAMTS-7 and ADAMTS-12 play a role in degradation of COMP (Liu CJ et al., 2006a; Liu CJ et al., 2006b), a prominent non-collagenous component of cartilage which catalyses and promotes collagen fibre formation (Halasz et al., 2007).

ADAMTS-13 mediates the catabolism of von Willebrand Factor (vWF), a glycoprotein involved in platelet adhesion to injured vessel walls under high-shear stress (Zimmerman and Ruggeri, 1987). ADAMTS-13 attenuates thrombus formation and growth on injured neointima (Moriguchi-Goto et al., 2009). Mutations in *ADAMTS-13* and auto-antibodies against ADAMTS-13

correlate with the occurrence of the hereditary and sporadic forms, respectively, of thrombotic thrombocytopenic purpura (TTP) disease, a rare disorder of the blood coagulation system (Levy et al., 2001; Soejima et al., 2003; Scheiflinger et al., 2003).

Finally, dysregulated expression and activity of several ADAMTSs have been associated with different forms of cancer **(See Section 1.2.4.5)**.

1.2.3. ADAMTS domain structure

ADAMTSs belong to the metallopeptidase family M12 and are evolutionarily and structurally related to the matrix metalloproteinases (MMPs) (family M10) (Rawlings et al., 2004). A common feature of these metallopeptidase families is the presence of a zinc-binding motif in the catalytic domain, containing the consensus sequence **HE**XX**H**XX**G**XX**H**, in which the three histidine residues coordinate a zinc atom and the glutamate residue exerts a catalytic role. This motif is followed C-terminally by a conserved methionine residue which constitutes a tight turn ("Met-turn") acting as a constraint in the topology of active site (Bode et al., 1993). The zinc-binding motifs and the Met-turn are also found in astacins, pappalysins, bacterial serralysins and enterotoxin (Bode et al., 1993; Goulas et al., 2011). All these families are collectively called "metzincins" (Bode et al., 1993).

Unlike ADAMs, which are transmembrane proteins, ADAMTSs are secreted proteins, and some of them bind to the ECM (Kuno and Matsushima, 1998; Kashiwagi et al., 2004; Gendron et al., 2007). They share a common domain composition consisting of a signal peptide, a prodomain, a metalloproteinase catalytic domain (Cat), followed by non-catalytic ancillary domains such as a disintegrin-like (Dis) domain, a thrombospondin-type I motif (TS) domain, a cysteine-rich (CysR) domain, a spacer (Sp) domain, and a various number of TS domains in the C-terminus (with the exception of ADAMTS-4, which has only the TS domain preceding the CysR region; TS domains are numbered here from the N-terminus TS-1, TS-2, etc) **(Figure 1.2)**. Some of the ADAMTSs have further C-terminal domains, such as a mucin domain (present in ADAMTS-7 and ADAMTS-12), a GON domain (in ADAMTS-20 and ADAMTS-9), and a PLAC (protease and lacunin) domain (in ADAMTS-2, -3,-6, -10, -12, 14, -16, -17, -18, and -19) (Porter et al., 2005). Moreover, ADAMTS-13 is unique among ADAMTs since it presents two CUB [complement subcomponent C1r/C1s/embryonic sea urchin protein Uegf (urchin epidermal growth factor)/bone morphogenic protein 1] domains (Soejima et al., 2001; Zheng et al., 2001).

For the ADAMTS family members, crystal structures have only been resolved for the Cat domains of ADAMTS-1, -4, and -5 (Gerhardt et al., 2007; Shieh et al., 2008; Mosyak et al., 2008) and for TS-1, CysR and Sp domains of ADAMTS-13 (Akiyama et al., 2009).

The Cat domain of ADAMTS-5 contains the active site (with the zinc-binding sequence **H**EIG**H**LLGLS**H**), the catalytic zinc ion, and two calcium-binding sites and has an α/β structure characteristic of the metzincin family (Shieh et al., 2008; Mosyak et al., 2008). There are two calcium-binding sites which have a structural role: one of them contains a single calcium ion whereas the other one comprises two calcium ions in a calcium cluster (Shieh et al., 2008). The latter calcium-cluster is not present in any known metalloproteinase structure. The Cat domain is stabilised by four disulphide bonds (Mosyak et al., 2008; Shieh et al., 2008); five cysteine residues are upstream of the zinc-binding sequence, and three residues are downstream of it. Downstream of this sequence is also present the methionine residue of the "Met-turn". The overall fold of the Cat domain of ADAMTSs is similar to that of other metzincins, with a central five-stranded β-sheet of which four strands are in a parallel configuration and a fifth one is in an antiparallel configuration (Shieh et al., 2008). This β-sheet is flanked with two helices on its concave side and one helix on its convex side. The main differences compared with the MMPs are the outward facing S2'and the inward facing S1' pockets (terminology is after Schechter and Berger, 1967). The S2' pocket is defined by a short disulphide-containing loop (containing the motif CGxxxCDTL) not present in any of the MMPs, called S2' loop (residues 371-379 in ADAMTS-5) (Mosyak et al., 2008). Unlike the large loop present in all the MMPs, this loop adopts a compact β-turn structure quite far from the catalytic zinc ion, which could impede sterically access of substrates into the S1' and S2'pockets (Mosyak et al., 2008). The S1'-loop (residues 437-451 in ADAMTS-5) occupies about half of the inner face of the S1' pocket, whereas in the MMPs it occupies almost the whole S1' pocket. The S1' pocket of ADAMTS-5 is smaller than ADAMTS-4 owing to more bulky side chains present in ADAMTS-5 (Leu^{301}, Leu^{438}, Leu^{443}, and Ile^{446} in ADAMTS-5 instead of Ala^{252}, Val^{390}, Met^{395}, and Val^{398} in ADAMTS-4) (Mosyak et al., 2008).

The disintegrin (Dis) domain of ADAMTSs does not share homology with disintegrins, a family of proteins from viper venoms, but it is very similar in structure to part of the CysR domain of P-III snake venom metalloproteinases in which it is involved in binding to platelet integrin receptors (Gerhardt et al., 2007; Mosyak et al., 2008; Akiyama et al., 2009). This prevents the association of platelets with their natural ligands such as fibrinogen, and results in a block of platelet aggregation at the wound site. In ADAMTS-5, the Dis domain lacks any integrin binding sequence and does not interact with integrin (Mosyak et al., 2008). It forms a unique fold of two α-helices, two β-sheets, and several loops throughout, connected to the Cat domain by a flexible linker 9 amino acids-long (Mosyak et al., 2008). The Dis domain lies on the prime side of the active site, where it shields the S1' pocket and, to a lesser extent, the S3' pocket from solvent (Mosyak et al., 2008). On the basis of their close proximity in the three-dimensional structure (Mosyak et al.,

2008) and the activity studies of ADAMTS-5 deletion mutants (Kashiwagi et al., 2004; Lauer-Fields et al., 2007; Gendron et al., 2007) (**See Section 1.3.3)**, Cat and Dis domains can be considered as a structural and functional unit.

The TS-1 domain is highly conserved within the ADAMTS family, including the CSR(T/S)C pentapeptide (Hurskainen et al., 1999). This pentapeptide is consistently different from the corresponding sequence (CSVTC) present in thrombospondins (Hurskainen et al., 1999). The CysR domain contains 10 conserved cysteine residues, whereas the Sp region does not contain cysteine residues, which could make this region quite flexible. In ADAMTS-13, the Sp domain has a β-sandwich structure where surface-exposed variable loops are potentially able to interact with target proteins (Akyama et al., 2009). Ancillary non-catalytic domains are involved in substrate binding and cleavage as well as ECM-binding. They comprise substrate-binding sites (exosites) which interact specifically with the substrate. For example, the four TS domains of ADAMTS-7 (Liu CJ et al., 2006a) and -12 (Liu CJ et al., 2006b) are necessary for binding to COMP. A critical step in both vWF binding and proteolysis by ADAMTS-13 is the docking of the Sp domain onto the C-terminal end of the VWF A2 domain (Zheng et al., 2003). The Dis domain of ADAMTS-13 also plays an essential role by enabling specific proteolysis (Gao et al., 2008; de Groot et al., 2009). Without these ancillary domains, the Cat domain of ADAMTS-13 binds to vWF with very low affinity and poor cleavage site specificity. The functions of non-catalytic ancillary domains of aggrecanases are described in **Section 1.3.3**.

1.2.4. ADAMTS regulation

ADAMTS activity is regulated by multiple interacting processes such as promoter activity, epigenetic modifications, regulation by microRNA (miRNA), alternative splicing, prodomain removal, post-translational modifications (e.g. C-terminal processing), presence of endogenous inhibitors and cofactors, and endocytosis. Since the ancillary domains are important in substrate recognition and cleavage efficiency, mechanisms able to produce variants lacking one or more of these domains (alternative splicing, C-terminal processing) could represent a potent strategy to modulate ADAMTS activity *in vivo*.

1.2.4.1. Regulation of expression

Expression of ADAMTSs has been shown to be regulated by cytokines, hormones, and epigenetic modifications. The effects produced by cytokines on ADAMTS expression vary greatly depending on the specific tissue/cell types examined. Major up-regulators of ADAMTS expression are interleukin-1 (IL-1) and tumour necrosis factor-α (TNF-α). *ADAMTS-1* messenger RNA

(mRNA) is up-regulated by IL-1 (Kuno et al., 1997), and *ADAMTS-1*, *-6*, and *-9* mRNA levels are up-regulated in response to TNF-α in retinal pigment epithelium-derived cells (Bevitt et al., 2003). Levels of pro-inflammatory cytokines are increased in arthritic joints and cartilage (Mills and Dunne, 2009). These cytokines are produced by mononuclear cells, chondrocytes and synoviocytes (Fernandes et al., 2002). Aggrecanase activity in bovine (Arner et al., 1998) and porcine (Powell et al., 2007) cartilage explants is inhibited by the inclusion of cycloheximide, thus indicating a requirement for *de novo* protein synthesis in IL-1 and TNF-α-mediated up-regulation. *ADAMTS-12* is induced by interferon-alpha (IFN-α) and IL-1β (Liu CJ et al., 2006b; Llamazares et al., 2007). *ADAMTS-4* mRNA expression by human synoviocytes is significantly inhibited by the TNF-α blocker etanercept and an anti-IL-1β neutralising antibody, whereas the expression of ADAMTS-5 in the same cells was not affected by neutralisation of IL-1β and/or TNFα (Bondeson et al., 2006). An additive effect of combination treatment with oncostatin M (OSM) and either IL-1α or TNF-α in human chondrocytes or cultured human cartilage explants led to a marked induction of *ADAMTS-4* gene expression and some induction of *ADAMTS-5* (Song et al., 2007).

ADAMTS-5 mRNA is constitutively expressed in human chondrocytes (Bau et al., 2002; Moulharat et al., 2004) and synovial fibroblasts (Vankemmelbeke et al., 2001; Yamanishi et al., 2002; Blaney Davidson et al., 2006). In mouse knee joint explants stimulated with IL-1α and TNF-α, *Adamts-5* mRNA was found induced in tenocytes, synovium, and in patellar, but not femoral or tibial articular cartilage (Wylie et al., 2012). In fibroblast-like synoviocytes the expression of *ADAMTS-4* mRNA was increased by IL-6 and soluble IL-6 receptor, whereas that of *ADAMTS-5* was decreased (Mimata et al., 2012). This regulation is mediated by both mitogen-activated protein kinase (MAPK)/ERK and the JAK/STAT signalling pathways (Mimata et al., 2012). IL-4 inhibits the expression of MMPs and ADAMTS-4, thus exerting protective effects on cartilage in animal models of OA (Yorimitsu et al., 2008). TGF-β strongly up-regulates *ADAMTS-4* mRNA and protein expression in human synovial fibroblasts, but does not affect *ADAMTS-5* (Yamanishi et al., 2002). The stress-induced calcium-binding protein, S100A8, enhances IL-1-induced ADAMTS-5 expression in mouse cartilage (van Lent et al., 2008). Fibroblast growth factor-2 (FGF-2) specifically inhibits IL-1-induced expression of *ADAMTS-4* and *-5* in primary human chondrocytes (Sawaji et al., 2008). ADAMTS-5 activity and aggrecan cleavage have been found increased in *fgf2*-null mice (Chia et al., 2009). The immunosuppressant drug cyclosporin A down-regulates *ADAMTS-4* and *ADAMTS-5* at mRNA levels (Little et al., 2002a) while a suppressive effect of n-3 fatty acids was observed for *ADAMTS-4* mRNA but not for *ADAMTS-5* (Curtis et al., 2000; Curtis et al., 2002).

The human *ADAMTS-4* promoter has two putative binding sites for the transcription factor nuclear factor of activated T cells-p (NFATp) and eight putative binding sites for the Runt-related transcription factor (RUNX) family of transcription factors (Thirunavukkarasu et al., 2006), and human *ADAMTS-5* promoter has four putative binding sites for the family of RUNX transcriptions factors (Thirunavukkarasu et al., 2007). *ADAMTS-5* promoter activity is up-regulated in response to RUNX-2 over-expression in primary bovine chondrocytes and human chondrosarcoma cells (Thirunavukkarasu et al., 2007). The human *ADAMTS-4* promoter contains at least one specificity protein-1 (Sp1) transcription factor-binding site (Mizui et al., 2000) which mediates induction by IL-1β (Sylvester et al., 2013). Sp1 regulates also TIMP-3 (Tissue Inhibitor of Metalloproteinase-3), an endogenous inhibitor of aggrecanases (Qureshi et al., 2005) **(See Section 1.2.4.4)**, and transcription factor SRY-box-containing gene 9 (SOX9), a master regulator of chondrocyte differentiation (Piera-Velazquez et al., 2007). Nuclear factor-κB (NF-κB) plays a role in inducible expression of ADAMTS-4 (Chockalingam et al., 2007; Bondeson et al., 2007; Ahmad et al., 2009).

Hormones play also a regulatory role in ADAMTS expression. In osteopenic mice, estradiol and pamidronate decrease *ADAMTS-4* and *ADAMTS-5* expression (Funck-Brentano et al., 2012). The thyroid hormone tri-iodothyronine (T3) up-regulates mRNA expression of *ADAMTS-5*, but not *ADAMTS-4*, with subsequent aggrecan degradation, in growth plate cartilage during endochondral ossification (Makihira et al., 2003).

Expression and/or activity of *ADAMTS-4* and *-5* can be regulated by mechanical loading in chondrocytes (Ding et al., 2010; Tetsunaga et al., 2011). Uni-axial cyclic tensile strain induced expression of *RUNX-2*, *MMP-13*, *ADAMTS-4*, *-5*, and *-9* by SW1353 chondrocytes-like cells (Tetsunaga et al., 2011). In this study, over-expression of RUNX-2 up-regulated expression of *MMP-13* and *ADAMTS-5*, but did not have any effect on expression of *ADAMTS-4* and *ADAMTS-9* (Tetsunaga et al., 2011). A ~40-fold increase of *ADAMTS-5* has been observed in cartilage explant cultures after mechanical injury (Lee JH et al., 2005).

ADAMTS-5 expression can be regulated by epigenetic modifications such as histone acetylation and changes in the methylation status of CpG sites in the gene promoter. Histone acetylation and deacetylation are generally associated with transcriptional activation and repression, respectively, and these modifications can be reversed by histone deacetylases (Kouzarides, 2000). In SW1353 chondrosarcoma cells and primary human chondrocytes, histone deacetylases inhibitors sodium butyrate and trichostatin A inhibited IL-1α/OSM-induced *ADAMTS-5* expression (Young et al., 2005). Methylation of CpG islands is associated with gene silencing. The percentage of non-methylated sites in *ADAMTS-4* promoter increased to 50% in OA cartilage from 0% in control

cartilage (Roach et al., 2005). Epigenetic modifications of ADAMTSs are involved in several types of cancer **(See Section 1.2.4.5)**.

1.2.4.2. Post-transcriptional regulation

ADAMTS transcripts have been shown to be regulated by alternative splicing, alternative promoter usage, and miRNAs. In human, alternative splicing has been reported for *ADAMTS-4* (2 isoforms) (Wainwright et al., 2006; Wainwright et al., 2013), *-6* (4 isoforms), *-9* (3 isoforms) (Bevitt et al., 2003; Bevitt et al., 2005), *-2* (2 isoforms), *-13* (3 isoforms), *-14* (2 isoforms) (Apweiler et al., 2004), *-12* (3 isoforms), *-16* (2 isoforms), *-17* (2 isoforms), *-18* (2 isoforms), *-20* (2 isoforms) and alternative promoter usage for *ADAMTS-14* (2 isoforms) (Uniprot database). The full 5'untranslated region (UTR) of *ADAMTS-6* mRNA contains multiple upstream ATG initiation codons followed by very short open reading frames which may decrease translation rate by recruiting ribosomes to non-productive sites (Bevitt et al., 2005); conversely, alternative transcripts lacking these 5'UTR codons may increase translation.

Another potential post-transcriptional regulation seems to be miRNA-mediated. miRNAs are a class of non-coding RNAs that negatively regulate genes involved in numerous biological processes. Mice with deletion of *miRNA140*, a miRNA specifically expressed in mouse cartilage and down-regulated in OA (Tuddenham et al., 2006; Miyaki et al., 2009), have significantly increased levels of *ADAMTS-5* mRNA and increased aggrecan loss *in vitro*, compared with wild-type mice (Miyaki et al., 2010).

1.2.4.3. Post-translational regulation

ADAMTSs can be regulated post-translationally by activation, C-terminal processing and endocytosis. In addition to *N* and *O*-glycosylation, which are common in secreted proteins, specific residues in the TS domains, occurring within conserved motifs, are modified by *C*-mannosylation and *O*-fucosylation (Ricketts et al., 2007; Wang et al., 2009).

ADAMTSs are synthesised as inactive zymogens. The mechanism by which the prodomains maintain ADAMTS latency is currently unknown. The "cysteine switch" mechanism has been proposed for pro-MMPs (Van Wart and Birkedal-Hansen, 1990), but only ADAMTS-1, -6, -7,-10, -12, and -15 contain a motif similar to the cysteine switch sequences found in the pro-MMPs (Porter et al., 2005). ADAMTSs are activated following proteolytic removal of the N-terminal propeptide by proprotein convertases (PC), a family of Ca^{2+}-dependent subtilisin-type serine proteases which include furin and paired-basic amino acid converting enzyme-4 (PACE-4) (Bergeron et al., 2000). These enzymes recognise a multibasic consensus sequence RXR/KR within the propeptide of

ADAMTSs (^{208}RRAKR^{212} in human ADAMTS-4 and ^{257}RRRRR^{261} in human ADAMTS-5) (Tortorella et al., 1999; Abbaszade et al., 1999).

PCs are located in the trans-Golgi network, in endosomes, at cell surface and in the ECM (Thomas, 2002). Consequently, activation of ADAMTSs may happen intracellularly as well as on the cell surface, although some PCs such as furin are more abundant inside the cell than on the cell-surface (Klimpel et al., 1992). Intracellular furin-dependent processing of ADAMTS-4 has been observed (Wang et al., 2004). It has also been proposed that ADAMTS-4 and ADAMTS-5 zymogens are deposited in cartilage ECM, where they may be activated by secreted PCs such as PACE4 (Malfait et al., 2008). Glucosamine interferes with ADAMTS-5 activation by impairing post-translational modification of furin (McCulloch et al., 2009b), and this could explain the suppression of aggrecan catabolism by hexosamines in cartilage explants cultures (Sandy et al., 1998; Sandy et al., 1999).

MMPs have been reported also to activate ADAMTSs. For example, ADAMTS-4 can be activated by MMP-9 (Tortorella et al., 2005) or can be processed on the cell membrane by the GPI-anchored membrane type 4 MMP (MT4-MMP/MMP-17), in partnership with the transmembrane proteoglycan syndecan-1 (Gao et al., 2004). The latter mechanism is similar to the activation of ADAMTS-5 by MMP-3 in conjunction with syndecan-4 (Echtermeyer et al., 2009), although the exact biochemical mechanism is not known. ADAMTS-1 presents four MMP cleavage sites in the Sp domain (Rodriguez-Manzaneque et al., 2000). The serine protease trypsin has been shown to activate ADAMTS-4 (Tortorella et al., 2005).

Cleavage in the C-terminal ancillary domains of ADAMTSs is a further regulatory level of ADAMTS activity which can affect both catalytic efficiency and binding to the ECM. Full-length ADAMTS-4 undergoes intramolecular autocatalytic C-terminal truncation to generate two isoforms, one lacking most of the Sp domain, the other lacking the Sp domain and most of the CysR domain, two regions which are essential for binding to GAGs (Flannery et al., 2002). A low molecular weight (37-kDa) form of ADAMTS-4 is prevalent in porcine chondrocyte-agarose cultures (Powell et al., 2007). C-terminal processing, with removal of the PLAC domain, has been observed for ADAMTS-2, resulting in an increase in procollagen peptidase activity (Colige et al., 2005). On the other hand, the same activity decreases after removal of the TS-2 and TS-4 domain (Colige et al., 2005). ADAMTS-5 is further regulated by endocytosis (Yamamoto et al., 2013). Low-density lipoprotein receptor-related protein-1 (LRP-1) is the main receptor which mediates ADAMTS-5 uptake by chondrocytes (Yamamoto et al., 2013).

1.2.4.4. Regulation by endogenous inhibitors and cofactors

TIMP-3 is a potent endogenous inhibitor of both ADAMTS-4 and ADAMTS-5, with K_i values in the nanomolar range (Hashimoto et al., 2001; Kashiwagi et al., 2001). TIMP-3, like many ADAMTSs, is normally bound to GAGs associated with ECM and cell surfaces and the biological function of this localisation may be inhibition of cell-surface or ECM-bound proteases (Yu et al., 2000). Other TIMPs (TIMP-1, -2, and -4) are ineffective inhibitors of these ADAMTSs, with K_i values in the high nanomolar range (Hashimoto et al., 2001). TIMP-3 also inhibits ADAMTS-1 (Rodriguez-Manzaneque et al., 2000), and ADAMTS-2 (Wang et al., 2006).

α2-macroglobulin (α2M) is a large plasma protein and is also present in the SF at concentrations of 1-2 mg/ml (Hadler et al., 1981). Most endopeptidases are inhibited by this macromolecular inhibitor and there is evidence that α2M may be an important inhibitor of ADAMTS-4 and -5 (Tortorella et al., 2004), as well as of ADAMTS-7 and ADAMTS-12 in the fluid phase (Luan et al., 2008). Other potential endogenous inhibitors reported so far are papilin for ADAMTS-2 (Kramerova et al., 2000) and the C-terminal domain of fibronectin for ADAMTS-4 (Hashimoto et al., 2004).

Interaction of ADAMTSs with cell surface or ECM molecules could enhance their aggrecanase activity. The interaction of ADAMTS-1 and ADAMTS-5 with fibulin-1, a secreted glycoprotein present in elastic matrix fibres and basement membranes, increases catalytic activities towards aggrecan or versican, respectively (Lee NH et al., 2005; McCulloch et al., 2009c). Fibulin-1 does not represent a substrate for both enzymes but it could mediate ADAMTS-5 localisation on aggrecan via interaction of its epidermal growth factor (EGF)-like repeats in domain II with aggrecan (Aspberg et al., 1999). In kidney, fibulin-1, aggrecan and ADAMTS-1 colocalise in apical epithelial tubules and in the basement membrane (Lee NH et al., 2005). Direct interactions with syndecan-4 (Echtermeyer et al., 2009; Wang et al., 2011) and syndecan-1 (Gao et al., 2004) can recruit ADAMTS-5 and ADAMTS-4, respectively, to the cell surface, where these enzymes undergo extracellular activation. During intervertebral disc degeneration, elevated levels of cytokines TNF-α and IL-1β, as well as syndecan-4 and ADAMTS-4 and -5 are observed (Wang et al., 2011). Treatment with TNF-α and IL-1β increases syndecan-4 expression through NF-κB signalling pathway and promotes syndecans-4 interaction with ADAMTS-5 but not with ADAMTS-4 (Wang et al., 2011).

1.2.4.5. ADAMTSs in cancer

In the last decade, increasing evidence for a role of ADAMTSs in cancer has emerged **(Table 1.1).** The role played by ADAMTSs in this complex pathology is a result of unregulated

expression as well as aberrant C-terminal processing (Liu YG et al., 2006). In particular, different effects on angiogenesis and metastasis have been observed for the same enzyme in different cancer types or even within the same cancer type, and several findings suggest that ancillary C-terminal domains play a crucial role in determining the pro- or anti-tumorigenic properties of these molecules.

ADAMTS	Cancer type	Role in cancer	Reference
1	Breast, colorectal cancers, pancreatic cancer, LLC	Anti- or pro-angiogenic, oncogenic	Vazquez et al., 1999; Liu YG et al, 2006; Masui et al., 2001
	NSCLC	Tumour suppressor	Lind et al., 2006
2	Not known	Anti-angiogenic	Dubail et al., 2010
4	Not known	Anti-angiogenic	Hsu et al., 2012
	Melanoma	Anti- or pro-angiogenic	Rao et al., 2013
	Glioblastoma	Oncogenic	Held-Feindt et al., 2006
5	Prostate cancer, HNSCC, breast cancer, colorectal cancer	Anti-angiogenic	Cross et al., 2005; Demircan et al., 2009; Stokes et al., 2010; Porter et al., 2006; Kim et al., 2011; Kumar et al., 2012; Sharghi-Namini et al., 2008
	LSCC	Oncogenic	Filou et al., 2013
	Gliobastoma	Oncogenic	Held-Feindt et al., 2006; Nakada et al., 2005
8	Brain cancer, NSCLC	Tumour suppressor	Vazquez et al., 1999; Dunn et al., 2004
	Breast cancer	Oncogenic	Porter et al., 2006
9	Not known	Anti-angiogenic *in vitro*	Koo et al., 2010
12	Colon cancer	Anti-angiogenic, tumour suppressor	Llmazares et al., 2007; Moncada-Pazos et al., 2009; El-Hour et al., 2010
13	Several types of cancer	Tumour suppressor	Koo et al., 2002; Oleksowicz et al., 1999
15	Breast cancer	Tumour suppressor	Porter et al., 2006
	Colorectal cancer	Tumour suppressor	Viloria et al.. 2009
18	Several types of cancer	Tumour suppressor	Jin et al., 2007
	Melanoma	Oncogenic	Wei et al., 2010
20	Brain, colon, breast cancer	Oncogenic	Llamazares et al., 2003

Table 1.1: Associations between ADAMTSs and several types of cancer. HNSCC, head and neck squamous cell carcinoma; LLC, Lewis lung carcinoma; LSCC, laryngeal squamous cell carcinoma; NSCLC, non-small lung cell carcinoma.

The pro-tumorigenic effects are generally mediated by cleavage of proteoglycans such as versican (Silver et al., 2008), brevican (Held-Feindt et al., 2006) or aggrecan (Filou e al., 2013) which promotes invasion. So far, the susceptibility of *Adamts-1*, *-4* and -5-null mice to tumour growth and metastasis has not been investigated.

ADAMTSs can act as tumour suppressors by different mechanisms. ADAMTS-1, -2, -4, -5, -8, -9 and -12 were shown to have anti-angiogenic activity. In the case of ADAMTS-2 (Dubail et al., 2010), -4 (Rao et al., 2013), -5 (Kumar et al., 2012), and -12 (Llamazares et al., 2007; El Hour et al., 2010) the catalytic activity is not required for the tumour suppressor and anti-angiogenic

activity. In the case of ADAMTS-9 the catalytic activity is required to exert anti-angiogenic effects *in vitro* (Koo et al., 2010). Inhibition of angiogenesis by ADAMTS-1 (Liu YG et al., 2006), -4 (Rao et al., 2013) and -5 (Kumar et al., 2012) is mediated by their TS domains, although the mechanisms are not fully elucidated. The TS-1 domain of ADAMTS-5 acts as an anti-angiogenic and pro-apoptotic peptide (Sharghi-Namini et al., 2008; Kumar et al., 2012). Suppression of angiogenesis is mediated by down-regulation of pro-angiogenic factors such as VEGF, placenta growth factor, plasminogen activator inhibitor-1 (PAI-1), insulin-like growth factor binding protein-3 (IGFBP-3), and platelet-derived endothelial cell growth factor (Kumar et al., 2012). The mechanism by which the TS-1 domain modulates transcriptions of these genes is not known. *ADAMTS-5* expression is down-regulated in breast cancer (Porter et al., 2004) and in head and neck squamous cell carcinoma (HNSCC) (Demircan et al., 2009; Stokes et al., 2010). Moreover, *ADAMTS-5* promoter has been found to be hyper-methylated in colorectal cancer (Kim et al., 2011) and T-cell acute lymphoblastic leukaemia (Roman-Gomez et al., 2005).

ADAMTS-4 and -5 have also been shown to play a pro-tumorigenic role. Both enzymes are over-expressed in human glioblastomas and, through cleavage of brevican, may contribute to invasiveness of glioblastoma cells (Gary et al., 1998; Held-Feindt et al., 2006; Viapiano et al., 2008). In glioblastoma *ADAMTS-5*, but not *ADAMTS-1* nor *ADAMTS-4*, are up-regulated (Nakada et al., 2005). In stimulation experiments performed with glioblastoma cells, *ADAMTS-4* is transiently up-regulated by TGF-β, and *ADAMTS-5* by IL-1β (Held-Feindt et al., 2006).

ADAMTS-4 is involved in aggrecan turnover in normal larynx, with its expression levels being 2.5- and 10-fold higher compared to those of ADAMTS-1 and -5, respectively (Filou et al., 2013). On the other hand, ADAMTS-5 is the main aggrecanase present in laryngeal squamous cell carcinoma (LSCC), both at the mRNA and at protein level (Filou et al., 2013). In human laryngeal cartilage aggrecan is the main ECM component (Skandalis et al., 2004a) and about 90% loss of aggrecan content compared to the normal was observed in late stage of laryngeal cancer (stage IV) (Skandalis et al., 2004b).

ADAMTS-1 is highly expressed in the colon 26 cachexigenic tumour *in vivo* (Kuno et al., 1997) and is inactivated through promoter hyper-methylation in colorectal cancer (Lind et al., 2006). Its expression is down-regulated in pancreatic tumours, but patients displaying higher levels of ADAMTS-1 are subject to more retroperitoneal invasion and lymph node metastasis associated with poor survival (Masui et al., 2001). ADAMTS-1 plays a dual role in pulmonary metastasis. Full-length ADAMTS-1 promotes tumour progression by stimulating the shedding of amphiregulin and heparin binding-epidermal growth factor (HB-EGF), and activation of EGF receptor (Liu YG et al., 2006). Binding of ADAMTS-1 to these factors is mediated by CysR/Sp domains. On the other

hand, an autocatalytically-truncated fragment of ADAMTS-1 containing TS domains inhibits bioactivity of amphiregulin and HB-EGF (Liu YG et al., 2006). An autocatalytic cleavage within the CysR/Sp domains also disrupts binding of ADAMTS-1 to both amphiregulin and EGF, thus abolishing its pro-tumorigenic activity (Liu YG et al., 2006). ADAMTS-1 acts also as an anti-angiogenic molecule. By binding to vascular endothelial growth factor (VEGF), ADAMTS-1 attenuates VEGF receptor 2 (VEGFR2) activation (Iruela-Arispe et al., 2003; Luque et al., 2003). A similar mechanism has been proposed to explain the anti-angiogenic activity of ADAMTS-4 (Hsu et al., 2012). ADAMTS-1 can also cleave thrombospondin-1 (TSP-1), an adhesive glycoprotein that mediates cell-cell and cell-matrix interactions, thus releasing anti-angiogenic peptides (Lee et al., 2006).

ADAMTS-1 and -8 are both down-regulated in non-small cell lung carcinoma (NSCLC) (Rocks et al., 2006; Dunn et al., 2004). ADAMTS-8 displays reduced expression levels in brain tumours (Dunn et al., 2006). Patients displaying high levels of ADAMTS-8 and low levels of ADAMTS-15 have a general poor clinical outcome in breast carcinoma (Porter et al., 2006). Genetic inactivation of *ADAMTS-15* in mice increases colony formation or invasion by colorectal cancer cells compared with wild-type animals (Viloria et al., 2009). This indicates that *ADAMTS-15* is a tumour suppressor gene.

Epigenetic silencing of *ADAMTS-9* (Lo et al., 2007) and *ADAMTS-12* (Moncada-Pazos et al., 2009) has been reported in different types of carcinomas suggesting their role of tumour suppressors for these enzymes. ADAMTS-9 suppresses tumour formation in nude mice and inhibits angiogenesis *in vivo* by down-regulating MMP-9 and VEGF (Lo et al., 2010). Lack of *Adamts-12* in mice results in increased angiogenesis and tumour progression (El Hour et al., 2010).

Patients with advanced metastasis display lower ADAMTS-13 levels and it has been hypothesised that the consequent accumulation of highly polymeric vWF may facilitate adhesive interactions between circulating tumour cells and platelets (Oleksowicz et al., 1999; Koo et al., 2002).

ADAMTS-18 has been indicated as a tumour suppressor in esophageal and nasopharyngeal cancer (Jin et al., 2007). Moreover, mutations of *ADAMTS-18* were reported in kidney and colorectal cancer (Sjöblom et al., 2006; Wood et al., 2007) and melanoma (Wei et al., 2010). *In vitro*, mutations of *ADAMTS-18* were shown to promote growth factor-independent cell proliferation, reduce adhesion to laminin and increase migration of melanoma cells and injections of mutant forms of ADAMTS-18 in immunodeficient mice result in increased metastasis (Wei et al., 2010). However, the underlying biochemical mechanism is not known.

Silencing of *Adamts-20* in mice results in increased melanoblast apoptosis, decreased soluble Kit ligand-stimulation of the pro-survival pathway and decrease processing of versican, suggesting a role of this enzyme as oncogene (Silver et al., 2008). In fact, *Adamts-20* is over-expressed in brain, colon and breast cancer (Llamazares et al., 2003).

1.3. AGGRECANASES

1.3.1. Aggrecan cleavage sites

Aggrecan is a multidomain glycoprotein whose 220 kDa protein core consists of two globular domains at the N-terminus, G1 and G2, separated by an interglobular domain (IGD) of 150 amino acids, and a third globular domain, G3, at the C-terminus (**Figure 1.3**). The region between the G2 and G3 domains is heavily modified with chondroitin sulphate (CS) and keratan sulphate (KS) GAGs, which cluster into CS-1 and CS-2 domains and a KS-rich region (Doege et al., 1991; Kiani et al., 2002). Negatively-charged groups on the GAGs are responsible for high osmotic pressure in cartilage, thus allowing aggrecan to swell and hydrate the network of collagen fibrils.

The aggrecan G1 domain interacts with link protein and HA to form large molecular weight aggregates containing up to approximately 100 proteoglycan molecules/HA (Hardingham et al., 1992). Although the G2 domain shares structural similarities with the HA binding region of the G1 domain, it lacks the ability to bind HA (Watanabe et al., 1997). The G3 domain, which is structurally distinct from the G1 and G2 domains, is involved in secretion, glycosylation and interaction of aggrecan with other ECM components (Aspberg et al., 1997; Chen et al., 2002).

Two autosomal recessive chondrodysplasias, cartilage matrix deficiency (*cmd*) in mice (Kimata et al., 1981; Rittenhouse et al., 1978) and nanomelia in chicken (Argraves et al., 1981; Li et al., 1993) are both caused by aggrecan gene mutations. Nanomelia is due to a point mutation which results in premature termination and retention of the truncated aggrecan molecule in the endoplasmic reticulum (Vertel et al., 1994). Cartilage matrix deficiency is caused by a deletion in exon 5 within the region coding the G1 domain, which results in the appearance of a premature termination codon and, ultimately, in the synthesis of a truncated protein (Watanabe et al., 1994). *Cmd* homozygotes show an extensive reduction in ECM content of the cartilage and die shortly after birth, while the heterozygotes are born normal and later develop spinal disorder (Rittenhouse et al., 1978; Vertel et al., 1994). In other mutants, such as the chubby (*cby*) (Wikstrom et al., 1987) and brachymorphic (*bm*) (Wikstrom et al., 1985) mice and the tibial dyschondroplasia (TD) chicken (Tselepis et al., 2000), the structure of aggrecan GAG chains is abnormal and growth plate presents

major defects. In TD chicken, an increase in the number of KS chains of aggrecan has been observed (Tselepis et al., 2000).

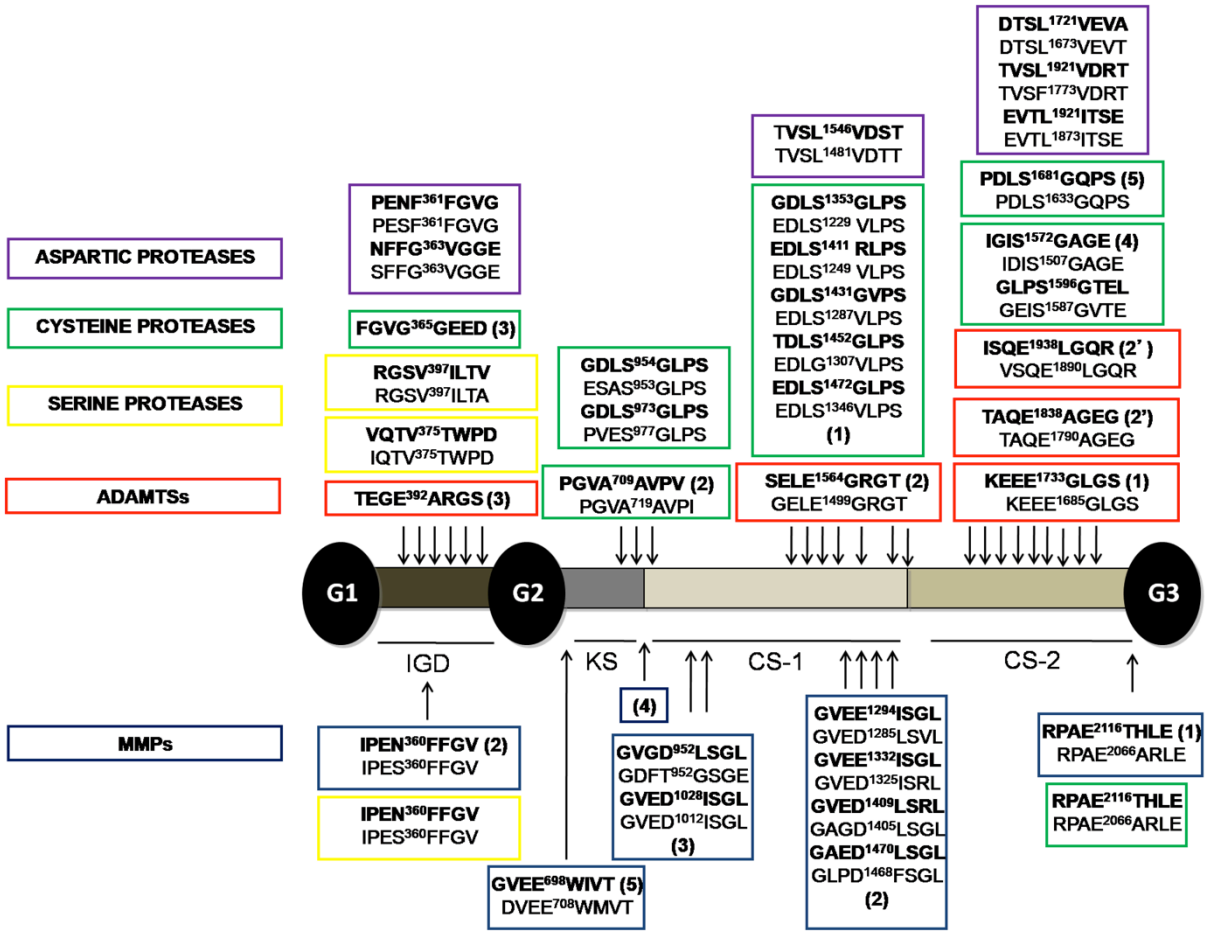

Figure 1.3: Domain structure of aggrecan proteoglycan. The boxes report the main cleavage sites by ADAMTSs (red), MMPs (blue), serine proteases (yellow), cysteine proteases (m calpain, cathepsins B and L) (green) and aspartic proteases (cathepsin D) (purple) for both human (bold) and bovine aggrecan sequences. Numbers in brackets indicate the preferred order for cleavage.

The proteases that are responsible for aggrecan degradation in cartilage are ADAMTSs as well as MMPs and cysteine proteases. In *ex vivo* cartilage explants systems, the initial enzymes responsible for degrading aggrecan are aggrecanases, followed by MMPs at a later stage (Little et al., 2002b). As the disease progresses and pH falls, cysteine proteases such as cathepsin B, cathepsin L (Lang et al., 2000) and cathepsin K (Konttinen et al., 2002) from chondrocytes may participate in further cartilage destruction.

In general, aggrecan cleavage sites are highly conserved in humans, bovines, mice and rats. In the following description of aggrecan cleavage sites I will follow the numbering of the full-length human aggrecan sequence (NCBI accession number P1612). It is worth noting that the classic numbering actually subtracts 19 residues from the NCBI database numbering to

accommodate the finding that the natural N-terminal of porcine aggrecan is VEVS (Barry et al., 1992) and this corresponds to ^{20}VETS in human aggrecan (Doege et al., 1991).

Aggrecanolysis is currently investigated by anti-neoepitope antibodies reacting with the new N- and C- termini of the cleavage products (Hughes et al., 1995). Cleavage sites which are most detrimental for cartilage integrity occur in IGD, since they lead to the release of the major portion of aggrecan core from the matrix meshwork (Sandy et al., 1991; Little et al., 2007). These sites comprise the NITEGE^{392}↓^{393}ARGSV, which is a signature of aggrecanase activity (Sandy et al., 1991), the MMP cleavage site at VDIPEN^{360}↓^{361}FFGVGG (Flannery et al., 1992) and the cysteine proteinase m-calpain cleavage site at TVQTV^{375}↓^{376}TWPDM (Struglics and Hansson, 2010).

In vitro, aggrecanases preferentially cleave aggrecan at FKEEE^{1733}↓^{1734}GLGSV in the CS-2 domain, then in the order at ASELE^{1564}↓^{1565}GRGTI in the CS-2 domain, and NITEGE^{392}↓^{393}ARGSV in the IGD (Tortorella et al., 2000a; Tortorella et al., 2002) **(Figure 1.3)**. Cleavages at PTAQE^{1838}↓^{1839}AGEGP and TISQE^{1938}↓^{1939}LGQRP in the CS-2 domain follow the primary cleavage at FKEEE^{1733}↓^{1734}GLGSV, contributing to further C-terminal processing (Tortorella et al., 2000a; Tortorella et al., 2002). These sites have a glutamic acid in the P1 position and a non-polar residue (Ala, Leu, Gly) in the P1' position, and are highly conserved in aggrecan from various species **(Figure 1.3)**. Aggrecanase cleavage in the CS-2 domain occurs preferentially relative to cleavage in the IGD in human (Struglics et al., 2006), bovine (Tortorella et al., 2001) and rat (Sandy et al., 2000) and C-terminal processing may be a pre-requisite for aggrecanase cleavage in the IGD (Ilic et al., 1998; Struglics et al., 2006).

MMPs recognise 6 main cleavage sites in human aggrecan with the following preferential order (Struglics and Hansson, 2012) **(Figure 1.3)**: 1) RPAE^{2116}↓^{2117}THLE at the border between the CS2 region and the G3 domain, 2) VDIPEN^{360}↓^{361}FFGV in the IGD and multiple sites GVED↓I(L)SGL in CS1; 3) GVGD^{952}↓^{953}LSGL and GVED^{1028}↓^{1029}ISGL in the CS1 domain; 4) an undefined site in the border between KS and CS1 regions; 5) GVEE^{698}↓^{699}WIVT in the KS region. MMP-1, -2, -3, -7, -8, -9, -12, -13, -14, -15 and -16 are able to cleave aggrecan at the MMP cleavage site (Malfait et al., 2002; Durigova et al., 2011a) with MMP-3 and -12 being the most efficient (Durigova et al., 2011a). MMP-14 (MT1-MMP) can cleave also at the aggrecanase site, although high concentrations and incubation times are required (Büttner et al., 1998).

The cysteine protease m calpain cleaves human aggrecan first at multiple cleavage sites in the CS1 domain (GDLS^{1353}↓^{1354}GLPS, EDLS^{1411}↓^{1412}RLPS, GDLS^{1431}↓^{1432}GVPS, TDLS^{1452}↓^{1453}GLPS, EDLS^{1472}↓^{1473}GLPS), then in the order at PGVA^{709}↓^{710}AVPV in the KS region, FGVG^{365}↓^{366}GEED in the IGD, IGIS^{1572}↓^{1573}GAGE and GLPS^{1596}↓^{1597}GTEL in the CS2 region and PDLS^{1681}↓^{1682}GQPS in the CS-2 region (Struglics and Hansson, 2010) **(Figure 1.3)**.

Calpains are calcium-dependent neutral proteases which are located mainly inside the cells (Hood et al., 2004) but have also been found in SF (Suzuki et al., 1990; Yamamoto et al., 1992) and in the culture medium of cartilage explants and chondrocytes (Szomor et al., 1999; Fushimi et al., 2004), suggesting that they may play a role in the cartilage degradation. Indeed, G1-PGVA^{709} fragments produced by m-calpain have been detected in bovine (Oshita et al., 2004) and human cartilage (Maehara et al., 2007), although in human OA and normal cartilage they constitute a small proportion (0.5-2%) compared with aggrecanase-generated G1-TEGE (71-76%) and MMP-generated G1-IPEN (23-29%) fragments (Struglics and Hansson, 2010). Abundance of m-calpain has been shown to correlate with the severity of arthritis in both animal models (Szomor et al., 1995) and human disease (Yamamoto et al., 1992).

The cysteine-proteases cathepsin B and L recognise the MMP cleavage site at VDIPEN^{360}↓^{361}FFGVGG (in the case of cathepsin B cleavage at the MMP site is secondary to cleavage at NFFG^{363}↓^{364}VGGE) (Fosang et al., 1992; Mort et al., 1998). Aspartic protease cathepsin D cleave at NFFG^{363}↓^{364}VGGE and PENF^{361}↓^{362}FGVG respectively (Handley et al., 2001), in the aggrecan IGD but no fragments derived from cathepsin cleavage sites have been detected *in vivo*. Cathepsin D cleaves bovine aggrecan also at TVSL^{1481}↓^{1482}VDTT between the CS-1 and CS-2 domains, and DTSL^{1673}↓^{1674}VEVT, TVSF^{1773}↓^{1774}VDRT and EVTL^{1873}↓^{1873}ITSE within the CS-2 domain (Handley et al., 2001). The ECM of cartilage is buffered at a pH of 7.4, so cathepsins may be active outside the cell just only when pH lowers upon cartilage degradation.

Serine proteases plasmin, urokinase and leucocyte elastase cleave within the IGD of aggrecan (Fosang et al., 1993; Mok et al., 1992). Cleavage by leucocyte elastase occurs at RGSV^{397}↓^{398}ILTV (Mok et al., 1992). Recently, cleavage by the serine protease HtrA1 at VQTV^{356}↓^{357}TWPD in human aggrecan core protein has been reported, although this neoepitope was present at about 5% of the level of NITEGE^{373} neoepitope in human OA cartilage protein extracts (Chamberland et al., 2009).

1.3.2. Physiological and pathological catabolism of aggrecan

Both aggrecan and HA constantly undergo turnover in healthy cartilage. Studies of precursor radiolabelling established that both the biosynthetic and turnover rates for HA and aggrecan are similar (Morales and Hascall, 1988).

Cleavage in the IGD of aggrecan is the most detrimental for cartilage integrity since it releases the bulk of aggrecan from its anchor to HA and releases the entire CS-rich region essential for the biomechanical properties of aggrecan (Little et al. 2007). This CS-2 region of aggrecan is lost from the cartilage by diffusion and found in the medium or SF (Sandy and Verscharen; 2001;

Fosang et al., 2000; Lohmander et al., 1993). Cartilage explant experiments have shown that C-terminal aggrecanase-produced ARGSV fragments are released into the culture media, with only very low ARGSV neoepitope content in the tissue (Malfait et al., 2002). Other studies have shown that these fragments are only in SF but not in cartilage samples (Struglics and Larsson, 2010; Struglics et al., 2006). On the other hand, cartilage contains significant amounts of both the N-terminal aggrecanase-generated G1-TEGE and MMP-generated G1-IPEN fragments (Lark et al, 1997; Struglics et al., 2006; Struglics and Hansson, 2010). The ratio between G1-IPEN and G1-TEGE fragments is approximately 1:3 in both OA and normal cartilage (Struglics and Hansson, 2010). G1-TEGE fragments can be detected also in the SF (Struglics et al., 2006) and can be internalised by chondrocytes through a mechanism involving HA/CD44-mediated endocytosis (Fosang et al., 2000; Embry and Knudson, 2003). Intact aggrecan molecules are not internalised, suggesting that only partial degradation of aggrecan is a pre-requisite for turnover (Embry and Knudson, 2003).

The G1-IPEN neoepitopes generated by MMPs are mostly abundant around the pericellular matrix, whereas G1-TEGE neoepitopes generated by aggrecanases are mostly abundant in the interterritorial matrix, thus indicating a spatial confinement for both MMP and aggrecanase activities (Lark et al, 1997; Struglics et al., 2006). Struglics et al. (2006) proposed a model where MMPs cleave full-length aggrecan in the IGD in the pericellular matrix, and secondarily aggrecanases process these fragments at the C-terminus in the interterritorial matrix; aggrecanases are also active against full-length aggrecan in the interterritorial matrix, cleaving first in the CS-2 domain and in the IGD. In normal mature cartilage, two distinct pools of aggrecan are present, a pool with short-lived aggrecan surrounding the chondrocytes and another pool with long-lived aggrecan in the interterritorial matrix (Mok et al., 1994).

SF of patients with various forms of arthritis, such as OA and RA, and joint injury, all show aggrecan products of cleavage at the aggrecanase site (Lohmander et al., 1993), and MMP-generated VDIPEN^{360} neoepitopes have been detected in human cartilages from normal, OA and RA patients (Fosang et al., 1996; Lark et al., 1997). Aggrecanase cleavage in the IGD increases in the SF of OA patients and in the acute injury phase as compared with the SF from knees of healthy patients, which is opposite to what is found for cleavage by MMPs (Larsson et al., 2009; Struglics et al., 2011). The amount of ARGSV fragments detected in SF of human healthy cartilage is approximately 2-fold the level of MMP-generated FFGV fragments, whereas in SF from knee-injured or OA patients, the levels of ARGSV fragments are 47- and 82-fold higher, respectively, than the levels of FFGV fragments (Struglics and Hansson, 2012). Moreover, the levels of SF ARGSV fragments increased 14-fold in the injury and OA samples compared with healthy samples,

whereas the levels of FFGV fragments slightly decreased (Struglics and Hansson, 2012). A marked increase in the ratio of G1-NITEGE to G1-VDIPEN has also been observed in human articular cartilage in the early post-injury period (Sandy and Verscharen, 2001).

In mouse models of arthritis, aggrecanase-generated NITEGE neoepitopes appear before the MMP-generated VDIPEN neoepitopes, but they disappear with the progression of the cartilage damage (Van Meurs et al., 1999a). In porcine explants cultures, MMPs are involved in baseline turnover of mature articular aggrecan (Fosang et al., 2000). In mice there are no phenotypic consequences of replacing endogenous aggrecan with aggrecan that is resistant to MMP cleavage by mutating the MMP cleavage site, suggesting that MMP activity is not required for aggrecan turnover during development (Little et al., 2005b). However, resistance to MMP activity is partially compensated by aggrecanase cleavage in the IGD (Little et al., 2005b). The cartilage of these mice show only 45% aggrecan release comparing with wild-type cartilage (Little et al., 2005b). MMP activity correlates with collagen breakdown, and not with aggrecan breakdown in cartilage explants after prolonged incubation with IL-1, which induces synthesis of pro-MMPs (Kozaci et al., 1997) and aggrecan degradation in porcine articular cartilage explants stimulated with IL-1α is inhibited by TIMP-3, an inhibitor of aggrecanases, but not by TIMP-1 or TIMP-2, two inhibitors of MMPs (Gendron et al., 2003). These data suggest a role for MMPs in normal aggrecan catabolism, whereas stimulated aggrecan loss is mediated by aggrecanases (Fosang et al., 2000; Sandy and Verscharen, 2001). Moreover, as it has been pointed out previously **(See Section 1.1)**, MMP activity is involved with the final stages of cartilage degradation through cleavage of both aggrecan and collagen *in vivo* (van Meurs et al., 1999a,b) and *in vitro* (Madsen et al., 2010; Durigova et al., 2011a; Little et al., 1999).

Collectively, these studies suggest that aggrecanase cleavage in the IGD of aggrecan is responsible for a major contribution to aggrecan catabolism relatively to MMP activity in arthritis and injury and promotes cartilage degradation during the early stages of disease. As a result, aggrecan fragments produced generally by aggrecanase activity have been tested as sensitive biomarkers of OA joint disease (Larsson et al., 2009; Struglics et al., 2009; Dufield et al., 2010; Swearingen et al., 2010) and are likely to be used in clinics in the near future.

Accumulation of aggrecanase-generated and MMP-generated neoepitopes in human articular and intervertebral cartilage has also been observed during ageing (Roughley et al., 1985; Sztrolovics et al., 1997; Lark et al., 1997). Cleavage by ADAMTS-4, but not ADAMTS-5, in the aggrecan IGD is affected by age in animal and human cartilage, with aggrecan from mature cartilage being cleaved more efficiently than aggrecan from young cartilage (Roughley et al., 2003, Pratta et al., 2000). A possible link between increase in aggrecan catabolism and ageing may be

represented by changes in GAG substitutions on the aggrecan molecule. A KS group near the aggrecanase site, which is associated with advanced age, has been thought to play a permissive role for aggrecanase digestion in mature bovines (Pratta et al., 2000). However, studies using recombinant IGD showed that cleavage by ADAMTS-4 can occur even in the absence of KS (Hughes et al., 1997; Mercuri et al., 1999; Miwa et al., 2006) and the absence of glycosylation has a lower impact on ADAMTS-5 than ADAMTS-4 (Roughley et al., 2003; Gendron et al., 2007). *In vitro*, deglycosylation of aggrecan with chondroitinase ABC and keratanase prior to digestion abolishes both aggrecanase (Pratta et al., 2000; Kashiwagi et al., 2004) and calpain activity (Struglics and Hansson, 2010), but has not effect on MMP activity. The presence of CS groups enhances ADAMTS-4 cleavage within the CS-2 domain and it has been proposed that the CS and KS groups may compete for binding to ADAMTS-4 (Miwa et al., 2006).

1.3.3. Role of exosites in aggrecanase activity

Exosites play important roles in the recognition and cleavage of aggrecan and in binding to ECM (**Table 1.2**). The function of non-catalytic domains in the recognition and cleavage of the substrate has been extensively investigated using C-terminal truncation forms of ADAMTS-1 (Kuno et al., 1999; Rodriguez-Manzaneque et al., 2000), ADAMTS-4 (Tortorella et al., 2000b; Gao et al., 2002; Kashiwagi et al., 2004) and ADAMTS-5 (Gendron et al., 2007; Fushimi et al., 2008). Localisation at the cell surface has been shown for ADAMTS-1 (Rodriguez-Manzaneque et al., 2000), -4 (Somerville et al., 2003a; Kashiwagi et al., 2004; Gao et al., 2004), -5 (Vankemmelbeke et al., 2001; Gendron et al., 2007), -7 (Somerville et al., 2004), and -9 (Somerville et al., 2003b) and likely occurs via ionic interactions with cell-surface or pericellular matrix molecules mediated by their ancillary domains.

The Sp region and two of the C-terminal TS repeats in ADAMTS-1 interact with heparin (Kuno and Matsushima, 1998) and their removal increases the solubility of the enzyme in tissue culture conditions and decreases its catalytic activity (Kuno et al., 1999; Rodriguez-Manzaneque et al., 2000). Studies where the Sp domain of ADAMTS-4 was removed by processing (Gao et al., 2002) or deletion (Kashiwagi et al., 2004; Gendron et al., 2007; Fushimi et al., 2008) highlight the role of this domain in binding to ECM, possibly through interaction with fibronectin (Hashimoto et al., 2004).

For ADAMTS-5, the CysR domain is necessary for binding to ECM (Gendron et al., 2007) but a significant role is exerted also by the Sp domain. This domain contains 86 basic residues, as well as an XBBXBX motif (N^{739}KKSKG^{744}), which may constitute a GAG-binding site (Troeberg et al., 2012). Deletion of the Sp domain markedly reduces both direct binding of ADAMTS-5 to

pentosan polysulphate (PPS) and the effect of PPS in increasing the affinity between TIMP-3 and ADAMTS-5 (Troeberg et al., 2012). Another domain important in ADAMTS-5 pericellular localisation is the Dis domain, which contains a pair of contiguous HA-binding motifs (Plaas et al., 2007). TS-1 domain mediates ADAMTS-5 endocytosis and this process is enhanced by the presence of the Sp domain (Yamamoto et al., 2013).

Domain deletion	ADAMTS-5	ADAMTS-4
Full-length	100% IGD-activity[1,2] 100% CS-2 activity[1]	100% IGD-activity[2] 100% CS-2 activity[1,2,3]
ΔC-terminal TS	Reduced IGD-activity (50% reduction)[1] 100% CS-2 activity[1]	N/A
Δ-Sp domain	Reduced IGD-activity (75% reduction)[1] Reduced CS-2 activity[1] (>99% reduction)	Reduced IGD-activity[2] (95% reduction) Reduced CS-2 activity (96% reduction) [2] Release into the medium
Δ-CysR domain	Reduced IGD-activity (99% reduction)[1] Reduced CS-2 activity[1] (>99% reduction) Release into the medium	Reduced IGD-activity (>99% reduction)[3] Reduced CS-2 activity[3] (>99% reduction)
Δ-TS	No IGD or CS-2 activity[1]	No IGD or CS-2 activity[1,3]
Δ-Dis	No IGD or CS-2 activity[1]	No IGD or CS-2 activity[1,3]

Table 1.2: Effects of C-terminal ancillary domain deletions on ADAMTS-5 and -4. [1](Gendron et al., 2007); [2](Fushimi et al., 2008); [3](Kashiwagi et al., 2004) (CS-2 activity: cleavage at GELE^{1499}↓^{1500}GRGT in bovine aggrecan); N/A, not applicable, ND, not determined.

Although it was reported that the Sp domain of ADAMTS-4 acts as an inhibitor since its removal increased the IGD-activity of ADAMTS-4 (Gao et al., 2002; Kashiwagi et al., 2004; Gendron et al., 2007), Fushimi et al. (2008) reported that full-length ADAMTS-4 is 20-times more active against aggrecan than its Sp domain deletion mutant. This was explained on the basis of inhibition of full-length ADAMTS-4 by heparin, particularly for cleavage at the Glu^{392}↓^{393}Ala bond of aggrecan (Fushimi et al., 2008) **(Table 1.2)**. Deletion of the Sp domain decreases the IGD-activity of ADAMTS-5 and -4 down to 25% and 5% of the full-length enzyme, respectively (Gendron et al., 2007). Moreover, removal of this region dramatically reduces the CS-2 activity of ADAMTS-4 (Fushimi et al., 2008) and ADAMTS-5 (Gendron et al., 2007).

The TS-1 and Dis domains of ADAMTS-4 are also considered important for recognition of a triple-helical FRET substrate (Lauer-Fields et al., 2007). Deletion of the TS-1 domain and/or the

Dis domain in ADAMTS-4 and -5 leads to a complete absence of catalytic activity (Kashiwagi et al., 2004; Gendron et al., 2007): the "minimal" aggrecanase comprises the Cat domain, the Dis domain and the TS-1 domain. Also ADAMTS-9 Cat domain alone is not correctly localised on the cell surface nor is it proteolytically active (Somerville et al., 2003b). The same is observed for ADAMTS-13, where the minimal fragment possessing proteolytic activity consists of the Cat/Dis domain (Gao et al., 2006).

In spite of these observations, the Cat domain seems to dictate a certain preference over macromolecular substrates. Combining ADAMTS-5 ancillary domains with ADAMTS-13 Cat domain does not produce chimeras able to cleave IGD or native aggrecan, reflecting the specificity of ADAMTS-13 Cat domain (Gao et al., 2012). When ADAMTS-5 ancillary domains (TS-1/CysR/Sp) are replaced with those of ADAMTS-13, ADAMTS-5 Cat domain acquires the ability to cleave the $Glu^{1615}\downarrow^{1616}Ile$ bond of vWF domain A2 in peptide substrates or vWF multimers that had been sheared, but native (unsheared) vWF multimers are resistant (Gao et al., 2012). This chimera is also able to cleave aggrecan at the aggrecanase site in the IGD but not in the CS-2 domain, thus underscoring the importance of ancillary domains in substrate recognition (Gao et al., 2012).

1.3.4. Other substrates of aggrecanases

Because of their preference for cleaving at the C-terminus of glutamic acid, ADAMTS-4 and ADAMTS-5 have been referred to as glutamyl endopeptidases. At least 32 residues at the N-terminal of the cleavage site (P residues of the substrate) and 13 residues at the C-terminal side (P' residues) are required for cleavage at the $Glu^{392}\downarrow^{393}Ala$ bond (Hörber et al., 2000). However, aggrecanases are not exclusively glutamyl endopeptidases. For example, ADAMTS-4 also cleaves aggrecan at $Asn^{360}\downarrow^{361}Phe$ bond (Westling et al., 2002) (**Table 1.3**). Both ADAMTS-4 and -5 cleave α_2M at $Met^{690}\downarrow^{691}Gly$ and this cleavage results in their inactivation (Tortorella et al., 2004). ADAMTS-4 cleavage of carboxymethylated transferrin occurs at Met↓Tyr, Gly↓Tyr, Ser↓Leu, and Leu↓Phe (Kashiwagi et al., 2004).

Biglycan, decorin, fibromodulin and keratocan belong to the family of small leucine-rich repeat proteoglycans (SLRPs), characterised by the presence of 6-10 adjacent leucine-rich repeats flanked by cysteine-rich domains (Iozzo, 1999). Biglycan interacts with type VI collagen and plays a role in establishing the type VI collagen network (Wiberg et al., 2001; Wiberg et al., 2002). Biglycan degradation products are present in the ECM of articular cartilage from OA and RA patients but not in normal adult human articular cartilage (Melching et al., 2006). Both ADAMTS-4 and -5 cleave human biglycan at an asparagines-cysteine bond ($Asn^{149}\downarrow^{150}Cys$) within the fifth

leucine-rich repeat (Rees et al., 2000; Melching et al., 2006; Gendron et al., 2007). This proteoglycan represents a substrate for ADAMTS-5 in cartilage (Zhen et al., 2008).

Substrate	Aggrecanase	Sequence	Reference
ADAMTS-4	ADAMTS-4	GSFR**K**FRYGY GSAL**T**FREEQ	Flannery et al., 2002
ADAMTS-5	ADAMTS-5	VRIP**E**GATHI	Georgiadis et al., 2002
Agg (Glu392)	ADAMTS-4,5	RNITEG**E**ARGSVI	Tortorella et al., 2000a
Agg (Glu1564)	ADAMTS-4,5	STASEL**E**GRGTIG	Tortorella et al., 2000a
Agg (Glu1733)	ADAMTS-4,5	TTFKEE**E**GLGSVE	Tortorella et al., 2000a
Agg (Glu1838)	ADAMTS-4,5	QAPTAQ**E**AGEGPS	Tortorella et al., 2000a
Agg (Glu1938)	ADAMTS-4,5	EPTISQ**E**LGQRPP	Tortorella et al., 2000a
Agg (Asn360)	ADAMTS-4,5	FVDIPE**N**FFGVGG	Westling et al., 2002
α2M (Met690)	ADAMTS-4,5	FYESDV**M**GRGHAR	Tortorella et al., 2004
Biglycan	ADAMTS-4,5	LRNM**N**CIEMG	Melching et al., 2006 Gendron et al., 2007
Brev (Glu393)	ADAMTS-4	QEAVES**E**SRGAIS	Matthews et al., 2000
Cm-tf (L195)	ADAMTS-4,5	FK*__C__LKD	Gendron et al., 2007
Cm-tf (L391)	ADAMTS-4,5	AM**S**LDG	Gendron et al., 2007
Cm-tf (L525)	ADAMTS-4,5	FR*__C__LVE	Gendron et al., 2007
COMP	ADAMTS-4	-	Dickinson et al., 2003
Decorin	ADAMTS-4,5	-	Kashivagi et al., 2004 Gendron et al., 2007
Fibromodulin (Y44)	ADAMTS-4,5	Y**A**YGSP	Kashiwagi et al 2004
Fibronectin		-	Gendron et al., 2007
Keratocan	ADAMTS-4,5	-	Rees et al., 2009
Matrilin-3		SATE**E**ARRLV	Hills et al., 2007
Neurocan	ADAMTS-4	-	Tauchi et al., 2012
Phosphacan	ADAMTS-4	-	Tauchi et al., 2012
Reelin	ADAMTS-4 ADAMTS-5	-	Hisanaga et al., 2012 Krstic et al., 2012
Ver V1(Glu441)	ADAMTS-4	KDPEAA**E**ARRGQY	Sandy et al., 2001

Table 1.3: Alignment of the known aggrecanase cleavage sites for human aggrecan (Agg), brevican (Brev), versican (Ver), and secondary substrates. For reduced, carboxymethylated transferrin (Cm-tf) major cleavage sites by ADAMTS-5 are reported, whereas ADAMTS-4 presents multiple cleavage sites. In bold are reported P1' residues. *C, S-carboxymethylated cysteine.

ADAMTS-4 and -5 are also able to cleave *in vitro* decorin (Kashiwagi et al., 2004; Gendron et al., 2007) and keratocan (Rees et al., 2009). Bovine fibromodulin is cleaved at $Tyr^{44}\downarrow^{45}Ala$ by recombinant ADAMTS-4 and -5 (Kashiwagi et al., 2004; Gendron et al., 2007). The hyalectan subfamily of CS proteoglycans includes aggrecan, brevican, neurocan, phosphacan and versican. These proteoglycans are related by the presence of homologous N-terminal G1 and C-terminal G3 globular domains, with a centrally located GAG attachment region. The G1 domain is highly homologous between the hyalectans and contains an immunoglobulin fold that mediates binding to

the family of small globular link proteins and two homologous proteoglycan tandem repeat (PTR) motifs responsible for binding to HA (Spicer et al., 2003).

Brevican is the main proteoglycan in the central nervous system; its expression in the brain coincides with periods of glial cell motility, such as in the developing brain during gliogenesis (Viapiano and Matthews, 2006). ADAMTS-4 and ADAMTS-5, but not ADAMTS-1 cleave brevican at $Glu^{395}\downarrow^{396}Ser$ (Matthews et al., 2000). The 23 amino acids surrounding the cleavage site are 50% identical to the cleavage site in aggrecan (Yamada et al., 1995). ADAMTS-4 has been reported to cleave *in vitro* phosphacan and neurocan (Tauchi et al., 2012).

Versican is found in ECM as four isoforms (V0, V1, V2, and V3) derived by alternative splicing. Each isoform is characterised by distinct structure, tissue localisation and signalling function. ADAMTS-1, -4, -5, -9, and -20 can cleave human versican V1 at the $Glu^{441}\downarrow^{442}Ala$ bond, within the sequence DPEAA**E**ARRGQ (Sandy et al., 2001; Somerville et al., 2003b) (See **Sections 1.2.2** and **1.3.5** for the biological significance of versican cleavage by hyalectanases). The equivalent ADAMTS cleavage site in V0 is $Glu^{1428}\downarrow^{1429}Ala$ (Sandy et al., 2001). ADAMTS-4 cleaves the versican V2 variant at $Glu^{405}\downarrow^{406}Gln$ (Westling et al., 2004).

Matrilins are adaptor proteins which connect fibrillar and network-like components such as aggrecan, fibrillar collagens, COMP, decorin and biglycan in the cartilage ECM. Cleavage of matrilins makes these molecules less efficient in providing matrix cohesion. ADAMTS-4 (Hills et al., 2007) and ADAMTS-5 (Groma et al., 2011) but not ADAMTS-1 (Ehlen et al., 2009) cleave matrilin-3 and -4 at $SATEE^{435}\downarrow^{436}ARRLV$. In mouse growth plate chondrocytes during endochondral ossification, ADAMTS-5, but not ADAMTS-4, colocalises with cleaved matrilin-4 in vesicles derived from the Golgi apparatus and cleaved matrilin-4 is absent in the growth plate of ADAMTS-5 knock-out mice (Groma et al., 2011).

ADAMTS-4 cleaves COMP, a pentameric disulphide-bonded glycoprotein present in cartilage, which represents a main substrate for ADAMTS-7 (Dickinson et al., 2003). ADAMTS-5 and -4 cleave Reelin, an important signalling glycoprotein in the nervous system (Hisanaga et al., 2012; Krstic et al., 2012) **(See Section 1.2.2)**. Cleavage of Reelin by ADAMTS-4 and -5 occurs both at the C- and N-terminal site, but ADAMTS-5 is also responsible for further N-terminal degradation (Krstic et al., 2012).

1.3.5. ADAMTS-5 (aggrecanase-2) as a target in OA

Members of the aggrecanases/hyalectanases subgroup of ADAMTSs (comprising ADAMTS-1, -4, -5, -8, -9, -15, -16) share the ability to cleave aggrecan at the aggrecanase site $Glu^{392}\downarrow^{393}Ala$ and are therefore potentially involved in dysregulated aggrecan catabolism which occurs in OA (Tortorella et al., 1999; Abbaszade et al., 1999; Collins-Racie et al., 2004; Zeng et al., 2006). However, if we look at different criteria such as specific activity, colocalisation with areas of aggrecan depletion in human OA cartilage, and correlation between loss of function and loss of aggrecan catabolism either *in vitro*, *ex vivo* and *in vivo*, ADAMTS-5 (aggrecanase-2) emerges as a major player in development of OA and as an attractive target for therapeutic intervention.

Only ADAMTS-1, -4, and -5 have been shown to cleave human aggrecan at all five aggrecanase sites ($Glu^{392}\downarrow^{393}Ala$, $Glu^{1564}\downarrow^{1565}Gly$, $Glu^{1733}\downarrow^{1734}Gly$, $Glu^{1838}\downarrow^{1839}Ala$, $Glu^{1938}\downarrow^{1939}Leu$) (Rodriguez-Manzaneque et al., 2002; Tortorella et al., 2004; Tortorella et al., 2002) (**Figure 1.3**), but, among these, ADAMTS-5 is the most active under physiological conditions (Gendron et al., 2007, Fushimi et al., 2008).

With the exception of *ADAMTS-8*, expression in human OA cartilage is widespread across all members of the hyalectanase subgroup (Kevorkian et al., 2004; Collins-Racie et al., 2004). In particular, *ADAMTS-4* and *ADAMTS-5* are expressed in cartilage and synovium from OA and RA patients (Vankemmelbeke et al, 2001; Yamanishi et al., 2002; Bau et al., 2002; Naito et al., 2007) and expression of *ADAMTS-4* mRNA and protein levels correlate with the progression of OA in humans (Naito et al., 2007). However, the specific relevance of ADAMTS-5 and ADAMTS-4 in human cartilage is evident from *in vitro* knock-down experiments (Song et al., 2007). Only *ADAMTS-4* or *ADAMTS-5* short interfering RNAs (siRNAs), once transfected, individually or in combination, into cytokine-treated human normal cartilage explants and primary human chondrocytes significantly decrease aggrecan catabolism by decreasing the expression of the targeted gene (Song et al., 2007). The same effect is observed following siRNA-mediated knock-down of either gene in human OA cartilage in the absence of cytokine stimulus, whereas transfection with *ADAMTS-1* siRNA fails to inhibit aggrecan degradation in either normal or OA cartilage (Song et al., 2007).

ADAMTS-5 is more highly expressed than *ADAMTS-4* in both normal and OA cartilage at the mRNA level (Bau et al., 2002; Kevorkian et al., 2004). However, mRNA levels for ADAMTS-5 in OA cartilage are not significantly elevated compared to that in normal cartilage (Naito et al., 2007; Bau et al., 2002; Kevorkian et al., 2004). ADAMTS-5 activity is down-regulated by endocytosis LRP-1-mediated in the normal cartilage, but LRP-1 shows a ~ 90% reduction in protein level in OA cartilage (Yamamoto et al., 2013) **(See Section 1.2.4.3)**. This suggests that ADAMTS-5

dysregulation in OA is principally due to impaired post-translational regulation. Interestingly, also TIMP-3 is endocytosed by an LRP-1-mediated pathway (Troeberg et al., 2008).

The two aggrecanases have been detected also in synovium from RA patients. In RA synovium, staining for ADAMTS-4 and –5 is mainly observed in the sublining layer of synovial membrane and pannus (Mimata et al., 2012). In another report, in RA synovium ADAMTS-5 was immunolocalised around cells lining the pannus and in some areas of ECM (Vankemmelbeke et al., 2001).

The importance of ADAMTS-5 in aggrecan breakdown and in facilitating progression of cartilage loss has been outlined by *in vivo* models of OA. *Adamts-4* and *Adamts-1* -null mice do not exhibit any significant protective effect on cartilage aggrecan loss (Glasson et al., 2004; Little et al., 2005a). These results suggest that neither ADAMTS-4 nor ADAMTS-1 is the major enzyme involved in cartilage aggrecan loss. On the other hand, studies with *Adamts-5*-null mice (catalytically inactivated homozygous allelic mice) showed that the lack of ADAMTS-5 protects against cartilage destruction when OA (Glasson et al., 2005) or inflammatory arthritis (Stanton et al., 2005) are induced. *Adamts-5*-null mice are resistant to OA development induced by the destabilisation of medial meniscus (DMM) surgery and to the associated mechanical allodynia (Malfait et al., 2010). *Adamts-4*$^{-/-}$*/Adamts-5*$^{-/-}$ double knockout mice are physiologically normal and also protected from developing OA (Majumdar et al., 2007). *Adamts-5*-null mice show essentially no cartilage erosion and fibrous overgrowth in DMM and in the OA model induced by the combination of TGF-β1 injection and enforced uphill treadmill running (TTR) (Li et al., 2011). In TTR model, these mice still show aggrecanase activity in the IGD (aggrecanase activity is present also in *Adamts-4*$^{-/-}$*/Adamts-5*$^{-/-}$ double knockout mice), but are protected from joint fibrosis and accumulate aggrecan in the articular cartilage (Li et al., 2011). In the TTR model, the deposition of versican was also observed (Li et al., 2011). These data indicate that the rate of aggrecan synthesis exceeds that of aggrecan degradation in *Adamts-5* null mice.

Collectively, these data point to a pivotal role exerted *in vivo* by ADAMTS-5, alone or in combination with ADAMTS-4, in mouse cartilage breakdown during the progression of OA, but other hyalectanases do not seem to be pathologically relevant. However, limitations of studies involving knock-out mice should be considered carefully before extrapolating to the human setting. First of all, ablating ADAMTS-5 function during development does not mimic clinical use of ADAMTS-5 inhibitors; in this case conditional knock-out mice involving specific ablation of ADAMTS-5 expression before or after onset of OA may represent a closer model of ADAMTS-5 inhibition in OA setting. Moreover, given the larger number of proteases in the murine (641) compared with human (565) proteome (Puente et al., 2003), mouse models may show a higher

degree of redundancy in performing protease functions. In the following paragraphs, we will first look at embryonic expression of *Adamts-5* and the effects of ADAMTS-5 ablation during development; successively, we will describe adult expression of *Adamts-5* and try to extrapolate the phenotypes of *Adamts-5*-null mice to the effects of a potential ADAMTS-5 inhibition in human setting.

Early reports showed that *Adamts-5*-null mice are viable, with a normal lifespan, and neither histological analysis of organs nor blood chemistry have identified any anomalies in the absence of challenge (Glasson et al., 2005; Stanton et al., 2005). However, recent studies have shown the presence of subtle phenotypes and these may be related to impaired cleavage of versican, rather than aggrecan.

Embryonic expression of *Adamts-5* is scarce prior to 11.5 days of gestation (E11.5) and limited to the floor plate of the developing brain at E9.5 (McCulloch et al., 2009c). After E11.5, continued expression in brain (choroid plexus, peripheral nerves, dorsal root ganglia, cranial nerve ganglia, spinal and cranial nerves and neural plexuses of the gut) is detected (McCulloch et al., 2009c). Aggrecan turnover is very high during embryonic skeletogenesis but there is no expression of *Adamts-5* in developing cartilage (McCulloch et al., 2009c). During chondrogenesis, *Adamts-1* and *-5* expression is down-regulated, whereas the expression of *Adamts-4*, *-9*, and *-16* is up-regulated (Boeuf et al., 2012). Aggrecanase cleavage products (NITEGE fragments) are not detected in human mesenchymal stem cells during chondrogenesis but cleavage products of MMPs (VDIPEN fragments) are detected 14 days after the induction of chondrogenesis (Boeuf et al., 2012). Expression of *Adamts-1* and *-5* can be up-regulated in these cells by IL-1β (Boeuf et al., 2012). When chondrogenesis is induced with conditioned medium containing bone morphogenetic protein-2 (BMP-2), *Adamts-4* is up-regulated after 2 days, thus this gene may be linked to early chondrogenesis (Djouad et al., 2007). In fact, *Adamts-4* expression is widespread during mouse embryonic development (McCulloch et al., 2009c). The lack of ADAMTS-5 expression in embryonic cartilage is consistent with the normal skeletal development reported in *Adamts-5*$^{-/-}$ mice (Glasson et al., 2005; Stanton et al., 2005) and *Adamts4*$^{-/-}$/*Adamts5*$^{-/-}$ double null mice (Majumdar et al., 2007).

Adamts-5 is expressed and colocalises with myosin heavy chain in embryonic mouse limbs when myoblasts initiate fusion into multinucleated tubes (McCulloch et al., 2009c; Jungers et al., 2005). Expression of *Adamts-5* during neuromuscular development and in smooth muscle cells coincides with that of versican (McCulloch et al., 2009c). *Adamts-5*$^{-/-}$ mice (Stupka et al., 2013) as well as *Adamts-5*$^{-/-}$*/Adamts-4*$^{-/-}$ double knock-out mice (Rogerson et al., 2008; McCulloch et al., 2009c) do not present overt myopathy or deficit in gait and mobility, likely due to compensation by

other hyalectanases such as *Adamts-15* during skeletal muscle development. However, higher levels of centrally positioned nuclei in myofibres during postnatal growth are observed, suggesting delayed maturation (Stupka et al., 2013).

ADAMTS-5 is found marked reduced in aortas of apolipoprotein E-null mice, which spontaneously develop atherosclerotic lesions, resulting in accumulation of biglycan and versican (Didangelos et al., 2012) **(See Section 1.2.2.)**. FGF-2, which suppresses *Adamts-5* expression and activity in cartilage (Sawaji et al., 2008; Chia et al., 2009), is up-regulated in atherosclerosis (Raj et al., 2006; Hughes et al., 1993) and accumulates in aortas of apoE-null mice (Didangelos et al., 2012). In the vasculature, the suppression of *Adamts-5* expression by FGF-2 could be related to the ability of this growth factor to increase neointima formation following arterial injury (Agrotis et al., 2004). Recombinant ADAMTS-5 reduces the LDL-binding ability of biglycan and releases LDL from human aortic lesions (Didangelos et al., 2012), thus suggesting a crucial role for this enzyme in mediating proteoglycan-mediated lipoprotein retention. These observations are supported by data from *Adamts-5*-null mice. In aortas of these mice, biglycan levels are increased, and no versican fragments are detectable (Didangelos et al., 2012). Moreover, *Adamts-5*-null mice display abnormally enlarged pulmonary valves in late foetal development and in the adult as a result of impaired cleavage of versican (Dupuis et al., 2011). *Adamts-5* is expressed by valvular endocardium during cardiac valve maturation and its loss cannot be compensated by *Adamts-1* or *-9* (Dupuis et al., 2011).

Recent data (Hattori et al., 2011; Velasco et al., 2011) suggest that ADAMTS-5 plays a critical role in dermal fibroblasts during dermal repair. Fibroblast to myofibroblast transition occurs physiologically during skin wound healing but may persist in pathologic situations such as hypertrophic scarring, contractures after burns, systemic and cutaneous scleroderma, and fibrosis of internal organs such as lung, kidney and liver (Abraham and Varga, 2005).

Whereas *Adamts-4*$^{-/-}$ mice show essentially normal wound contracture and collagen fibrillogenesis, *Adamts-5*$^{-/-}$ mice exhibit impaired contraction and dermal collagen deposition in an excisional wound healing model (Velasco et al., 2001). This phenotype is associated with accumulation in the dermal layer of cell aggregates and fibroblastic cells surrounded by a pericellular matrix enriched in full-length aggrecan which resemble immature skin appendages such as hair follicles and sweat glands (Velasco et al., 2011). According to Velasco et al. (2011), the impaired repair response observed in dermal fibroblast from *Adamts-5*$^{-/-}$ mice is due to accumulation of complexes between aggrecan, HA and CD44 on the cell surface which ultimately results in an altered signalling of TGF-β1, a key regulator of multiple processes in wound healing.

Dermal fibroblasts from *Adamts5*$^{-/-}$ mice show reduced versican proteolysis, increased pericellular matrix volume due to accumulation of versican, altered cell shape, enhanced α-smooth muscle actin expression and increased contractility within 3D-collagen gels. This myofibroblast-like phenotype is associated with activation of TGF-β signalling (Hattori et al., 2011). Since versican binds to fibrillin-1, which interacts with the large latent complex of TGF-β/TGF-β-binding proteins (Isogai et al., 2002), accumulation of versican in the pericellular matrix due to absence of ADAMTS-5 could affect sequestration and consequent activation of TGF-β (Hattori et al., 2011). Moreover, *aggrecan,* but not collagen (*col2*), is expressed during murine dermal wound healing and by newborn fibroblasts so aggrecan cleavage as well as versican cleavage may be important in dermal fibroblasts and can be impaired in *Adamts-5*$^{-/-}$ mice (Velasco et al., 2011).

In mouse adult tissues, *Adamts-5* is expressed in synovium, tenosynovium, bone marrow sinusoids, tendons, ligaments, ligament insertions, periosteal cells, and bone vasculature (Wylie et al., 2012), in arterial smooth muscle cells, mesothelium lining the peritoneal, pericardial and pleural cavities (endocardium, pericardium, pleural and peritoneal mesothelial cells), smooth muscle cells in bronchi and pancreatic ducts, glomerular mesangial cells in the kidney, dorsal root ganglia and in Schwann cells of the peripheral and autonomic nervous system (McCulloch et al., 2009c). Since *ADAMTS-5* expression is not detected in human mesenchymal stem cells during chondrogenesis, therapeutic inhibition of ADAMTS-5 would not impair regenerative self-healing pathways based on chondrogenesis of local progenitor cells in the joint (Boeuf et al., 2012). Moreover, since lacking of ADAMTS-5 is followed by activation of Smad1, 5, 8, resulting in chondrogenic response and pro-anabolic activity in chondrocytes (Velasco et al., 2011), inhibition of this enzyme can represent a dual strategy for both attenuation of cartilage degradation and induction of articular cartilage repair.

However, given the importance of ADAMTS-5 as a versicanase and the co-expression of *Adamts-5* with versican in arterial smooth muscle cells and pericardial cavities in adult mice (McCulloch et al., 2009c) a potential side effect of anti-ADAMTS-5 therapy may be related to accumulation of versican in these tissues (Dupuis et al., 2011) and development of aortic lesions (Didangelos et al., 2012). ADAMTS-5 also plays a role in myoblast fusion (Stupka et al., 2013). Skeletal muscle regeneration occurs after mechanical stress such as intense physical activity or trauma, thus, inhibiting ADAMTS-5 could be potentially detrimental in patients with compromised skeletal muscle due to immobilisation. ADAMTS-5 inhibition could also potential impair wound healing (Hattori et al., 2011; Velasco et al., 2011). The degree of these side effects mostly depend on the contribution of ADAMTS-5 to versican cleavage relative to that of other hyalectanases such as ADAMTS-9 and -20 with whom it has been shown to cooperate (McCulloch et al., 2009a).

1.4. Strategies to develop disease-modifying osteoarthritic drugs

There are currently no cures for OA, and no effective pharmacological treatments exist that slow or halt its progression (Sun, 2010). OA treatment is currently limited to steroidal and non-steroidal anti-inflammatory drugs, which provide symptomatic relief for pain and inflammation (Fajardo and Di Cesare, 2005). However, analgesic agents are only slightly superior to placebo in controlling OA-related pain (Zhang et al., 2008) and physical activity is one of the most widely prescribed non-pharmacological therapies for OA management (Fransen et al., 2002; Roddy et al., 2005). So there is strong urgency for a drug able to halt disease progression and improve the quality of life of OA patients. Recently, considerable effort has been put on the discovery and development of drugs able to slow down or halt the progression of OA, i.e. disease modifying osteoarthritic drugs.

1.4.1. Small molecule inhibitors of metalloproteinases

Inhibition of members of both MMP and ADAM families has a long and well-established tradition. Nevertheless, most synthetic inhibitors against MMPs such as Batimastat or Ilomastat (GM6001) failed in clinical trials. The primary cause of the high rate of failure is the musculoskeletal syndrome (MSS), a side-effect associated with the clinical administration of broad-spectrum MMP inhibitors and involving arthralgia, myalgia, joint stiffness and tendonitis. These symptoms are predominantly in the upper limbs, do not respond to analgesics and non-steroidal anti-inflammatory agents, and are to large extent reversible following the discontinuation of the drug (Tierney et al., 1999; Wojtowicz-Praga et al., 1998).

Most of the compounds which reached phase I and II in clinical trials have common structural features: they contain a zinc-chelating group, such as hydroxamate, and a peptidic or peptidomimetic backbone that lies in the side of the active site cleft, and side chains binding to the different enzyme pockets. Since members of the metzincin clan of metallopeptidases show a high similarity of their catalytic site structure and they all bind to the catalytic zinc with similar geometry, it is very likely that MSS is due to lack of selectivity by synthetic MMP inhibitors. However, the identity of the metalloproteinase(s) involved in MSS is not known. An early hypothesis was that inhibition of MMP-1 (collagenase-1) activity induced MSS but this syndrome was observed following treatment with MMP-1 sparing inhibitors, indicating that inhibition of this enzyme is not essential for this side effect (Whittaker et al., 1999).

Over-expression of TIMP-1 and TIMP-3 is protective in mouse models of RA (Schett et al., 2001; van der Laan et al., 2003), thus some MMPs represent a real target of arthritis therapy. However, it is evident that cross-inhibition of certain MMPs is detrimental. For example, based on

studies in mice lacking MMP-2 (Itoh et al, 2002), MMP-3 (Clements et al., 2003) or MMP-14 (Holmbeck et al., 1999), inhibition of MMP-2, -3, and -14 appears to facilitate aggrecan degradation.

It has been proposed that inhibition of ADAMs by broad-spectrum MMP inhibitor is responsible for MSS (Bird et al., 1999). An alternative hypothesis is that MSS is not due to MMP inhibition. For example, GM6001 is also a potent inhibitor of neprilysin, leucine aminopeptidase and dipeptidylpeptidase III, three metallopeptidases lacking any sequence homology with MMPs (Saghatelian et al., 2004). However, none of these enzymes has been associated with MSS.

Because of chronic administration in an old population with multiple co-morbidities, candidates for OA therapy must demonstrate utmost safety. To circumvent cross-inhibition-related issue, an approach is to engineer TIMPs to obtain inhibitors directed only against one or few enzymes. Following this strategy, a mutant N-terminal domain of TIMP-3 that selectively inhibits only aggrecanases has been developed (Lim et al., 2010). An alternative approach is using monoclonal antibodies (mAbs) directed against a target enzyme.

1.4.2. Monoclonal antibodies (mAbs)

mAbs were proved potent and selective binders of many biologically relevant targets and are well established as therapeutic agents for several diseases including cancer, autoimmune disorders, and infectious diseases (Weisser and Hall, 2009). Antibodies now represent one third of the total number of recombinant proteins used for therapy in developed countries (Hagemeyer et al., 2009). In 2011, there were 34 US Food and Drug Administration-approved mAbs in the market (Aggarwal, 2011).

In 1975, Köhler and Milstein described hybridoma technology, a method to generate monoclonal antibodies based on the fusion of B-lymphocytes from an immunised animal with immortal myeloma cells (Köhler and Milstein, 1975). Soon this method became popular for generation of antibodies for a variety of applications. This technology was subsequently used by many labs to generate metzincin inhibitors with a focus on the Cat domain. For example, REGA-3G12 mAb is a selective inhibitor of MMP-9 which does not inhibit MMP-2 (Paemen et al., 1995). This antibody recognises the amino terminal part of the catalytic domain of MMP-9 but not the zinc -binding region (Martens et al., 2007). More unusually, in order to produce MMP-blocking antibodies, Sela-Passwell et al. (2011) immunised mice with a synthetic molecule (a tris-imidazole-zinc complex) that mimics the conserved structure of the metalloenzyme catalytic zinc-histidine complex and isolated monoclonal antibodies by hybridoma technology. The resulting blocking antibodies were directed against the catalytic zinc-protein complex and enzyme surface

conformational epitopes of endogenous MMP-2 and MMP-9 (Sela-Passwell et al., 2011). These antibodies did not show cross-reactivity with free zinc ions or analogous metal-protein motifs present in carbonic anhydrase, alcohol dehydrogenase and myoglobin as well as a plethora of MMPs (Sela Passwell et al., 2011). Atapattu et al. (2012) reported the generation by hybridoma technology of mAbs which specifically bound to a distal substrate binding pocket in the CysR domain of ADAM-10 and inhibited ephrin cleavage, thus acting as exosite inhibitors.

An alternative way to generate mAbs is phage display, which has superseded hybridoma technology through the creation of large natural and synthetic *in vitro* repertoires of antibody fragments. The display of antibody fragments on filamentous phage was first described in 1990 (McCafferty et al., 1990). Phage display exploits a vast number of possibilities from a combinatorial biology approach and the linkage between genotype and phenotype to isolate antibodies against a desired antigen. The genotype-phenotype linkage permits the rapid determination of the amino acid sequence of the specific binding molecule by DNA sequencing of the specific insert in the phage genome. Phage display allows to manipulate *in vitro* conditions during selections and screening to tailor the properties of the antibodies isolated. For example, antibodies may be selected for features like affinity to the antigen, stability or yield.

The most popular vectors for display are phagemids, which are hybrid of phage genome and plasmid vectors. Phagemids are designed to contain the origin of replications for both the M13 phage and *E. coli* in addition to gene III (which codes for a protein necessary for infection of male *E. coli* or competent *E. coli* strains like TG1), appropriate multiple cloning sites, and an antibiotic-resistance gene (Mead and Kemper, 1988). However, phagemids lack all other structural and non-structural gene products required for phage biology (phage genome consists of 11 genes). Phagemids can be grown as plasmids, or, alternatively, packaged as recombinant M13 phages with the aid of a helper phage that contains a defective origin of replication (such as M13KO7 or VCSM13) and supplies, *in trans*, all the structural proteins required for generating a complete phage. The latter process is named "phage rescue" **(See Section 2.2.3)**. The resulting phage particles may thus incorporate either pIII derived from the helper phage (wild-type pIII) or the pIII-antibody fragment from the phagemid.

To construct an antibody library, genes of variable heavy (V_H) and variable light (V_L) chains of antibodies are prepared by reverse transcription of mRNA obtained from B-lymphocytes. The V_H and V_L gene products are then amplified by polymerase chain reaction (PCR) and assembled into a single gene using a DNA linker. The assembled scFv DNA insert is then cloned into a phagemid vector which is transformed into competent *E. coli* cells (Schofield et al., 2007).

Phage display libraries can be classified as antigen-biased (immune) or antigen unbiased (non-immune). Immune libraries are created by using V genes derived from the immunoglobulin G (IgG) mRNA of B-cells from immunised animal or naturally immunised/infected patients. Humanised immune repertoires can also be prepared using immunised transgenic mice (xenomice) thus combining immunisation and phage display (Yang et al., 1999). Xenomice harbour most of the human immune system V genes in the germline (instead of the native murine immune repertoire) (Yang et al., 1999). In this case the immune library will be enriched in antigen-specific antibodies which, potentially, have already undergone affinity maturation (Clackson et al., 1991).

Non-immune libraries comprise naïve, synthetic and semi-synthetic libraries and show several advantages over other techniques such as hybridoma technologies or immune libraries. A first, plain, advantage is the ability to isolate human antibodies against human (self) antigens with no need of animal immunisation. Since phage display does not depend on an animal immune system, antibodies against antigens which are particular problematic (non-immunogenic, cell-surface, toxic antigens, etc) can be generated. Cross-reactive antibodies are often difficult to obtain by hybridoma technology owing to tolerance by immune system but are commonly isolated by phage-display. Naïve libraries are derived from natural, non-immunised, rearranged V genes, which are amplified using family-based oligonucleotides. Heavy and light chains are then randomly combined and cloned. Synthetic libraries introduce wholly novel sequences into an antibody framework. Semi-synthetic libraries are created by engineering the non-immune repertoire to increase natural diversity, for example by randomisation of complementarity determining region-3 (CDR-3), which has an estimated potential diversity of 10^{23} sequences (Sanz, 1991).

Antibody fragments such as scFv (single-chain variable fragment) and Fab (antigen- binding fragment) had been displayed on filamentous phages. scFvs comprise the variable regions of the V_H and V_L of immunoglobulins connected with a short glycine-rich linker. This fusion protein retains the specificity of the immunoglobulin, thus it constitutes a minimal paratope. Fabs are composed of one constant and one variable domain from the heavy and light chains of the antibody. Since the heavy and light chains in the Fab molecule are connected by a disulphide bond, folding and assembly of Fab fragments in the periplasm of *E. coli* is less efficient than for scFvs (Skerra et al., 1991). A further disadvantage of Fabs is the tendency of light chains to form homo-dimers, which are known as Bence-Jones proteins (Kirsch et al., 2005).

Phage display can be used for mapping epitopes of monoclonal and polyclonal antibodies, identifying peptide ligands, and to define substrates for different enzymes (Matthews and Wells, 1993). Antibodies isolated by phage display have been shown to act as agonists and antagonists of receptors (Cortese et al., 1994; Doorbar and Winter, 1994). Catalytic antibodies (i.e. mAbs with

catalytic activity) are generated by immunisation with haptens that are analogous of rate-determining state structures in a particular chemical reaction (Lerner et al., 1991). Phage display has been proved successful in providing both selective and potent inhibitors of MMPs (Koivunen et al., 1999; Björklund et al., 2004; Devy et al., 2009; Bahudhanapati et al., 2011), human neutrophil elastase (Roberts et al., 1992) and ADAM-17 (Tape et al., 2011). DX-2400 is a highly selective human MMP-14-blocking antibody selected from a human Fab phage display library that reduces angiogenesis, tumour growth and metastasis of MMP-14-expressing tumours in mice (Devy et al., 2009).

1.5. Aim of the thesis

On the basis of the *in vitro* and *in vivo* data accumulated so far, ADAMTS-5 plays a major role in cartilage degradation. Thus it is appealing to inhibit this enzyme for therapeutic purposes. In particular, I hypothesised that exosite inhibitors of ADAMTS-5 would suffer from less side effects than active-site inhibitors due to specific targeting of enzyme regions involved in substrate recognition and binding.

The aim of this thesis is the isolation and characterisation of selective ADAMTS-5 inhibitors. Owing to the high selectivity shown by mAbs, we chose to select by phage display mAbs able to block aggrecanase activity of ADAMTS-5.

My specific objectives were:

(i) Isolation of antibodies against ADAMTS-5 by selection from a human antibody phage display library.

(ii) Characterisation of ADAMTS-5 binding antibodies as inhibitors: investigation of their mechanism of action (active site-directed *versus* exosite inhibition) and assessment of their selectivity against other members of metalloproteinase family, in particular MMPs and ADAMTSs families.

(iii) Assessment of inhibitory efficacy in *in vitro* systems.

Selective inhibition of ADAMTS-5 could pave the way for the therapeutic blocking of cartilage breakdown in OA and could help to further investigate the functional role of this enzyme in OA pathology.

Chapter 2
Material and Methods

2.1. REAGENTS

2.1.1. Tissue and cell culture reagents

Human embryonic kidney-Epstein Barr nuclear antigen (HEK293-EBNA) and FreeStyle™ HEK293-F cell lines were from Invitrogen (Paisley, UK); human chondrosarcoma cells (HTB-94) were from American Culture Type Collection (Manassas, VA, USA). HEK293-EBNA cells transfected with pCEP4 vector expressing different deletion mutants of ADAMTS-5, ADAMTS-4 or TIMP-3, and HTB-94 cells expressing mouse ADAMTS-5 were obtained from frozen stocks prepared in this lab. Porcine joints were supplied by Fresh Tissue (London, UK) and dissected on site within 24 h of slaughter.

Cell and tissue culture reagents were from the following sources: heparin, pluronic F68, sodium chlorate, polyethyleneimine (PEI), trypan blue, oncostatin-M (OSM), Dimethylmethylene Blue (DMMB) and shark chondroitin sulphate from Sigma-Aldrich (Dorset, UK); Falcon plates from Beckton-Dickinson (Oxford, UK); Dulbecco's modified Eagle's medium (DMEM), penicillin/streptomycin from Biowhittaker (Berkshire, UK); fetal calf serum (FCS), trypsin-EDTA and hygromycin B from PAA Laboratories (Pashing, Austria), FreeStyle™ 293 Expression Medium from Invitrogen (Paisley, UK); vented polycarbonate Erlenmeyer flasks and HYPERflask™ cell culture vessels from Corning (Corning, NY); Deep-well 24 well block from Qiagen (Manchester, UK).

Purified IL-1α was a gift from Professor J. Saklatvala (Kennedy Institute of Rheumatology, University of Oxford). Human articular cartilage was obtained from patients after they provided informed consent and following approval by the Riverside Research Ethics Committee (Riverside Health Authority, London, UK). Non-OA cartilage was obtained from the knee following amputation due to soft tissue sarcoma and osteosarcoma with no involvement of the cartilage. Tissues were obtained from 3 patients. Anti-desmin scFv-Fc antibody was kindly provided by Dr Mike Dyson, Iontas, Ltd.

2.1.2. Sodium dodecyl sulphate-Polyacrylamide Gel Electrophoresis (SDS-PAGE) and Western blot reagents

Materials were from the following sources: 30 % (w/v) acrylamide/bis-acrylamide from Severn Biotech (Worcestershire, UK); 2-amino-2-methyl-1,3-propanediol (amediol), Bovine Serum Albumin (BSA), Tween®20 and mouse monoclonal anti-FLAG M2-antibody from Sigma-Aldrich (Dorset, UK); pre-stained and unstained Precision Protein Standards, Trans-Blot® Turbo™ Transfer System, Trans-Blot® Turbo™ polyvinylidene difluoride (PVDF) transfer packs and

BioRad GS-710 densitometer from Bio-Rad (Hemel Hempstead, UK); the rabbit anti-ADAMTS-5 Cat domain antibody, the rabbit anti-AGEG antibody (which recognises the N-terminal AGEG fragment generated by aggrecanase cleavage of bovine aggrecan at $Glu^{1790}\downarrow^{1791}Ala$) and the rabbit anti-GELE antibody (which recognises the C-terminal GELE fragment generated by aggrecanase cleavage of bovine aggrecan at $Glu^{1499}\downarrow^{1500}Gly$) were prepared by Masahide Kashiwagi in this laboratory; antibody 2-B-6 (raised against the aggrecan CS stubs that remain after deglycosylation with chondroitinase ABC and keratanase) was a kind gift from Dr. Clare Hughes and Professor Bruce Caterson (University of Wales, Cardiff, UK); mouse monoclonal BC-3 antibody (which recognises the N-terminal ARGSV fragment generated by aggrecanase cleavage of bovine aggrecan at $Glu^{392}\downarrow^{393}Ala$) and anti-TIMP-3 antibody were from Abcam (Cambridge, UK); rabbit polyclonal anti-G3 was from Pierce Biotechnology (Rockford, USA); mouse monoclonal anti-NITEGE antibody (BC-13) was from MD Bioproducts (Zürich, Switzerland); Western Blue® stabilised substrate (5-bromo-4-chloro-3-indolyl-1-phosphate and nitroblue tetrazolium) for alkaline phosphatase (AP), streptavidin AP-linked, anti-mouse AP-linked antibody, anti-human IgG AP-linked and anti-rabbit AP-linked antibodies from Promega (Southampton, UK).

2.1.3. Protein chemistry reagents

2.1.3.1. Proteins and protein purification

Materials were from the following sources: anti-FLAG M2-agarose, Brij®35 solution 30% (w/v), trichloroacetic acid (TCA) and imidazole were from Sigma-Aldrich Ltd (Dorset, UK); FLAG peptide (D-K-Y-D-D-D-D-K) from Advanced Biotechnology Centre (Imperial College, London, UK); Vivacell 250 filters (MWCO 5000) from Sartorius Ltd (Epsom, UK); PD-10 Desalting Columns from GE Healthcare (Buckinghamshire, UK); bacterial recombinant N-TIMP-3 from Dr Ngee Han Lim and Dr. Linda Troeberg in this laboratory; MMP-1 Cat domain, MT-1 MMP and MMP-13 from Dr Rob Visse in this laboratory.

2.1.3.2. Biotinylation

Materials were from the following sources: Zeba Spin Desalting columns (7 kDa cut-off) and EZ-link Sulpho-*N*-Hydroxysuccinimide (NHS)-biotin containing a 19 atoms spacer (Sulpho-NHS-LC) were from Pierce Biotechnology; Fluoreporter Biotin Quantitation Assay Kit was from Invitrogen; CHES was from Sigma.

2.1.3.3. Quenched-Fluorescent (QF) peptide cleavage assay and aggrecan cleavage assay

QF peptide substrates ortho-aminobenzoyl-Thr-Glu-Ser-Glu~Ser-Arg-Gly-Ala-Ile-Tyr-(N-3-[2,4-dinitrophenyl]-L-2,3-diamino-propionyl)-Lys-Lys-NH_2 [*Abz*-TESE↓SRGAIY-*Dpa*-KK, "↓" indicates the cleavage site] and carboxyfluorescein-Ala-Glu↓Leu-Asn-Gly-Arg-Pro-Ile-Ser-Ile-Ala-Lys-N,N,N',N'-tetramethyl-6-carboxyrhodamine [*Fam*-AE↓LQGRPISIAK-*Tamra*] were custom-synthesised by Bachem. QF peptide substrate (7-methoxycoumarin-4-yl) acetyl-Lys-Pro-Leu-Gly↓Leu-(N-3-[2,4-dinitrophenyl]-L-2,3-diaminopropionyl)-Ala-Arg-NH_2 (*Mca*-KPLG↓L-*Dpa*-AR) (FS-6) was from Sigma. Chondroitinase ABC and keratanase were from Seikagaku (Tokyo, Japan). Bovine nasal aggrecan was prepared in this lab according to the method of Hascall and Sajdera (1969).

2.1.4. Phage display and molecular biology reagents

Phage display library was provided by Dr John McCafferty (Department of Biochemistry, Cambridge University). *TG1* electrocompetent cells were from Lucigen; streptavidin-coated paramagnetic beads (Dynabeads M-280) were from Invitrogen; skimmed milk powder from Marvel; TPCK-Trypsin, ampicillin, kanamycin, streptavidin from *Streptomyces avidinii* were from Sigma; GM6001 was from Elastin Products Co. (Owensville, MO); 96 Deep-well plates and polystyrene tubes from Nunc (Roskilde, DK); Qiagen Plasmid Miniprep Kit from Qiagen (Qiagen, Valencia, CA); T4 DNA Ligase, *Nco*I, *Not*I and *Bstn*I restriction enzymes were from New England Biolabs. ZymoClean™ Gel DNA recovery was from ZymoResearch (Orange, CA). pSANG-10 and pBIOCAM-5 expression vectors was kindly provided by Dr John McCafferty.

2.1.5. Primary screening

Materials were from the following sources: Black Nunc MaxiSorp plates and Abgene 800 µl 96-well block from Fisher Scientific (Loughborough, UK); BL21(DE3) cells from Merck; isopropyl β-D-1 thiogalactopyranoside (IPTG), kanamycin, ampicillin, Greiner 96 well polypropylene plates, anti-M13 antibody were from Sigma; anti-6x His tag antibody from R&D; CircleGrow ® broth from Krackeler Scientific; Whatman MBPP 25 micron filter plate from GE Healthcare; Nucleobond Anion II anion exchange resin was custom-produced by Machery-Nagel (Fisher Scientific); Quant-IT double strand DNA assay Kit from Invitrogen; Nickel-nitrilotriacetic (Ni-NTA) resin was from Qiagen; Generon Proteus 1-step batch midi-spin columns from Generon (Maidenhead, UK); imidazole and anti-FLAG antibody F3165 was from Sigma; europium-labelled anti-mouse and anti-human IgG antibodies, europium-labelled streptavidin and dissociation-enhanced lanthanide

fluorescence immunoassay (DELFIA enhancement solution were from Perkin Elmer (Beaconsfield, UK).

2.1.6. scFv-Fc characterisation

CM5 biosensor chip and anti-human IgG were from GE Healthcare; gelatin from Sigma; heparin-binding plates from Beckton Dickinson Life Science; anti-mouse antibody coupled with horseradish peroxidase (HRP) from Dako (Ely, UK); anti-human HRP from Promega; tetramethylbenzidine substrate from KPL (Wembley Middlesex, UK), Dynabeads Protein G from Invitrogen.

2.2. METHODS

2.2.1. SDS-PAGE and Western Blot

2.2.1.1.SDS-PAGE

Proteins were resolved by SDS-PAGE using either a modification of the ammediol/glycine/HCl buffer system of Wyckoff et al. (1977) or the Tris-glycine buffer system according to Laemmli (1970). Polyacrylamide gels were made with 6-12 % total acrylamide, depending on the size of the proteins to be separated. Samples were diluted with an equal volume of double strength sample buffer [42 mM ammediol, 0.01% (w/v) sodium azide, 2 % SDS, 0.1% (w/v) bromophenol blue, 50% (w/v) glycerol] and loaded into the wells of the upper gel (4% total acrylamide). Unless otherwise specified, sample buffer contained 1% β-mercaptoethanol. Typically, ammediol gels were run at 200 V for 45-60 min and Tris-glycine gels were run at 70 V for 120 min.

2.2.1.2. Gel staining

2.2.1.2.1. Coomassie Brilliant Blue (CBB) R-250 staining

SDS-PAGE gels were stained with Coomassie Brilliant Blue R-250 stain [0.1 % (w/v) CBB, 50 % (v/v) methanol and 20 % (v/v) acetic acid] for 30 min before several 30 min-washes with destaining solution [30 % (v/v) methanol and 1 % (v/v) formic acid]. Gels were then scanned with a BioRad GS710 calibrated imaging densitometer and dried.

2.2.1.2.2. Silver staining

SDS-PAGE gels were stained using silver stain (Shevchenko et al., 1996). Gels were incubated with fixing solution [50 % (v/v) methanol and 5 % (v/v) acetic acid] for 20 min and washed for 10 min with 50 % (v/v) methanol. Next, gels were washed with distilled water (dH_2O) and then incubated with sensitizer [0.02 % (w/v) sodium thiosulphate] for 1 min. After washing two times with dH_2O, gels were incubated with cold silver reagent [0.1 % (w/v) silver nitrate] for 1 h at 4ºC. Following this incubation, gels were washed twice with dH_2O and protein bands were detected by addition of developer [0.04 % (v/v) formalin and 2 % (w/v) sodium carbonate]. The developer was discarded and replaced as soon as it turned yellow so that protein bands were developed in an absolutely transparent solution. Once protein bands could be detected, the developing reaction was stopped using 5 % (v/v) acetic acid. Gels were then scanned with a BioRad GS710 calibrated imaging densitometer and dried.

2.2.1.3. Western blot analysis

Proteins separated by SDS-PAGE were analysed by Western blotting using Trans-Blot® Turbo™ Transfer System according to the manufacturer's instructions (BioRad). Proteins were transferred onto PVDF at 1.3 A for 7 min (Mixed Molecular Weight Protocol, 5-150 kDa proteins) or for 10 min (High Molecular Weight Protocol, >150 kDa proteins) Following transfer, the membranes were blocked with 5% BSA in Tris-Buffered saline (TBS, 50 mM Tris, 200 mM NaCl, pH 7.5) for 1 h at room temperature (RT). In general, membranes were incubated overnight with primary antibodies in 1 % BSA/TBS at 4 ºC. Antibody dilutions were as follows: anti-FLAG M2 1:1000, anti-ADAMTS-5 Cat domain 1:500; anti-NITEGE 1:100; anti-AGEG 1:500; anti-GELE, anti-ARGSV 1:200; anti-G3 1: 500, anti-TIMP-3 1:1000. Membranes were then washed three times with TBS containing 0.1% Tween 20 and incubated with AP-linked secondary antibody (1:5000). Membranes were subsequently washed three times with TBS containing 0.1% Tween 20 before development. AP Western blots were developed with Western Blue AP substrate until bands appeared. The AP reaction was then stopped with AP stop solution [20 mM Tris-HCl pH 7.5, 10 mM EDTA]. Membranes were then scanned with a BioRad GS710 calibrated imaging densitometer and dried.

2.2.2. Antigen preparation and characterisation

2.2.2.1. Expression and purification of recombinant proteins

Recombinant human ADAMTS-4 and ADAMTS-5 deletion mutants and mouse ADAMTS-5 containing a FLAG tag (*N*- D-K-Y-D-D-D-D-K *C*) at the C-terminus were expressed and purified from stably transfected cell lines following the procedure established in our laboratory (Gendron et al., 2007). The vector used for expression of human ADAMTS-4 (Kashiwagi et al., 2004) and -5 (Gendron et al., 2007), as well as mouse ADAMTS-5, was pCEP4.

Stably transfected HEK293-EBNA cells were selected for hygromycin B resistance (100 μg/ml) in DMEM containing 10% FCS, 100 units/ml penicillin and 100 units/ml streptomycin. HTB94 cells stably expressing mouse ADAMTS-5 were selected with 300 μg/ml hygromycin and maintained in Corning HYPERflask cell culture vessels. The culture medium was replaced to serum-free DMEM containing penicillin, streptomycin, and 100 μg/ml heparin. After 3 days, the conditioned media were harvested, centrifuged for 20 min, at 3,000 rpm to remove cells, filtered through a 0.2 μm filter to eliminate any cell debris, supplemented with 0.02% sodium azide and stored at -20° C until purification. The collected conditioned media (0.5 L) were passed over a 3-ml anti-FLAG M2 agarose column at 4°C, which was previously equilibrated with TNC buffer (50 mM Tris-HCl pH 7.5, 100 mM NaCl, 10 mM $CaCl_2$, 0.02% NaN_3 and 0.05% Briji). After loading the media, the column was washed with 1 M NaCl to remove heparin (Kuno & Matsushima, 1998), and the bound protein was eluted with 200 μg/ml FLAG peptide. All the fractions were checked by Western blot analysis with anti-FLAG M2 and anti-ADAMTS-5 Cat domain antibodies and purity was assessed by silver stain. All stocks were passed through PD-10 pre-calibrated gel-filtration column in TNC buffer to remove excess of FLAG peptide and stored at -80°C before use.

Recombinant C-terminally FLAG-tagged TIMP-3 was purified following the procedure described by Troeberg et al. (2009). HEK293-EBNA cells stably transfected with pCEP4-TIMP-3 construct were initially selected for hygromycin resistance (800 μg/ml) in DMEM containing 10% FCS, penicillin and streptomycin, then switched to serum-free DMEM containing 30 mM sodium chlorate ($NaClO_3$) for protein expression.

Active concentrations of all enzymes were determined by titration against known concentrations of N-TIMP-3 in the QF peptide cleavage assay (see **Section 2.2.2.2**). Active concentrations of TIMP-3 were determined by titration against known concentrations of MMP-1 Cat domain.

2.2.2.2. QF peptide cleavage assay

All enzyme assays were conducted in TNC buffer at 37°C, using a Gemini microplate spectrofluorometer (Molecular Devices, Sunnyvale, CA, USA). The activity of ADAMTS-5 was monitored using the QF peptide substrate *Abz*-TESE↓SRGAIY-*Dpa*-KK. This peptide is based on the ADAMTS-4 cleavage site in rat brevican (Matthews et al., 2000) and recombinant ADAMTS-5 cleaves this substrate more readily than ADAMTS-4 *in vitro* (Troeberg et al., 2009). The substrate was used at a final concentration of 20 μM with an excitation wavelength of 300 nm and an emission wavelength of 430 nm (420 nm cut-off). The activity of ADAMTS-4 was monitored using the QF peptide substrate *Fam*-AE↓LQGRPISIAK-*Tamra* at a final concentration of 0.5 μM with an excitation wavelength of 485 nm and an emission wavelength of 538 nm (495 nm cut-off) (Wayne et al., 2007). The activity of MMP-1 Cat domain, MT1-MMP, and MMP-13 was measured using the QF peptide substrate *Mca*-KPLG↓L-*Dpa*-AR at 2 μM final concentration (Knight et al., 1992). Enzymatic rates were corrected for spontaneous hydrolysis of the substrate.

2.2.2.3. Aggrecan digestion assay

Bovine nasal aggrecan (50 μg, 670 nM, MW=1500 kDa) was incubated with ADAMTS-5 in 50 μl TNC at 37°C for 2 h. The reaction was stopped by adding 2 volumes of sodium acetate buffer (200 mM sodium acetate, 250 mM Tris HCl pH 8.0 and 100 mM EDTA). Aggrecan was then deglycosylated by incubating with 0.1 mU/μl of chondroitinase ABC and 0.1 mU/μl of keratanase overnight at 37°C. The samples were precipitated by adding 5 volumes of cold acetone, incubated at -20°C for 4 h, and then centrifuged at 13,000 x *g* for 30 min. The dried pellet was dissolved in 50 μl of reducing sample buffer, run on SDS-PAGE (6% total acrylamide), and subjected to Western blot analysis as described in **Section 2.2.1.3**.

2.2.2.4. Biotinylation of ADAMTS-5 and ADAMTS-4

ADAMTS-5 and ADAMTS-4 were biotinylated with EZ-link Sulpho-NHS-LC biotin. This biotinylation reagent contains a long alkyl spacer arm which guarantees that the interaction between biotin and avidin/streptavidin occurs far away (22 angströms) from the biotinylated protein. The NHS ester present on the biotinylation reagent reacts with primary amines in alkaline conditions such as the side chains of lysines or the N-termini of proteins to yield stable amide bonds. Protein samples were passed through Zebaspin gel filtration columns (7 kDa cut off), recovered in CHES buffer (20 mM CHES pH 8.8, 200 mM NaCl, 10 mM $CaCl_2$) and incubated with Sulpho-NHS-LC-biotin for 30 min RT. Reaction was stopped with an equal volume of TNC buffer (final [Tris]=25 mM) and excess of biotin was removed by gel filtration. Biotinylated enzyme was finally recovered

in TNC buffer and stored at -80°C before use. ADAMTS-5 was titrated before and after biotinylation and the estimated recovery was ~90%.

The level of biotinylation was first assessed by anti-biotin Western blot using AP-conjugated streptavidin A (1:1000). Next, FluoReporter ® Biotin Quantitation Assay Kit was used following the manufacturer's protocol. This Kit provided a fluorescence displacement assay for accurately determining the degree of labelling (DOL) of protein samples. The assay is based on a modified form of avidin which has been labelled both with a fluorescent donor group and a quenching acceptor. Both chromophores occupy the biotin binding sites on the avidin molecule, at a distance which allows for highly efficient Förster resonance energy transfer (FRET). Since the interaction between biotin and avidin is characterised by high affinity (dissociation constant, K_D, around 10^{-15} M) (Green, 1963), biotin molecules covalently attached to the protein sample are able to displace the quencher groups from avidin. The separation of donor and quencher chromophores abolishes the FRET and leads to an increase in fluorescence which is proportional to the number of biotin molecules in the sample. In order to expose any biotin group which could be sterically inaccessible to the avidin, biotinylated ADAMTS-5 was digested overnight at 37°C with 2 U/ml of protease type XIV from *Streptomyces griseus*. Each reaction was performed in phosphate buffered saline (PBS) in a total volume of 100 µl (all samples in triplicate). After 5 minute incubation at room temperature with fluorescently-labelled avidin, fluorescence was measured at excitation wavelength of 495 nm and emission wavelength of 519 nm. Background represented by unbiotinylated protein was subtracted and the fluorescence detected was compared to that of a standard curve of 1.5-200 pmoles of biocytin (biotinylated lysine), which represents the form of biotin upon proteolytic cleavage of a biotinylated protein sample.

2.2.3. Phage display selections

Solution phase scFv phage display selection was performed using protocols and library provided by Dr John McCafferty (Department of Biochemistry, University of Cambridge). McCafferty's library (with a diversity of 1.1 x 10^{10} clones) was created by sequentially cloning an antibody repertoire of light chain variable domains (V_L) followed by cloning of an antibody repertoire of heavy chain variable domains (V_H) (Schofield et al., 2007). The V_H and V_L repertoires were created by PCR amplification from human lymphocytes from 43 non-immunised donors (Schofield et al., 2007). This results in a "naïve" or non-immunised antibody library that can be used to isolate antibodies to any given antigen including antibodies recognising "self" proteins. The format is an scFv fragment (the fragment antibody containing the antigen binding domain) (scFv), with V_H and V_L fragments joined by a flexible linker (Gly_4 Ser Gly_4 Ser Gly_3 Ala Ser) and fused to

the minor coat protein pIII of filamentous phage M13 (5 copies per virion). The cloning vector is the pSANG4 phagemid, which carries an ampicillin resistance marker, bacterial and phage origins of replication, and a phage-packaging signal (**Figure 2.1**). Moreover, it contains the signal sequence from M13 gene III, restriction sites for *Nco*I and *Not*I, a myc tag and the pIII gene under the control of *lac* promoter.

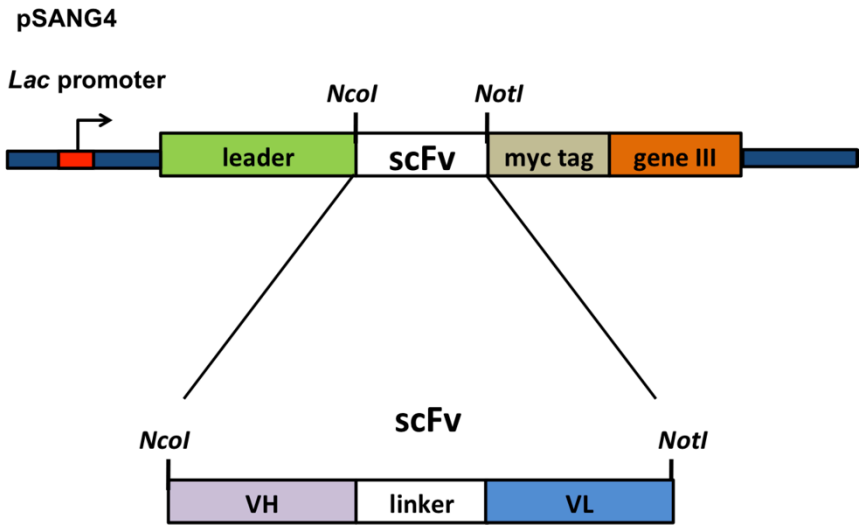

Figure 2.1: Schematic representation of pSANG4 vector and scFv insert.

The pIII protein begins phage infection when it attaches to the F pilus of a susceptible *E. coli* strain and assists in the release of phage from the bacterial cell (Rakonjac and Model, 1998). The scFv insert is cloned via *Nco*I and *Not*I so that the recombinant protein is expressed at the N-terminus of pIII, which extends into solution, without interfering with pIII functions. The following protocol uses a KingFisher 96 Well System (Thermoscientific) and is schematically reported in **Figure 2.2**.

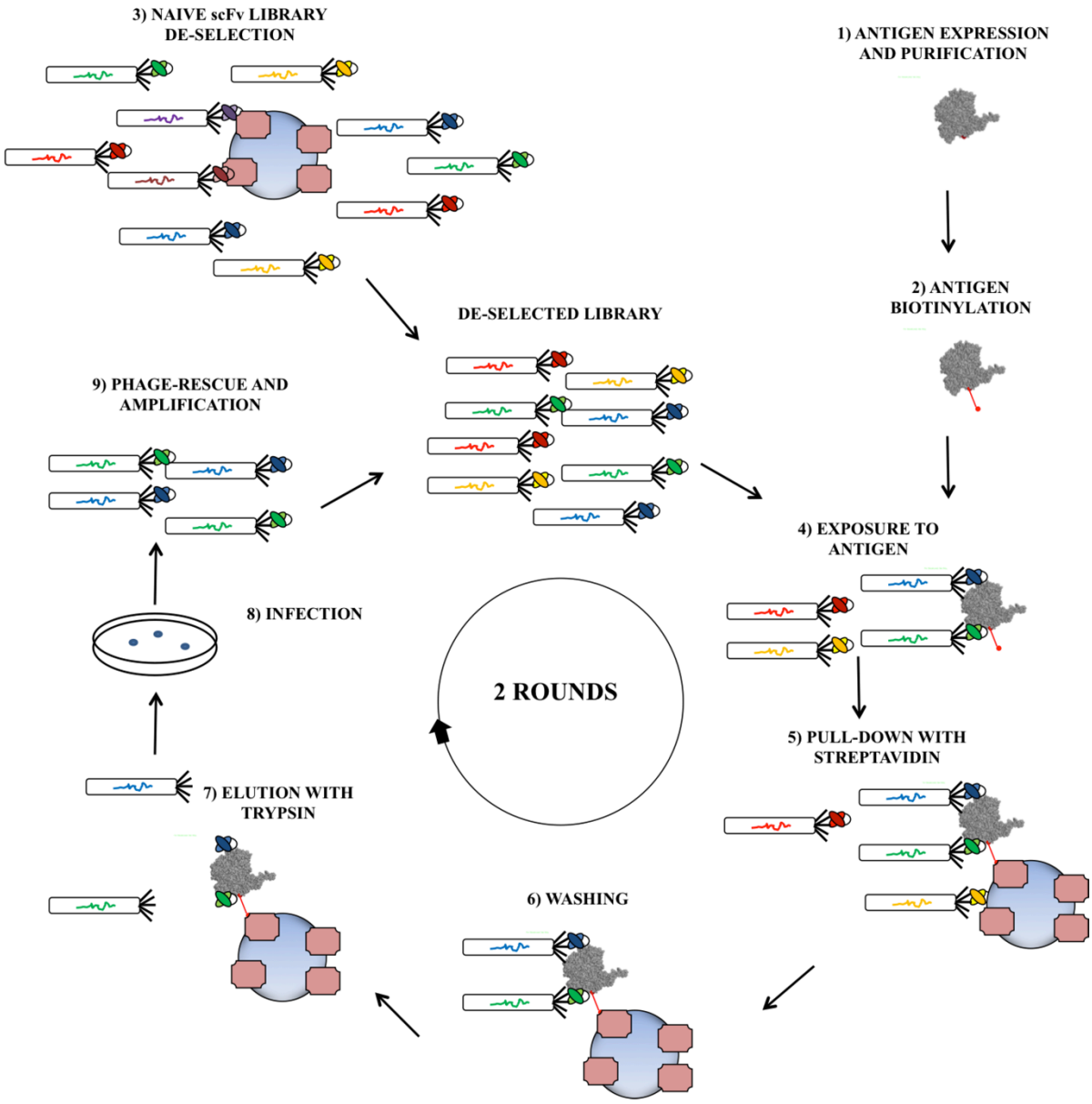

Figure 2.2: Solution-phase scFv Phage Display. 1) ADAMTS-5 is expressed, purified, and **2)** biotinylated with Sulpho-NHS-LC-biotin. **3)** A naïve human scFv phage display library (McCafferty's library) is exposed to unwanted binding partners such as streptavidin (here represented by beads coated with streptavidin) and FLAG peptide. **4)** The de-selected library is then exposed to biotinylated ADAMTS-5 and **5)** the phage-antigen complex is captured by streptavidin-coated paramagnetic beads. **6)** The bead-antigen-phage complex is washed several times to remove weak-binding or aspecific phages. **7)** The specifically-bound phages are eluted from the antigen-bead complex using trypsin-mediated proteolytic digestion of pIII. **8)** Specifically-eluted phages are used to infect *TG1 E. coli*. The bacteria are plated out and selected for ampicillin resistance (only *TG1* cells containing an ampicillin-resistant phagemid are able to grow). After overnight growth, the cells are used to prepare glycerol stocks. **9)** For the second round of selection, bacteria are harvested, grown in liquid phase and super-infected with helper-phage, which confers kanamycin resistance. Double-infected cells are lysed in solution to release a polyclonal (and amplified) mixture of selected phages (phage rescue). The polyclonal phage population can be tested in ELISA to check antigen-binding activity (polyclonal phage ELISA). Glycerol stocks from step **8** can be used to grow and rescue phages for additional rounds of selection or, as an alternative, as a source of DNA for subcloning the scFv inserts into an expression vector.

2.2.3.1. Solution-phase phage-display selection

2.2.3.1.1. Preparation of host *TG1*. A 100 ml culture of 2x TY (Trypton yeast extract) was inoculated from a single colony of *E. coli TG1* cells (taken from a freshly grown minimal media plate). The monoculture was grown at 37°C/250 rpm and placed on ice when optical density at 600 nm (OD_{600}) was around 0.5-0.8 (i.e. logarithmic growth phase).

2.2.3.1.2. Blocking of streptavidin magnetic beads. Pre-washed streptavidin-coated magnetic beads (1 mg, 100 µl) were pelleted using a Dynal Magnetic separator, re-suspended in 1 ml 3% Marvel/TNC in a deep-well plate and mixed on a microtitre plate mixer for 15 min at RT.

2.2.3.1.3. Library De-Selection. The selection of binders to the fusion partner (FLAG) or streptavidin beads can be reduced by de-selection in the presence of an excess of the unwanted partner. McCafferty library (50 µl, 10^{12} phages) was blocked with 900 µl of 3% milk/TNC and used to re-suspend streptavidin-coated magnetic beads (1 mg). FLAG peptide was added to the mixture of phages and beads at a final concentration of 5 µM. The phage-bead solution was mixed and then resolved by magnetic separation on the KingFisher 96. The supernatant (preliminary de-selection phage library) was transferred to a separate plate.

2.2.3.1.4. Exposure to antigen. Biotinylated ADAMTS-5 (10 or 100 nM) was added to the de-selected library in the presence and absence of a 100-fold excess of GM6001. The mixture was incubate at RT for 1 h in a microtitre plate mixer**.**

2.2.3.1.5. Capture and pull-down of phage-antigen complex. Following incubation, the phage-antigen solution described in **Section 2.2.3.1.4** was used to re-suspend the blocked streptavidin coated magnetic beads described in **Section 2.2.3.1.2**. The bead-antigen phage solution was mixed at RT for 10 minutes, then resolved using paramagnetic separation. The supernatant containing non-bound phage was discarded.

2.2.3.1.6. Washing. The bead-antigen-phage complexes were washed 5 times with 3% marvel/TNC. All wash steps were performed in solution and magnetic separation was used to re-isolate the bead-antigen-phage complexes.

2.2.3.1.7. Elution. The plate was then taken out from KingFisher and 10 µl of 1.25 mg/ml L-1-tosylamide-2-phenylethyl chloromethyl ketone (TPCK)-Trypsin in trypsin buffer (50 mM Tris-HCl pH 8.0, 20 mM $CaCl_2$) to the bead-antigen-phage complexes. Trypsin cleaves the scFv antibody from the gene III fusion protein, releasing the bound phage. The gene III protein is still functional after removal of the scFv molecule, thus allowing the phage to infect *TG1* host cells. The solution was incubated at RT for 15 min, then the elution mixture was returned to the KingFisher and resolved for the final time by magnetic separation.

2.2.3.1.8. Infection. Supernatant from step **2.2.3.1.7** (120 µl) containing eluted phage was transferred to a new deep-well plate and combined with 800 µl mid log phase *TG1* (OD_{600}=0.3-0.5) from **step 2.2.3.1.1** and incubated at 37°C, 150 rpm for 60 min.

2.2.3.1.9. Selection for phage-infected *TG1*. A small aliquot of infected *TG1* cells was diluted (1:10, 1:100, 1:1000) and plated out on 2xTYAG (containing ampicillin as a resistance marker and glucose to suppress expression of scFv antibodies) agar plates to titrate the number of selected clones. The rest of the infected cells was pelleted at 3000 x g for 10 min at 20°C, re-suspended in 500 µl 2xTYAG, plated on 2xTYAG agar plates and incubated overnight at 30°C (only *TG1* cells containing an ampicillin-resistant phagemid were able to grow). An aliquot of uninfected *TG1* cells was also plated on 2xTYAG to assess eventual phagemid contamination.

2.2.3.1.10. Phage rescue. Positively-infected *TG1* cells were re-suspended in 2 ml 2xTYAG and either stored as glycerol stocks at -80°C or used to inoculate a poly-culture in 1 ml 2xTYAG. The culture was grown at 37°C, 600 rpm till mid-log phase (OD_{600}= 0.3-0.5) was achieved, then exposed to 10^{10} M13K07 helper phage at a multiplicity of infection of ~ 10 (approximately 10 helper phages per infected *TG1* cell) and incubated at 37°C, 150 rpm, for 1 h. This helper phage brings a gene which confers kanamycin-resistance and will preferentially package phagemid DNA rather than its own helper phage DNA. Moreover, it encodes a modified pIII with an additional trypsin-sensitive site between domains D2 and D3, which are essential for phage infectivity. Thus 'bald' phage with no scFv molecule which were bound non-specifically to the antigen or have not been removed by the wash step are inactivated, giving a more efficient selection process. All cells were centrifuged at 3,200 rpm for 10 min at 20°C and re-suspended in 10 ml 2xTYAK (only *TG1* cells which bring both the ampicillin-resistance carried by the phage display phagemid and the kanamycin-resistance by the helper phage can survive). Dual-infected cells were incubated overnight at 30°C, 600 rpm. During this period the combined burden of phage infection and aggressive agitation results in *TG1* cells lysis and release of packaged phages into the growth medium.

2.2.3.1.11. Polyethylene-glycol (PEG) precipitation. The 10 ml culture described in **Section 2.2.3.1.10** was centrifuged at 8000 rpm for 10 min. The supernatant was transferred to a new tube, supplemented with 3 ml 20% PEG/2.5 M NaCl and incubated on ice for 1 h. Precipitated phages were pelleted at 10,000 rpm for 10 min and re-suspended in 0.5 ml PBS. In order to remove any bacterial debris, re-suspended phages were centrifuged at 10,000 rpm for 20 min at 4°C and the supernatant containing purified selected phages was stored as a glycerol stock at -80°C and/or used in the second round of phage display (thus replacing the de-selected phage library described in **Section 2.2.3.1.3**).

2.2.3.2. Solid-phase phage display selection (biopanning)

The antigen was immobilised by passive adsorption on Nunc Maxisorp polystyrene tubes and all the phage display steps (selection, washing, elutions, etc.) described in **Section 2.2.3.1** were performed manually.

2.2.3.3. Polyclonal Phage Enzyme-Linked Immunosorbent Assay (ELISA)

Black Nunc MaxiSorp plates were coated overnight at 4°C with streptavidin (50 µl/well, 10 µg/ml), blocked for 1 h at RT with 5% BSA/TNC and incubated for 30 min with biotinylated ADAMTS-5 (50 µl/well of 50 nM dilution in 1% BSA/TNC). After three washes with TNC buffer, a dilution in PBS of rescued phages was added for 1 h at RT. Plates were washed 3-times with TNC/0.1% Tween and 3-times with TNC before incubation with anti-M13 antibody (50 µl/well, 1:500 dilution in 1% BSA/TNC) for 1 h at RT. After washing, bound phages were detected by time-resolved fluorescence using europium-labelled anti-mouse-antibody (50 µl/well, 1:1500 dilution in 1% BSA/TNC) and DELFIA enhancement solution (50 µl/well for 3-5 min on a shaker) followed by europium signal acquisition (330 nm excitation, 620 nm emission) on a plate reader.

2.2.4. Primary Screening

2.2.4.1. Subcloning selected populations into pSANG10-3F and pBIOCAM5 expression vectors

After phage display selection, the selected antibody population exists as a polyclonal phagemid mixture in *E. coli*. The glycerol stocks described in **Section 2.2.3.1.10** (containing bacteria which were selected for the presence of a phagemid by ampicillin resistance) can be used directly as a source of DNA in a PCR reaction to amplify scFv sequences. The scFv inserts can then be subcloned into a vector suitable for soluble expression of antibody fragments (glycerol stocks can also be used to grow and rescue phage for additional rounds of selection if necessary). Plasmid DNA of selected clones from the second round of each selection was extracted following the Qiagen Plasmid Miniprep Kit and amplified by PCR using M13 LeadSeq and NotMycSeq primers. The amplified DNA was run on a 1% agarose gel and the insert excised and purified using Zymoclean™ Gel DNA recovery Kit. Purified PCR products were digested with *Nco*I and *Not*I restriction enzymes and then ligated into the *Nco*I/*Not*I digested p-SANG10 or p-BIOCAM5 expression vectors using T4 DNA ligase. The ligation product was used to transform BL21 (DE3) (pSANG-10) or DH5α (pBIOCAM5) chemically competent cells by thermic shock. Transformed cells are then plated out and individual colonies are picked and transferred to separate wells in

microtitre plates. After overnight growth, glycerol is then added to the plates to a final concentration of 16-17% and the plates are stored at -70°C. These archive plates are then be used to inoculate replica plates for primary screening.

A schematic representation of pSANG-10 and pBIOCAM-5 vectors is shown in **Figure 2.3**. Both vectors contain 6 His and triple FLAG tags for antibody detection and purification. pSANG10 vector contains a leader for expression in the bacterial periplasm. The insert is under the control of the T7 promoter. pBIOCAM-5 vector contains a signal peptide for secretion of protein under the control of an enhanced cytomegalovirus promoter (CMV). In this case scFv are expressed in mammalian cells as fusion proteins with the Fc of a human IgG1 (scFv-C_H2-C_H3 dimers).

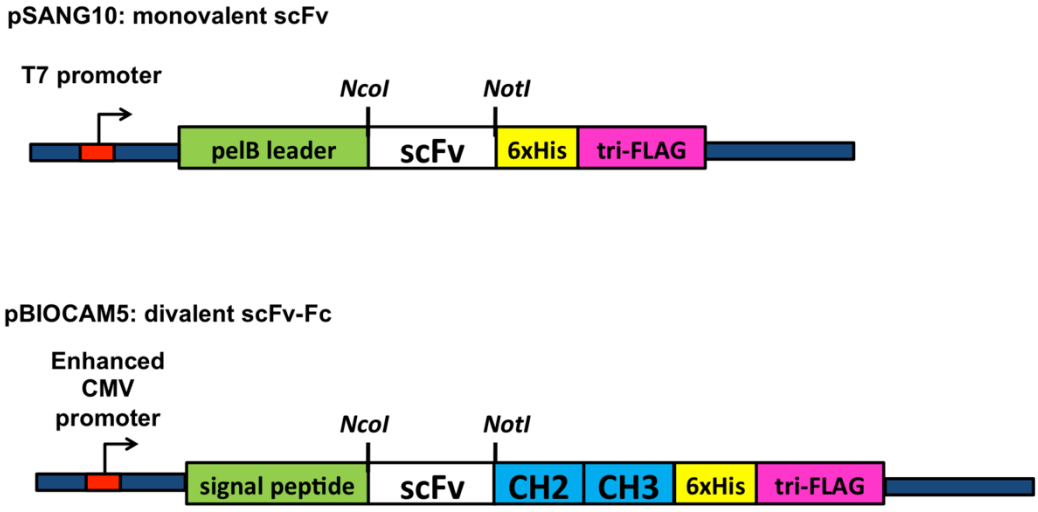

Figure 2.3: Schematic representation of pSANG10 and pBIOCAM5 expression vectors. CMV, cytomegalovirus promoter.

2.2.4.2. Bacterial Screening

2.2.4.2.1. Expression of scFv in *E. coli*

The strain BL21 (DE3) carries a chromosomal copy of T7 RNA polymerase, under the control of the *lacUV5* promoter. Expression is controlled by the *lac* promoter driving expression of T7 RNA polymerase which in turn acts on the T7 promoter of pSANG-10 vector to induce scFv expression. The *lac* promoter can be induced using isopropyl β-D-1 thiogalactopyranoside (IPTG) in mid-log phase growth or auto-induction (Studier, 2005).

2.2.4.2.1.1. Isolation of individual clones. Transformed BL21 (DE3) cells described in **Section 2.2.4.1** were plated and selected on 2x TY, containing 50 µg/ml kanamycin and 2% glucose (2x TYKG). One-hundred ninety colonies were picked and used to inoculate 100 µl 2x TYKG in 96-well polypropylene plates. Isolated cultures were incubated at 37°C, 150 rpm for 4-5 h. Cultures

were replicated in 2x TYKG and 2% glucose and, following overnight incubation, stored as 10% glycerol stocks.

2.2.4.2.1.2. Induction. Cultures were centrifuged at 2,000 rpm for 5 min. All supernatant was removed and each pellet was re-suspended in 200 µl of 2x TY containing 0.02 mM IPTG and 50 µg/ml kanamycin. Induced cultures were incubated overnight at 30°C, 200 rpm.

2.2.4.2.1.3. Isolation of scFv from *E. coli* periplasm. Inoculated cultures were centrifuged at 4,000 rpm for 10 min and cell pellets were re-suspended in 150 µl TES (50 mM Tris-HCl pH 8.0, 0.5 mM EDTA and 0.5 M sucrose). After 10 min, as osmotic shock was initiated by supplementing each re-suspended culture with 150 µl of 20% TES and incubating on ice for 30 min. All cultures were then centrifuged at 4,000 rpm for 10 min and 180 µl of each supernatant (containing soluble scFv) was transferred to a 96 well polypropylene plate. In alternative, after centrifugation of bacterial cultures, supernatant was directly tested on ELISA **(See Section 2.2.4.2.2)**.

2.2.4.2.2. scFv-ELISA

Black Nunc MaxiSorp™ plates were coated overnight at 4°C with streptavidin (50 µl/well, 10 µg/ml), blocked for 1 h at RT with 5% BSA/TNC and incubated for 30 min with biotinylated ADAMTS-5 (50 µl/well of 50 nM dilution in 1% BSA/TNC). After three washes with TNC buffer, bacterial supernatant or periplasm extract was added (50 µl/well, final 1% BSA/TNC) for 1 h at RT. Plates were then washed 3-times with TNC/Tween and 3-times with TNC before incubating with anti-6x his-tag antibody (50 µl/well, 1:500 dilution in 1% BSA/TNC). After washing, bound antibodies were detected by time-resolved fluorescence using europium-labelled anti-mouse antibody (50 µl/well, 1:500 dilution in 1% BSA/TNC) and DELFIA enhancement solution (50 µl/well for 3-5 min on a shaker) followed by europium signal acquisition (330 nm excitation, 620 nm emission) on a plate reader.

2.2.4.3. Mammalian Screening

2.2.4.3.1. High-throughput DNA purification

DH5α glycerol stocks described in **Section 2.2.4.1** were used to inoculate 1.5 ml of CircleGrow ® broth, containing 100 µg/ml ampicillin in 96 deep-well blocks, at 37°C, 800 rpm for 20-24 h (OD_{600}>2). Blocks were spinned for 5 min at 5300 x *g* on a Sorvall RC12 centrifuge and cultures were re-suspended in TE Re-suspension Buffer (50 mM Tris pH 8.0, 10 mM EDTA, 0.1 mg/ml RNAse) and lysed with 0.2 M NaOH, 1% SDS. Suspensions were neutralised with 2.8 M potassium acetate pH 5.1 and centrifuged for 30 minutes at 5300 x *g* to pellet the lysate. To clear

the lysate, supernatant was transferred to a Turbofilter 96 well plate placed over a 96-deep-well plate and centrifuged at 750 x *g* for 5 minutes. The clear lysate was then transferred to a 25 µm Whatman MBPP filter plate containing Nucleobond Anion II anion exchange resin previously equilibrated with Equilibration buffer (100 mM Tris-phosphoric acid pH 6.3, 15% ethanol, 900 mM KCl, 0.15% Triton-X-100) and centrifuged for 10 minutes at 300 x *g* to bind DNA. DNA was washed 3-times with Wash Buffer (100 mM Tris-phosphoric acid pH 6.3, 15% ethanol, 1.15 M KCl) and eluted with Elution Buffer (100 mM tris-phosphoric acid pH 8.5, 15% ethanol, 1M KCl). DNA was then precipitated in isopropanol, washed with 70% ethanol, re-suspended in 10 mM Tris-HCl pH 8.0 and finally quantified by OD_{260} or Quant-IT double strand DNA assay Kit.

2.2.4.3.2. Transient transfection of HEK293-F cells

HEK293-F cells were maintained in serum-free FreeStyle™ 293 Expression Medium in agitated vented polycarbonate Erlenmeyer flasks at 120 rpm (orbital throw 25 mm), 37°C, 5 % CO_2 and 40 % humidity. Cells were routinely maintained at > 95 % viability and passaged when cell density reached 1–4 $\times 10^6$ cells/ml. Cell number and viability was determined using trypan blue exclusion staining and manual cell counts on haemocytometer. For screening, HEK293-F cells (2 ml) were seeded at 1 x 10^6 cells/ml and transfected with 2.4 µg DNA in 24 well blocks containing 0.1% pluronic F68 (Chapple et al., 2006). Linear PEI was used as a transfection reagent (Boussif et al., 1995; Durocher et al., 2002). Blocks were sealed with an air-pore membrane and incubated in an Infors Multitron II incubator (37°C, 5 % CO_2, 75 % humidity, 400 rpm). After 5 days supernatant was collected by centrifugation at 4000 rpm, 5 min, supplemented with sodium azide and stored at 4°C before analysis by ELISA.

2.2.4.3.3. scFv-Fc-ELISA

Black Nunc MaxiSorp™ plates were coated overnight at 4°C with streptavidin (50 µl/well, 10 µg/ml), blocked for 1 h at RT with 5% BSA/TNC and incubated for 30 min with biotinylated ADAMTS-5 (50 µl/well of 50 nM dilution in 1% BSA/TNC). After three washes with TNC buffer, supernatant from transfected HEK cultures was added (50 µl/well, final 1% BSA/TNC) for 1 h at RT. After washing, bound antibodies were detected by time-resolved fluorescence using europium-labelled anti-human antibody (50 µl/well, 1:500 dilution in 1% BSA/TNC) and DELFIA enhancement solution (50 µl/well for 3-5 min on a shaker) followed by europium signal acquisition (330 nm excitation, 620 nm emission) on a plate reader.

2.2.5. Secondary Screening

2.2.5.1. Sequence analysis

Clones were sequenced using primers 2151 (5'-TTAGGAGGGAA CAGGAACACGGAG-3') and 2152 (5'-TTTCTCTCCACAGGTGTCCACTCC-3') for DH5α. Sequences were analysed using FinchTV (GeospizaTM, Seattle, USA) and aligned by BLAST. Following alignment, different clones were identified while duplicate clones were discarded. The consensus DNA sequence was subjected to 3 frame translations and scFv linker (Gly_4 Ser Gly_4 Ser Gly_3 Ala Ser), 6-His tag and triple FLAG tag sequences were identified. Subsequently, the framework regions and CDRs were identified.

2.2.5.2. Determination of scFv-Fc concentration in cell supernatant by sandwich ELISA

Black Nunc MaxiSorp^{TM} plates were coated overnight at 4°C with anti-FLAG antibody (50 µl/well, 5 µg/ml) and blocked for 1 h at RT with 5% BSA/PBS. After three washes with PBS, supernatant from transfected HEK cultures was added (50 µl/well of a 1:50 dilution in PBS) for 1 at RT. After washing, bound antibodies were detected by time-resolved fluorescence using europium-labelled anti human antibody (50 µl/well, 1:500 dilution in 1% BSA/TNC) and DELFIA enhancement solution (50 µl/well for 3-5 min on a shaker) followed by europium signal acquisition (330 nm excitation, 620 nm emission) on a plate reader. Purified scFv-Fc antibodies were used as a standard.

2.2.5.3. Purification of scFv and scFv-Fc antibodies

Antibodies were purified by one-step immobilised metal chromatography (IMAC). For scFv-Fc expression, HEK293-F cells (25 ml) were transfected as described in **Section 2.2.4.3.2** and medium was harvested by centrifugation for 30 min at 2000 x g and stored at 4°C. For scFv expression, bacterial periplasm from 50 ml-induced culture was harvested as described in **Section 2.2.4.2.1**. Conditioned medium (supplemented with 10 x Binding buffer: 10x PBS + 100 mM imidazole, pH 8.0) or bacterial periplasm (dialysed in 10 x Binding Buffer) were incubated Ni-NTA slurry for 2 h at 4°C on a rotating wheel. After this binding step, the mixture was centrifuged at 4000 rpm for 5 minutes to collect beads; the resin was re-suspended in 1 ml supernatant, loaded onto a Generon Proteus spin column and centrifuged at 50 x *g* for 1 min at 4°C. Resin was washed twice with 10 ml Washing Buffer (PBS, 300 mM NaCl, 25 mM imidazole, pH 8.0) and bound antibodies were eluted in Elution buffer (PBS, 300 mM NaCl, 300 mM imidazole, pH 8.0). Eluted fractions were analysed by SDS-PAGE and Coomassie Blue staining. Antibodies were dialysed 3

times in TN buffer (50 mM Tris HCl, 400 mM NaCl, pH 7.5) and once in TNC buffer. The final yield was determined from the UV absorption at 280 nm and the theoretical extinction coefficient was calculated from its amino acid composition. Antibody stocks were stored at 4°C.

2.2.6. scFv-Fc characterisation

2.2.6.1. Surface Plasmon Resonance (SPR)

SPR measurements were carried out on a BIAcore-T100 instrument (GE Healthcare). Anti-human IgG was chemically immobilised on CM5 biosensor chips, and the anti-ADAMTS-5 antibodies were captured to give ~300 response units (RU). For kinetics measurements, 3-fold serial dilutions of ADAMTS-5 (1-100 nM) were injected in TNC buffer containing 0.05% Tween-20 at 25°C with a flow rate of 30 µl/min. The surface of the chip was regenerated after each injection of sample with 3M $MgCl_2$. Binding was corrected for background binding to a non-coated control channel. The binding kinetics were derived from the SPR sensorgrams after subtraction of baseline responses. Association rate constants (k_{on}) and dissociation rate constants (k_{off}) were obtained by using a simple one-to-one binding model (BIACore Evaluation Software).

2.2.6.2. Investigation of inhibition mechanism

To characterise the inhibition mechanism of scFv-Fc antibodies, their inhibitory effect on ADAMTS-5 was measured at different concentrations of the QF substrate Abz-TESE~SRGAIY-Dpa-KK (10, 20, 40 and 80 µM). Data for the reciprocal of the rate of peptide hydrolysis ($1/v$) *versus* antibody concentration (Dixon Plot) were fitted to a linear polynomial equation using Prism software version 5.0 (GraphPad Software, Inc., La Jolla, CA) (Dixon et al., 1979).

2.2.6.3. Dual inhibition studies

Double-inhibitor experiments were conducted as described by Yonetani and Theorell (1964). Inhibition by two inhibitors is examined by varying the concentration of one inhibitor, *i*, over a range of concentrations in the absence or in the presence of a second inhibitor, *j*, held at a constant concentration (generally corresponding to its apparent inhibition constant, $K_{i\ app}$). A plot of the reciprocal of the rate of peptide hydrolysis in the presence of both inhibitors ($1/v_{ij}$) *versus* the concentration of inhibitor *i* will yield: a) two parallel lines if the two inhibitors compete for the same site; b) two lines intersecting the abscissa if the inhibitors bind at two independent sites.

2.2.6.4. Solid-phase binding assay for ADAMTS-5 binding to heparin

Heparin (10 μg/ml TBS) was coated overnight at 25°C on to heparin-binding plates (Mahoney et al., 2004). Wells were washed in TNC buffer containing 0.1%Tween 20 between each subsequent incubation. Wells were blocked with 0.2% gelatin in TNC buffer and then incubated with recombinant ADAMTS-5 in blocking solution for 3 h at 37°C. Bound proteins were detected using either an M2 anti-FLAG antibody followed by anti-mouse antibody coupled to horseradish peroxidase (HRP) or anti-human HRP antibody for 1 h at 37°C. Hydrolysis of tetramethylbenzidine (TMB) substrate was measured at 450 nm using a BioTek EL-808 absorbance microplate reader.

2.2.6.5. Immunoprecipitation of ADAMTS-5 with scFv-Fc antibodies

Purified scFv-Fc antibodies (5 μg) were incubated with Protein G paramagnetic beads (0.6 mg) for 30 min at RT. The mixture was resolved using magnetic separation and the beads containing bound scFv-Fc were incubated with purified ADAMTS5-2 (100 nM, 100 μl), TIMP-3 (100 nM) or both for 1 h at RT. The beads were washed 3 times with TNC buffer containing 0.02 % Tween, re-suspended in 100 μl reducing sample buffer and heated at 90°C for 10 minutes. The mixture was resolved by magnetic separation and the supernatant was collected for Western blot analysis.

2.2.7. Cartilage explant degradation studies

2.2.7.1. Cartilage explant culture

Porcine articular cartilage from the joints of 3-9 month old pigs was dissected into small pieces approximately 3 mm long and 3-4 mm wide. Each piece weighed roughly 10 mg. Human articular cartilage was dissected into small pieces approximately 1-2 mm thick, 2 mm long, and 2 mm wide. Each piece weighed roughly 20 mg. After dissection, the cartilage was allowed to acclimatise for 24 h at 37°C under 5% CO_2 in DMEM containing 100 U/ml penicillin, 100 μg/ml streptomycin, 10 % FCS.

2.2.7.2. Cartilage explant culture conditions for aggrecan degradation

Each cartilage piece placed in one well of a round bottom 96-well plate was incubated in 200 μl of serum-free DMEM (Dulbecco's modified Eagle's medium) with or without IL-1α (10 ng/ml) and OSM (50 ng/ml) to stimulate aggrecan degradation. To test the ability of anti-ADAMTS-5 scFv-Fc antibodies to block aggrecan degradation, each scFv-Fc was added at a concentration of 1 μM. N-TIMP-3 (0.1 μM) was used as a positive control. Three pieces of cartilage

were subjected to each treatment. After 24 h incubation, the conditioned media were harvested and stored at -20°C.

2.2.7.3. Dimethylmethylene blue (DMMB) assay

GAG-released into the conditioned medium was measured in duplicate using a modification of the DMMB assay as described by Farndale et al. (1986). A 200 µl portion of the DMMB assay reagent (16 mg/L DMMB dye, 41 mM sodium chloride, 40 mM glycine, 9.5 mM HCl) was added to 2 µl sample and the absorbance was read at 540 nm. Shark chondroitin sulphate was used as a standard. All data were analysed by unpaired one-tail *t*-test with Welch's correction using the software package GraphPad Prism.

2.2.7.4. Analysis of aggrecan fragments in the conditioned medium

Conditioned medium from cartilage explant culture was mixed with an equal volume of double strength GAG buffer. Aggrecan fragments released into the conditioned medium were deglycosylated using chondroitinase ABC and keratanase, acetone-precipitated and subjected to SDS-PAGE as described in **Section 2.2.1.3**. Membranes were probed with BC3 anti-ARGSV antibody and scanned with a BioRad GS710 calibrated imaging densitometer. Densitometric data were analysed by unpaired one-tail *t*-test with Welch's correction using the software package GraphPad Prism.

2.2.8. Phylogram

A computer sequence analysis of the 19 known ADAMTS family members plus 7 ADAMTS-like (ADAMTSL) proteins was performed. Using the full-length protein sequence for each of the family members, a multiple sequence alignment was generated using CLUSTAL W. CLUSTAL W was run under the default settings. The ".dnd" tree file created was then used as input to TREEVIEW (Page, 1996; http://taxonomy.zoology.gla.ac.uk/rod/treeview.html) for the generation of a phylogram. ADAM-10 was chosen as outgroup. The following human ADAMTS/ADAMTSL family member proteins (UniProt identifiers given in parenthesis) were collected for the generation of the phylogram: ADAMTS-1 (Q9UHI8), ADAMTS-2 (O95450), ADAMTS-3 (O15072), ADAMTS-4 (O75173), ADAMTS-5 (Q9UNA0), ADAMTS-6 (Q9UKP5), ADAMTS-7 (Q9UKP4), ADAMTS-8 (Q9UP79), ADAMTS-9 (Q9P2N4), ADAMTS-10 (Q9H324), ADAMTS-12 (P58397), ADAMTS-13 (Q76LX8), ADAMTS-14 (Q8WXS8), ADAMTS-15 (Q8TE58), ADAMTS-16 (Q8TE57), ADAMTS-17 (Q8TE56), ADAMTS-18 (Q8TE60), ADAMTS-19 (Q8TE59), ADAMTS-20 (P59510), ADAMTSL-1 (A2A344),

ADAMTSL-2 (Q86TH1), ADAMTSL-3 (P82987), ADAMTSL-4 (Q6UY14), ADAMTSL-5 (Q6ZMM2), ADAMTSL-6 (Q6ZMP0), papilin (O95428), ADAM-10 (O14672).

Chapter 3

Preparation of antigen for phage display selection

3.1. Introduction

This chapter focuses on purification and characterisation of ADAMTS-5 which was used as an antigen in phage display selections with the ultimate aim of isolating anti-ADAMTS-5 mAbs. The quality of the antigen is one of the most important factors that affect the success of a phage display selection. Both the purity and the biological activity of a protein antigen are crucial. If the antigen is denatured or incorrectly folded or in an aggregate form, or if it tends to auto-degrade during the selection conditions, the antibodies isolated from primary screening may not have the desired properties. These antibodies may score as positive in ELISA settings but result ineffective in functional assays (for example they would not be able to block catalytic activity of their target enzyme or receptor signalling). This is particularly important when selecting antibodies for therapeutic use. The biological activity of the antigen can be measured in the same assay that will be used later during secondary screening.

Our phage-display protocol uses streptavidin beads to pull down biotinylated antigen/phage complexes during selection **(See Section 2.2.3)**, so biological activity of biotinylated antigens must be assessed and this must be theoretically as similar as possible to that of the native (unbiotinylated) protein. Source of antigen may be also relevant. Antigens expressed in bacteria can be incorrectly folded. Moreover, glycosylation patterns may be significant for biological activity of a mammalian antigen and these are completely absent in a bacterial-expressed antigen or very different in yeast (Powers et al., 2001) and insect cells (Kost and Condreay, 1999). Glycosylation sites on the antigen may also affect antibody binding. The formulation of the antigen is also important. For example, it should not contain carrier protein. As the carrier (usually BSA) is generally at much higher concentration than the antigen, the majority of phage display antibody will bind only to the carrier. Minor contaminants can also cause serious problems. For example, FLAG peptide used to elute FLAG-tagged antigens from anti-FLAG-resin if not removed can be biotinylated and outnumber the antigen during liquid-phase selections. Another factor which plainly influences the choice of an antigen is the expression level. For example, point or deletion mutants of enzymes may be expressed at higher levels than the wild type/full-length enzyme. Since high amounts of purified antigen are needed for selection and primary screening, the final yield should be reasonably high.

Taking in account all these factors, we chose to use ADAMTS5-2 as an antigen for phage display selection **(Fig 3.1)**. This form of ADAMTS-5 lacks the C-terminal TS domain (TS-2); deletion of this domain has no detectable effect on matrix binding or general aggrecanolytic activity of ADAMTS-5, but produces a 2-fold decrease in IGD aggrecanolysis (Gendron et al., 2007) **(See Section 1.3.3)**. However, expression of full-length ADAMTS-5 (ADAMTS5-1) is approximately

10% the expression of ADAMTS5-2 (only 2 µg from 1 L conditioned medium). For this reason, we chose ADAMTS5-2 as an antigen.

3.2. ADAMTS-5 purification

The ADAMTS5-2 construct consists of a signal peptide necessary for extracellular secretion, a prodomain, a Cat domain, a Dis domain, a TS domain, a Sp domain and a FLAG tag at the C-terminus **(Fig 3.1)**. This enzyme was expressed in stably-transfected HEK293-EBNA cells and purified from the conditioned media in the presence of heparin using anti-FLAG affinity chromatography as described in **Section 2.2.2.1**. Heparin was added to enhance the release of the mature enzyme in the conditioned medium owing to its ability to compete with ECM for binding to ADAMTS exosites (Kuno & Matsushima, 1998; Gendron et al., 2007). Since heparin also inhibits aggrecanase activity (Fushimi et al., 2008), high concentrations of salt (1 M) were used to remove heparin from anti-FLAG resin. A typical Western blot from affinity step is shown in **Figure 3.2**.

Figure 3.1: Schematic representation of ADAMTS-5 construct. S, signal peptide; Pro, prodomain; Cat, catalytic domain; Dis, disintegrin domain; TS, thrombospondin domain; CR, cysteine-rich domain; Sp, spacer domain; F, FLAG tag.

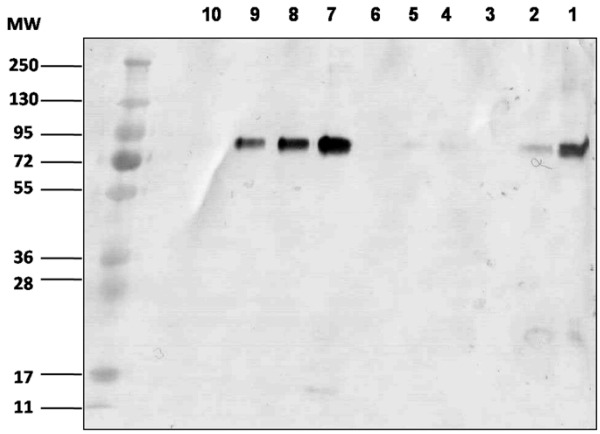

Figure 3.2: SDS-PAGE and Western blot analysis of samples collected from anti-FLAG M2 affinity chromatography. Lanes: 1) Conditioned medium. 2) Unbound. Medium was harvested after 3 days of culture and 1 ml was precipitated with 5% TCA. Unbound was precipitated in the same way. 3), 6) and 10) wash. 4) and 5) wash with 1 M NaCl; 7), 8) and 9) FLAG peptide-eluted fractions. The membrane was probed with anti-FLAG antibody. MW, Molecular weight (kDa).

The eluted fractions were concentrated and applied to a PD-10 gel filtration column to remove excess of FLAG peptide. The purified protein was analysed by Western Blot analysis using both the anti-ADAMTS-5 Cat domain and the anti-FLAG antibodies, and purity was assessed by silver stain **(Figure 3.3)**. The enzyme ran at a molecular weight that was higher than that predicted

for the active form: 75-80 kDa *versus* the predicted 68 kDa, as previously shown in our lab (Gendron et al., 2007). This may be due to glycosylation of the protein.

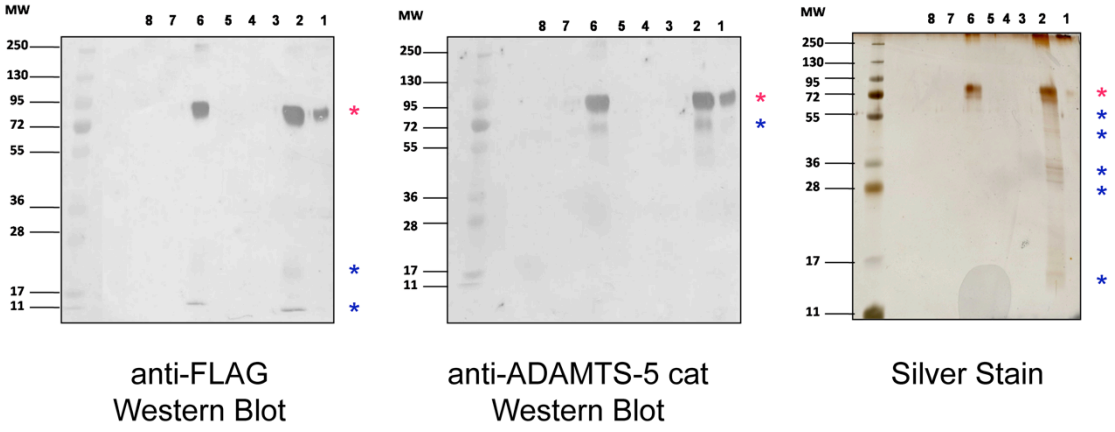

Figure 3.3: SDS-PAGE and Western blot analysis of ADAMTS-5. Purified ADAMTS5-2 was concentrated, passed through a PD-10 column and then subjected to SDS-PAGE (10% total acrylamide) and Western blot analysis using either the anti-FLAG M2 or the anti-ADAMTS-5 Cat domain antibodies. Proteins were stained with silver. Lanes: 1) Pool of eluted fractions from affinity chromatography; 2) 6-folds concentrated pool; 3) flow-through from concentration cell; 4) TNC-buffer; 5) Flow-through; 6), 7) and 8) TNC-eluted fractions. Red stars indicate mature ADAMTS5-2, blue stars C-terminally truncated products. Mw, molecular weight (kDa).

ADAMTS-5 is predicted to undergo *N*-glycosylation (where the glycan is attached to an asparagine residue present in the tripeptide consensus sequence Asn-X-Ser/Thr, with X being any amino acid except proline), *O*-glycosylation (in which the glycan is attached to a serine or threonine residue) and *C*-mannosylation (where a mannose sugar is added to the first tryptophan residue in the sequence Trp-X-X-Trp) and these modifications are linked to protein secretion (Wang et al., 2009; Ricketts et al., 2007). In particular, four *N*-glycosylation sites (one in the Dis domain, one in the CysR domain and two in the Sp domain), one *O*-glycosylation site (in the Sp domain) and five C-mannosylation sites (one in the Cat domain, three in the TS-1 domain and one in the TS-2 domain) are predicted in mature ADAMTS-5. Glycosylation sites for human and mouse sequences are reported in **Table 3.1**. A change in electrophoretic mobility of recombinant ADAMTS-5 after digestion with *N*-glycosidase F confirmed *N*-linked glycosylation in ADAMTS-5 Sp (Zeng et al., 2006) and Dis (Gendron et al., 2007) domain. Moreover, also two C-mannosylation modifications of tryptophan and a glucose-fucose disaccharide on the TS-1 domain of recombinant ADAMTS-5 were experimentally confirmed (Wang et al., 2009).

The protein was mainly present in its processed, active form, as a result of intracellular processing by furin (Gendron et al., 2007). A minor band of approximately 20 kDa was detected with anti-FLAG M2 antibody (**Figure 3.3**); Western blot using the anti-ADAMTS-5 Cat domain antibody also showed a ~60 kDa band which was absent in the anti-FLAG Western Blot. The

combined molecular weights of the 20-kDa band detected in anti-FLAG Western blot and the 60-kDa band detected in the anti-ADAMTS-5 Cat domain Western blot gave the original molecular weight of the enzyme.

Post-translational Modification	Aa residue	Human	Mouse	Domain
N-glycosylation*	498	+	+	Dis
N-glycosylation	728	+	+	CysR
N-glycosylation	802	+	+	Sp
N-glycosylation	807	+	+	Sp
O-glycosylation	25	+	-	Propeptide
O-glycosylation	211	+	+	Propeptide
O-glycosylation	215	+	-	Propeptide
O- glycosylation**	582	+	-	TS-1
O-glycosylation	840	+	-	Sp
C-mannosylation	255	+	-	Propeptide
C-mannosylation	452	+	+	Cat
C-mannosylation**	570	+	+	TS-1
C-mannosylation**	573	+	+	TS-1
C-mannosylation	576	+	+	TS-1
C-mannosylation	884	+	+	TS -2

Table 3.1: Post-translational modifications of ADAMTS-5. Positions were predicted by NetNGlyc 1.0, NetOGlyc 3.1 and NetCGly1.0 (Julenius et al., 2005; Julenius, 2007) softwares. *Gendron et al., 2007, ** Wang et al., 2009.

The final concentration of ADAMTS-5 was determined by active-site titration with N-terminal domain of TIMP-3 (N-TIMP-3). Approximately 150 μg of ADAMTS-5 was routinely obtained from 1 L of conditioned medium.

3.3. Characterisation of aggrecanase activity of ADAMTS5-2

The enzyme concentration-dependence of aggrecan cleavage was characterised by incubating purified bovine aggrecan (670 nM) with different amounts of purified ADAMTS5-2 for 2 h. The products were deglycosylated and subjected to SDS-PAGE and Western blot analysis with the anti-AGEG, anti-GELE, anti-ARGSV (BC3), anti-NITEGE, 2-B-6 (which recognises the chondroitinase-resistant chondroitin 4-sulphate stubs), and anti-G3 antibodies **(Fig. 3.4)**. ADAMTS5-2 showed a general preference for cleavage in the CS-2 domain relative to cleavage in the IGD of aggrecan. Both the 130-kDa AGEG- and 250-kDa GELE- reactive fragments were generated with as low as 1 pM enzyme **(Fig. 3.4 A, B)**; generation of these species peaked at around

5 and 50 pM, respectively, and then declined **(Fig 3.4 G)**, suggesting further C-terminal cleavage. The anti-GELE antibody detected also a second band at around 370 kDa at high (10-100) pM concentrations of enzyme. This fragment was not observed at around 0.5 nM of enzyme **(Fig. 3.4 B).** Interestingly, at this concentration, 250-kDa ARGSV-reactive fragments start to be detected **(Fig 3.4 C)**, thus it is likely that the 370-kDa band represents a product of cleavage at both the GELE^{1499}↓^{1500}GRGT and NITEGE^{392}↓^{393}ARGSV sites (bovine aggrecan numbering).

The 250-kDa ARGSV-reactive fragments peaked at 1 nM ADAMTS5-2 and showed little or no signal at picomolar concentration of enzyme **(Figure 3.4 C)**. As it has previously been shown (Tortorella et al., 2002), the anti-NITEGE neoepitope antibody detected two bands at around 80-70 kDa, which for sake of clarity we define here as "70-kDa band"'. As expected, the 70-kDa NITEGE^{391}-reactive fragments showed a similar pattern with a peak around 1-5 nM, notwithstanding the differences in the relative sensitivities of the two antibodies **(Figure 3.4 G)**.

In the absence of ADAMTS5-2, both the anti-CS stubs antibody and the anti-G3 antibody detected a 500-kDa band representing intact aggrecan. With increasing concentration of enzyme (1-100 pM) 4 different species appeared: 1) a ~250-kDa band which reacted with both the anti-ARGSV antibody **(Fig 3.4 C)** and the anti-GELE antibody **(Fig 3.4 B)**, indicating that this fragment was generated by cleavage at the NITEGE^{392}↓^{393}ARGSV and GELE^{1499}↓^{1500}GRGT sites; 2) a 140-kDa band, which cross-reacted with both the anti-CS stub and the anti-G3 antibodies and was likely to be generated by cleavage at KEE^{1685}↓^{1686}GLGS within the CS-2 domain; 3) a 130-kDa band, which reacted with anti-CS stub, anti-G3 antibody and anti-AGEG antibody, was generated by cleavage at PTAQE^{1790}↓^{1791}AGEG in the CS-2 domain; 4) a 98-kDa band, which cross-reacted with both the anti-CS stub and the anti-G3 antibodies, was likely generated by cleavage at TVSQE^{1890}↓^{1891}LGQR in the CS-2 domain.

In summary, cleavage in the CS-2 domain is favoured over cleavage in the IGD; in particular, cleavage at GELE^{1499}↓^{1500}GRGT, PTAQE^{1790}↓^{1791}AGEG and TVSQE^{1890}↓^{1891}LGQR is preferred over cleavage at NITEGE^{392}↓^{393}ARGSV. These preferences are inferred from comparison between neoepitope antibody Western blots and anti-CS stubs/anti-G3 Western blots, thus overcoming difficulties related with different antibody sensitivities.

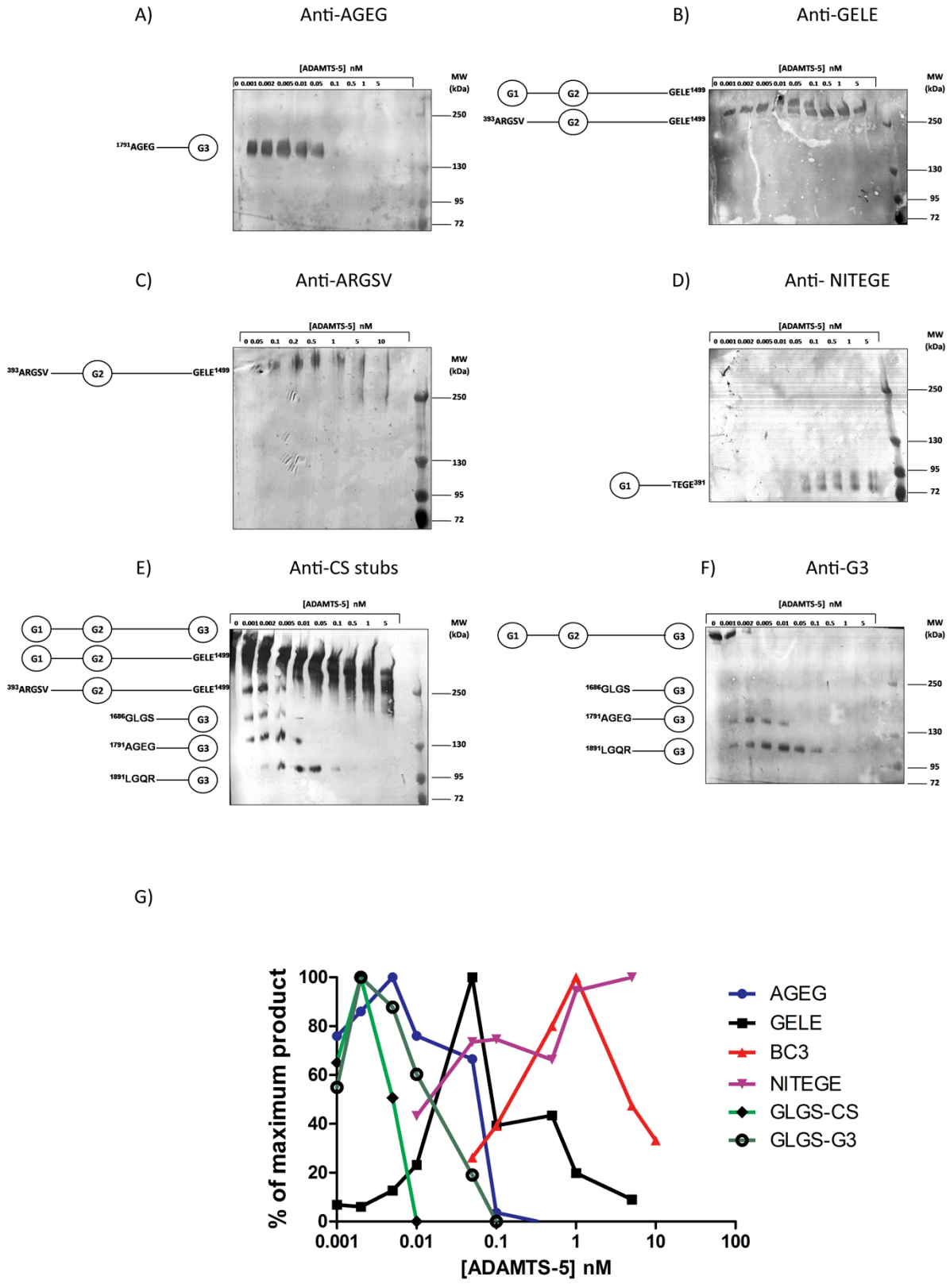

Figure 3.4: Enzymatic characterisation of ADAMTS5-2. ADAMTS5-2 was incubated with aggrecan (670 nM) for 2 h at 37°C. The reaction was stopped with 50 mM EDTA and the samples were deglycosylated. After acetone precipitation, the protein pellets were re-suspended in reducing sample buffer, run on SDS-PAGE (6% total acrylamide), and subjected to Western Blot analysis. Membranes were probed with anti-AGEG (A), anti-GELE (B), anti-ARGSV (C), anti-NITEGE (D), anti-CS stub (E) or anti-G3 (F) antibodies. Detected molecular species are reported on the left side of each blot. G) Plot of ADAMTS-5 generated neoepitopes over the concentration of enzyme (continued). Blots were quantified by scanning densitometry and the intensity of the bands was plotted as a percent

(continued) maximum of reactivity against enzyme concentration. For GELE, only the 250 kDA band is plotted; GLGS indicates the intensity of the band corresponding to 140 kDa-^{1686}GLGS fragment as detected by anti-CS stub or anti-G3 antibodies.

Fragments that react with both the anti-ARGSV and the anti-AGEG antibodies were not detected; instead, only fragments cross-reacting with both the anti-ARGSV and the anti-GELE neoepitope antibodies were observed, thus it may be concluded that cleavage at GELE^{1499}↓^{1500}GRGT is favoured over cleavage at PTAQE^{1790}↓^{1791}AGEG. Bands with size corresponding with cleavage at KEE^{1685}↓^{1686}GLGS are also readily detected with the 2B-6 and anti-G3 antibodies, with intensities peaking at around 2 pM and then declining **(Fig.3.4 G)**. Taken altogether, the data suggest the following order of cleavage (minimum amount necessary to generate maximum cleavage product): 1) cleavage at KEE^{1685}↓^{1686}GLGS; 2) cleavage at GELE^{1499}↓^{1500}GRGT; 3) cleavage at NITEGE^{392}↓^{393}ARGSV in the IGD and at PTAQE^{1790}↓^{1791}AGEG of ^{1500}GRGT-G3 fragments.

3.4. ADAMTS-5 biotinylation

In order to perform solution-phase phage display selections, purified ADAMTS5-2 was biotinylated with EZ-link Sulpho-NHS-LC biotin. This biotin-derivative contains a 19-atom spacer which guarantees that streptavidin binding will not interfere with any local scFv-antigen binding. In fact, the high-affinity ($K_D \sim 10^{-5}$ M, Green, 1963) biotin-streptavidin interaction occurs significantly far away from ADAMTS-5 during antigen pull-down.

Owing to the relatively low enzyme stock concentration (200-300 nM, 15-23 μg/ml) to enhance the efficiency of biotinylation protein/biotin ratios higher than unity (1:4.5; 1:13.5; 1:27; 1:46; 1:90) were explored. Biotinylation was confirmed by anti-biotin Western blot and the degree of labelling (DOL, number of molecules of biotin per molecule of enzyme) was determined by florescence displacement assay **(See section 2.2.2.4)** (**Figure 3.5. and Table 3.2**). Enzyme/biotin ratios up to 1:90 resulted in incorporation of up to 12.5 molecules of biotin per molecule of enzyme. At 1:13.5 and 1:4.5 enzyme/biotin ratios the fluorescence detected was the same of the background and the DOL was calculated as ≤ 1.

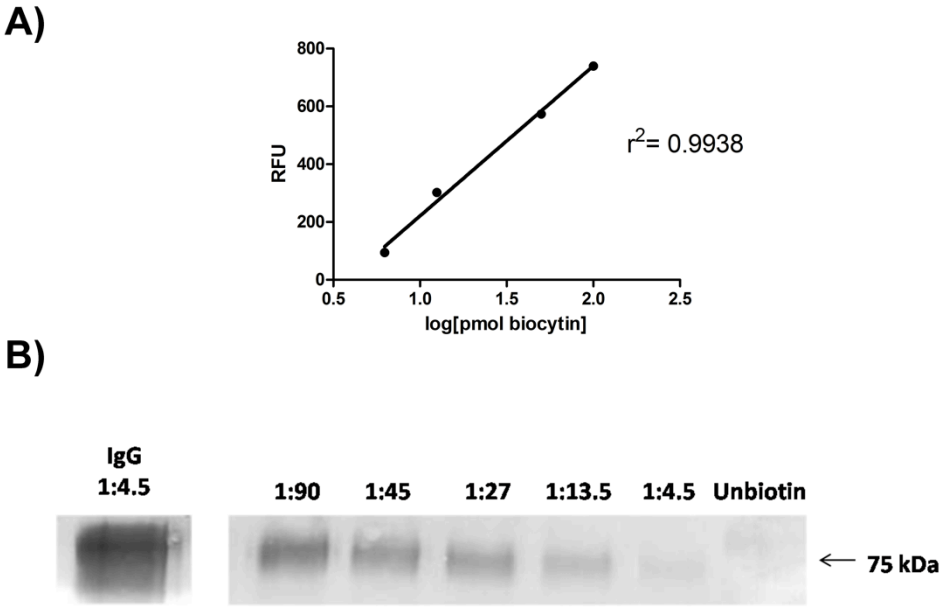

Figure 3.5: Assessment of biotinylation level for ADAMTS-5. A) Standard curve of biocytin (range: 6-100 pmoles biocytin). **B)** Western blot with streptavidin A conjugated with AP. 0.9 pmoles of samples were loaded in each lane. Positive control for Western blot is represented by biotinylated IgG provided by the manufacturer.

Enzyme/Biotin ratio	Degree of labelling (DOL)
1:4.5	<1
1:13.5	<1
1:27	2
1:45	2.7
1:90	12.5

Table 3.2: **Determination of biotinylation level (DOL) for different enzyme/biotin ratios by fluorescence displacement assay.**

Activity of ADAMTS-5 labelled with different numbers of molecules of biotin was tested both in a QF peptide cleavage assay and in the aggrecan digestion assay to ensure that biotinylated antigen retained the activity of the native one. No significant difference in activity was detected between unbiotinylated and biotinylated ADAMTS-5 in the QF peptide cleavage assay even at the highest level of biotinylation **(Figure 3.6 A)**. However, the aggrecan digestion assay revealed a marked decrease in anti-AGEG and anti-ARGSV neoepitope detection for ADAMTS-5 with DOL of 12.5 and 2.7 **(Figure 3.6 B, C)**.

Taken altogether DOL and activity of biotinylated samples, a 1:20 enzyme/biotin ratio was chosen for antigen labelling. This ratio resulted in an average DOL of 1.5 (on average each molecule of enzyme is labelled with 1.5 molecules of biotin). A DOL less than unity would produce

non-biotinylated molecules which will not be pulled down during phage display-selection, thus leading to loss of binders.

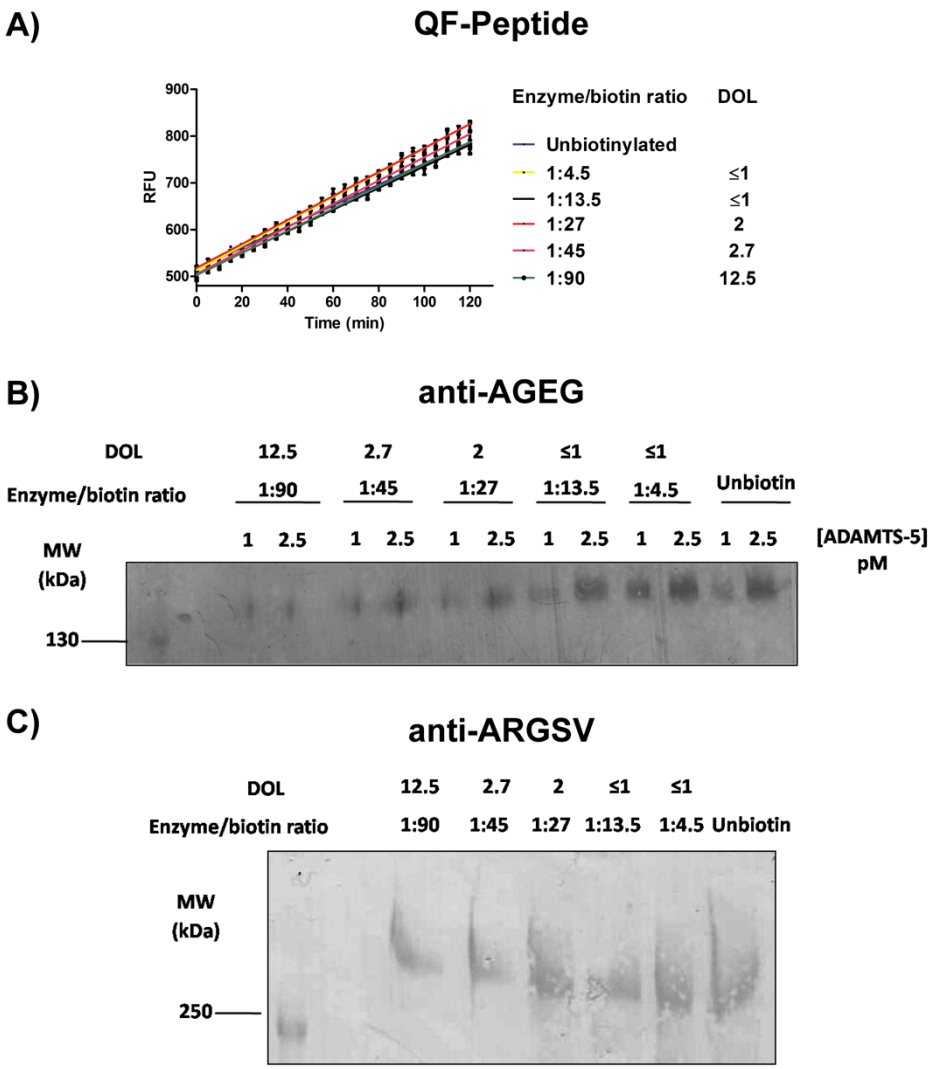

Figure 3.6: Enzymatic activity of biotinylated ADAMTS-5. A) QF-peptide cleavage by biotinylated ADAMTS-5. Enzyme (5 nM) was pre-incubated for 10 min at 37°C before adding 20 µM of QF-peptide substrate ortho-aminobenzoyl-Thr-Glu-Ser-Glu~Ser-Arg-Gly-Ala-Ile-Tyr-(N-3-[2,4-dinitrophenyl]-L-2,3-diamino-propionyl)-Lys-Lys-NH_2. The assay was performed in triplicate in a total volume of 200 µl per well in 96-well microtitre plates. For each DOL mean and standard deviation are reported. **B, C)** Aggrecanase activity by biotinylated ADAMTS-5. Bovine aggrecan (50 µg) was digested for 2 h at 37°C with 1 and 2.5 pM (B) or 1 nM (C) unlabelled ADAMTS-5 or with ADAMTS-5 labelled with increasing number of molecules of biotin. The reactions were stopped with 50 mM EDTA and the products were deglycosylated overnight with chondroitinase ABC and keratanase and analysed by Western blotting for ARGSV-containing fragments using anti-AGEG (B) and anti-ARGSV (C) neoepitope antibodies. For all these assays, activity of unlabelled ADAMTS-5 is reported for comparison.

3.5. Discussion

In this chapter we presented a detailed characterisation of ADAMTS-5 which was preliminary to phage display selection and following screening. A deletion form lacking the C-terminal TS (TS-2) domain (ADAMTS5-2) was expressed in HEK293 cells and purified from the

conditioned medium in the presence of heparin, which enhances release of aggrecanases from ECM (Gendron et al., 2007). The preparation contained mainly the desired enzyme form, although a proportion of the purified protein was C-terminally cleaved, as evidenced by Western blot analysis and silver stain (**Figure 3.3**). On the basis of the observed molecular weight and Western blot data it is very likely that the cleavage sites for autocatalytic processing lie in the Sp and CysR domain. A cleavage site in the Sp domain at $Glu^{753}\downarrow^{754}Gly$ has been reported by Georgiadis et al. (2002) and Zeng et al. (2006). This cleavage generated a 60-kDa band on SDS PAGE (Zeng et al., 2006). However, identification of the cleavage sites may require N-terminal amino acid analysis.

The aggrecanase activity of the antigen was then characterised. ADAMTS5-2 cleaves preferentially in the CS-2 domain of aggrecan with the following order of cleavage 1) cleavage at $KEE^{1685}\downarrow^{1686}GLGS$; 2) cleavage at $GELE^{1499}\downarrow^{1500}GRGT$; 3) cleavage at $NITEGE^{392}\downarrow^{393}ARGSV$ in the IGD and at $PTAQE^{1790}\downarrow^{1791}AGEG$ of $^{1500}GRGT$-G3 fragments. The observed order is in agreement with previous studies reporting time-dependent aggrecanase cleavage of bovine aggrecan (Tortorella et al., 2000a; Tortorella et al., 2002).

The antigen was biotinylated and both peptidolytic and aggrecanolytic activity were checked. High biotinylation levels resulted in a substantial decrease in aggrecanase activity as evaluated by detection of AGEG- and ARGSV-fragments with no effect on cleavage of a QF-peptide. ADAMTS5-2 displays 51 sites for biotinylation, comprising 48 lysine residues (10 in the Cat domain), the N-terminus and 2 lysine residues in the FLAG tag. Therefore, it is statistically more likely that biotinylation reaction involves residues in the ancillary domains rather than in the Cat domain. Since these domains are important in cleavage of macromolecular substrates such as aggrecan **(See section 1.3.3)** but may not be necessary in cleavage of small peptides, the discrepancy in activity between the two assays observed at high biotinylation levels may be explained on the basis of biotinylation of critical lysine residues in the ancillary domains. For example, ADAMTS-5 presents a lysine-rich sequence ($^{739}NKKSKG^{744}$) in the Sp which represents a consensus motif for interaction with GAGs (Troeberg et al., 2012; Cardin and Weintraub, 1989) thus over-biotinylation may impair binding to macromolecular substrates/ECM.

A 1:20 enzyme/biotin ratio resulted in a reasonable labelling (1.5 molecules of biotin/molecule of enzyme) without any effect on aggrecanolytic activity and was chosen for biotinylation of ADAMTS5-2 in preparation for liquid-phase phage display selections.

Chapter 4

Phage display selection and screening

4.1. Introduction

Phage display provides a powerful tool to isolate antibodies against a desired antigen. The possibility to manipulate conditions during selection and screening allows to target or, alternatively, exclude specific epitopes on the target antigen. This is particularly important if the isolated antibodies are required for therapeutic use.

The aim of the selection process is to isolate a small subset of phages that recognise the target antigen from a large and diverse library. One main parameter which modulates the size and diversity of the selected population is the stringency. Stringency is defined as "the degree to which peptides with higher fitness are favoured over peptide with lower fitness", the fitness itself being defined in its Darwinian terms as the contribution to the gene pool of the next generation by an individual with a specific genotype and phenotype (Smith and Petrenko, 1997). Stringency is inversely proportional to the yield (or output), i.e. "the fraction of particles with a given fitness that survive selection" (Smith and Petrenko, 1997). Most common parameters affecting stringency are the duration of incubation of library with the target, conditions of washing steps (e.g. detergent concentration, pH value of washing buffer) (D'Mello and Howard, 2001; Lunder et al., 2005; Yu et al., 2004) and target concentration/density (Kretzschmar et al., 1995). Antibodies can also be selected on the basis of kinetic parameters ("off-rate selection") by incubating the library with the biotinylated antigen in the presence of an excess of unlabelled antigen (Vaughan et al., 1996). The same principle can be exploited to direct the selection towards particular epitopes by adding an excess of a ligand (small molecule or protein) during incubation of the library with the antigen, thus actually negatively selecting antibodies sharing an epitope with the ligand. Finally, screening of the selected phage population can be tailored to enhance the chance to identify antibodies with desired properties. Primary screening usually involves isolation of antibodies for antigen-binding activity by ELISA. This allows for screening of large numbers of clones in parallel. Eventually, secondary screening can be performed to further identify antibodies on the basis of their ability to interfere with the biological activity of the antigen.

In pursuing our aim to isolate ADAMTS-5-blocking antibodies, we exploited the versatility of phage display selection by varying parameters such as antigen concentration and presence of ligand. Moreover, after primary screening by ELISA, ADAMTS-5-binding antibodies were tested for their ability to inhibit peptidolytic and aggrecanolytic activity of the enzyme. Screening for inhibition of a QF peptide cleavage identifies antibodies able to inhibit ADAMTS-5 activity by interacting with Cat/Dis domain; on the other hand, screening for inhibition of aggrecan cleavage not only allows to assess the inhibitory potency of antibodies against an endogen (native) substrate

but may also identify antibodies able to inhibit specifically cleavage of macromolecular substrates by interaction with enzyme ancillary domains.

4.2. Phage display selections

Different approaches for panning of phage display libraries are available. For example, antigen columns can be used where the library is passed through a column with immobilised antigen; selections can also be performed on antigen adsorbed on plastic surface (solid-phase selection) or using biotinylated antigen which can be captured by streptavidin-coated magnetic beads (liquid-phase selection). Alternatively, libraries can be incubated with monolayers of cells or on cells in suspension which express the antigen and then target cells are sorted by Fluorescence-Activated Cell Sorting (FACS) using antibodies against an irrelevant antigen (de Kruif et al., 1995). Finally, in *in vivo* selections phage libraries are directly injected into animals and then tissues are collected and examined for phage bound to tissue-specific markers (Pasqualini and Ruoslahti, 1996).

I chose to perform phage display selection against ADAMTS-5 in liquid phase. Biotinylated human recombinant ADAMTS5-2 was exposed to a naïve scFv antibody phage-display library for two rounds of solution-phase phage display selections. Owing to the presence of a FLAG tag at the C-terminus of the antigen, the library was previously deselected against 5 μM FLAG peptide.

Two antigen concentrations (10 and 100 nM) were explored and for each condition exposure to the library was carried out both in the presence and in the absence of a 100-fold excess of the broad-spectrum metalloprotease inhibitor GM6001 (Grobelny et al., 1992). GM6001 is a zinc-chelating hydroxamate-based compound which inhibits ADAMTS-5 with a $K_{i\ app}$ of 600 nM in QF peptide cleavage assay **(Figure 4.1)**. Notably, no differences in GM6001 inhibition between unbiotinylated and biotinylated form of ADAMTS-5 are detected ($K_{i\ app}$ 630 ± 50 and 590 ± 80, respectively), thus confirming that under these biotinylation conditions ADAMTS-5 is fully active. The use of a large excess of a small molecule inhibitor has two possible effects: 1) to redistribute the conformational distribution of the antigen towards a closed, stable form, preventing potential auto-catalysis; 2) competition with scFv-antibodies with epitopes localised in the proximity of the active site zinc.

A solid phase selection (biopanning), using passive adsorption to polystyrene tubes for antigen immobilisation, was performed using 50 nM ADAMTS5-2. Although this method can induce conformational changes in the structure of native antigens, it generally provides a robust alternative for generate a large number of binders.

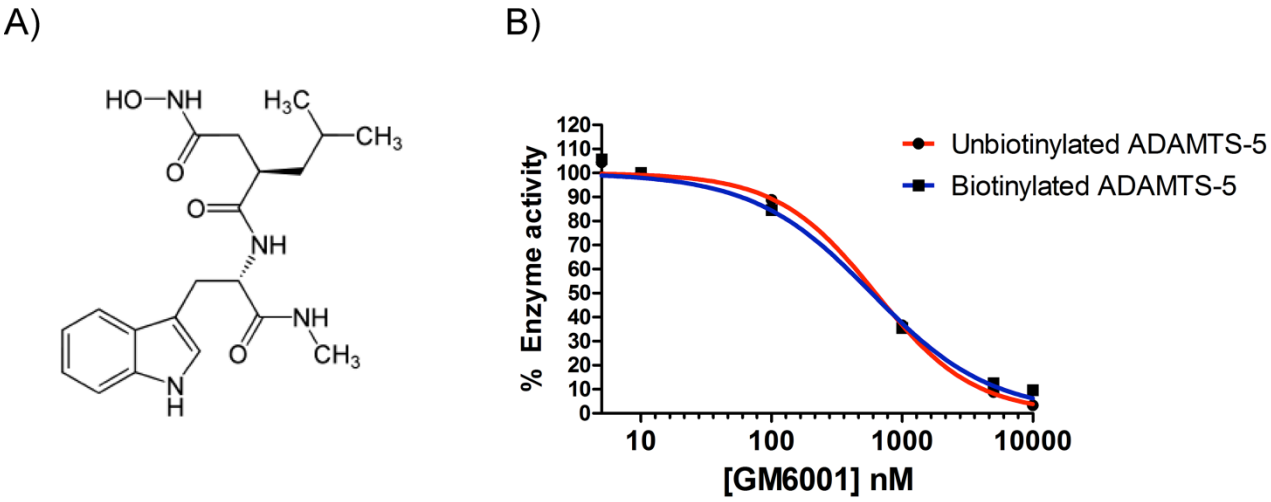

Figure 4.1: Inhibition of ADAMTS-5 by broad-spectrum MMP inhibitor GM6001. A) Structure of GM6001; **B)** Dose-response inhibition of biotinylated and unbiotinylated ADAMTS5-2. Enzyme (5 nM) was pre-incubated for 2 h at 37°C with different concentrations of inhibitor before adding 20 µM of QF peptide substrate ortho-aminobenzoyl-Thr-Glu-Ser-Glu~Ser-Arg-Gly-Ala-Ile-Tyr-(N-3-[2,4-dinitrophenyl]-L-2,3-diamino-propionyl)-Lys-Lys-NH_2.

As a positive control for phage display selections, a well-characterised antigen (kindly provided by Dr John McCafferty, University of Cambridge), SHC-transforming protein 1 (Shc1) was biotinylated and used as an antigen (100 nM concentration) for solution-phase phage display selections.

Following two rounds of phage display selection, the estimated enrichment ratio (calculated by the number of colony-forming units, cfu, eluted in the second round of selection *versus* the number of cfu present in the first round) was between 5- and 13.5-folds for the selections performed in the absence of the inhibitor and between 22.5- and 29-folds in the presence of inhibitor (**Table 4.1**). The solid-phase selection gave 4.5-folds of enrichment, comparable with liquid-phase selections performed in the absence of GM6001. For comparison, the positive control (Shc1) gave about 4000-fold enrichment. The enrichment after round II is explained by a selective increase in targeted-eluted phage pool and the degree of this enrichment depends on the nature of the antigen. Further rounds of selection may provide a greater enrichment ratio but at the same time may decrease final phage diversity. In fact, since phage selection is a function of display level (i.e. expression) as well as binding affinity, excessive rounds of selection can lead to artefacts such as the biased production of better expressing clones or "monster" phage clones lacking any displayed ligand (Jackson et al., 1995).

Selection	[Ag] nM	Inhibitor*	Output Round I	Output Round II	Enrichment (Round II/ Round I)
ADAMTS-5 solid-phase	50	-	2.2 x10^4	1x10^5	4.5
ADAMTS-5 liquid-phase	10	-	5.7 x 10^4	7.7x10^5	13.5
ADAMTS-5 liquid-phase	10	+	6.5 x 10^4	1.9x10^6	29
ADAMTS-5 liquid-phase	100	-	3.5 x 10^5	2x10^6	6
ADAMTS-5 liquid-phase	100	+	4 x 10^5	9x10^6	22.5
Shc1 liquid-phase	100	-	3. 9x 10^3	15x10^6	4000

Table 4.1: Number of phages (cfu) present in pools from the selection experiments. Success rate is defined as the number of ELISA-positive clones over the total number of screened clones and the values reported are for mammalian expression system (See section 4.3.4). *100-fold excess of GM6001.

The trypsin-based phage elution specifically targets only phages bound *via* scFv by cleaving the scFv and the D1 domain of pIII **(Figure 4.2)**. This results in a low phage background when compared with other elution methods, such as pH shift, which also removes phages which bind to the antigen through aspecific interactions (i.e. non-scFv-mediated). The pIII protein is still functional after removal of the scFv molecule, thus allowing the phage to infect *TG1* host cells.

Another advantage of trypsin elution is the specific removal of so-called "bald" phages lacking an scFv molecule derived by the helper phage. When the phagemid is rescued by infection with helper phage, the cell contains pIII protein from the helper and pIII-scFv fusion protein from the phagemid. Approximately 90% of all phage particles produced have only pIII protein from the helper phage and do not carry an scFv molecule. During packaging and rescue of the library, the pIII protein from the helper phage competes with the scFv-pIII fusion protein for incorporation into the phage particles. The helper phage KM13, however, encodes a modified pIII with an additional trypsin-sensitive sequence between domains N1 and N2. Thus, whereas the wild-type pIII protein of the phagemid is resistant to trypsin treatment and retains the infectivity, the modified pIII from the helper phage loses infectivity after trypsin treatment. The net result is the inactivation of phages not carrying an scFv molecule.

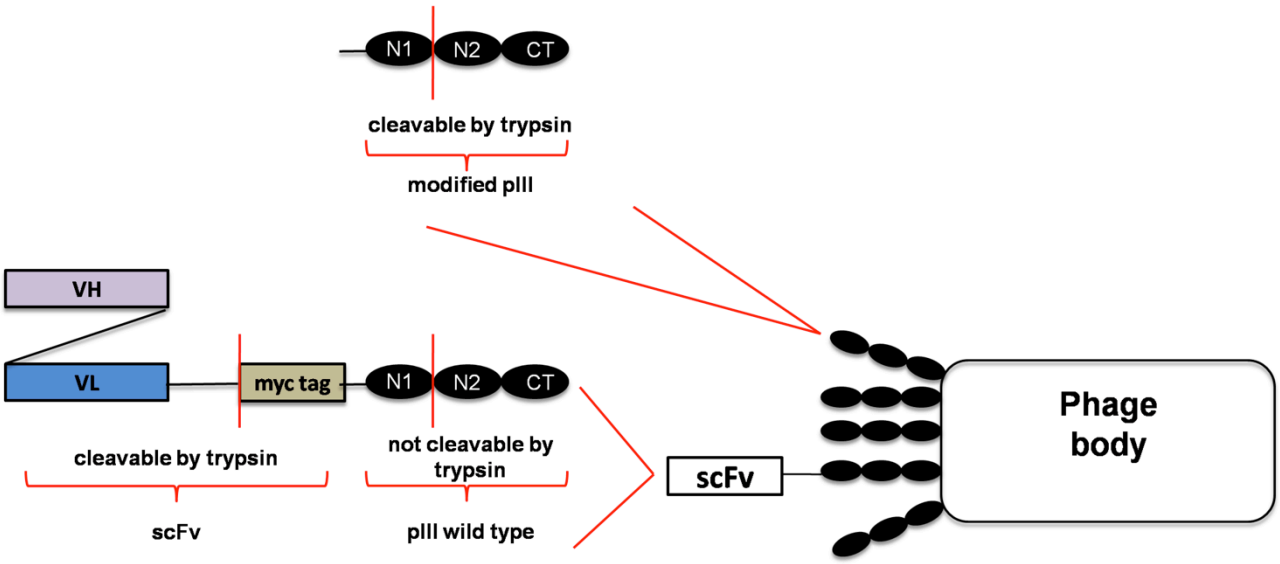

Figure 4.2: Principle of trypsin-based elution.

To check the quality of selections, polyclonal phage ELISA was performed **(Figure 4.3)**. **Figure 4.3 A** shows the results for the 10 nM antigen selections (liquid-phase), the control selection using biotinylated Shc1 as an antigen (liquid-phase) and a standard biopanning selection in immunotubes using 45 nM ADAMTS-5 as an antigen (solid-phase). The solid-phase selection produced a low cognate *versus* non-cognate (ADAMTS-5/streptavidin) signal ratio. This is may be due to the general lower efficiency in the selection procedures in immunotubes coated with streptavidin compared with the pull down mediated by streptavidin-coated paramagnetic beads. We therefore chose to focus our efforts on solution-phase selections. **Figure 4.3 B** reports the results after two rounds of selection for liquid-phase selections using 100 nM ADAMTS-5 as an antigen. In this case the antigen-specific binding after round II increased by around 100 folds with respect to round I. As a negative control, phages from liquid-phase selection against an unrelated antigen (lysozyme) were rescued and incubated with biotinylated ADAMTS-5 to check aspecific binding. These phages gave a signal about 1000 RFU, comparable with the signal from ADAMTS-5 selections after round I, whereas the specific signal from ADAMTS-5 selections after round II increased to around 100,000 RFU. Thus, the signal detected after round I, in the absence of any amplification, is undistinguishable from background signal coming from a phage population selected against a non-cognate antigen.

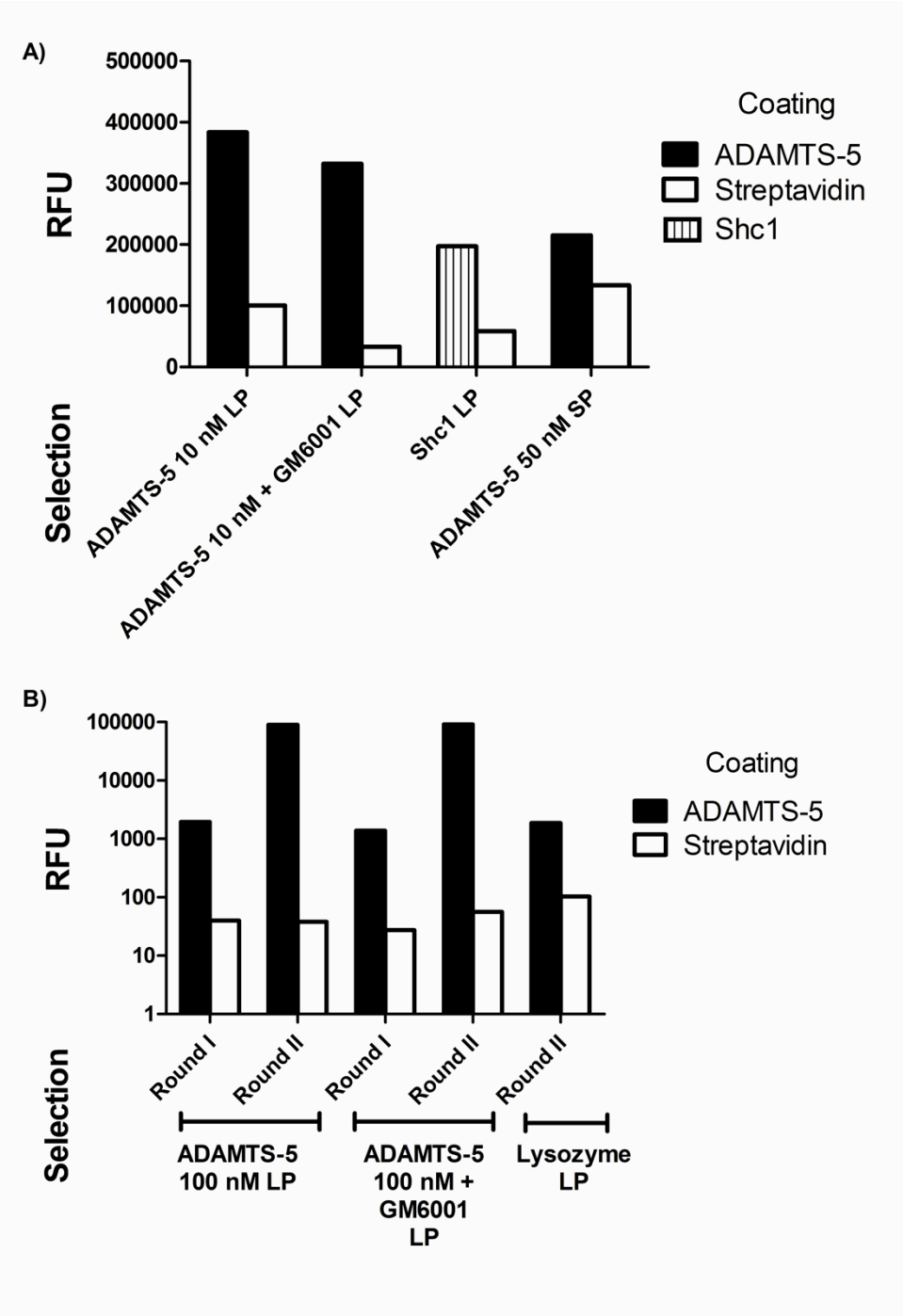

Figure 4.3: Polyclonal Phage ELISA. A) After two rounds of selection, polyclonal ELISA was performed by incubating the polyclonal phage population (5-fold dilution in TNC) from each selection after round II with biotinylated ADAMTS-5 (50 nM) coated on streptavidin plates (black bars) or with streptavidin alone control (white bars). As a comparison, phage population from a selection against Shc1 was incubated with biotinylated Shc1 coated on streptavidin plates or with streptavidin alone. **B)** Enrichment in antigen-specific phages after round II. To check aspecific binding to ADAMTS-5, phages rescued from a selection against lysozyme were incubated with biotinylated ADAMTS-5 coated on streptavidin plates. Phage binding was detected by a M13 europium-conjugated secondary antibody. The ELISA signal is represented as raw fluorescent units (RFU) on the *y*-axis. LP, liquid-phase selection; SP, solid-phase selection.

4.3. Primary screening

The vector used for phage display selection (pSANG4) is not designed for expression of soluble antibody fragments since scFvs are expressed at the N-terminus of pIII of filamentous phage. Moreover, although trypsin-based elution is highly efficient in removing bald phages, still some phagemids may not contain a complete scFv sequence. Therefore, an additional cloning step is required.

For primary screening, selected libraries are usually subcloned into a vector suitable for soluble expression of scFvs by bacterial cells. Although bacterial expression is sufficient for most purposes, some sensitive biological assays and lead validation protocols prefer a mammalian expression system which can provide an antibody format whose features (stability, glycosylation, pharmacokinetics, etc) closely mimic those expected to occur with therapeutic agents. We therefore subcloned selected libraries in pBIOCAM5 vector for screening in HEK293-F suspension cells where antibodies were expressed as fusion proteins with the crystallizable fragment of human IgG1 (scFv-C_H2-C_H3 dimers or scFv-Fc) (Chapple et al, 2006) **(Figure 4.4)**. In parallel, the same eluted polyclonal scFv populations were subcloned into pSANG10-3F for expression of soluble scFv (Martin et al., 2006) to compare success rates (i.e. the number of positive clones over the total number of screened clones) and general performances between the two formats.

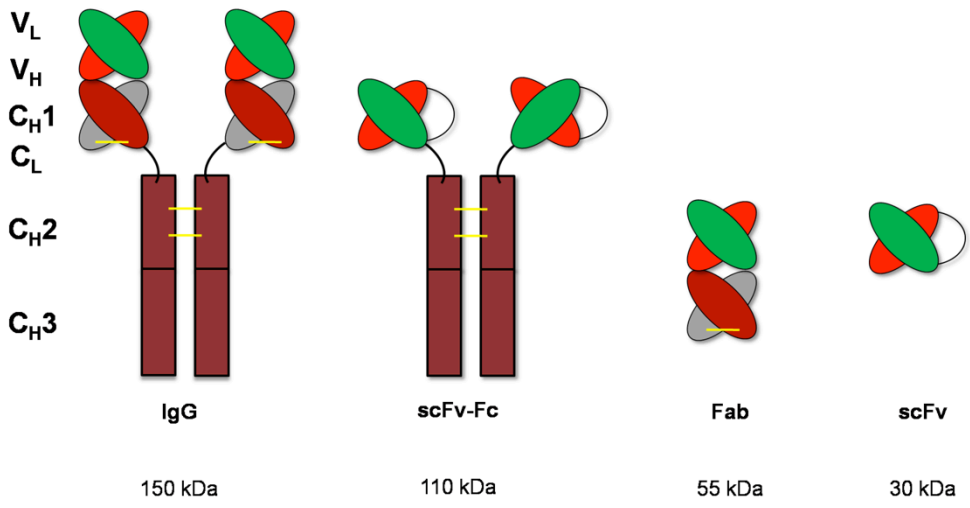

Figure 4.4: Schematic representation of different antibody formats, showing intact IgG molecules alongside scFv and scFv-Fc antibody fragments. Approximate size in kDa is reported. Yellow bars indicate interchain disulphide bonds (intrachain disulphide bonds are omitted).

In both cases, the primary screening was performed in an ELISA setting in the absence of GM6001, using as an antigen biotinylated ADAMTS-5 coated on streptavidin plates or streptavidin alone. Binding specificity was estimated as the ratio between the signal from the antigen plates over the

signal from streptavidin plates. The general strategy for isolation of ADAMTS-5 inhibitory antibodies is depicted in **Figure 4.5**.

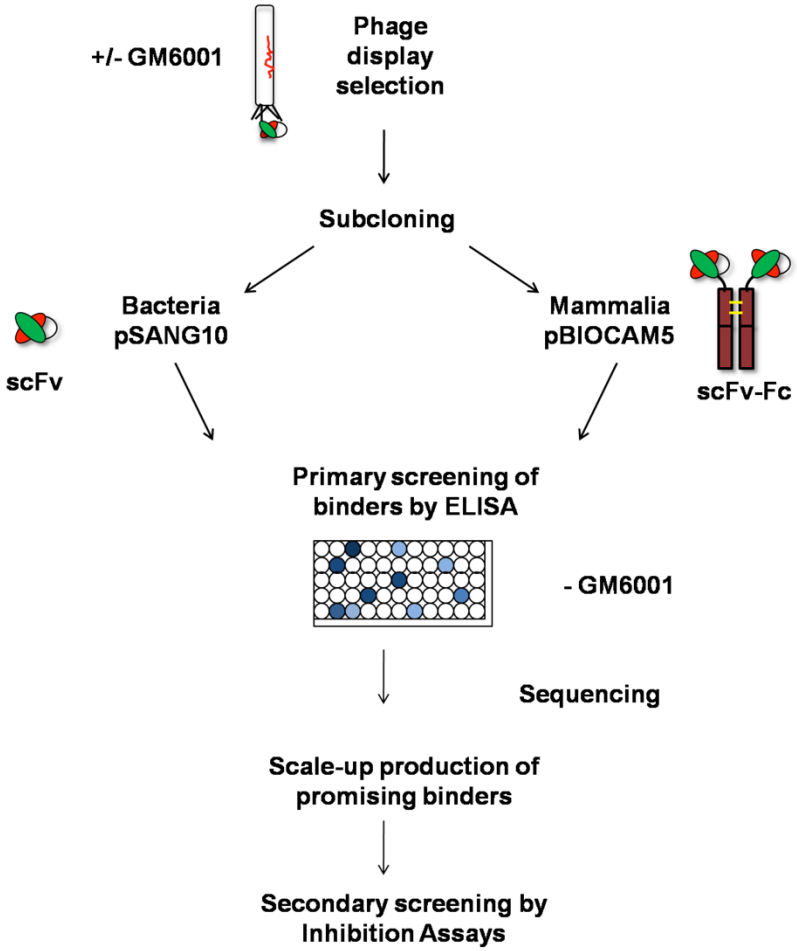

Figure 4.5: Strategy for isolation of ADAMTS-5-inhibitory antibodies. Libraries selected against ADAMTS-5 in the presence and absence of small molecule inhibitor GM6001 were subcloned into both bacteria and mammalian expression vectors. Individual clones were then isolated. Antibodies were first screened for binding to ADAMTS-5 in ELISA (primary screening) in the absence of GM6001. For bacterial screening, BL21 colonies expressing scFvs were directly screened after IPTG induction. For mammalian screening, DH5α colonies were used as a source of DNA which was successively transfected in HEK293-F cells for expression of scFv-Fc antibodies. After DNA sequencing, non-redundant clones were expressed in high amounts and tested in functional assays (secondary screening).

4.3.1. Bacterial screening

The scFv DNA sequences from the final round of selection pools were amplified by colony PCR, isolated by agarose gel extraction and re-cloned into the pSANG10-3F expression vector (Martin et al., 2006) for bacterial expression via *Nco*I/*Not*I. After transformation in BL21, colonies were picked and transferred to 96-well plates (masterplates). Ninety-five clones from the second round of the 100 nM antigen selections (total 190 clones, x 2 96-well plates) were isolated and used to express recombinant scFv antibodies **(Figure 4.6)**. The capacity of each clone to bind to biotinylated recombinant human ADAMTS-5 was investigated by ELISA using anti6x His-tag-antibody/europium-labelled anti-mouse-antibody as a detection system. Supernatant from a

bacterial clone specific for Shc1 and a purified anti-Shc1 scFv were used as positive controls for expression and ELISA, respectively.

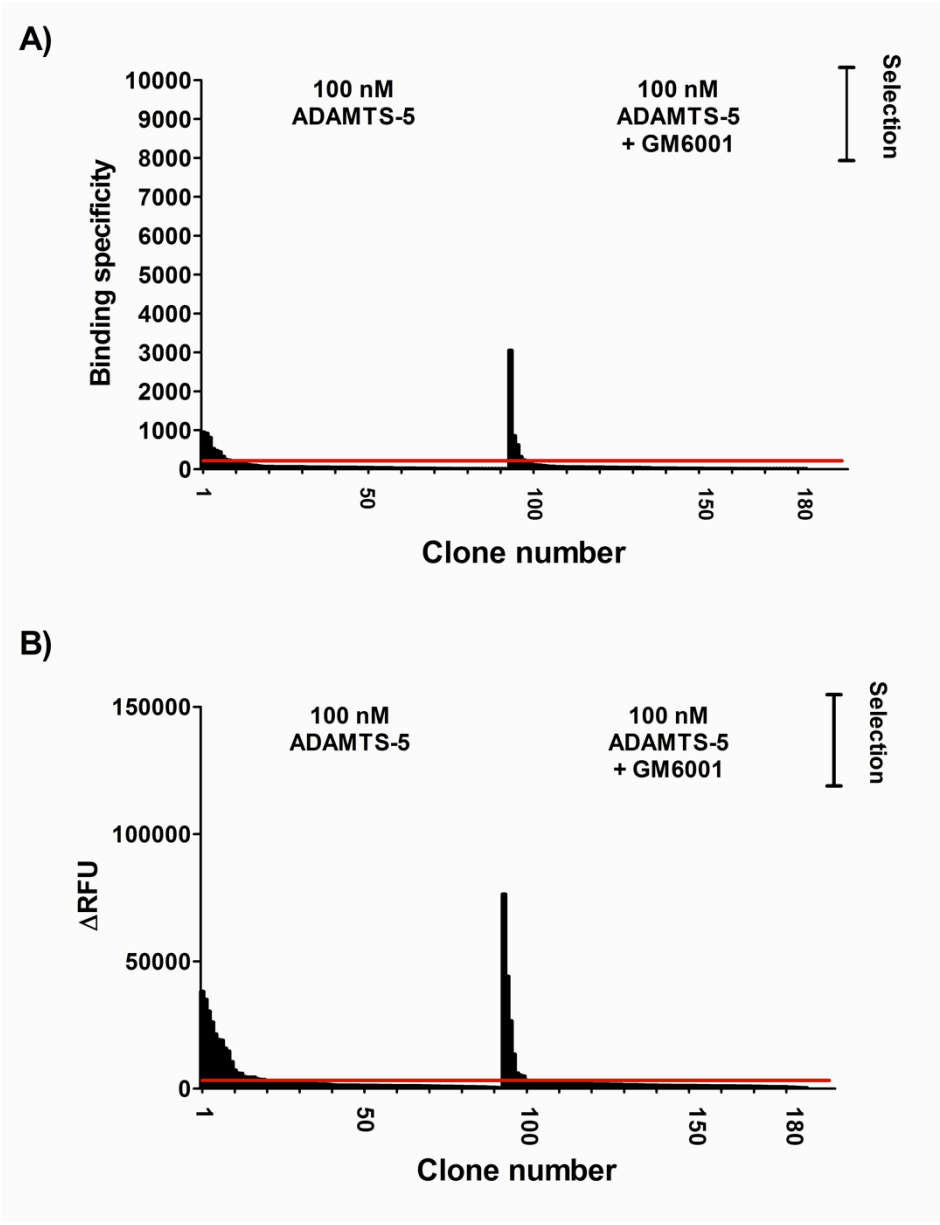

Figure 4.6: Isolation of anti-ADAMTS-5 antibodies expressed in *E. coli*. Following two rounds of solution-phase phage display selections against biotinylated ADAMTS-5 (in the presence and in the absence of a 100-fold excess of zinc-chelating inhibitor GM6001), the eluted phagemid populations were transferred into pSANG10-3F vector and antibodies were expressed as soluble scFvs in *E. coli*. Each clone was ELISA-screened against biotinylated ADAMTS-5 (in the absence of GM6001) on streptavidin plate or streptavidin alone. Results are expressed as **(A)** binding specificity (fold of difference between ADAMTS-5 and streptavidin: $RFU_{ADAMTS\text{-}5}/RFU_{streptavidin}$) or, alternatively **(B)**, as ΔRFU (difference in signal between antigen and streptavidin: $\Delta RFU = RFU_{ADAMTS\text{-}5} - RFU_{streptavidin}$). Red line indicates the arbitrary threshold for signal (~ 5000 RFU, 300 folds of difference).

Both gave a signal of 10,000 RFU after binding biotinylated Sch1, showing saturation of the signal for this antigen **(Figure 4.7)**. A threshold of 5000 RFU was chosen and gave a total success rate of

about 13% (19% for selection with 100 nM antigen without inhibitor and 7% for selection in the presence of inhibitor). In all cases, bacterial supernatant gave a signal of about 50-100 RFU when incubated with streptavidin alone controls. This proves the efficiency of the deselection strategy adopted before the actual phage display selection.

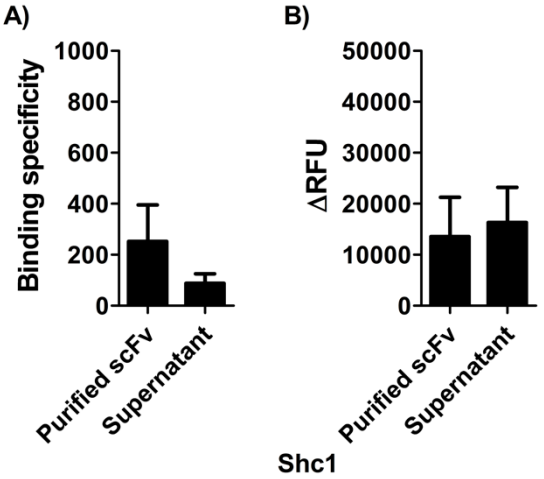

Figure 4.7: Positive controls for bacterial screening. Culture supernatant from a bacterial clone positive for Shc1 binding and purified anti-Shc1 scFvs from the same clone were incubated with biotinylated Shc1 on streptavidin wells as positive controls for induction and ELISA, respectively. Results are expressed as binding specificity (fold of difference between ADAMTS-5 and streptavidin: RFU_{Sch1}/ $RFU_{streptavidin}$) **(A),** or, alternatively, as ΔRFU (difference in signal between antigen and streptavidin: $\Delta RFU = RFU_{Sch1} - RFU_{streptavidin}$ **(B)**. Error bars indicate standard deviation (n=3).

To check expression levels, scFvs were purified from bacterial periplasm after auto-induction using immobilised metal affinity chromatography (IMAC) **(Figure 4.8)**. Purified scFvs run as a single band of around 30 kDa on 12% SDS-PAGE. In this case, scFv expression was controlled by growth in a chemically-defined auto-induction medium, which removes the necessity to monitor bacterial growth by optical density and switches on recombinant protein expression (Studier, 2005). The growth medium contains a controlled amount of carbon sources and the expression is tightly controlled by catabolite repression. As the bacterial culture density increases, the catabolite repression is released by loss of carbon sources and expression from the *lac* promoter is turned on due the presence of lactose in the induction medium. The Studier-defined auto-induction media greatly reduces unintended induction of cultures. In our case, we found that scFv expression induced by auto-induction medium is equivalent to IPTG-induction, as previously reported (Martin et al., 2006). scFvs are mainly present in the periplasmic fraction, although some expression "leaks" into the medium (**Figure 4.8**). However, although recovery of scFv from culture medium is achievable, it is not a straightforward one-step Ni-NTA purification procedure (Bannister et al., 2006). Thus we chose to work with the periplasmic fraction to facilitate

purification of resulting antibodies. Yields between 30-100 µg from 50 ml-scale cultures were routinely obtained for different antibodies **(Table 4.2)**.

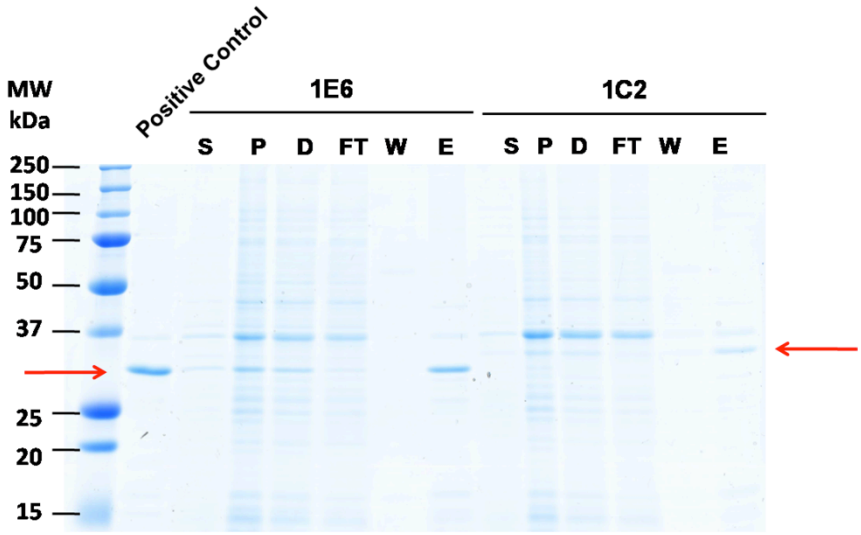

Figure 4.8: scFv purification from bacterial periplasm. A typical purification of clone C2 is compared with that of a positive control (E6) for expression and purification. The first lane from left reports a positive control of E6 clone for SDS-PAGE. S, supernatant; P, periplasmic fraction; D, periplasmic fraction after dialysis in binding buffer; FT, flow-through from Ni-NTA column; W 20 mM imidazole wash; E, 300 mM imidazole-eluted fraction. The red arrows indicate the scFv band at around 30 kDa. Samples were run on a 12% SDS-PAGE under reducing conditions and stained with CBB.

Antibody	Purified scFv (µg, total)
1	120
2	47
3	36
4	106
5	68
6	50
7	91

Table 4.2: Yields of purified scFvs from 50-ml auto-induction cultures. Antibodies were purified by IMAC and concentrations were determined by OD reading at 280 nm.

4.3.2. Mammalian Screening

Phagemid populations were subcloned in pBIOCAM5 vector for expression in HEK293-F suspension cells. For transient expression, the recombinant expression vector was propagated in the *E. coli* strain DH5α. Colonies were picked and transferred to 96-well plates (masterplates). Each bacterial clone from master plates was used to inoculate a replica clone in 96 deep-well blocks for high-throughput plasmid DNA purification **(See Section 2.2.4.3.1)**. On average, DNA yield for 1.5 ml culture was ~ 25 μg, with OD_{260}/OD_{280} ~ 1.9 and OD_{260}/OD_{230} > 2. DNA was then used to transfect HEK293-F cells (2 ml) and 5 days after transfection supernatant was harvested and assayed directly by ELISA against biotinylated ADAMTS-5 coated on streptavidin plates. Antibody binding was detected by europium-labelled anti-human antibody **(Figure 4.9)**. Ninety-five clones from the second round of the 100 nM antigen selections (total 190 clones, x 2 96 well plates) were tested. A threshold of 5000 RFU gave a total success rate of about 24% (29% for selection with 100 nM antigen without GM6001 and 19% for selection in the presence of GM6001). In all cases, supernatant gave a signal of about 10-20 RFU when incubated with streptavidin alone controls. A similar signal was detected when supernatant from mock-transfected cells was incubated with biotinylated ADAMTS-5 or streptavidin **(Figure 4.10)**.

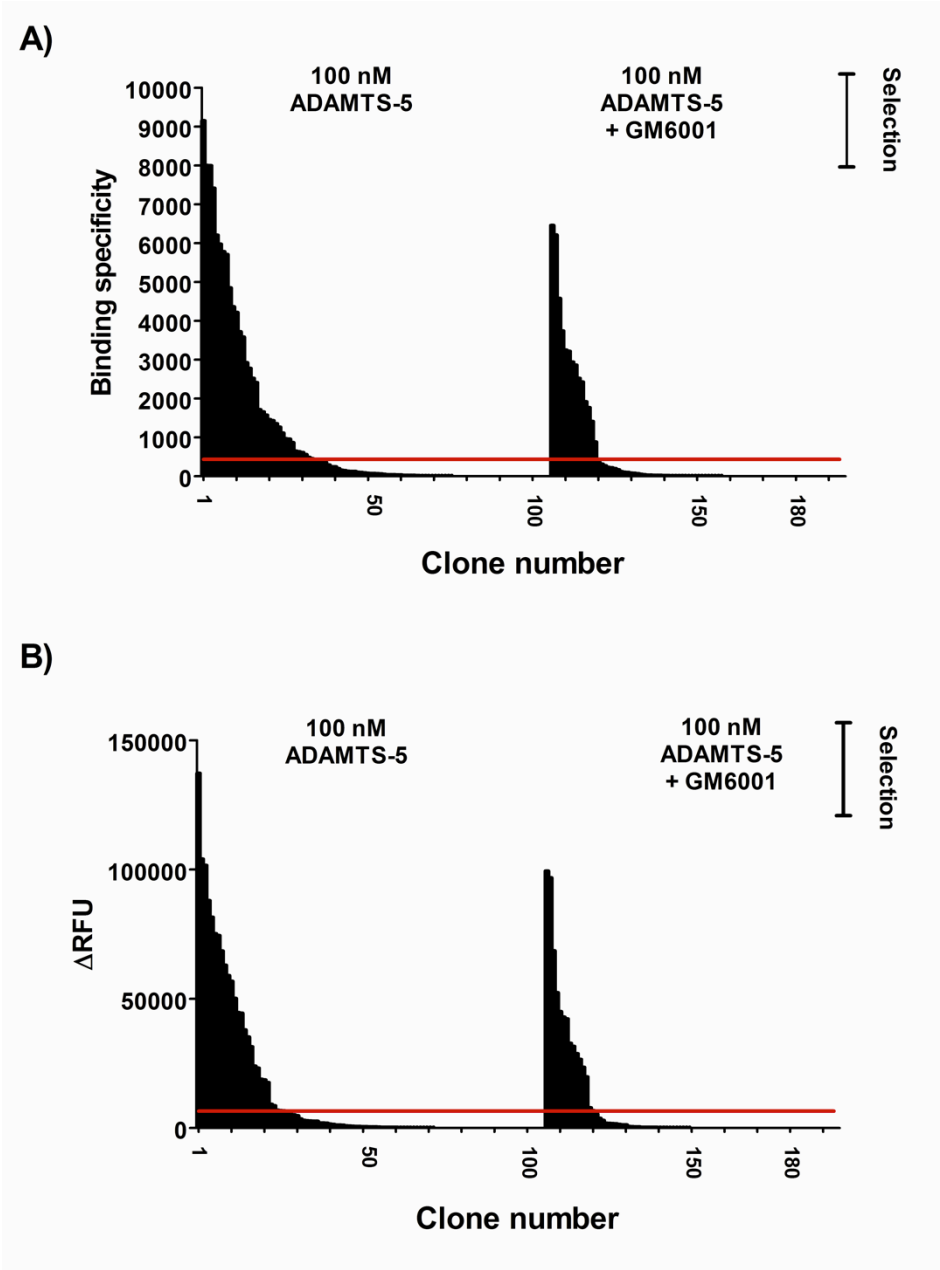

Figure 4.9: Isolation of anti-ADAMTS-5 antibodies expressed in HEK293-F. Following two rounds of solution-phase phage-display selections against biotinylated ADAMTS-5 (in the presence and in the absence of a 100-fold excess of the zinc-chelating inhibitor GM6001), the eluted phagemid populations were transferred into pBIOCAM5 vector and antibodies were expressed as soluble scFv-Fc in HEK293-F cells. Each clone was ELISA-screened against biotinylated ADAMTS-5 (in the absence of GM6001) on streptavidin plate or streptavidin alone. Results are expressed as binding specificity (fold of difference between ADAMTS-5 and streptavidin: $RFU_{ADAMTS\text{-}5}/RFU_{streptavidin}$) **(A)** or, alternatively as ΔRFU (difference in signal between antigen and streptavidin: $\Delta RFU = RFU_{ADAMTS\text{-}5} - RFU_{streptavidin}$) **(B)**. Red line indicates the arbitrary threshold for signal (~ 5000 RFU, 300 folds of difference).

Supernatant from a clone specific for Shc1 was incubated with biotinylated Shc1 as a positive control for transfection and ELISA, giving a signal of about 10,000 RFU **(Figure 4.10)**.

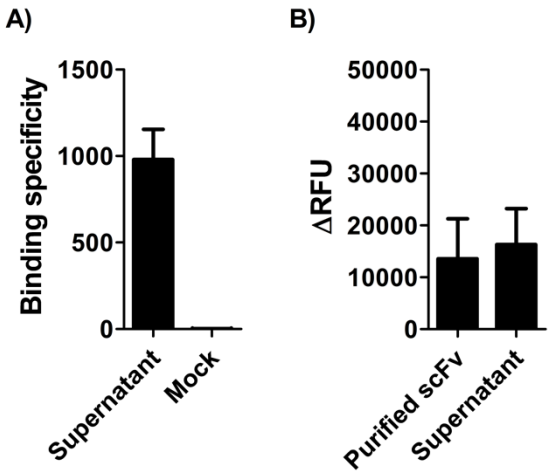

Figure 4.10: Positive controls for mammalian screening. HEK293-F cells were transfected with an anti-Shc1 antibody and after 5 days supernatant was harvested and incubated with biotinylated Shc1 on streptavidin wells as positive controls for transfection and ELISA. As a negative control, HEK293-F cells were mock-transfected and supernatant was incubated with biotinylated ADAMTS-5. Results are expressed as binding specificity (fold of difference between ADAMTS-5 and streptavidin: $RFU_{antigen}/RFU_{streptavidin}$) **(A)**, or, alternatively, as ΔRFU (difference in signal between antigen and streptavidin $\Delta RFU = RFU_{antigen} - RFU_{streptavidin}$). Error bars indicate standard deviation (n=3).

To estimate the concentration of scFv-Fc antibodies in the conditioned medium, a sandwich ELISA was developed. scFv-Fc antibodies were captured with anti-FLAG antibody and detected by an anti-human-europium labelled secondary antibody. A purified scFv-Fc, whose concentration was previously determined by OD reading, was diluted to give a standard curve with linearity in the range of 5-100 ng/ml (r^2=0.98) **(Figure 4.11).** The lower detection limit was 0.5 ng/ml. Conditioned medium was diluted (10-, 50- and 100-folds in PBS) and concentration values were interpolated from the standard curve under conditions where the anti-human signals were proportional to bound scFv-Fc.

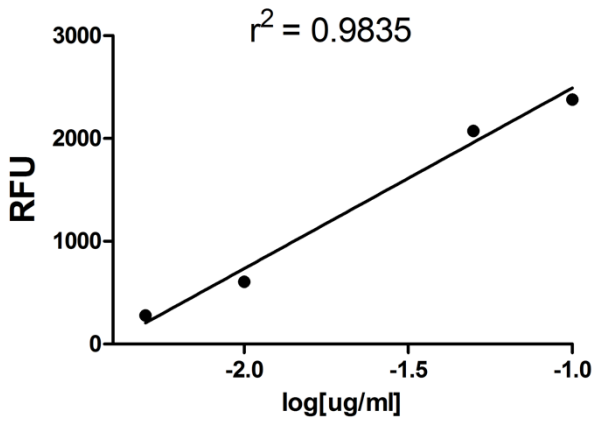

Figure 4.11: Representative standard curve of scFv-Fc antibodies (range 5-100 ng/ml)**.**

Concentrations in the conditioned medium from 2 ml-scale transfections ranged between 0.5 and 20 µg/ml **(Table 4.3)**. The average concentration was around 1 µg/ml, corresponding to 9 nM.

Antibody	[scFv] µg/ml	[scFv] nM	Purified scFv-Fc (µg, total)
1 (1D)	2.2	20	4.4
2 (1F)	0.95	9	1.9
3 (5A)	0.55	5	1.1
4 (2B)	1.85	17	3.7
5 (2F)	1.55	14	3.1
6 (5C)	0.8	7	1.6
7 (2A)	20	180	40

Table 4.3: Concentrations of scFv-Fc antibodies in conditioned medium from 2-ml cultures as determined by sandwich-ELISA.

Differences in expression up to an order of magnitude were observed among different antibodies. It has been reported that even a single amino acid difference at the sequence level may affect the expression of antibodies in mammalian cells, possibly influencing folding, glycosylation, chaperone association and retention in the endoplasmic reticulum (Bentley et al., 1998; Swaroop et al., 1997).

A limitation of the sandwich ELISA described here is the potential loss of C-terminal FLAG tag from the antibody molecule, which may result in an underestimation of antibody concentration in conditioned medium. To directly compare antibody yields between bacterial and mammalian expression systems, scFv-Fc were expressed in 25 ml-scale transfection and purified by IMAC **(Figure 4.12)**. Purified scFv-Fc run as a single band (monomer) of around 60 kDa on a 12% SDS PAGE under reducing conditions. The observed size was in general slightly higher than the expected 55 kDa, probably due to post-translational modifications.

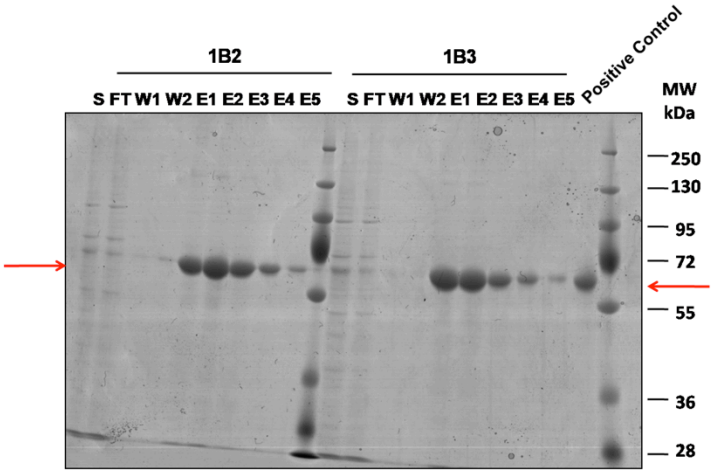

Figure 4.12: scFv-Fc purification from HEK293-F conditioned medium. Representative purifications for two clones are reported. The last lane on the right reports a positive control (purified scFv-Fc) for SDS-PAGE. S, supernatant; FT, flow-through from Ni-NTA column; W, 20 mM imidazole wash; E, 300 mM imidazole-eluted fraction. The red arrows indicate the scFv-Fc band at around 60 kDa. Samples were run on a 12% SDS-PAGE under reducing conditions and stained with CBB.

Yields between 140-300 µg were obtained for different antibodies **(Table 4.4)**. These correspond to concentrations of 5-12 µg/ml in the conditioned medium, with an average concentration of 6 µg/ml (50 nM). One reason for the discrepancy between the average yields determined by sandwich ELISA and the actual yields obtained after IMAC may be the loss of the FLAG peptide (the FLAG peptide is located C-terminal to the 6-His tag); another possibility is that the scale up from 2 ml cultures in 24 well blocks to 25 ml cultures in vented caps may lead to a more robust expression of scFv-Fc antibodies by HEK293-F cells.

Antibody	Purified scFv-Fc (µg, total)
1 (1D)	245
2 (1F)	140
3 (5A)	150
4 (2B)	220
5 (2F)	290
6 (5C)	180
7 (2A)	260

Table 4.4: Yields of purified scFv-Fc antibodies from 25-ml cultures. Antibodies were purified by IMAC and concentrations were determined by OD reading at 280 nm.

It is noteworthy that for screening, supernatant from HEK293-F conditioned medium was used as a source of scFv-Fc antibodies directly without further purification. Thus, scFv concentration was not assessed and the bias represented by different expression levels of different clones could potentially affect the binding of one clone relative to the other, meaning that it is not possible to compare directly antibody signal and affinity. We can assume on the basis of the sandwich ELISA and purification data reported here that the scFv-Fc concentration in the conditioned medium ranged between 10-50 nM. If we compare these values with the concentration of antigen coated on ELISA plates (50 nM), a large excess of antigen was not provided in ELISA. However, it was not possible to increase further the antigen concentration on the plate due to the limited ADAMTS5-2 purification yield.

4.3.3. Comparison between bacterial and mammalian screening

Traditionally in phage display, antibody populations are selected as scFv or Fab fragments fused to coat proteins on the phage surface. For primary screening, these antibodies are then subcloned in *E. coli* for expression of soluble antibody fragments. Within two days, cultures can be transformed, propagated and induced, and periplasm or bacterial supernatant can be tested for binding to the target antigen by ELISA. However, there are some drawbacks related to the use of scFvs during the screening procedure. First, the expression level of human antibody fragments in bacteria is relatively low; secondly, scFvs suffer from a lack of stability. As a result, unless a low molecular weight is desired for specific applications (like *in vivo* imaging), these antibodies need to be reformatted as Fabs or IgGs and, consequently, subcloned in a mammalian expression vector for functional characterisation.

On the other hand, mammalian cells such as HEK or Chinese hamster ovary (CHO) cells can express whole IgGs in a fully glycosylated form although the complete procedure takes 7-10 days to get the purified protein from DNA purification and transfection to antibody purification. A list of factors affecting bacteria and mammalian screening of antibody fragments is reported in **Table 4.5**. Here we were able to compare performances of these two systems by subcloning the same phagemid populations in two vectors optimised for expression of soluble antibody fragments in bacteria and mammalia, respectively. Although the detection system used was different (anti6x-tag followed by europium-labelled anti-mouse antibody in the case of *E. coli*-expressed scFv *versus* europium-labelled anti-human antibody in the case of mammalian-expressed scFv-Fc antibdies), it is evident that the mammalian system presented a superior performance in terms of success rate (~30% versus ~15%, threshold: 5000 RFU or 300 folds of difference with respect streptavidin) (compare **Figures 4.9** with **Figure 4.6** and **Figure 4.10** with **Figure 4.7**). This may be mainly due

to a combination of higher expression and an avidity effect due to the presence of two antigen-binding sites on an scFv-Fc molecule. The yield of purified antibody was in the range of 30-200 μg scFvs from a 50 ml-induced *E. coli* culture and 100-500 μg scFv-Fc antibodies from 25 ml-transfected HEK293-F culture. Moreover, in the case of scFvs, precipitation was observed after short storage at 4°C. Precipitation and inactivation of scFvs are a well documented phenomenon (Marks et al., 1992) and they may be due to the exposure and subsequent aggregation of hydrophobic patches that are in contact with the C_H1 and C_L domains in natural antibodies (Nieba et al., 1997, Reiter et al., 1996). In the case of scFv-Fc antibodies, little or no precipitation was observed after prolonged storage at 4°C, thus it is likely that the fusion of Fcγ1 to the scFv through the hinge region and the consequent dimerisation resulted in stabilisation of the antibody fragment.

	Bacteria scFv	**Mammalia scFv-Fc**
Success rate	**15%**	**30%**
Expression	++*	+++**
Stability	+	+++
Glycosylation	Absent	Present
Time consuming	+ (2 days)	+++ (7-8 days)

Table 4.5: Comparison between bacteria and mammalian systems for expression of antibody fragments. *30-200 μg from 50-ml culture; **100-500 μg from 25-ml culture.

Taken altogether data from ELISA and purification, we chose scFv-Fc expression by HEK293-F cells as a system to screen ADAMTS-5-binding antibodies.

4.3.4. Primary screening of anti-ADAMTS-5 antibodies

Three hundred-three (303) clones from different selections were ELISA-screened in HEK293-F cells (**Figure 4.13**). To check selectivity, 72 clones were randomly chosen and screened again by ELISA against ADAMTS-5 and its most similar ADAMTS member, ADAMTS-4 **(Figure 4.14)**. Both recombinant human proteases are FLAG-tagged at the C-terminus (domain structure of the recombinant human proteins is reported in **Figure 4.14 B**). Biotinylated ADAMTS-4 gave approximately the same signal of ADAMTS-5 on two different types of ELISA (**Figure 4.14 C**).

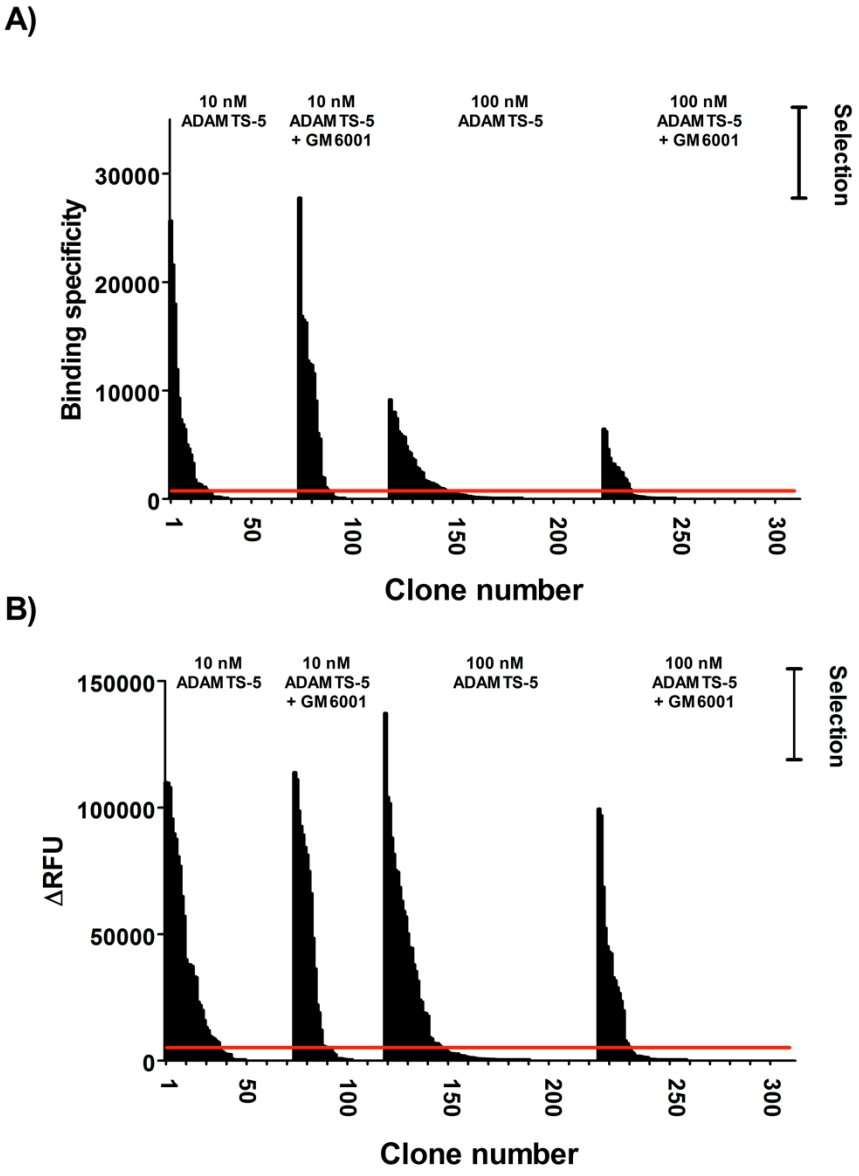

Figure 4.13: Isolation of anti-ADAMTS-5 human antibodies expressed in HEK293-F cells. After high-throughput DNA plasmid purification and transfection in HEK293-F cells, individual clones were ELISA-screened against biotinylated ADAMTS-5 (in the absence of GM6001) on streptavidin plates or streptavidin alone. Results are expressed as binding specificity (fold of difference between ADAMTS-5 and streptavidin: $RFU_{ADAMTS\text{-}5}/RFU_{streptavidin}$) **(A)** or, alternatively as ΔRFU (difference in signal between antigen and streptavidin: $\Delta RFU = RFU_{ADAMTS\text{-}5} - RFU_{streptavidin}$) **(B)**. Red line indicates the arbitrary threshold for signal (~ 5000 RFU, 300 folds of difference).

First, biotinylated ADAMTS-5 and -4 were captured on streptavidin plates and binding was detected by europium-labelled anti-FLAG antibody; in the second ELISA setting, both enzymes were captured by anti-FLAG M2 antibody and the binding was detected by europium-labelled streptavidin. All 72 clones bound only to ADAMTS-5 but not to ADAMTS-4 or streptavidin. Since both enzyme forms used in this experiment are FLAG-tagged, we can exclude that these antibodies are directed against this tag. Moreover, since the scFv-Fc antibodies also contain a triple-FLAG tag, anti-FLAG tag scFv-Fc antibodies would compete each other for the binding or aggregate.

Out of 303 clones, 116 clones were sequenced and 72 different antibodies were identified. **Table 4.6** reports the success rate (number of hits/total number of clones screened), the final diversity (number of different sequences/total number of clones sequenced) and the number of different sequences which have been identified for each selection. The total diversity of the selected phagemid populations was around 62%.

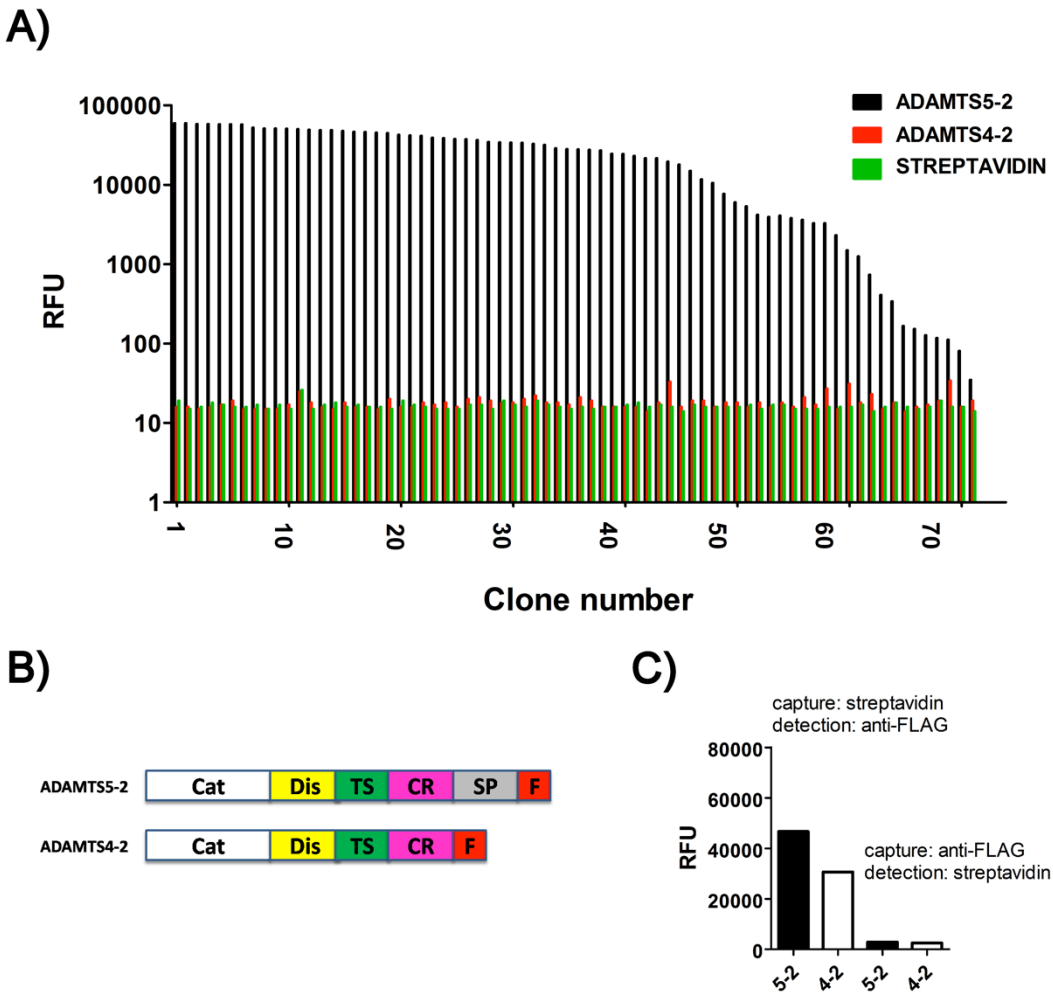

Figure 4.14: Specificity of anti-ADAMTS-5 antibodies. A) Supernatant from HEK293-F cells containing scFv-Fc antibodies was incubated with biotinylated ADAMTS5-2 and ADAMTS4-2 on streptavidin plates or with streptavidin alone, and binding was detected by anti-human europium-labelled IgG (note logarithmic scale); **B)** Domain structure of ADAMTS antigens; F, FLAG tag; **C)** To check that equal levels of biotinylated antigens were coated on streptavidin plates, binding was detected by anti-FLAG europium-labelled IgG; alternatively, 50 nM of each antigen were captured on anti-FLAG wells and binding was detected by europium-labelled streptavidin.

Selection	[Ag] nM	Inhibitor*	Success rate (total clones)	Final diversity (total sequences)	Number of different clones
ADAMTS-5 liquid-phase	10	-	39% (64)	69% (32)	22
ADAMTS-5 liquid-phase	10	+	34% (45)	94% (16)	14
ADAMTS-5 liquid-phase	100	-	29% (106)	66% (44)	28
ADAMTS-5 liquid-phase	100	+	19% (88)	100% (12)	14

Table 4.6: Success rate and final diversity for ADAMTS-5 phage display selections. Sequencing was used to determine final diversity. Numbers in brackets indicate the number of clones which were screened and sequenced, respectively. *100-fold excess of GM6001. Note: the number of different clones is higher than 72 owing to clones being shared between different selections.

Three antibodies were identified both in the 10 and in the 100 nM selection in the absence of GM6001, whereas just one antibody out of 72 was isolated irrespective of the selection conditions. For each clone, the variable heavy and light chain subclasses as well as the 3 CDRs (CDR-1, -2, and -3) of each chain were identified (**Table 4.7**). CDRs represent a set of structural elements which determine the specificity of an antibody to the target (Jones & Thornton, 1996), namely the residues on the antibody that contact the epitopes (paratopes). The third CDR of the heavy chain (CDR-H3) is the most diverse and most important for antigen recognition (Xu and Davis, 2000; Zemlin et al., 2003) and, in naturally occurring human antibodies, its size varies from 4 to >35 residues (Johnson and Wu, 2000). An analysis of the germ line contribution to CDR-H3 diversity points out that naïve loops are dominated by tyrosine and small residues (glycine, serine, alanine and threonine) (Zemlin et al., 2003). Tryptophan residues are not particularly abundant, and arginine residues are rare but become more abundant in antibodies that have undergone affinity maturation (Zemlin et al., 2003). The sequences of anti-ADAMTS-5 antibodies show an over-representation of a few amino acids (tyrosine, serine, asparagine and tryptophan), as previously reported (Ofran et al., 2008). Tyrosine residues mediate about 25% of the antigen contacts in functional antibodies (Mian et al., 1991). Aspartate and glycine are over-represented in the CDRs of the heavy chain. High abundance of tyrosine, serine and glycine has been correlated with increased antibody specificity (Birtalan et al., 2008).

Clone	Variable Heavy				Variable Light			
	CDR-1	CDR-2	CDR-3	Subclass	CDR-1	CDR-2	CDR-3	Subclass
MP2 A1	GFTFSSYGMH	VISYDGSNKYYADSVKG	LFYNNYYYVMDV	III	QGDSLRSYYAS	GKNNRPS	NSRDSSGNHVV	Lambda IV
MP2 A3	GFTFSSYGMH	VISYDGSNKYYADSVKG	DRDSSGYWYGMDV	III	RASQSISSYLN	DASNLET	QQSHSTPYT	Kappa I
MP2 A7	GFPFSSYGMH	VISYDGSNKYYADSVKG	DSGSSWHRYMDV	II	RASQSISSYLN	AASSLQS	QQSYSTPPT	Lambda I
MP2 A11	GYSFTSYWIS	RIDPSDSYTNYSPSFQG	GGDSSSLYDAFDI	I	TGTSSDVGGYNYVS	EGSKRPS	SSYTSTNSVV	Lambda II
MP2 B1	GYTLTELSMH	GFDPEDGETIYAQKFQG	FGRGY	I	TGSNGTIDSNFVQ	EDNQRPS	QSYDSTTVI	Lambda VI
MP2 B3	GFTFDDYAMH	SISWNSGSIGYADSVKG	DAVDGYYHYVDV	III	RASQSISSYLN	AASSLQS	QQSYSTPSRT	Kappa I
MP2 B8	GYSFTSYWIG	IIYPGDSDTRYSPSFQG	GTGTTIADAFDI	I	RASQSISSYLN	AASSLQS	QQTYKTPQT	Kappa I
MP2 B9	GFTFSSYAMS	AISGSGGSTYYADSVKG	DQTPLGGFYFDY	III	RASQSISSYLN	AASSLQS	QQSYSTPGT	Kappa I
MP2 C1	GGTFSSYAIS	GIIPIFGTANYAQKFQG	VLQGYSYGYWVFDY	I	TRSSGSIASNYVQ	EDNQRPS	QSYDSNNVV	Lambda VI
MP2 C7	GYTLTELSMH	GFDPEDGETIYAQKFQG	SGLLDY	I	TGSSGSIASNYVQ	EDNQRPS	QSYDSSNHCWV	Lambda VI
MP2 C9	GYTFTSYGIS	GIIPIFGTANYAQKFQG	DLYQLLYPGGAFDI	I	TGSGGSIASNDVQ	EDDQRPS	QSYDSVNRGI	Lambda VI
MP2 D3	GGTFSSYAIS	GIIPIFGTANYAQKFQG	EGRLVVGATTDYYYYYGMDV	I	RASQNINTYLN	KASSLES	QQYDNLPIT	Kappa I
MP2 D5	GFTFDDYAMH	GISWNSGSIGYADSVKG	ESSSWYLRYFDY	III	RASQSISSYLN	AASSLQS	QQSYSTPFT	Kappa I
MP2 D9	GGTFSSYAIS	GIIPIFGTANYAQKFQG	ALTVRYSSGWYIPPFNYYYYGMDV	I	GGNNIGSKNVH	DDTDRPS	QVWDSSTEEVV	Lambda III
MP2 D11	GFTFTDYYMS	YIDTGSGGTYTKYADSVKG	LWTLGGWYFDL	III	QASQDISNYLN	DASNLET	QQYDNLRLT	Kappa I
MP2 E2	GGIFSSYVIS	GIIPIFGTANYAQKFQG	LPTYGPSY	I	TGSSGSIASNYVQ	EDNQRPS	QSYDSSNVV	Lambda VI
MP2 E4	GYTLTELSIH	GFDPEDGETIYAQKFQG	DLVRGYDFWSGYTPPRDY	I	TGTGGNIADNFVQ	EDDLRPS	QSYDSSSWV	Lambda VI
MP2 E6	GFTFDDYAMH	GISWNSGSIGYADSVKG	TAGGLSAADNPYYYYGMDV	III	KSSQSVLYSSNNKNSLA	WASTRES	HQYYNAPLT	Kappa IV
MP2 E7	GYSFTSYWIS	RIDPSDSYTNYSPSFQG	GGDSSSLHDAFDI	I	SGRSANIGSNYVS	RNNQRPS	ASWDDLLSGWV	Lambda I
MP2 E10	GFTFDDYAMH	GISWSSGSIGYADSVKG	DRVAISGLLYAFDI	III	TRSSGSIASNYVQ	EDNQRPS	QSYDSSNVV	Lambda VI
MP2 F5	GFTLSDYYMDW	RTRNKANGYTTEYAASVKG	DFWSGYYDSGLGSGYFQH	III	GGENIGAKPVH	YDSDRPS	QVWDSSTVV	Lambda III
MP2 G7	GYTLTELSMH	GFDPEDGETIYAQKFQG	DYY	I	TGTSGSIASNYVQ	EDDKRPS	QSYDSSNHRWV	Lambda VI
MP2 G9	GGTFSSYAIS	GIIPIFSTANYAQKFQG	GDLRRDAFDI	I	SGSSSNIEFNTVN	SNNQRPS	AAWDDSLNGYV	Lambda I
MP2 H2	GGTFSSYAIS	GIIPIFGTANYAQKFQG	APSHGSGDY	I	TRSSGSIASNYVQ	EDNQRPS	QSYDSNNRV	Lambda VI
MP2 H5	GYTFTDYYMH	LVDPEDGETIYAEKFQG	DLLTTGDYGMDV	I	RASQGISNYLN	DASNLET	QQFDNLPIT	Kappa I
MP2 H9	GFTFSSYAMH	LISYDGSNKYYADSVKG	VSRFQLSLPFDY	III	RARQSIRDYLN	GASSLQS	QQSYSLPLT	Kappa I
MP1 A3	GYSLTQLAMH	GFDPERGETIYAQQIQG	HPRH	I	TGSSGSIASNFVQ	EDKKRPS	QSFDTSNWV	Lambda VI
MP1 A4	GFTFSSYGMH	VISYDGSNKYYADSVKG	DSGSSWHRYMDV	III	RASQSISSYLN	AASSLQS	QQSYSTPYT	Lambda I
MP1 A5	GYSFTSYWIG	IIYPGDSDTRYSPSFQG	LINGWYFDY	I	TRSGGDIANNFVQ	EDNQRPS	QSYDSTNHWV	Lambda VI
MP1 A6	GYTLTELSMH	GFDPEDGETIYAQKFQG	DTYYGVDY	I	TGSSGSIASNFVQ	EDSQRPS	QSYDSSNWV	Lambda VI
MP1 A7	GFTFSSYWS	NIKQDGSEKYYVDSVKG	DWNGDV	III	RASQSVTTYLA	SASARAT	QQYNSWPLT	Kappa III
MP1 A8	GYSFTSYWIG	IIYPGDSDTRYSPSFQGQ	GMVRGVISSAFDI	I	TRSSGSIASNYVQ	EDNQRPS	QSSDSIIVV	Lambda VI
MP1 A9	GYTFTSYGIS	WISAYNGNTNYAQKLQG	AAFGWFDP	I	SGDRLGDKYAY	QDSKRPS	QAWDSSTAV	Lambda III
MP1 A11	GFTFSSSDMH	AIGTGGDSYYSDSVKG	EGYSYNWNDWYFDL	III	QARQDISNYLN	AASSLQS	QQYNSYPYT	Lambda I
MP1 A12	GHTFTGYYMH	RINPNSGGTNYAQKFQG	QGYGVFYYYYGMDV	I	TGSSGSIASNYVQ	EDNQRPS	QSYDSSNHVV	Lambda VI
MP1 B1	GYTFTGYYMH	WINPNSGGTNYAQKFQG	DGGYCSSTSCHDAFDI	I	TRSSGSIARNYVQ	GDNQRPS	QSYDSNNHVV	Lambda VI
MP1 B3	GYTLTELSMH	GFDPEDGETIYAQKFQG	FASLLPGLNWFDP	I	GGNNIGSKSVH	YDRDRPS	QVWDSSSDHPG	Lambda III
MP1 B2	GFTFSSYAMH	VISYDGSNKYYADSVKG	DVGSNWHHWFDP	III	RASQSISSYLN	AASSLQS	QQSYSTPPSIT	Kappa I
MP1 B4	GGTFSSYTIS	RIIPILGIANYAQKFQG	VTGTVKGAFDI	I	RGDNIGHKLVH	YDNDRPS	QAWDSSHVVF	Lambda III
MP1 B6	GYSFTSYWIG	IIYPGDSDTRYSPSFQG	PILALGAFDI	I	GGNNIGSKSVH	YDSDRPS	QVWDSSSDHPGYV	Lambda III

Table 4.7: Paratope sequences and immunoglobulin subclasses of anti-ADAMTS-5 antibodies.

Clone	Variable Heavy				Variable Light			
	CDR-1	CDR-2	CDR-3	Subclass	CDR-1	CDR-2	CDR-3	Subclass
MP1 B7	GGTFSSYAIS	RIIPILGIANYAQKFQG	PGYSGYDAVTTDYYYYYGMDV	I	SGSSSNIGSHTVD	SDYHRPS	AAWDDSLNGYV	Lambda I
MP1 B9	GFTFSNFGMS	SISGHGYDKFYADSVKG	DSSSNWWGLTRHFDN	III	TRSSGNIASNSVH	EDNQRPS	QSYDSSNLWV	Lambda VI
MP1 B11	GFTFSSYAMH	VISYDGSNKYYADSVKG	DLGSGWWVFDY	III	GGNNIGSKSVH	YDSDRPS	QVWDSSSDHPNVV	Lambda III
MP1 C1	GFTFDDYAMH	GISWNSGSIGYADSVKG	VSSSSWYHWFDP	III	RASQSISSYLN	AASSLQS	QQSYSTPYT	Kappa I
MP1 C8	GYTLTELSMH	GFDPEDGETIYAQKFQG	DYY	I	TGTSGSIASNYVQ	EDDKRPS	QSYDSSNHHWV	Lambda VI
MP1 D1	GFTFSSYAMS	AISGSGGSTYYADSVKG	DQTPLGGFYFDY	III	RASQSISSYLN	AASSLQS	QQSYSTPQT	Kappa I
MP1 D6	GGTFSSYTIS	RIIPILGIANYAQKFQG	GGVVPDTQGQGDDAFDI	I	RSSHSLLYTDGNTYLN	KVSNRDS	MQGRHWSTT	Kappa II
MP1 D9	GFTFSSYSMN	AIFGSGGSTYYADSVKG	DFGYYYGMDV	III	TRSSGSIASNYVQ	EDDQRPS	QSYDSGIVV	Lambda VI
MP1 D10	GYTFTDYGIT	RIIPILGIANYAQKFQG	HGGPRTFDI	I	TRTSGDIANNYVQ	EDSQRPS	QSYDSSNIWV	Lambda VI
MP1 D11	GGTFSSYAIS	GIIPIFGTANYAQKFQG	NSSSWYWPWADAFDI	I	RASQSISRYLN	AASSLQS	QQTYTTPWT	Kappa I
MP1 D12	GFTVSSNYMS	VIYSGGSTYYADSVKG	DSYQATYDFWSGYFPNYYYYGMDV	III	RSSQSLLHSNGYNYLD	LGSNRAS	MQALQTPRT	Kappa II
MP1 E2	GFTFDDYAMH	LISWDGGSTYYADSVKG	PLDIVVVVGVTTGYYGMDV	III	TRSSGSIDSNYVQ	EDNLRPS	QSYDDSNHLV	Lambda VI
MP1 E3	GFTFSSYSMN	SISSSSSYIYYADSVKG	PQEYGDYGMDV	III	TRSSGGIASNYVQ	EDKQRPS	QSFDSTNHWV	Lambda VI
MP1 E4	GGNFRNYAIS	WINTNTGNPTYAQGFTG	DRFEGAIFDY	I	TGSSGSIASNYVQ	EDNQRPS	QSYDSNNRV	Lambda VI
MP1 E5	GFTFDDYAMH	GISWNSGSIGYADSVED	DSADYYYYYMDV	III	RASQSISSYLN	AASSLQS	QQSYSTPRT	Kappa I
MP1 E6	GFTFSSYAMS	AISGSGGSTYYADSVKG	SYSSSVLRWLI	III	RSSQSLVFSDGNTYLN	KVSNRDS	MQGTHWPLT	Kappa II
MP1 E9	DELETION	DELETION	DELETION		RASQGISNRLA	AASSLQS	QHYYNTPPT	Kappa I
MP1 E10	GYSFTNYWIS	RIDPSDSYTNYSPSFQG	QPSPYSIGYYGMDV	I	GNNIGSKNVH	RDSNRPS	QVWDSSTAEVV	Lambda III
MP1 E11	GYSFTSYWIG	IIYPGDSDTNYSPSFQG	LYYGGYVDY	I	GGDNIGGKSVH	DTDRPS	QVWDDSAHAAI	Lambda III
MP1 E12	GGTFSSYAIS	GIIPIFGTANYAQKFQG	DRDLVVANAEALDI	I	RSSQSLVYSDGNTHLQ	KVSKRDS	MQGAHWPRT	Kappa II
MP1 F1	GFSLSTSGMRMN	RIDWDDDKYYSTSLKT	IPPLWWYGMD	II	TRSSGSIASNYVQ	EDNQRPS	QSYDSGNEAV	Lambda VI
MP1 F2	GFTFSSYAMH	VISYDGSNKYYADSVKG	DEWELLGGGAFDI	III	RASQGIGTYLN	AASSLQS	QQSYSTPYT	Kappa I
MP1 F3	GYSFTSYWIG	IIYPGDSDTRYSPSFQG	PRAGTTGGIDY	I	GGNNIGSKNVH	RDSNRPS	QVWDSSTAV	Lambda III
MP1 F4	GGTFSSYAIS	GIIPIFGTANYAQKFQG	GRGYCSGGSCYPDY	I	TRSSGDIASNYVQ	EDKQRPP	QSYHNDNWI	Lambda VI
MP1 F5	GFTFDDYAMH	GISWNSGSIGYADSVKG	GGYSSSWYGDY	III	TRSSGSIASNYVQ	EDDERPS	QSLDGRDWV	Lambda VI
MP1 F7	GGTFSSYTIS	RIIPILGIANYAQKFQG	DKYYGSGSYPFDAFDI	I	TRSSGSIARNYVQ	EDNQRPS	QSYDSSAVV	Lambda VI
MP1 F8	GFTFDDYAMH	GISWNSGSIGYADSVKG	EGGGTWAFDY	III	TRSSGSIASNYVQ	EDNQRPS	QSYGDNTVI	Lambda VI
MP1 F9	GYTFTGYYMH	WINPNSGGTNYAQKFQG	ASGSYHNWFDP	I	TGSRGSIASNYVQ	EDDQRPS	QSYDSLNPWV	Lambda VI
MP1 F10	GFTFDDYAMH	GISWNSGSIGYADSVKG	AQYSSPLSYFDY	III	TRSSGSIASNYVH	EDSQRPS	QSYDSNILV	Lambda VI

Table 4.7: Paratope sequences and immunoglobulin subclasses of anti-ADAMTS-5 antibodies (continued)**.**

Figure 4.15 shows the frequency of different combinations of the V_H, V_L kappa and V_L lambda subfamilies in the selected repertoire. In agreement with previous work (Schofield et al., 2007), we observed a disproportionate occurrence of certain germline families, in particular V_H1, V_H3, V_L kappa I and V_L lambda VI. Since the relative contribution of each germline family was normalised during the construction of the library, the over-representation of certain subfamilies in the selected repertoire may reflect a greater degree of diversity within these families or may be the result of improved expression (Schofield et al., 2007).

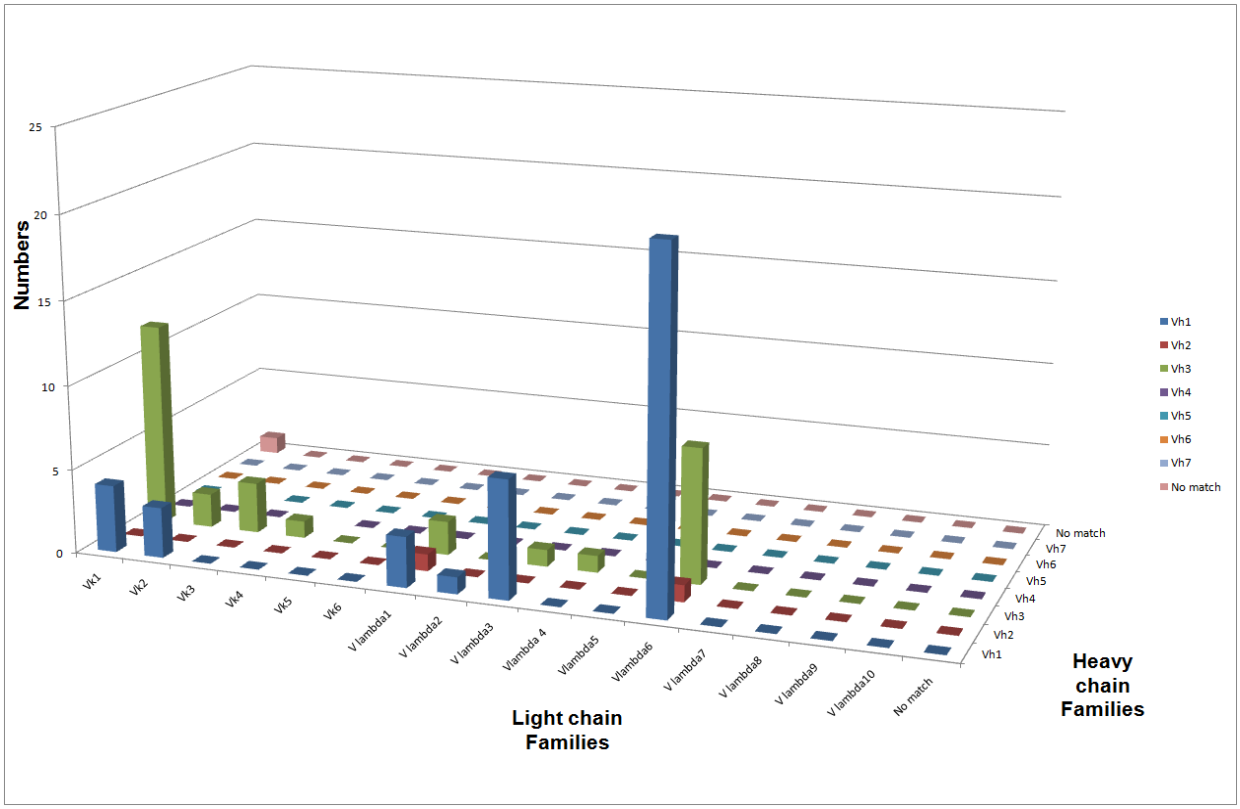

Figure 4.15: Frequency of V_H and V_L germline gene combinations in the selected antibody populations.

4.4.Secondary screening

4.4.1. Expression and purification of scFv-Fc lead antibodies

Theoretically, conditioned medium from HEK cells could be directly assayed for inhibitory potential. However, functional characterisation requires high concentrations of antibody and I found that antibody concentration in the conditioned medium ranged between 10-50 nM **(See Section 4.3.2)**. Moreover, concentration of medium may also lead to concentration of contaminants which can affect functional assays. I then chose to purify individually candidate antibodies. Fifty-four different antibodies were expressed in 25-ml transfection scale and affinity-purified by IMAC **(Figure 4.16)**. Purified scFv-Fc antibodies displayed different sizes on SDS-PAGE, as predicted on the basis of their physical and chemical properties (**Table 4.8**). Most of the sequences of the isolated scFv-Fc antibodies show isoelectric point (pI) values which are slightly acidic (average and mode of pI values were 6.2. and 6.5, respectively). Generally, pI values of IgG1 antibodies are basic (pI values around 8.6) (Tracy, 1982). Although the scFv-Fc antibodies lack the constant regions C_H1 and C_L of IgGs, these do not significantly affect the overall charge of the antibody molecule. Also the presence of the 6x His tag and the acidic triple-FLAG tag sequences (2 6x-His/3xFLAG

tags per dimer) does not dramatically affect the pI of the antibody, thus it is possible that observed acidity may be antigen-selected (i.e. CDRs on scFv-Fc molecules are responsible for the predicted acidity).

One antibody (1E6) was successfully expressed (supernatant was assayed by ELISA against biotinylated ADAMTS-5) but rapidly degraded after purification and was thus discarded from analysis; antibodies 2B3 and 1B9 were discarded due to low expression levels.

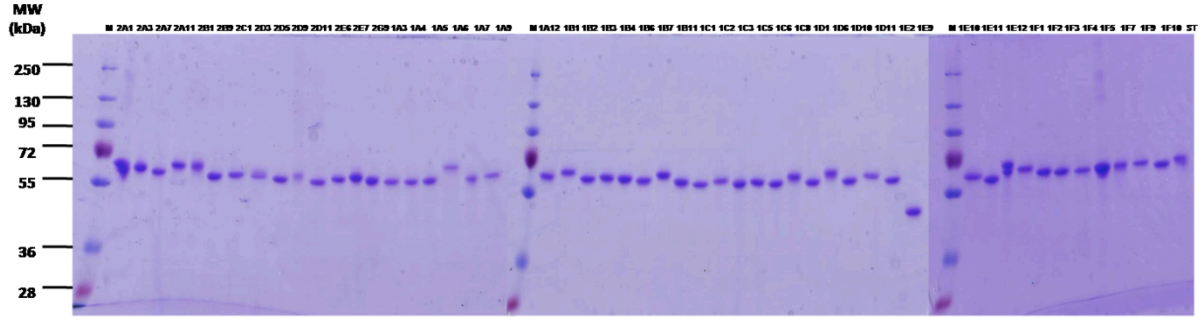

Figure 4.16: **Expression and purification of lead anti-ADAMTS-5 antibodies.** scFv-Fc antibodies were expressed in HEK293-F cells (25 ml) and purified using Ni-NTA resin. After dialysis in TNC buffer, 580 ng of purified protein were loaded under reducing conditions on a 10% Tris-glycine gel and stained with CBB. Variations in size correlate with predicted molecular weight.

Clone 1E9 is a "light chain only" antibody. This antibody is a "domain antibody" or (dAb), and comprises only the V_L chain of an antibody fused to the Fc portion, so the original scFv is half the size of an scFv comprising both the V_H and V_L chains. Individual V_H and V_L domains can exist *in vivo* in some human diseases such as heavy chain disease (isolated heavy chains) (Hendershot et al., 1987; Prelli and Frangione, 1992) and as Bence-Jones proteins in multiple myeloma (isolated light chains) (Hilschmann and Craig, 1965). Camels naturally produce heavy chain dAbs (Ungar-Waron et al., 1987) and these dAbs are usually endowed with excellent biophysical properties such as thermostability (Dumoulin et al., 2002).

Table 4.9 reports the summary of results for phage display selection and mammalian screening.

CLONE	pI	MW	Number of residues	Extinction coefficient cm^{-1} M^{-1} (secreted protein)
2A1	6.20	111415.77	1018	178650
2A3	6.46	112603.26	1020	191710
2A7	7.43	111852.67	1018	177730
2A11	6.02	111539.5	1026	191710
2B1	5.58	110492.53	1010	157790
2B3	6.40	111794.36	1020	177730
2B9	6.46	111017.50	1018	166730
2C1	5.98	112136.48	1028	177730
2D3	6.13	113340.43	1034	172690
2D5	6.49	112056.72	1018	188730
2D9	5.82	113942.67	1044	194690
2D11	6.12	112581.53	1020	191710
2E6	6.20	114565.49	1044	194690
2E7	6.15	111696.08	1026	201790
2G9	6.03	110847.21	1020	165810
1A3	5.95	110426.73	1008	162830
1A4	6.84	111714.11	1018	180710
1A5	5.94	112214.59	1020	210730
1A6	5.33	111174.86	1016	174750
1A7	6.79	109888.43	1000	193770
1A9	6.12	109966.07	1008	199730
1A12	6.36	112965.28	1030	172690
1B1	6.26	113259.61	1034	175000
1B2	6.69	112461.24	1022	185750
1B3	5.70	111521.99	1022	179790
1B4	6.43	110953.84	1016	179790
1B6	6.11	111225.98	1020	196750
1B7	5.86	112837.01	1034	211650
1B9	6.13	113379.26	1032	181850
B11	6.33	111808.39	1022	196625
1C1	6.66	111880.60	1018	196750
1C2	6.02	110606.81	1008	154810
1C3	6.52	111087.89	1014	169710
1C5	6.33	112575.19	1018	171770
1C6	6.66	111179.81	1016	182770
1C8	5.61	110850.80	1010	174750
1D1	6.46	111215.76	1018	166730
1D6	6.67	113518.83	1038	171770
1D10	6.02	111449.93	1020	171770
1D11	6.46	112441.35	1024	204770
1E2	5.83	113984.79	1040	174750
1E6	7.07	112888.02	1028	190790
1E9	6.66	82492.32	740	106660
1E10	6.33	112356.78	1024	202710
1E11	6.23	110559.20	1024	199730
1E12	6.30	113310.57	1032	162830
1F1	5.90	112967.82	1026	190790
1F2	6.37	111874.82	1020	174875
1F3	6.37	110591.13	1014	196750
1F4	6.03	112402.78	1028	177980
1F5	5.95	112156.24	1022	193770
1F7	6.37	114299.14	1048	166730
1F9	6.15	112504.80	1024	199730
1F10	6.06	112016.30	1024	177730

Table 4.8: Predicted physical and chemical properties of lead scFv-Fc antibodies. Molecular weight (MW), extinction coefficient and isoelectric points (pI) were predicted by Expasy Proteomic Server.

Number of selections performed	4
Total number of analysed clones	308
Primary hits	116
Success rate	30%
Confirmed different antibody clones (sequencing)	72
Final diversity	69%
Different antibody clones carried forward for secondary screening	54

Table 4.9: Summary of selections and mammalian screening results.

4.4.2. Investigation of the inhibitory potential of scFv-Fc lead antibodies on ADAMTS-5

Fifty-four (54) purified antibodies were then screened for their ability to inhibit ADAMTS-5 cleavage of a QF peptide and bovine aggrecan **(Table 4.10)**. Although 15 of these antibodies (~29%) were found to inhibit ADAMTS-5 cleavage of QF peptide in a dose-dependent manner, only 9 antibodies (~17%) showed a certain degree of inhibition of bovine aggrecan cleavage **(Table 4.10 and Figures 4.17 and 4.18)**. Some antibodies, like 2A3 and 1B11, showed a modest increase in aggrecanase activity (2-2.5 folds) **(Figure 4.18 D)** which was not matched by an equivalent increase in peptidolytic activity (**Figure 4.17 D**).

Antibodies 2D3, 2D5 and 2D11 were the most potent in the QF peptide cleavage assay and retained their activity when tested for inhibition of aggrecan cleavage at the $Glu^{392}\downarrow^{393}Ala$ site. On the other hand, antibodies 2B9 and 2D9 inhibited aggrecan cleavage in a dose-dependent manner although they did not show any inhibitory potential in the QF peptide cleavage assay. For comparison, 10 nM N-terminal domain of TIMP-3 (N-TIMP-3) was sufficient to completely block ADAMTS-5 activity in both assay **(Figures 4.17 and 4.18)**.

We observed a constant increase in $K_{i\ app}$ values (about 10-folds) in the aggrecan digestion assay compared with the QF peptide cleavage assay **(Table 4.10)**. A possible explanation for this phenomenon may be the different K_m of ADAMTS-5 for these two substrates. The K_m for aggrecanase cleavage at $Glu^{392}\downarrow^{393}Ala$ in the bovine aggrecan digestion assay was estimated to be around 4 μM **(Figure 4.19)**. The estimated K_m value for aggrecan cleavage is much lower than the estimated K_m calculated for ADAMTS-5 cleavage of the Abz-TESE~SRGAIY-Dpa-KK peptide substrate (76 μM) (Troeberg et al., 2009).

Clone	Inhibition ($K_{i\ app}$ nM)		Clone	Inhibition ($K_{i\ app}$ nM)	
	QF peptide	Aggrecan ($Glu^{392}\downarrow^{393}Ala$ cleavage)		QF peptide	Aggrecan ($Glu^{392}\downarrow^{393}Ala$ cleavage)
2A1	120	NI	1B7	300	NI
2A3	NI	NI	1B9	ND	ND
2A7	530	NI	1B11	NI	NI
2A11	150	NI	1C1	NI	NI
2B1	NI	NI	1C2	NI	NI
2B3	ND	ND	1C3	NI	NI
2B9	NI	300	1C5	NI	NI
2C1	NI	NI	1C6	500	NI
2D3	5	30	1C8	NI	NI
2D5	23	300	1D1	NI	NI
2D9	NI	400	1D6	1400	NI
2D11	60	100	1D10	NI	NI
2E6	NI	NI	1D11	NI	NI
2E7	250	NI	1E2	NI	NI
2G9	NI	NI	1E6	ND	ND
1A3	NI	NI	1E9	1000	NI
1A4	1040	NI	1E10	1800	NI
1A5	NI	>500	1E11	NI	NI
1A6	NI	>500	1E12	NI	>500
1A7	NI	>500	1F1	NI	NI
1A9	NI	NI	1F2	NI	NI
1A12	NI	NI	1F3	NI	NI
1B1	NI	NI	1F4	NI	NI
1B2	850	NI	1F5	NI	NI
1B3	NI	NI	1F7	NI	NI
1B4	NI	NI	1F9	930	>500
1B6	NI	NI	1F10	NI	NI

Table 4.10: Inhibition data of scFv-Fc antibodies. Fifty-four antibodies were selected for expression in 25 ml-scale transfection, purified by IMAC and tested for their ability to inhibit ADAMTS-5 cleavage of both a QF-peptide and bovine aggrecan. NI, not inhibiting at 500 nM concentration; ND, not determined (failed expression or stability issues).

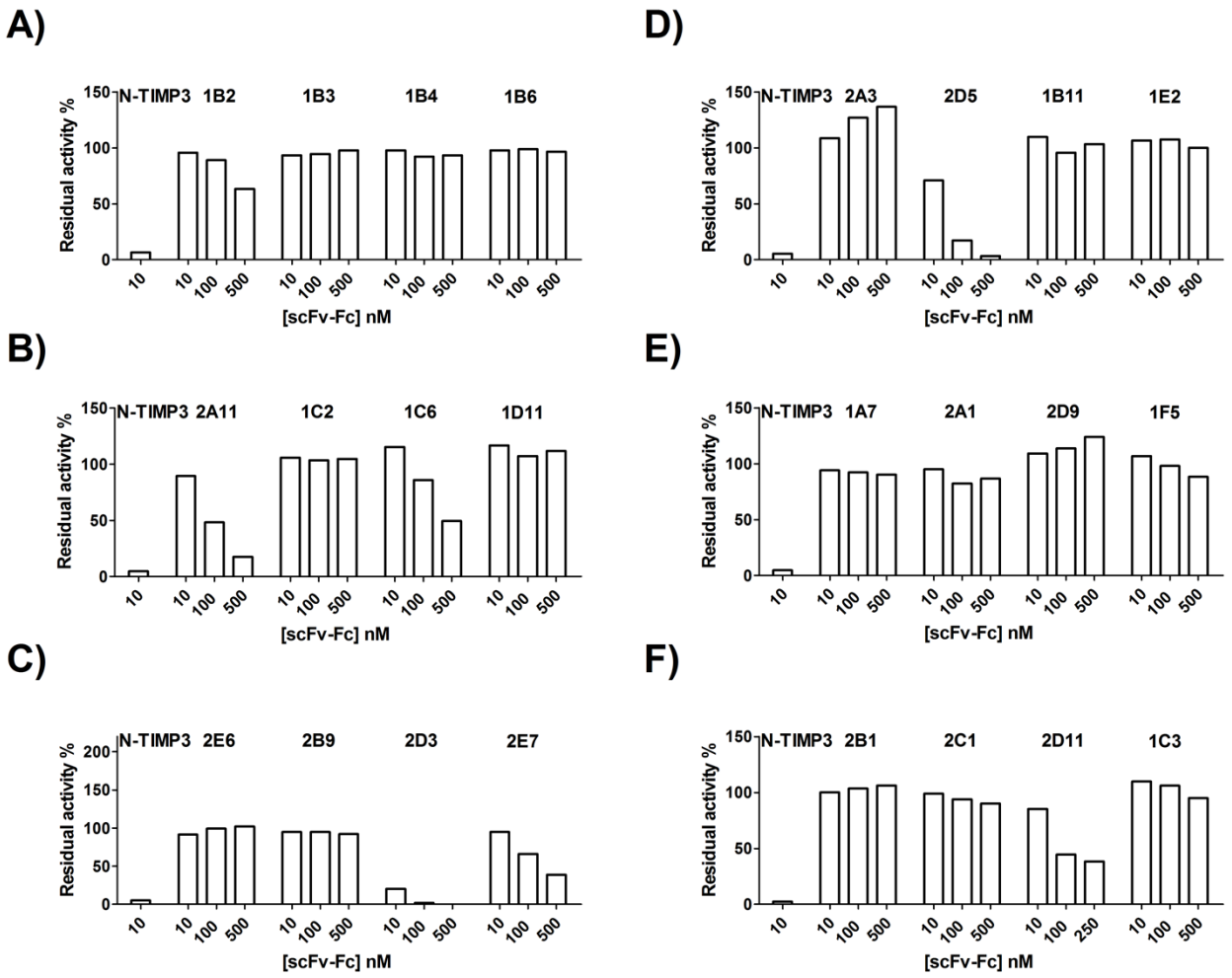

Figure 4.17: Inhibition of QF peptide cleavage by scFv-Fc antibodies. ADAMTS5-2 at a concentration of 5 nM was incubated alone or with N- TIMP-3 (10 nM) and different concentrations of scFv-Fc antibodies (10, 100 and 500 nM) for 2 h. Residual activities against Abz-TESE~SRGAIY-Dpa-KK (1 h, 37°C) were determined.

The estimated K_m value for aggrecan cleavage may reflect additional interactions which arise between aggrecan and enzyme exosites, such as TS-1 and Sp domains. On the other hand, the higher K_m value for the peptide substrate appear to reflect a much weaker interaction with the active site of ADAMTS-5. As a result, inhibition of ADAMTS-5 by scFv-Fc antibodies is affected to a different degree by the presence of the two substrates, with $K_{i\ app}$ values reflecting the relative affinity between antibody, enzyme and substrate.

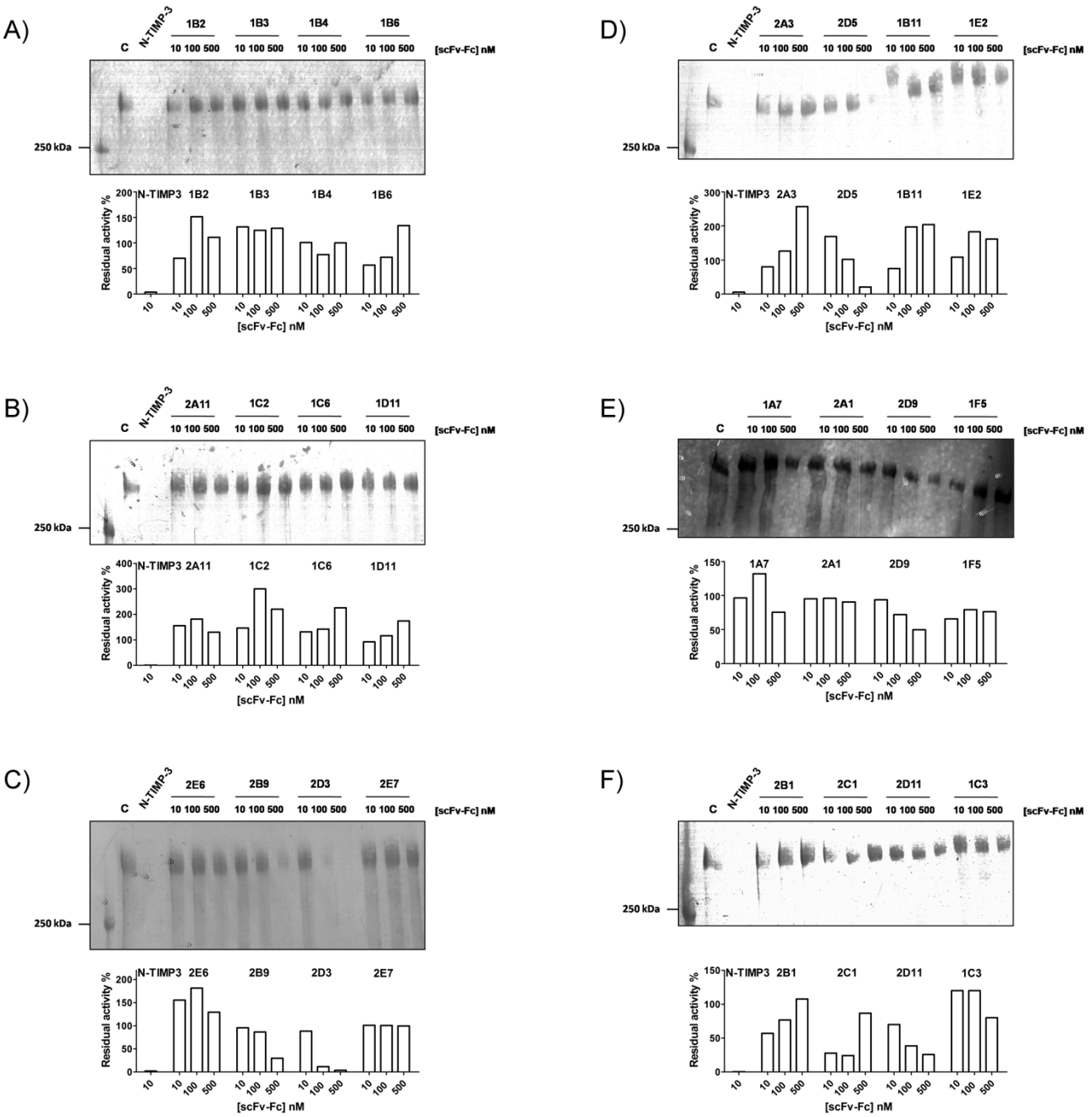

Figure 4.18: Inhibition of aggrecan cleavage at the Glu^{392}↓^{393}Ala by scFv-Fc antibodies. ADAMTS5-2 at a concentration of 0.5 nM was incubated alone (C, control) or with N- TIMP-3 (10 nM) and different concentrations of scFv-Fc antibodies (10, 100 and 500 nM) for 2 h. Bovine aggregan (50 µg) was added and the mixture was incubated for 2 h at 37°C. The reactions were stopped with 50 mM EDTA and the product was deglycosylated overnight with chondroitinase ABC and keratanase and analysed by Western blot for ARGSV-containing fragments using BC3 mAb. Representative Western blots and densitometric analysis are shown.

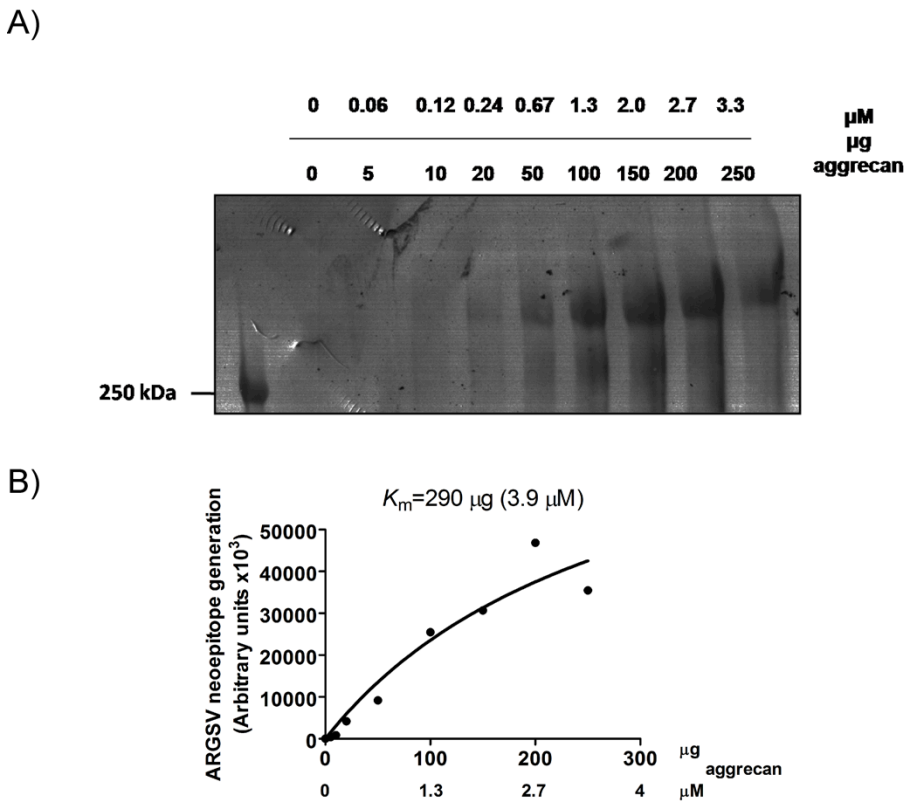

Figure 4.19: Estimate of Michaelis-Menten constant for bovine aggrecan cleavage by ADAMTS-5. ADAMTS5-2 was incubated with bovine aggregan (0-250 µg) for 2 h at 37°C. The reactions were stopped with 50 mM EDTA and the products were deglycosylated overnight with chondroitinase ABC and keratanase and analysed by Western blot for ARGSV-containing fragments using BC3 mAb **(A)**. Membranes were scanned with a BioRad GS710 calibrated imaging densitometer and data were fitted to the Michaelis Menten equation **(B)**.

4.4.3. Recognition of ADAMTS-5 deletion mutants on Western blot

To evaluate how denatured forms are recognised by scFv-Fc antibodies, ADAMTS5-2 was subjected either to reduction/heat denaturation or non-reducing conditions followed by SDS PAGE and immunoblotting with isolated scFv-Fc antibodies **(Figure 4.20)**. Bands were visualised with an AP-conjugated anti-human IgG antibody. Out of 51 different antibodies tested, 47 showed binding to ADAMTS-5 under non-reducing conditions **(Table 4.11)**. Just one antibody (1A6) was able to recognise ADAMTS5-2 in both reducing and non-reducing conditions, whereas all the other scFv-Fc antibodies recognised ADAMTS5-2 only in non-reducing conditions. Thus scFv-Fc performed well in ELISA and in Western blotting, despite folded antigen having been used for the selection, suggesting that a mixture of linear and conformational epitopes are recognised by these antibodies. Alternatively, a positive reaction on Western blot can also be achieved by non-linear epitopes where reacting residues are in relatively close proximity.

scFv-Fc antibodies which scored as positive in Western blots were successively tested for their ability to recognise different deletion mutants of ADAMTS-5 **(Table 4.11 and Figure 4.20)**. This screening allowed us to map the main epitope of these antibodies. Representative blots for

antibodies recognising the different ADAMTS-5 domains are shown in **Figure 4.21** and **Figure 4.21 A** reports the domain composition of different forms of ADAMTS-5. As a comparison, membranes were probed with anti-FLAG mAb and anti-Cat polyclonal antibody. We can exclude that the anti-ADAMTS-5 scFv-Fc antibodies recognise the FLAG tag on ADAMTS-5 deletion mutants for two main reasons. First, these antibodies showed differential binding on equimolar concentrations of FLAG-tagged ADAMTS-5 deletion mutants **(Figure 4.21)**. Moreover, as mentioned before, since the scFv-Fc antibodies also contain a triple-FLAG tag, antibodies directed against the FLAG sequence would aggregate.

Under non-reducing conditions, all ADAMTS-5 deletion forms migrated at a molecular weight which was in agreement with the predicted molecular weight: ~70 kDa for ADAMTS5-2, ~50 kDa for ADAMTS5-3, ~40 kDa for ADAMTS5-4. ADAMTS5-5 is present as two distinct bands between 30 and 36 kDa that were recognised by the anti-FLAG M2, the polyclonal rabbit anti-Cat and by anti-Cat/Dis scFv-Fc antibodies. It has been shown (Gendron et al., 2007) that treatment of this deletion form of ADAMTS-5 with N-glycosidase F results in a single band, indicating that the higher molecular weight band is a N-glycosylated form of ADAMTS5-5 (**See Table 3.1**). Both forms as well as intermediate bands were recognised by anti-Cat/Dis antibodies as well as anti-FLAG and polyclonal rabbit anti-Cat antibodies. In total, 8 antibodies recognised the Sp domain, 8 antibodies the CysR domain, 19 antibodies the TS-1 domain and 12 antibodies the Cat/Dis domain (**Figure 4.22**). Domain mapping of lead antibodies 2A11, 2B9, 2D3, 2D5, and 2D11 is discussed in **Chapter 5**.

Clone	ADAMTS5-2		5-3	5-4	5-5	Domain
	Reducing	Non-reducing	Non-reducing	Non-reducing	Non-reducing	
2A1	-	+	+	+	Faint	TS-1
2A3	-	+	+	+	-	TS-1
2A7	-	-				-
2A11	-	+	+	+	+	Cat/Dis*
2B1	-	+	+	+	+	Cat/Dis
2B9	Faint	+	+	+	-	Sp*
2C1	-	+	+	+	-	TS-1
2D3	-	+	+	+	+	Cat/Dis*
2D5	-	+	+	+	-	Cat/Dis*
2D9	-	+	+	+	-	TS-1
2D11	-	+	+	+	+	Cat/Dis*
2E6	-	+	+	+	-	TS-1
2E7	-	+	+	+	+	Cat/Dis
2G9	-	+	+	-	-	CysR
1A3	-	+	+	+	+	Cat/Dis
1A4	-	+	+	-	-	CysR
1A5	-	+	+	-	-	CysR
1A6	+	+	+	-	-	TS-1
1A7		+	+	-	-	CysR
1A9	-	+	+	-	-	CysR
1A12	-	+	+	-	-	CysR
1B1	-	+	-	-	-	Sp
1B2	-	+	+	+	-	TS-1
1B3	-	+	+	+	-	TS-1
1B4	-	+	-	-	-	Sp
1B6	-	+	-	-	-	Sp
1B7	-	+	+	+	+	Cat/Dis
1B11	-	+	-	-	-	Sp
1C1	-	Faint				-
1C2	-	+	+	+	-	TS-1
1C3	-	+	+	+	-	TS-1
1C5	-	+	+	-	-	CysR
1C6	-	+	+	+	-	TS-1
1C8	-	+	+	+	+	Cat/Dis
1D1	-	+	+	+	-	TS-1
1D6	-	-				-
1D10	-	+	+	+	+	Cat/Dis
1D11	-	+	+	+	-	TS-1
1E2	-	+	+	+	-	TS-1
1E9	-	+	+	+	-	Cat/Dis
1E10	-	+	+	+	-	TS-1
1E11	-	+	+	+	-	TS-1
1E12	-	+	+	+	-	TS-1
1F1	Faint	+	-	-	-	Sp
1F2	-	+	-	-	-	Sp
1F3	-	+	+	+	+	Cat/Dis
1F4	Faint	+	-	-	-	Sp
1F5	-	+	+	-	-	CysR
1F7	-	Faint				-
1F9	-	+	+	+	-	TS-1
1F10	-	+	+	+	-	TS-1

Table 4.11: Summary of results obtained by Western blot analysis of ADAMTS-5 deletion mutants using scFv-Fc antibodies. Plus signs denotes positive reactivity toward the respective ADAMTS-5 form; minus sign, no signal detected Antibodies 2A11, 2B9, 2D3, 2D5 and 2D11 (*) were characterised by SPR (See Section 5.4).

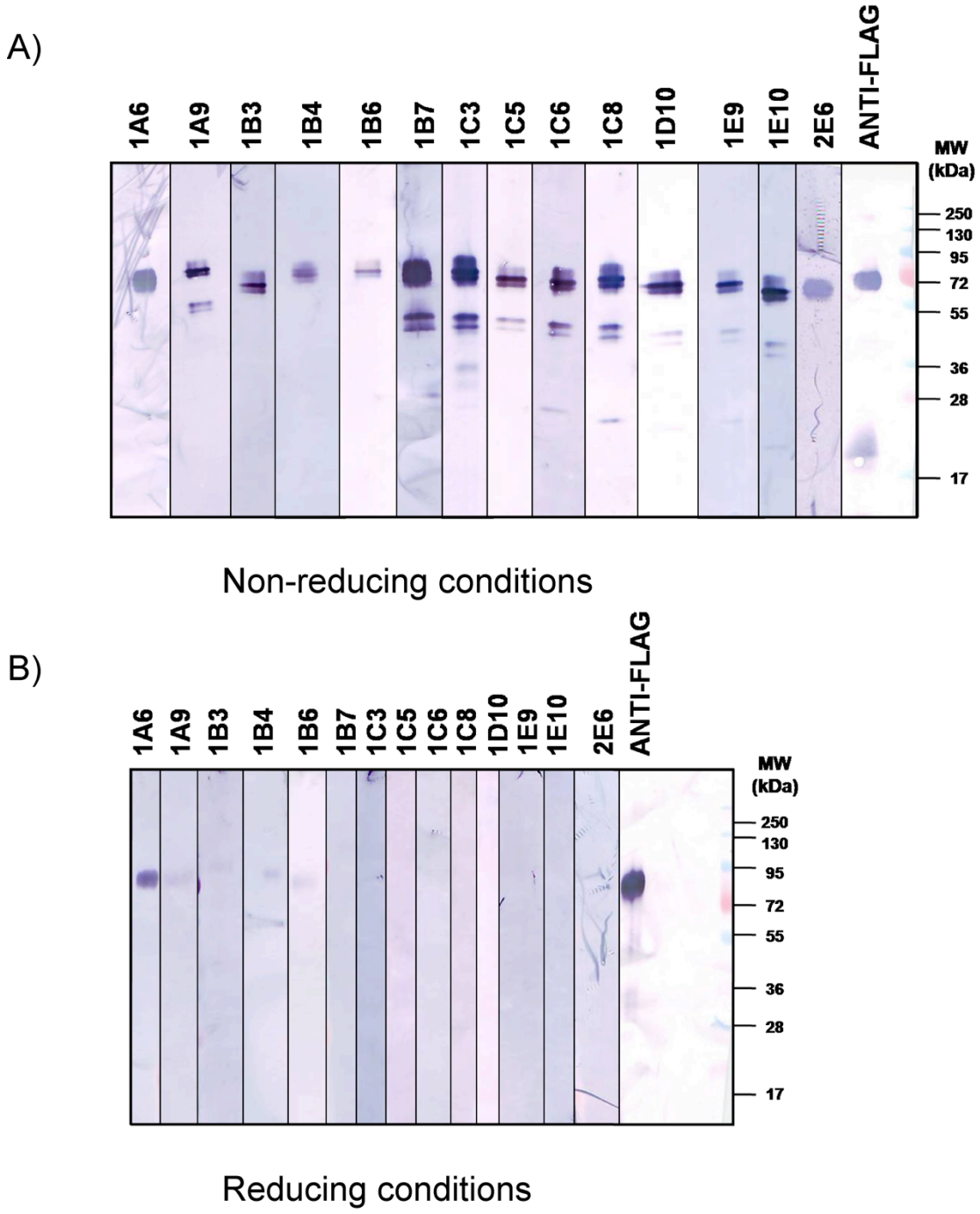

Figure 4.20: Immunoblots with anti-ADAMT-5 scFv-Fc antibodies. ADAMTS5-2 (115 ng) was run on a 10% SDS-PAGE gel under non-reducing **(A)** and reducing **(B)** conditions. Under reducing conditions the samples were boiled at 90°C for 5 minutes in the presence of β-mercaptoethanol. scFv-Fc antibodies were used to stain the membranes and signal was detected with AP-conjugated anti-human IgG. Anti-FLAG M2 antibody was used as a positive control.

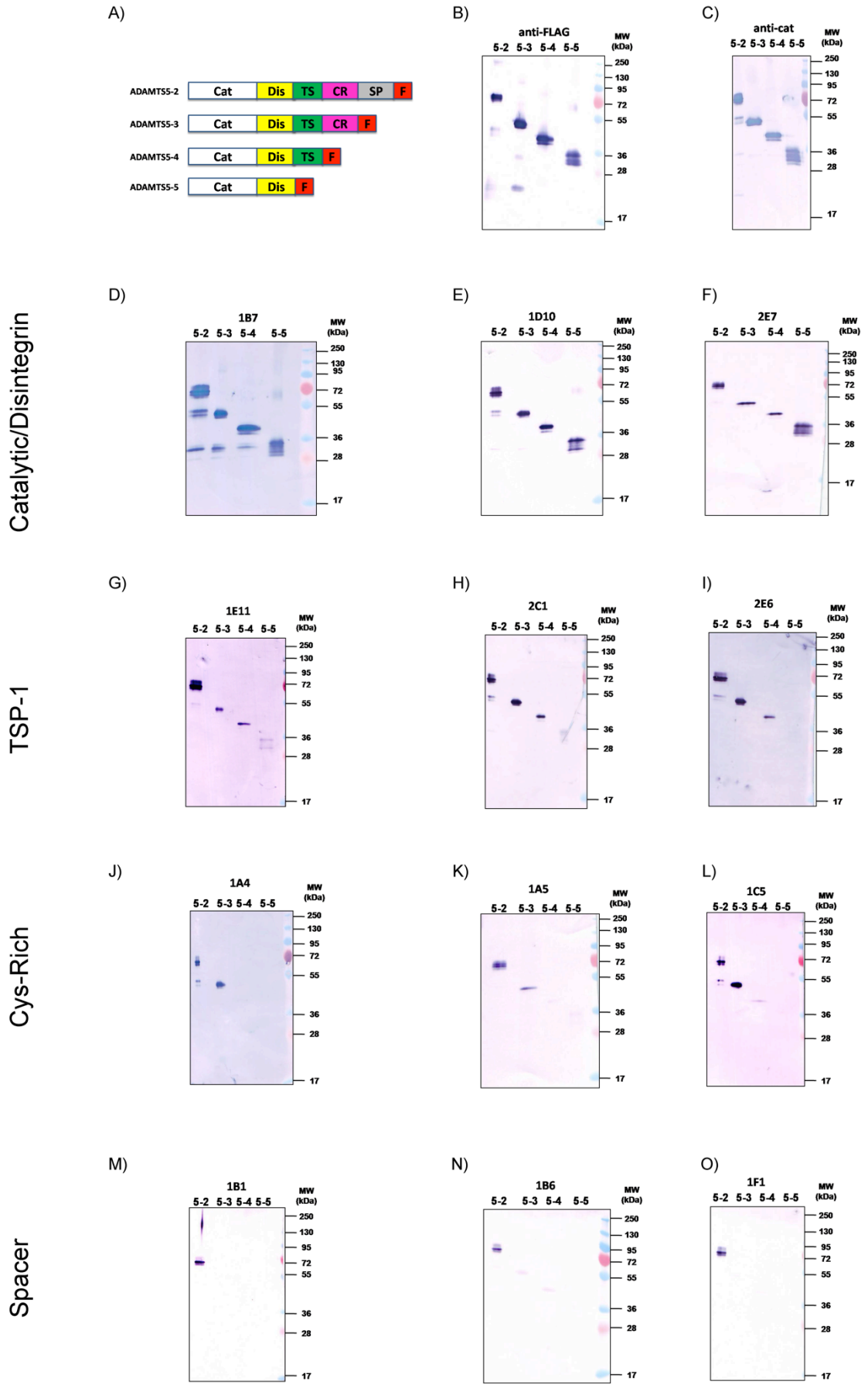
A)
ADAMTS5-2
Cat
Dis
TS
CR
SP
F
ADAMTS5-3
Cat
Dis
TS
CR
F
ADAMTS5-4
Cat
Dis
TS
F
ADAMTS5-5
Cat
Dis
F
B)
anti-FLAG
C)
anti-cat
5-2 5-3 5-4 5-5
MW (kDa)
250
130
95
72
55
36
28
17
Catalytic/Disintegrin
D)
1B7
E)
1D10
F)
2E7
TSP-1
G)
1E11
H)
2C1
I)
2E6
Cys-Rich
J)
1A4
K)
1A5
L)
1C5
Spacer
M)
1B1
N)
1B6
O)
1F1

Figure 4.21 (page 126). Immunoblots with anti-ADAMTS-5 scFv-Fc antibodies. Each purified ADAMTS-5 deletion mutant (115 ng) was run on a 10% SDS-PAGE gel under non-reducing conditions. **A)** Domain structure of ADAMTS-5 deletion forms **B)** mouse monoclonal anti-FLAG M2 or rabbit polyclonal anti-cat antibodies were used to stain the membranes. **J-O)**: scFv-Fc antibodies were used to stain the membranes and signal was detected with AP-conjugated anti-human IgG.

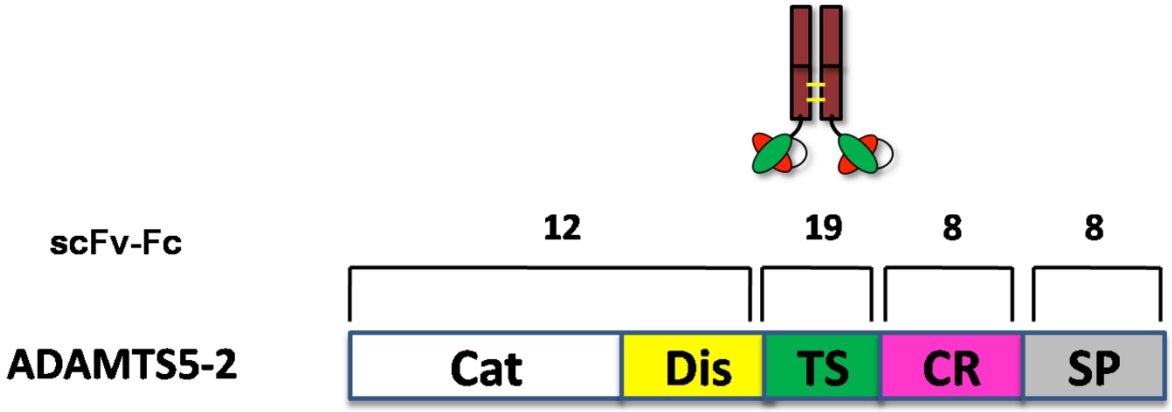

Figure 4.22: Summary of domain mapping results for scFv-Fc antibodies. On top of a schematic representation of ADAMTS5-2, the number of antibodies recognizing each domain is reported. See Table 4.11 for details.

4.5. Discussion

The purpose of a phage display selection is to isolate a small subset of ligands able to bind a desired antigen from huge (diversity ~10^{10} clones) libraries. Purified ADAMTS5-2 was exposed to a human naïve scFv antibody phage-display library for two rounds of solution-phase selections (Schofield et al., 2007). From a therapeutic point of view, the use of a human library should dramatically reduce the potential for immunogenicity in humans. On the other hand, mouse antibodies may generate human anti-mouse antibodies which affect clinical outcomes by neutralising therapeutic antibodies, increasing rates of clearance and, ultimately, reducing efficacy (Pendley et al., 2003).

Ligands selected from phage-display libraries can interact specifically with distinct conformations of their target antigen. One way to drive the selection against other epitopes on the antigen is the epitope masking selection which exploits competitive blocking of epitopes on the antigen using antibodies or ligands (Ditzel et al., 1995). In our case exposure of ADAMTS-5 to the library was carried out both in the presence and in the absence of a 100-fold excess of the broad-spectrum metalloprotease inhibitor GM6001 (Grobelny et al., 1992). The presence of the inhibitor can stabilise ADAMTS-5 to a particular conformation. Another effect that GM6001 may have on phage display selection is competition with phages sharing epitopes deep in the active site cleft. Although it is possible that some molecules of ADAMTS-5 are not blocked by GM6001 under these conditions, the presence of the competitor for two rounds of selection should bias the selection against this kind of antibodies. This strategy has been used before. For example, Nizak et al. (2003),

used a GTP-locked form of inactive mutant of Rab6, a small GTPase, as a target antigen to select conformation-specific antibody fragments by phage display. Gao et al. (2009) reported a strategy for identifying conformation-specific antibodies by using small molecule ligands to lock target proteins into the conformation of interest. By this approach, two different Fabs were identified, each one recognising a distinct conformation of caspase-1, induced by an irreversible active site and an allosteric inhibitor, respectively (Gao et al., 2009). In this case, antibodies binding to the catalytically competent conformer were found to increase the catalytic activity of caspase-1, whereas antibodies binding to the inactive conformer acted as inhibitors (Gao et al., 2009). Ecotin, a macromolecular inhibitor specific for trypsin-fold serine proteases has been used during phage display selection to isolate potent allosteric inhibitors of serine protease MTSP1 which did not bind to the active site (Sun et al., 2003). Addition of a small molecule active-site inhibitor has been shown to be successful in isolating an antibody with preference for TNF-α converting enzyme (TACE) ectodomain over the isolated Cat domain (Tape et al., 2011).

For primary screening, selected libraries are usually subcloned into a vector suitable for soluble expression of scFv by bacterial cells. Although bacterial expression is sufficient for most purposes, antibody fragments expressed in bacteria show several limits such as stability, lack of glycosylation patterns, and poor pharmacokinetics *in vivo*. Here we chose transient transfection of mammalian cells grown in liquid culture to screen libraries selected by phage display, using the cationic polymer PEI as a vehicle for the introduction of plasmid DNA (Boussif et al., 1995; Durocher et al., 2002). We therefore subcloned selected libraries in pBIOCAM5 vector for screening in HEK293-F suspension cells where antibodies were expressed as fusion proteins with the crystallizable fragment of human IgG1 (scFv-C_H2-C_H3 dimers or scFv-Fc) (Chapple et al, 2006). In parallel, the same eluted polyclonal scFv populations were subcloned into pSANG10-3F for expression of soluble scFv (Martin et al., 2006) to compare success rates (i.e. the number of positive clones over the total number of screened clones). It was evident that the mammalian system gave a superior performance in terms of success rate (~30% vs ~15%), likely due to a combination of higher yield and an avidity effect for the presence of two antigen-binding sites on an scFv-Fc molecule. The primary screening was therefore performed using the mammalian expression system. A similar strategy has been recently reported to isolate antibodies against CD9 by cell panning (Yoon et al., 2012), although in our case we took advantage of high-throughput DNA purification and transfection to screen a number of clones (308) comparable with those screened when using *E. coli* cells expressing scFvs.

We were able to exclude general cross-reactivity and non-specific binding of this antibody format since randomly-chosen clones did not recognise ADAMTS-4 (aggrecanase-1) in the same

ELISA setting **(Figure 4.14)**. Three-hundred-three clones from different selections were ELISA-screened in HEK293-F cells (**Figure 4.13**); out of 116 hits, 72 different clones were identified after sequencing; among them, 54 were chosen to be expressed in 25-ml transfection scale and affinity-purified by IMAC for functional characterisation (**Table 4.9**).

Antibodies 2D3, 2D5 and 2D11 were the most potent in the QF peptide cleavage assay and retained their activity when tested for inhibition of aggrecan cleavage at the $Glu^{392}\downarrow^{393}Ala$ site. On the other hand, antibodies 2B9 and 2D9 inhibited aggrecan cleavage in a dose-dependent manner although they did not show any inhibitory potential in the QF peptide cleavage assay. These data highlight the importance of tailoring the screening strategy to meet the conditions as close as possible to those in *vivo*. To our knowledge, this is the first report of the usage of a native macromolecular substrate to screen a relatively high number of inhibitors (54 antibodies tested in functional screening). Moreover, the parallel use of QF peptide allowed the identification of both active-site directed and exosite-directed antibodies. Characterisation of antibodies 2A11, 2B9, 2D3, 2D5, 2D11 is reported in **Chapter 5**.

In parallel to inhibitory screening, anti-ADAMTS-5 antibodies were tested for their ability to bind to denatured ADAMTS-5 on Western blots. Forty-seven antibodies were able to recognise ADAMTS-5 after SDS-PAGE under non-reducing conditions. The fact that just one antibody out of 47 was able to recognise ADAMTS-5 under both reducing and non-reducing conditions suggests a critical role for disulphide bonds in maintaining the epitopes of anti-ADAMTS-5 antibodies. Since all the analysed scFv-Fc antibodies were screened for binding to native ADAMTS-5 on a liquid-phase ELISA, they may recognise a mixture of linear/conformational epitopes. Antibodies such as 1E11 (**Figure 4.21 G**) or 2E6 (**Figure 4.21 I**) bound strongly to ADAMTS5-2 but not to ADAMTS5-3 or 5-4 on Western Blot. This may indicate that the TS-1 domain has a different exposure (at least in the presence of SDS under non-reducing conditions) in ADAMTS5-2 compared to ADAMTS5-3 or 5-4. The same was observed for antibodies such as 1A5 **(Figure 4.21 K**) which bound more strongly to ADAMTS5-2 compared to ADAMTS5-3, indicating different conformations of the CysR domain under these conditions. On the other hand, antibodies such as 1A4 (**Figure 4.21 J**) or 1C5 (**Figure 4.21 L**) react similarly with ADAMTS5-2 and 5-3, thus the epitope recognised by these antibodies likely is not conformational. Domain mapping using different deletion mutants of ADAMTS-5 allowed the identification of antibodies targeting different domains of this enzyme. These antibodies may represent important tools and useful in-house reagents to deepen our knowledge of ADAMTS-5 biology (**See Section 6.2**).

Chapter 5
Characterisation of scFv-Fc antibodies

5.1 Introduction

As was discussed in Chapter 4, antibodies 2B9, 2D3, 2D5, and 2D11 were identified from a secondary screening as inhibitors of ADAMTS-5. In particular, antibodies 2D3, 2D5 and 2D11 inhibited ADAMTS-5 cleavage of both a QF peptide substrate and aggrecan, whereas antibody 2B9 inhibited cleavage only of the macromolecular substrate. We therefore hypothesised that antibodies 2D3, 2D5, and 2D11 interfere directly with the catalytic activity of ADAMTS-5, whereas 2B9 may represent an allosteric (exosite) inhibitor.

Our first aim was then the characterisation of these antibodies and the mapping of the binding epitope. Inhibition of lead scFv-Fc antibodies was tested against different deletion mutants of ADAMTS-5 and interactions between scFv-Fc antibodies and ADAMTS-5 were studied by surface plasmon resonance (SPR) studies. I also examined the extent of *in vitro* inhibition of mouse ADAMTS-5, since this information is useful to establish whether these antibodies can be tested in *in vivo* models of OA. Moreover, we were interested in the effects that GM6001 and TIMP-3, a small molecule and an endogenous inhibitor of ADAMTS-5, respectively, exert on the inhibitory potency of lead scFv-Fc antibodies. Finally, the ability of lead antibodies to inhibit aggrecan degradation was tested in an *ex vivo* model of OA using both porcine articular cartilage explants and human knee cartilage explants co-stimulated with IL-1α and OSM.

5.2. Inhibition of ADAMTS-5 cleavage of QF peptide

scFv-Fc antibodies 2A11, 2D3, 2D5, and 2D11 showed the ability to inhibit cleavage of a QF peptide by ADAMTS5-2 with different potency ($K_{i\ app}$ values ranging from 2.8 nM for 2D3 to 180 nM for 2A11). (**Table 5.1 and Figure 5.1**). Inhibitory activity was also tested against other truncated forms of ADAMTS-5 (**Figure 5.1 and Table 5.1**). The smallest fragment of ADAMTS-5 with detectable proteolytic activity consists of Cat/Dis domains (Gendron et al., 2007) and crystallographic data shows that these two domains are structurally integrated (Mosyak et al., 2008). For this reason, ADAMTS5-5 (comprising Cat/Dis domains) was used as a representative of the Cat domain.

Clone	TS5-2	TS5-3	TS5-4	TS5-5	Mouse TS5-2	TS4-2	MMP-1 Cat	MMP-13	MT1-MMP
2A11	180 ± 38	Nd	nd	150 ± 10	360 ± 50	ni	nd	nd	nd
2B9	ni	Ni	ni	ni	ni	ni	nd	nd	nd
2D3	2.5 ± 0.6	3.2 ± 0.2	5.5 ± 0.3	8.3 ± 0.8	14 ± 2	ni	ni	ni	ni
2D5	20 ± 5	37 ± 2.5	35 ± 2.6	53 ± 2.8	180 ± 30	ni	ni	ni	ni
2D11	70 ± 8	79 ± 16	73 ± 11	130 ± 31	590 ± 320	ni	ni	ni	ni

Table 5.1: $K_{i\ app}$ values (nM) for inhibition of ADAMTS-5, -4 and MMPs by lead antibodies. The QF substrates used were Abz-TESE~SRGAIY-Dpa-KK (ADAMTS-5), FAM-AE~LQGRPISIAK-TAMRA (ADAMTS-4) and Mca-KPLGL-Dpa-AR (MMPs); ni, not inhibiting at 500 nM; nd, not determined. Data are $K_{i\ app}$ values of the mean data ± S.D. (n = 3-6).

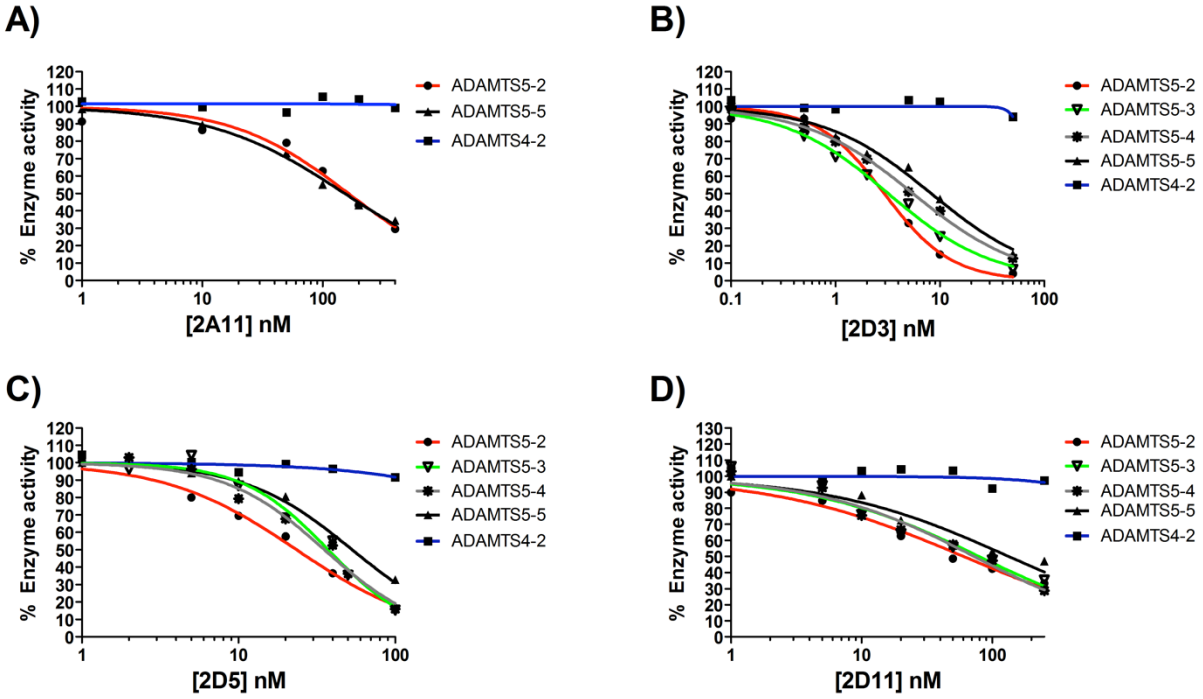

Figure 5.1: Inhibition of ADAMTS-5 and ADAMTS-4 by scFv-Fc antibodies 2A11 (A), 2D3 (B), 2D5 (C) and 2D11 (D). Enzyme (5 nM) was incubated with different concentrations of scFv-Fc antibodies for 2 h and residual activities against Abz-TESE~SRGAIY-Dpa-KK (ADAMTS-5, 1 h, 37°C) and FAM-AE~LQGRPISIAK-TAMRA (ADAMTS-4, 15 min, 37°C) were determined. For 2D3, 0.5 nM of different deletion forms of ADAMTS-5 were incubated with substrate for 18 h at 37°C before end-point reading. Representative curves are shown.

Figure 5.2 reports a schematic representation of active forms of FLAG-tagged ADAMTS-5 and ADAMTS-4 deletion mutants used to characterise scFv-Fc antibodies.

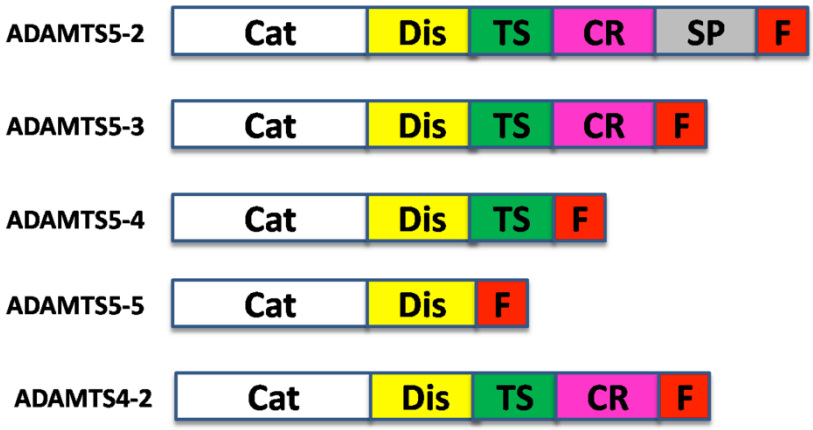

Figure 5.2: Domain structure and nomenclature of active ADAMTS-5 and ADAMTS-4 deletion mutants. F, FLAG tag.

With the exception of 2A11, all the lead antibodies showed a 2-3-fold increase in $K_{i\ app}$ against ADAMTS5-5, with values ranging from 8 nM for 2D3 to 150 nM for 2A11. For 2D3 a ~2-fold increase in $K_{i\ app}$ was observed against the forms of ADAMTS-5 lacking the CysR domain (ADAMTS5-4 and 5-5) ($K_{i\ app\ 5\text{-}4}$ 5.5 ± 0.3 nM; $K_{i\ app\ 5\text{-}5}$ 8.3 ± 0.8 nM). Similarly, for 2D5 a ~2-fold increase in $K_{i\ app}$ was observed after removal of the Sp domain ($K_{i\ app\ 5\text{-}2}$ 20 ± 5 nM; $K_{i\ app\ 5\text{-}3}$ 37 ± 2.5 nM) and for 2D11 after removal of the TS-1 domain ($K_{i\ app\ 5\text{-}4}$ 73 ± 11 nM; $K_{i\ app\ 5\text{-}5}$ 130 ± 31 nM). Thus, although these antibodies recognise the Cat/Dis domain of ADAMTS-5, they establish additional interactions with non-catalytic domains such as CysR (2D3), Sp (2D5), and TS-1 (2D11). It is also possible that these domains do not interact directly with the antibodies but positively modify the structure of their binding site(s).

Lead scFv-Fc antibodies were tested for their ability to inhibit ADAMTS-4. Unfortunately, expression of human recombinant full-length ADAMTS-4 (ADAMTS4-1), which most resembles ADAMTS5-2 (38% identity), is very poor (Gendron et al., 2007), thus a form lacking the Sp domain was tested for inhibition. Moreover, since all four antibodies are able to inhibit ADAMTS5-5, the presence of the Sp domain is not necessary for interaction with ADAMTS-5 (**Table 5.1**). Antibodies 2A11, 2D3, 2D5 and 2D11 did not inhibit cleavage of a QF-peptide by ADAMTS4-2 at 500 nM concentration. Lead scFv-Fc antibodies did not inhibit MMP-1 (Cat domain), -13, and -14, thus being selective for ADAMTS-5 over other members of the MA family of metallopeptidases.

5.3. Inhibition of mouse ADAMTS-5

In order to assess therapeutic potential for future *in vivo* applications, the ability of antibodies 2A11, 2D3, 2D5 and 2D11 to inhibit mouse ADAMTS-5 was investigated using both the QF peptide substrate and bovine aggrecan. When the QF peptide substrate was used, all four

antibodies showed the ability to inhibit the murine version of ADAMTS-5, although with decreased potency ($K_{i\ app}$ values ranging from 14 nM for 2D3 to 590 nM for 2D11) **(Table 5.1)**.

Mouse ADAMTS5-2 cleaves bovine aggrecan *in vitro* at the aggrecanase site $Glu^{392}\downarrow^{393}Ala$, thus the ARGSV cleavage products are detectable by the anti-ARGSV neoepitope antibody in Western blot. Antibodies 2A11, 2B9, 2D3, 2D5 and 2D11 inhibited mouse ADAMTS5-2 cleavage of bovine aggrecan with comparable potency to the human version (**Figure 5.3**). The non-inhibitory antibody 1B3 also showed inhibition of aggrecanase activity of mouse ADAMTS-5. The reasons for this discrepancy are not known although we may hypothesise subtle structural differences between mouse and human ADAMTS-5.

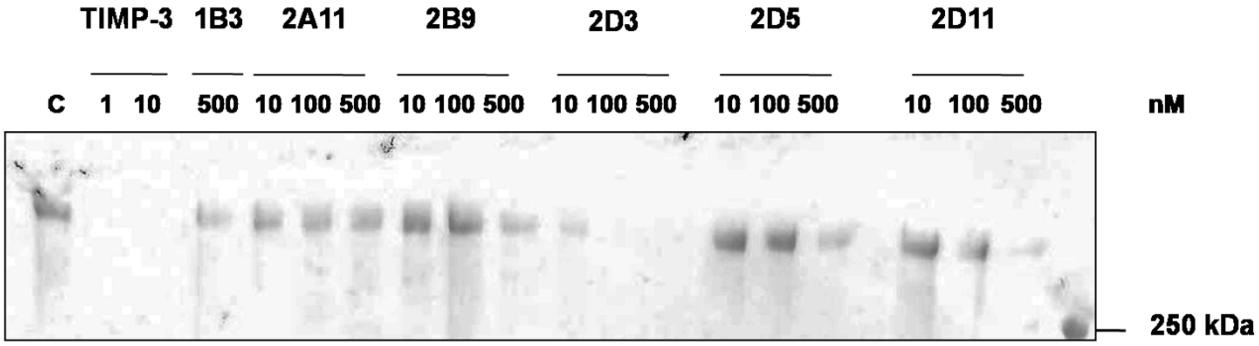

Figure 5.3: Inhibition of mouse ADAMTS-5 by scFv-Fc antibodies. Mouse ADAMTS-5 at a concentration of 1 nM was incubated alone (C, control) or with various concentrations of TIMP-3 and scFv-Fc antibodies for 2 h. Bovine aggregan (50 µg) was added and the mixture was incubated for 2 h at 37°C. The reactions were stopped with 50 mM EDTA and the products were deglycosylated overnight with chondroitinase ABC and keratanase and analysed by Western blot for ARGSV-containing fragments using BC3 monoclonal antibody. The result shown is representative of three independent experiments.

Figure 5.4 shows alignment of amino acid sequences of mature ADAMTS-5 lacking C-terminal TS (TS-2) domain from different species (residues not homologous to human are shown in red). ADAMTS-5 sequences are highly conserved between human and cynomolgus monkey (99.3% identity), mouse (96.6% identity), rat (96.3% identity), rabbit (96.3% identity), pig (90.7% identity) and cow (97.2%).

Seq	262 Catalytic domain
Human	RSISRARQVELLLVADASMARLYGRGLQHYLLTLASIANRLYSHASIENHIRLAVVKVVVLGDKDKSLEVSKNA
Cynom	RSISRARQVELLLVADASMARLYGRGLQHYLLTLASIANRLYSHASIENHIRLAVVKVVVLGDKDKSLEVSKNA
Mouse	RSISRARQVELLLVADSSMARMYGRGLQHYLLTLASIANRLYSHASIENHIRLAVVKVVVLTDKDTSLEVSKNA
Rat	RSISRARQVELLLVADSSMAKMYGRGLQHYLLTLASIANRLYSHASIENHIRLAVVKVVVLTDK--SLEVSKNA
Rabbit	RSISRSRQVELLLVADSTMARMYGRGLHHYLLTLASIANRLYSHASIENHIRLAVVKVVVLGDKDKSLEVSKNA
Pig	RSISRARQVELLLVADASMARMYGRGLQHYLLTLASIANRLYSHASIENHIRLTVVKVVVLGDKDKTLEVSKNA
Bovine	RSISRARQVELLLVADASMARMYGRGLQHYLLTLASIANKLYSHASIENHIRLVVVKVVVLGDKDKSLEVSKNA

Seq	
Human	ATTLKNFCKWQHQHNQLGDDHEEHYDAAILFTREDLCGHHSCDTLGMADVGTICSPERSCAVIEDDGLHAAFTV
Cynom	ATTLKNFCKWQHQHNQLGDDHEEHYDAAILFTREDLCGHHSCDTLGMADVGTICSPERSCAVIEDDGLHAAFTV
Mouse	ATTLKNFCKWQHQHNQLGDDHEEHYDAAILFTREDLCGHHSCDTLGMADVGTICSPERSCAVIEDDGLHAAFTV
Rat	ATTLKNFCKWQHQHNQLGDDHEEHYDAAILFTREDLCGHHSCDTLGMADVGTICSPERSCAVIEDDGLHAAFTV
Rabbit	ATTLKNFCKWQHQHNQLGDDHEEHYDAAILFTREDLCGHHSCDTLGMADVGTICSPERSCAVIEDDGLHAAFTV
Pig	ATTLKNFCKWQHQHNQLGDDHEEHYDAAILFTREDLCGHHSCDTLGMADVGTICSPERSCAVIEDDGLHAAFTV
Bovine	ATTLKNFCKWQHQHNQLGDDHEEHYDAAILFTREDLCGHHSCDTLGMADVGTICSPERSCAVIEDDGLHAAFTV

Seq	476	477
Human	AHEIGHLLGLSHDDSKFCEETFGSTEDKRLMSSILTSIDASKPWSKCTSATITEFLDDGHGNCLLDLP	RKQILG
Cynom	AHEIGHLLGLSHDDSKFCEETFGSTEDKRLMSSILTSIDASKPWSKCTSATITEFLDDGHGNCLLDQP	RKQILG
Mouse	AHEIGHLLGLSHDDSKFCEENFGTTEDKRLMSSILTSIDASKPWSKCTSATITEFLDDGHGNCLLDLP	RKQILG
Rat	AHEIGHLLGLSHDDSKFCEENFGSTEDKRLMSSILTSIDASKPWSKCTSATITEFLDDGHGNCLLDVP	RKQILG
Rabbit	AHEIGHLLGLSHDDSKFCEENFGSTEDKRLMSSILTSIDASKPWSKCTSATITEFLDDGHGNCLLDVP	RKQILG
Pig	AHEIGHLLGLSHDDSKFCEENFGSTEDKRLMSSILTSIDASKPWSKCTSATITEFLDDGHGNCLLDLP	RKQILG
Bovine	AHEIGHLLGLSHDDSKFCEENFGSTEDKRLMSSILTSIDASKPWSKCTSATITEFLDDGHGNCLLDLP	RKQIPG

Seq	Disintegrin domain
Human	PEELPGQTYDATQQCNLTFGPEYSVCPGMDVCARLWCAVVRQGQMVCLTKKLPAVEGTPCGKGRICLQGKCVDKTK
Cynom	PEELPGQTYDATQQCNLTFGPEYSVCPGMDVCARLWCAVVRQGQMVCLTKKLPAVEGTPCGKGRICLQGKCVDKTK
Mouse	PEELPGQTYDATQQCNLTFGPEYSVCPGMDVCARLWCAVVRQGQMVCLTKKLPAVEGTPCGKGRVCLQGKCVDKTK
Rat	PEELPGQTYDATQQCNLTFGPEYSVCPGMDVCARLWCAVVRQGQMVCLTKKLPAVEGTPCGKGRICLQGKCVDKTK
Rabbit	PEELPGQTYDATQQCNLTFGPEYTVCPGMDVCARLWCAVVRQGQMVCLTKKLPAVEGTPCGKGRICLQGKCVDKTK
Pig	PEELPGQTYDASQQCNLTFGPEYSVCPGMDVCARLWCAVVRQGQMVCLTKKLPAVEGTPCGKGRICLQGKCVDKTK
Bovine	PEELPGQTYDASQQCNLTFGPEYSVCPGMDVCARLWCAVVRQGQMVCLTKKLPAVEGTPCGKGRICLQGKCVDKTK

Seq	566	567 TS-1 622	623
Human	KKYYSTSS	HGNWGSWGSWGQCSRSCGGGVQFAYRHCNNPAPRNNGRYCTGKRAIYRSCSLMPCP	PNGKSFRH
Cynom	KKYYSTSS	HGNWGSWGSWGQCSRSCGGGVQFAYRHCNNPAPRNNGRYCTGKRAIYRSCGLMPCP	PNGKSFRH
Mouse	KKYYSTSS	HGNWGSWGPWGQCSRSCGGGVQFAYRHCNNPAPRNSGRYCTGKRAIYRSCSVTPCP	PNGKSFRH
Rat	KKYYSTSS	HGNWGSWGPWGQCSRSCGGGVQFAYRHCNNPAPRNSGRYCTGKRAIYRSCSVIPCP	PNGKSFRH
Rabbit	KKYYSTSS	HGNWGSWGPWGQCSRSCGGGVQFAYRHCNNPAPRNSGRYCTGKRAIYRSCSVTPCP	ANGKSFRH
Pig	KKYYSTSS	HGNWGSWGSWGQCSRSCGGGVQFAYRHCNNPAPRNSGRYCTGKRAIYRSCSVTPCP	ANGKSFRH
Bovine	KKYYSTSS	HGNWGSWGSWGQCSRSCGGGVQFAYRHCNNPAPRNNGRYCTGKRAIYRSCSVTPCP	ANGKSFRH

Figure 5.4: Amino Acid Sequences of human ADAMTS-5 and corresponding sequences of other animal species. Alignment of human (accession number Q9UNA0), cynomolgus monkey (G8F2G2) mouse (Q9R001), rat (QSTY19), rabbit (G1SIH2), pig (F1SHP0) and bovine (F1MRZ2) ADAMTS-5 sequences was performed with Clustal Omega. C-terminal TS (TS-2) domain is not shown.

Seq	Cys-Rich Domain
Human	EQCEAKNGYQSDAKGVKTFVEWVPKYAGVLPADVCKLTCRAKGTGYYVVFSPKVTDGTECRLYSNSVCVRGKCVR-
Cynom	EQCEAKNGYQSDAKGVKTFVEWVPKYAGVLPADVCKLTCRAKGTGYYVVFSPKVTDGTECRPYSNSVCVRGKCVR
Mouse	EQCEAKNGYQSDAKGVKTFVEWVPKYAGVLPADVCKLTCRAKGTGYYVVFSPKVTDGTECRPYSNSVCVRGRCVR-
Rat	EQCEAKNGYQSDAKGVKTFVEWVPKYAGVLPADVCKLTCRAKGTGYYVVFSPKVTDGTECRPYSNSVCVRGRCVR-
Rabbit	EQCEAKNGYQSDAKGVKTFVEWVPKYAGVLPADVCKLTCRAKGTGYYVVFSPKVTDGTECRPYSNSVCVRGRCVR-
Pig	EQCEAKNGYQSDAKGVKTFVEWVPKYAGVLPADVCKLTCRAKGTGYYVVFSPKVTALTRN-----SRCLCEFCIYT
Bovine	EQCEAKNGYQSDAKGVKTFVEWVPKYAGVLPGDVCKLTCRAKGTGYYVVFSPKVTDGTECRPYSNSVCVRGKCVR-

Seq	731	732 Spacer domain
Human	-TGCDGIIGSKLQYDKCGVCGGDNSSC	TKIVGTFNKKSKGYTDVVRIPEGATHIKVRQFKAKDQTRFTAYL
Cynom	-TGCDSIIGSKLQYDKCGVCGGDNSSC	TKIVGTFNKKSKGYTDVVRIPEGATHIKVRQFKAKDQTRFTAYL
Mouse	-TGCDGIIGSKLQYDKCGVCGGDNSSC	TKIIGTFNKKSKGYTDVVRIPEGATHIKVRQFKAKDQTRFTAYL
Rat	-TGCDGIIGSKLQYDKCGVCGGDNSSC	TKIIGTFNKKSKGYTDVVRIPEGATHIKVRQFKAKDQTRFTAYL
Rabbit	-TGCDGIIGSKLHYDKCGVCGGDNSSC	TKIIGTFNKKSKGYTDVVRIPEGATHIKVRQFKAKDQTRFTAYL
Pig	YINHDYLLGSSL---ECHLCGSTGETC	RKFLFVYSFVNKGYTDVVRIPEGATHIKVRQFKAKDQTRFTAYL
Bovine	-TGCDGIIGSKLQYDKCGVCGGDNSSC	TKVVGTFNKKSKGYTDVVRIPEGATHIKVRQFKAKDQTRFTAYL

Seq	Spacer domain
Human	ALKKKNGEYLINGKYMISTSETIIDINGTVMNYSGWSHRDDFLHGMGYSATKEILIVQILATDPTKPLDVRYSFFV
Cynom	ALKKKNGEYLINGKYMISTSETIIDINGTVMNYSGWSHRDDFLHGMGYSATKEILIVQILATDPTKPLDVRYSFFV
Mouse	ALKKKTGEYLINGKYMISTSETIIDINGTVMNYSGWSHRDDFLHGMGYSATKEILIVQILATDPTKALDVRYSFFV
Rat	ALKKKTGEYLINGKYMISTSETIIDINGTVMNYSGWSHRDDFLHGMGYSATKEILIVQILATDPTKALDVRYSFFV
Rabbit	ALKKKNGEYLINGKYMISTSETIIDINGTVMNYSGWSHRDDFLHGMGYSATKEILIVQILATDPTKALDVRYSFFV
Pig	ALKKKNGEYLINGKYMISTSETIIDLNGTVMNYSGWSHRDDFLHGMGYAATKEILIVQILATDPTKALDVRYSFFV
Bovine	ALKKKNGEYLINGKYMISTSETIIDINGTVMNYSGWSHRDDFLHGMGYSATKEILIVQILATDPTKALDVRYSFFV

Seq	Spacer domain 874
Human	PKKSTPKVNSVTSHGSNKVGSHT
Cynom	PKKSTPKVNSVTSHGSNKVGSHT
Mouse	PKKTTQKVNSVISHGSNKVGPHS
Rat	PKKTTQKVNSVISHSSNKVGLHS
Rabbit	PKKSTQNLNSVTNHGSNKVVSHT
Pig	PKKSTPKVNSVTSQGSNKVGSHT
Bovine	PKKSAPKANSVTSQGSNKVGSPT

Figure 5.4 (continued).

5.4. Determination of dissociation constant (K_D) and domain mapping by SPR

To characterise the kinetics of interactions between ADAMTS-5 and scFv-Fc antibodies, antibodies 2A11, 2B9, 2D3, 2D5, and 2D11 were captured by rabbit anti-human IgG amino-coupled to a CM5 Biacore chip and titrated concentrations of ADAMTS-5 deletion mutants were injected **(Figure 5.5)**. As negative controls, two scFv-Fc antibodies selected against unrelated antigens were not able to capture ADAMTS5-2 at the highest concentration tested (100 nM) **(Figure 5.6)**.

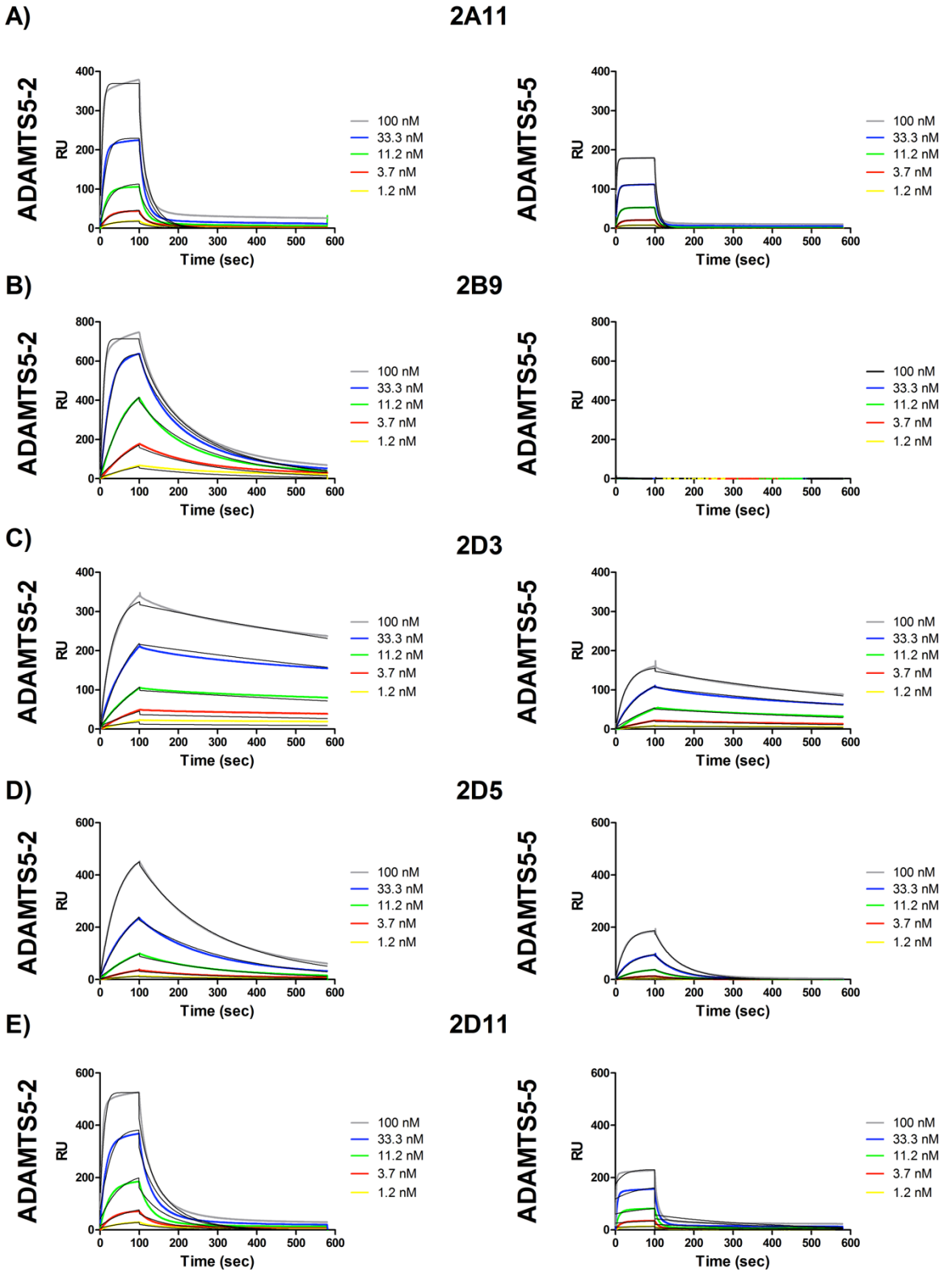

Figure 5.5: Binding kinetics of ADAMTS-5 and scFv-Fc antibodies. scFv-Fc antibodies (100 nM) were captured by an anti-human IgG antibody immobilised onto a CM5 chip and ADAMTS-5 or -4 deletion mutants were injected at different concentrations ranging from 1.2 to 200 nM at a flow rate of 30 µl/min. Representative binding curves are shown.

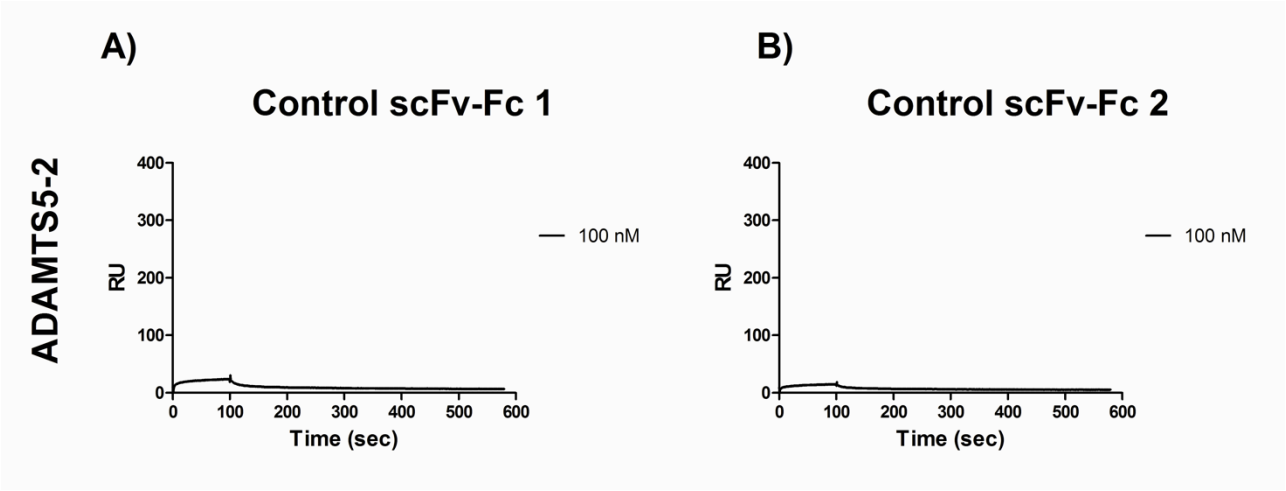

Figure 5.6: Control scFv-Fc antibodies do not bind to ADAMTS5-2 in the SPR setting. Two different scFv-Fc antibodies **(A, B)** isolated from phage display selections against unrelated antigens were captured on CM5 chip by immobilised anti-Fc IgG and a single (100 nM) concentration of ADAMTS5-2 was injected.

Generally, the dissociation constants (K_D) values determined by SPR were found to be in good agreement with the $K_{i\ app}$ values obtained from steady-state inhibition studies **(Table 5.2)**. For 2A11, it was not possible to accurately estimate the K_D for ADAMTS5-2 (approximate K_D: 94 ± 72 nM) since this approaches the maximum ADAMTS5-2 concentration tested (100 nM). Interestingly, 2A11 bound to the Cat/Dis domain with higher affinity ($K_{D\ 5\text{-}5}$: 35.6 ± 0.21 nM); this was mainly due to a substantially higher association rate, suggesting that this interaction might be conformation-dependent, with the epitope partially masked in the full-length molecule. The reason for the relatively high K_D values for the two forms is the poor off rate ($k_{off\ 5\text{-}2}$: 0.121 sec^{-1}, $k_{off\ 5\text{-}5}$: 0.181 sec^{-1}) **(Table 5.2).**

Antibody 2B9 was able to bind to ADAMTS5-2 with relatively high affinity ($K_{D\ 5\text{-}2}$: 6.7 ± 0.8 nM) but was not able to bind to all the other truncation forms of ADAMTS-5 at the highest concentration tested (100 nM) in the SPR setting, indicating the Sp domain as the main epitope **(Table 5.2 and Figures 5.5 and 5.7)**. The binding kinetics of 2B9 to ADAMTS5-2 was characterised by high values of association and dissociation rate constants (~10^6 M^{-1} sec^{-1} and ~10^{-2} sec^{-1}, respectively).

Antibodies 2D3, 2D5, and 2D11 bound to both ADAMTS5-2 and ADAMTS5-5 but with some remarkable differences. Antibody 2D3 bound to ADAMTS5-5 with essentially the same affinity as ADAMTS5-2 ($K_{D\ 5\text{-}5}$: 3.4 ± 1.0 nM; $K_{D\ 5\text{-}2}$: 2.8 ± 1.2 nM). Although antibody 2D11 showed a comparable equilibrium dissociation constant for the two enzyme forms ($K_{D\ 5\text{-}2}$: 22 ± 7.2 nM; $K_{D\ 5\text{-}5}$: 24 ± 4.6 nM) both dissociation and association rate constants were 2-fold higher in the case of the interaction with ADAMTS5-5 than with ADAMTS5-2. Antibody 2D5 exhibited a 2-fold

increase in K_D for ADAMTS5-5 (71 ± 29 nM) compared with ADAMTS5-2 (29 ± 11 nM) and this was due to a 2 fold increase in dissociation rate constant.

	k_{on} (M^{-1} sec^{-1})	k_{off} (sec^{-1})	K_D (x 10^{-9} M)	ΔG (kJ/mol)	ΔΔG (kJ/mol)	Epitope
2A11						**Dis-Cat**
ADAMTS5-2	1.58 x10^6	0.121	94 ± 72	-40.6		
ADAMTS5-5	5.11 x 10^6	0.182	36 ± 0.2	-42.6	~ -1.9	
2B9						**Spacer**
ADAMTS5-2	(2.4 ± 0.3) x 10^6	(1.6 ± 0.2) x 10^{-2}	6.7 ± 0.8	-46.7		
ADAMTS5-3	-	-	NB			
ADAMTS5-4	-	-	NB			
ADAMTS5-5	-	-	NB			
ADAMTS4-2	-	-	NB			
2D3						**Dis-Cat**
ADAMTS5-2	(2.8 ± 0.8) x 10^5	(7.0 ± 0.8) x 10^{-4}	2.8 ± 1.2	-48.8		
ADAMTS5-5	(3.3 ± 1.1) x 10^5	(1.1 ± 0.1) x 10^{-3}	3.4 ± 1.0	-48.3	0.5	
ADAMTS4-2	-	-	NB			
2D5						**Cross-domain**
ADAMTS5-2	(2.3 ± 0.7) x 10^5	(5.9 ± 0.2) x 10^{-3}	29 ± 11	-43.0		
ADAMTS5-5	(2.3 ± 1.2) x 10^5	(1.4 ± 0.5) x 10^{-2}	71 ± 29	-40.8	2.2	
ADAMTS4-2	-	-	NB			
2D11						**Dis-Cat**
ADAMTS5-2	(1.9 ± 1.0) x 10^6	(4.9 ± 1) x 10^{-2}	22 ± 7.2	-43.7		
ADAMTS5-5	(4.70 ± 1.9) x 10^6	(0.11 ± 0.2)	24 ± 4.6	-43.5	0.2	
ADAMTS4-2	-	-	NB			

Table 5.2: ADAMTS-5 Surface Plasmon Resonance (SPR). Association (k_{on}) and dissociation (k_{off}) rate constants and the equilibrium dissociation constant (K_D) were determined by global fitting of the SPR data to a 1:1 binding model. ΔΔG is the difference in free energy of binding (calculated from K_D) relative to ADAMTS5-2. Free energies of binding were calculated from K_D according to $\Delta G = -RT\ln(1/K_D)$; NB, no measurable binding at 100 nM concentration of ADAMTS-5 and 200 nM concentration of ADAMTS4-2. Mean values ± S.D. are reported (n=3).

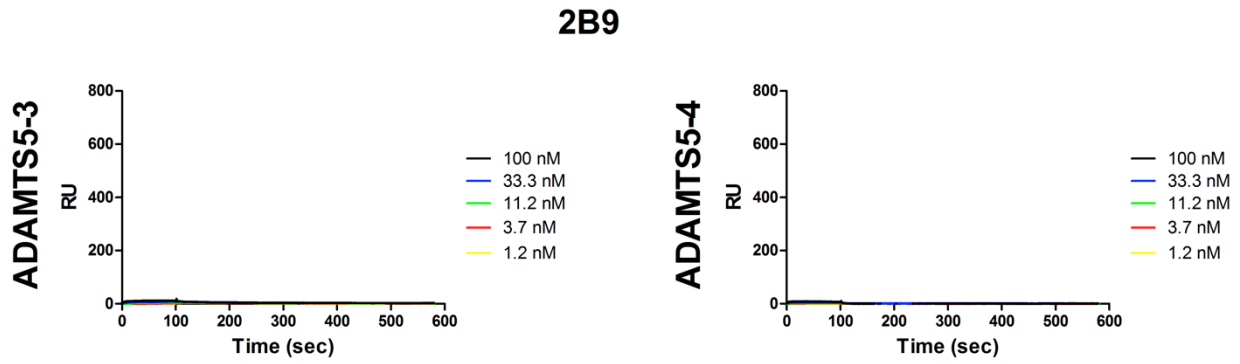

Figure 5.7: Antibody 2B9 does not bind to ADAMTS5-3 and ADAMTS5-4. scFv-Fc antibodies (100 nM) were captured by an anti-human IgG antibody immobilised onto a CM5 chip and ADAMTS5-3 or 5-4 were injected at different concentrations ranging from 1.2 to 100 nM at a flow rate of 30 µl/min.

To test selectivity, the ability of anti-ADAMTS-5 antibodies to bind to ADAMTS-4 was investigated. Antibodies 2B9, 2D3, 2D5, and 2D11 did not bind to ADAMTS4-2 at the highest concentration of enzyme tested (200 nM) **(Table 5.2 and Figure 5.8)**.

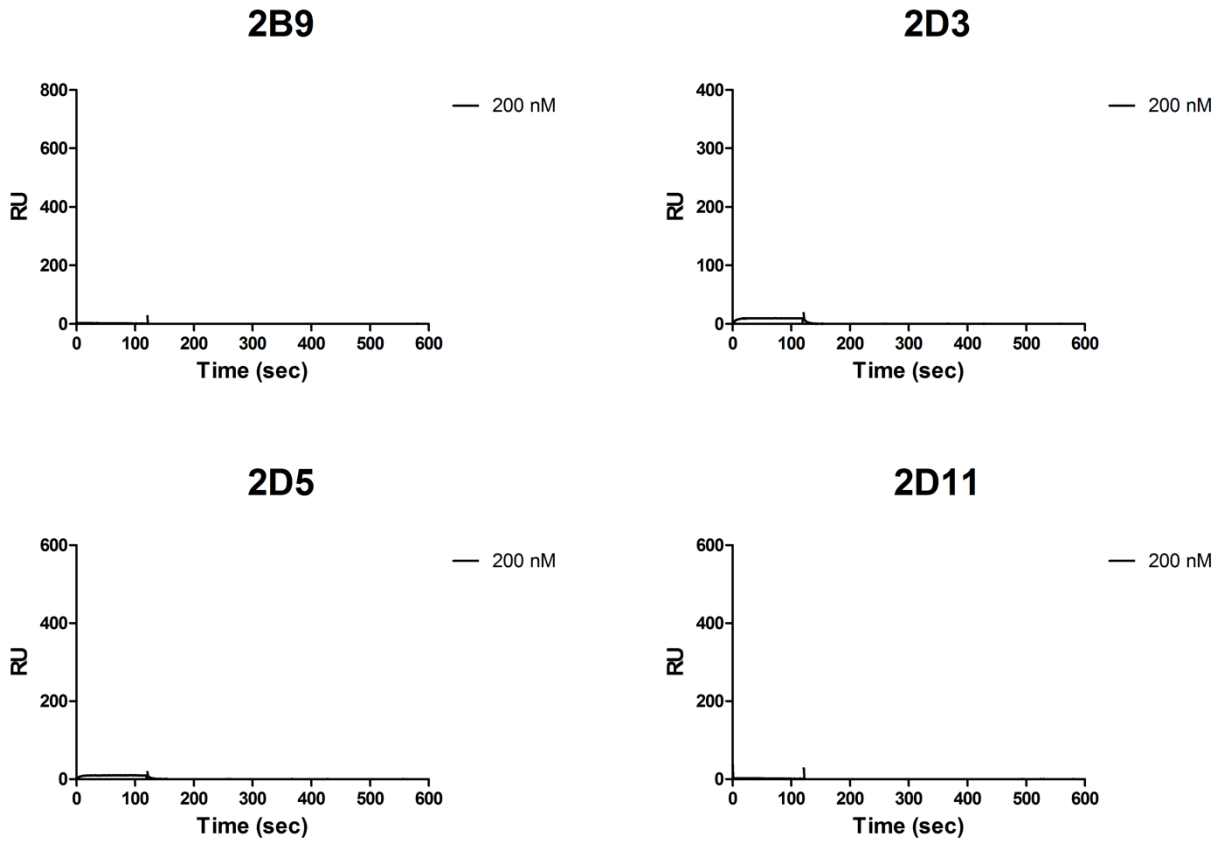

Figure 5.8: scFv-Fc antibodies 2B9, 2D3, 2D5, and 2D11 do not bind to ADAMTS-4. scFv-Fc antibodies (100 nM) were captured by an anti-human IgG antibody immobilised onto a CM5 chip and ADAMTS4-2 (200nM) was injected at a flow rate of 30 µl/min.

5.5. Recognition of ADAMTS-5 on Western blot

scFv-Fc antibodies 2A11, 2B9, 2D3, 2D5, and 2D11 were able to recognise ADAMTS-5 on Western blots only when the protein was run under non-reducing conditions and the sample was not previously heat-denatured **(Figures 5.9 and 5.10)**. This implies that the epitopes recognised by these antibodies are a mixture of three-dimensional and linear sequences, as reported for other anti-ADAMTS-5 scFv-Fc antibodies **(See Section 4.4.3)**. With antibody 2B9, a faint band was detected under reducing conditions **(Figure 5.9)**.

Antibodies 2A11, 2D3, 2D5, 2D11 could recognise all the truncated ADAMTS-5 forms, thus confirming the SPR data. Interestingly, 2D5 recognised ADAMTS5-5 with much decreased sensitivity and this confirms the increase in K_D value for ADAMTS5-5 compared to ADAMTS5-2 as measured by SPR. 2B9 recognised not only ADAMTS5-2 but also ADAMTS5-3 and ADAMTS5-4 on a Western blot, and this implies that the antibody, due to its size, shields some epitopes in CysR and TS-1 domains, other than in the Sp domain. These epitopes may not be exposed in solution and therefore not bound by 2B9 in the SPR setting. The polyclonal rabbit anti-Cat antibody and the anti-Cat/Dis antibodies 2D3, 2A11 and 2D11 could detect lower bands at 55 and 36 kDa in the ADAMTS5-2 lane. These bands were not detected by anti-FLAG antibody and correspond in size to recombinant truncated forms of ADAMTS-5 consisting of Cat/Dis (ADAMTS5-5) and Cat/Dis/TS-1/CysR domains (ADAMTS5-3); they therefore should be products of C-terminal truncation, probably due to autolysis.

All the antibodies showed a certain ability to detect mouse ADAMTS-5 on Western Blot, although with decreased sensitivity (an exception being 2D3 and 2D11, **Figure 5.10 E, G**). The polyclonal rabbit anti-ADAMTS-5 Cat domain antibody was raised against the peptide sequence ^{426}CEETFGSTEDKRL^{438} which is different from the mouse ^{426}CEENFGTTEDKRL^{438} (residues not homologous to human are shown in red) thus it cannot recognise mouse ADAMTS-5 **(Figure 5.10 B)**.

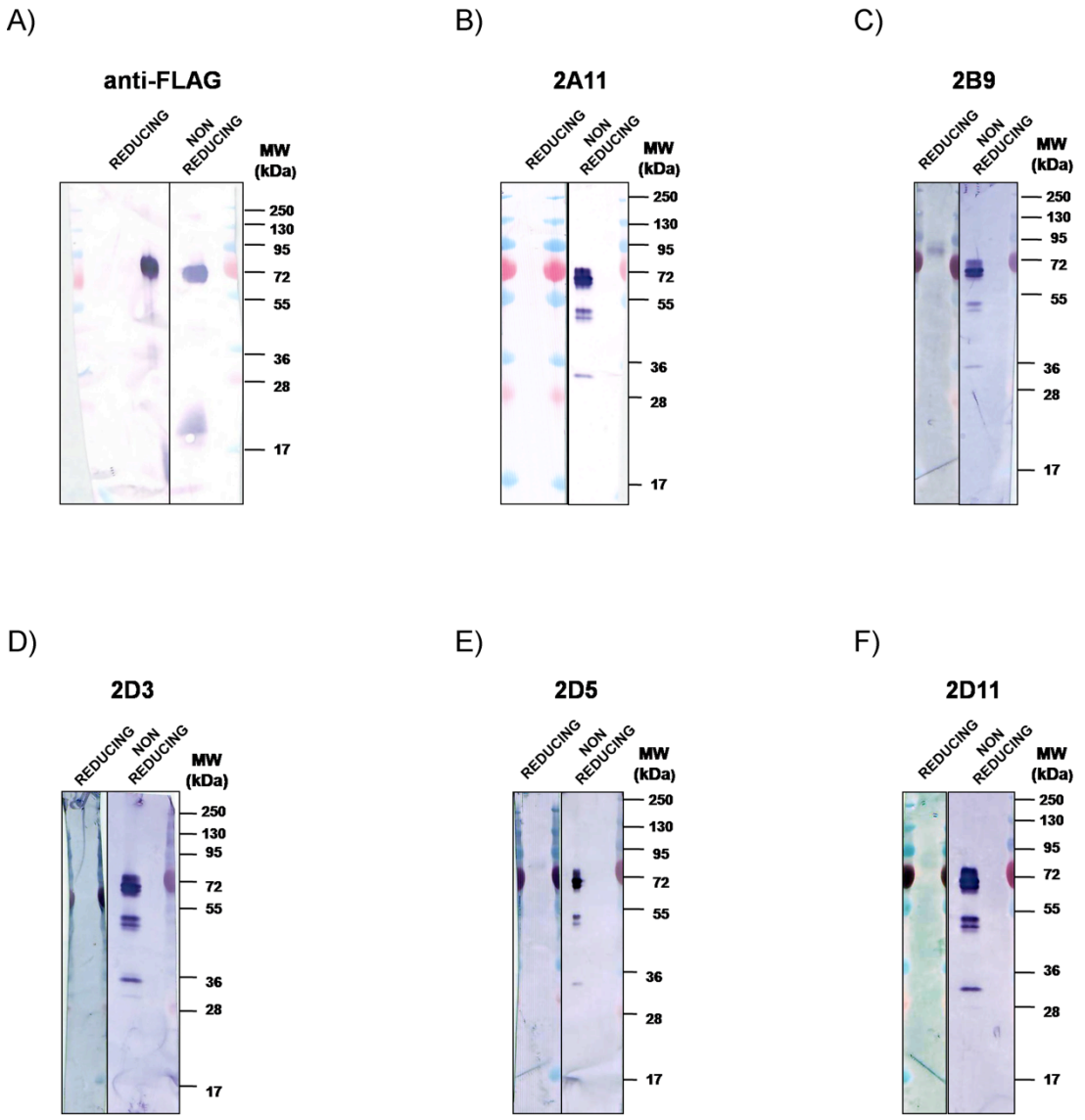

Figure 5.9: Immunoblots with scFv-Fc antibodies. ADAMTS5-2 (115 nanograms) was run on a 10% SDS-PAGE gel under non-reducing and reducing conditions. Under reducing conditions the samples were boiled at 90°C for 5 minutes in the presence of β-mercaptoethanol. scFv-Fc antibodies were used to stain the membranes and signal was detected with AP-conjugated anti-human IgG. Anti-FLAG M2 antibody was used as a positive control.

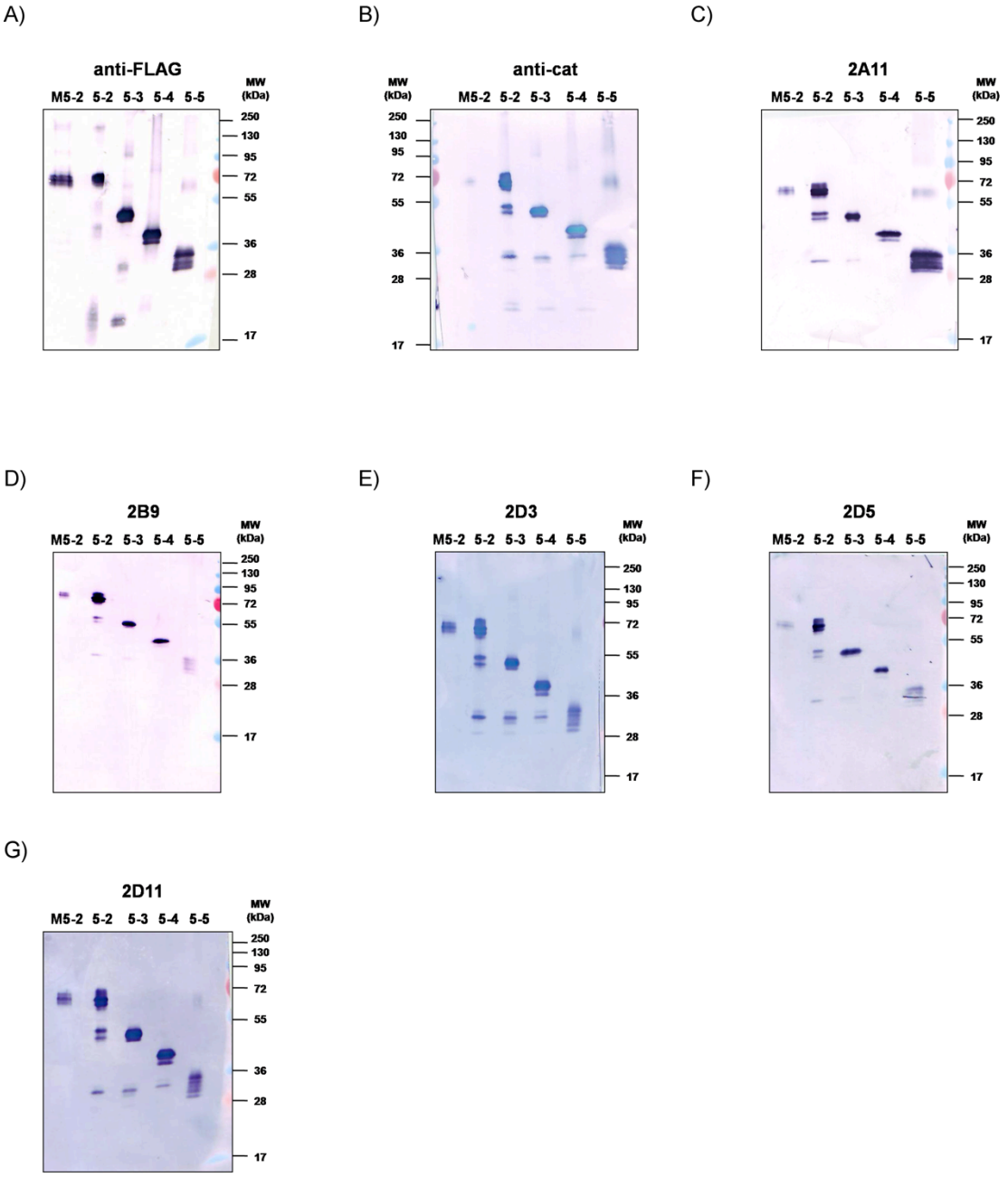

Figure 5.10. Immunoblots with scFv-Fc antibodies. Purified ADAMTS-5 deletion mutants (115 nanograms) were run on a 10% SDS-PAGE gel under non-reducing conditions. **A), B)** mouse monoclonal anti-FLAG M2 or rabbit polyclonal anti-Cat antibodies were used to stain the membranes. **C-G)**: scFv-Fc antibodies were used to stain the membranes and signal was detected with AP-conjugated anti-human IgG. M5-2: mouse ADAMTS5-2.

5.6. Investigation of mechanism of inhibition of QF peptide cleavage

To investigate the mechanism of inhibition of antibodies 2A11, 2D3, 2D5, 2D11 inhibition kinetic studies were performed using the QF-peptide. Dixon plots were used as a graphical method for determination of the type of enzyme inhibition and as an independent way to calculate the K_i values of the enzyme-inhibitor complexes. In this case the effect on the enzyme rate ($1/v$) was determined at 4 substrate concentrations (10, 20, 40, and 80 μM, corresponding to 0.13, 0.26, 0.53, and 1.05 $[S]/K_m$ ratios) over a range of scFv-Fc concentrations which produce between 5-70%

inhibition. In a plot of the reciprocal of the rate of peptide hydrolysis ($1/v$) against the inhibitor concentration ([I]), data for each substrate concentration fall on straight lines that intersect at a concentration of inhibitor equal to the inhibition constant above the x axis ([I] = $-K_i$ and $1/v = 1/v_{max}$) (competitive inhibition), or on the x axis ($1/v = 0$) (noncompetitive inhibition). In the case of uncompetitive inhibition, these lines are parallel. Examination of the kinetic data by a linearised Dixon plot graphic approach suggested a competitive inhibition modality for antibodies 2A11 and 2D5, and a noncompetitive inhibition modality for antibodies 2D3 and 2D11 (**Figure 5.11**).

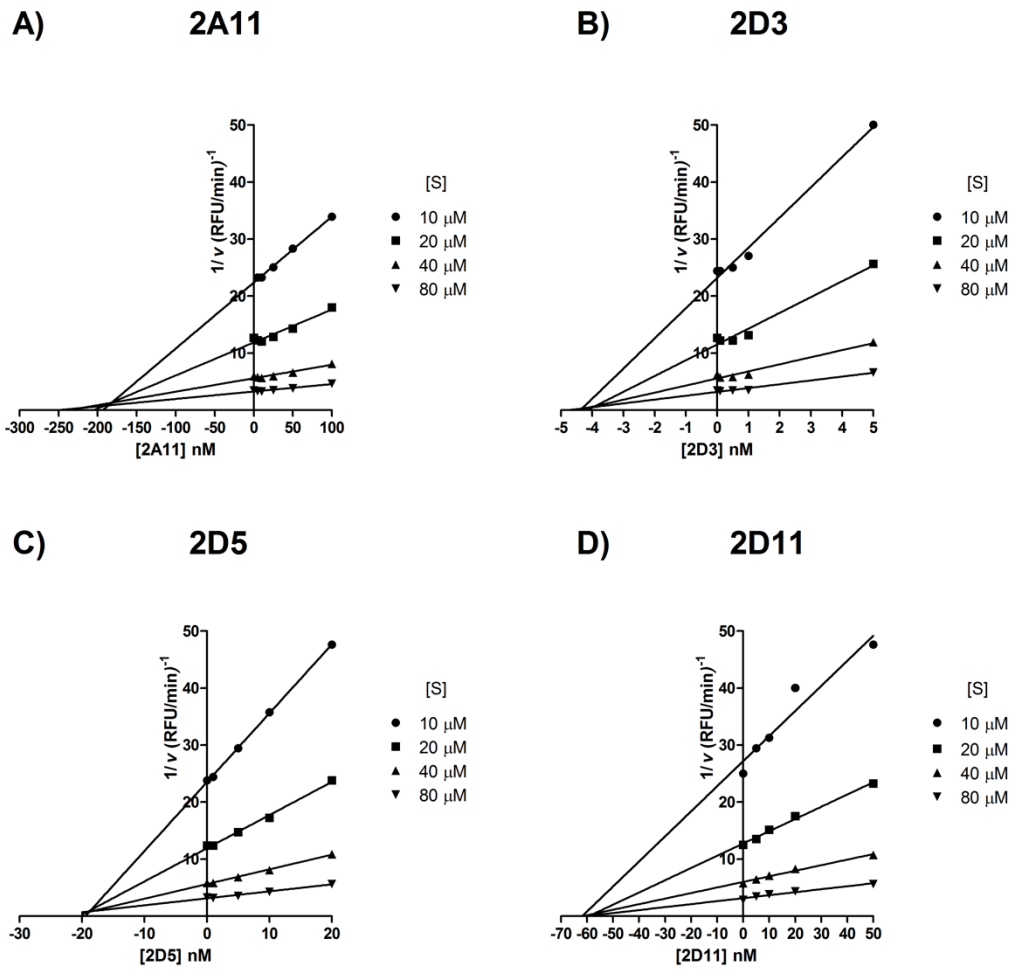

Figure 5.11: **Dixon Plots for ADAMTS-5 inhibition by 2A11 (A), 2D3 (B), 2D5 (C), and 2D11 (D) scFv-Fc antibodies.** Enzyme (5 nM) was incubated with different concentrations of scFv-Fc antibodies for 2 h and reciprocal rates against Abz-TESE~SRGAIY-Dpa-KK (1 h, 37°C) were determined at 10, 20, 40, and 80 µM substrate concentrations.

The K_i values estimated from the intercepts of the plots were found to be in good agreement with the values determined by dose-response inhibition at [S]= 20 µM **(Table 5.3)**. In the case of the tight-binding inhibitor 2D3 (K_i value 2.5 nM), these values were higher because 5 nM enzyme was used instead of 0.5 nM due to detection limits at substrate concentrations lower than 20 µM (20 µM

substrate should be incubated with 0.5 nM enzyme for approximately 18 h to generate a reasonable signal).

Clone	K_i (nM)
2A11	180 ± 12
2D3	4.4 ± 0.2
2D5	18 ± 0.7
2D11	60 ± 1.0

Table 5.3: K_i **values for inhibition of ADAMTS-5 by scFv-Fc antibodies as estimated by the intercepts of the Dixon plots on the *x* axis.**

However, a limitation of this method is that only low concentrations of substrate relative to the K_m could be used. This is due to auto-quenching and solubility limits at high substrate concentrations. In fact, if we plot the data above in a classical Lineweaver-Burk plot (i.e. the reciprocal of the rate of peptide hydrolysis, $1/v$, versus the reciprocal of the substrate concentration, 1/[S]), intercepts are too close to the origin so accurate determination of both K_m (intercept on the *x* axis) and V_{max} (intercept on the y axis) is not possible **(Figure 5.12 A, C, E, G)**. This is confirmed by a plot of the rate *versus* the substrate concentration where it is evident that V_{max} is not reached at any substrate concentration **(Figure 5.12 B, D, F, H)**.

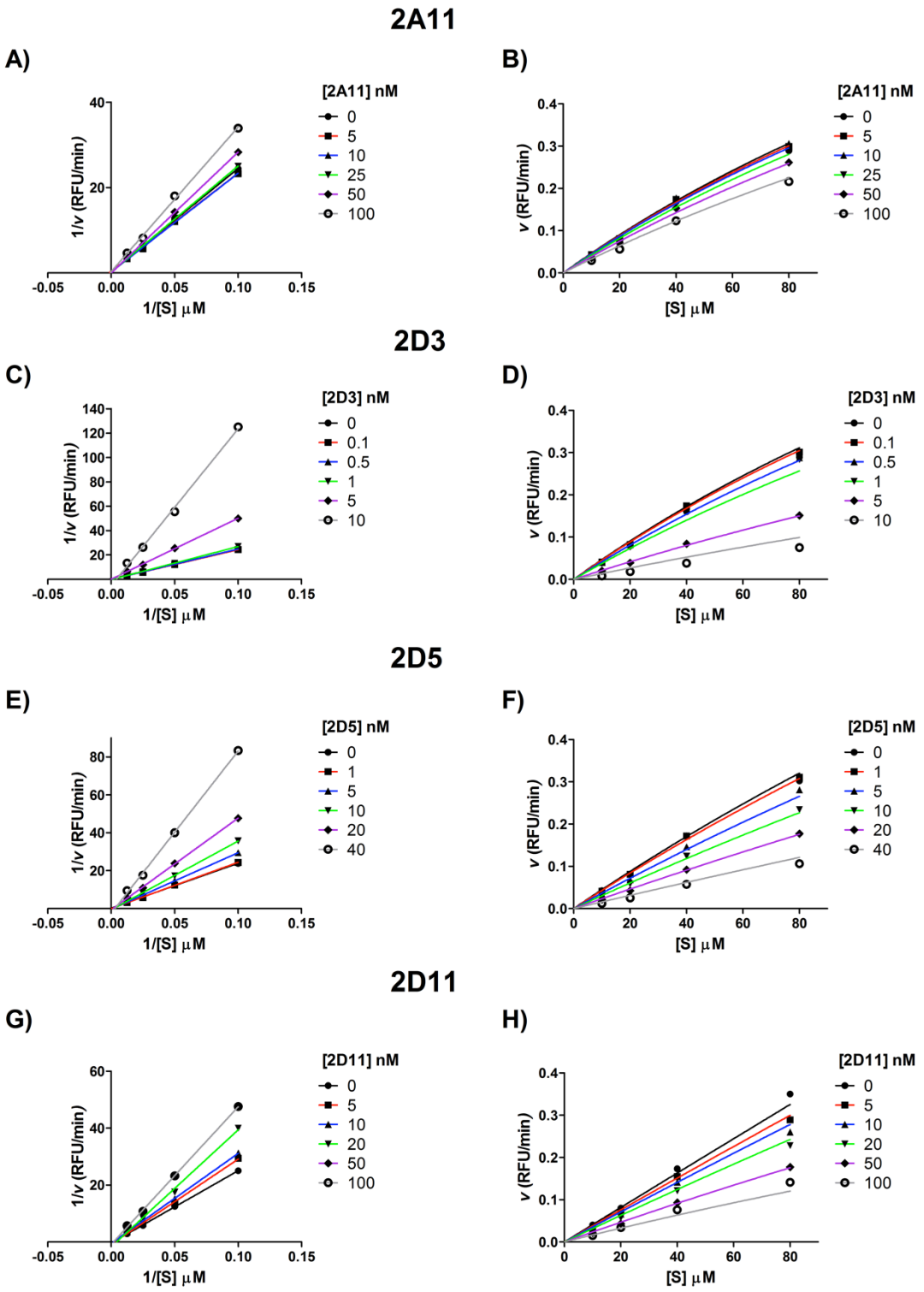

Figure 5.12: Dependence of ADAMTS-5 activity on the concentration of the QF peptide substrate in the presence of scFv-Fc antibodies. Lineweaver-Burk **(A, C, E, G)** and rate versus substrate concentration **(B, D, F, H)** plots are shown.

5.7. Dual inhibition studies

Since the studies described in **Section 5.6** did not elucidate unequivocally the mechanism of inhibition of anti-ADAMTS-5 antibodies, I chose to test the effect of addition of other ligands such as GM6001, heparin and TIMP-3 on the inhibitory potency of scFv-Fc antibodies. These studies could help to clarify if these antibodies inhibit ADAMTS-5 through a zinc-chelating mechanism or share an epitope deep in the active site cleft (combination with GM6001) and if they are potentially affected by TIMP-3 or GAG binding to the enzyme (combination with TIMP-3 or heparin, respectively). Therefore, double-inhibitor experiments were conducted as described by Yonetani and Theorell (1964). In such experiments, the effect of the concurrent presence of two inhibitors is examined by varying the concentration of one inhibitor in the absence or presence of a second inhibitor held at a constant concentration. These studies will show zero interaction if the effect of the combination is that expected from the dose-response curves of the single inhibitors; synergy if the effect is greater than expected and antagonism if the effect is less than expected. Factor γ represents the mutual influence of the two inhibitors on the binding of each other. If the binding of two inhibitors to the enzyme is mutually exclusive ($\gamma = \infty$), plotting $1/v$ against different concentrations of the first inhibitor at a fixed concentration of the second inhibitor would result in parallel lines. If the inhibitors can bind simultaneously to the enzyme ($\gamma \neq 1$), the slope will depend on the concentration of the inhibitor held at constant concentration and the lines will intersect above or below the *x* axis. In this case the two inhibitors will show positive interaction since use of the combination means that the total concentration needed to obtain a certain level of inhibition is less than the concentrations of each inhibitor taken separately. When $\gamma = 1$, the effects of the two inhibitors are independent and the lines in the Yonetani-Theorell plot will converge at the *x* axis.

5.7.1. Effect of GM6001

To investigate whether antibodies 2A11, 2D3, 2D5 and 2D11 act via a zinc-binding mechanism or share epitopes deep in the active site cleft, we performed dual inhibition kinetics using GM6001, a known zinc chelator and competitive inhibitor of many metalloproteinases (Grobelny et al., 1992) **(Figure 5.13 and Table 5.4)**.

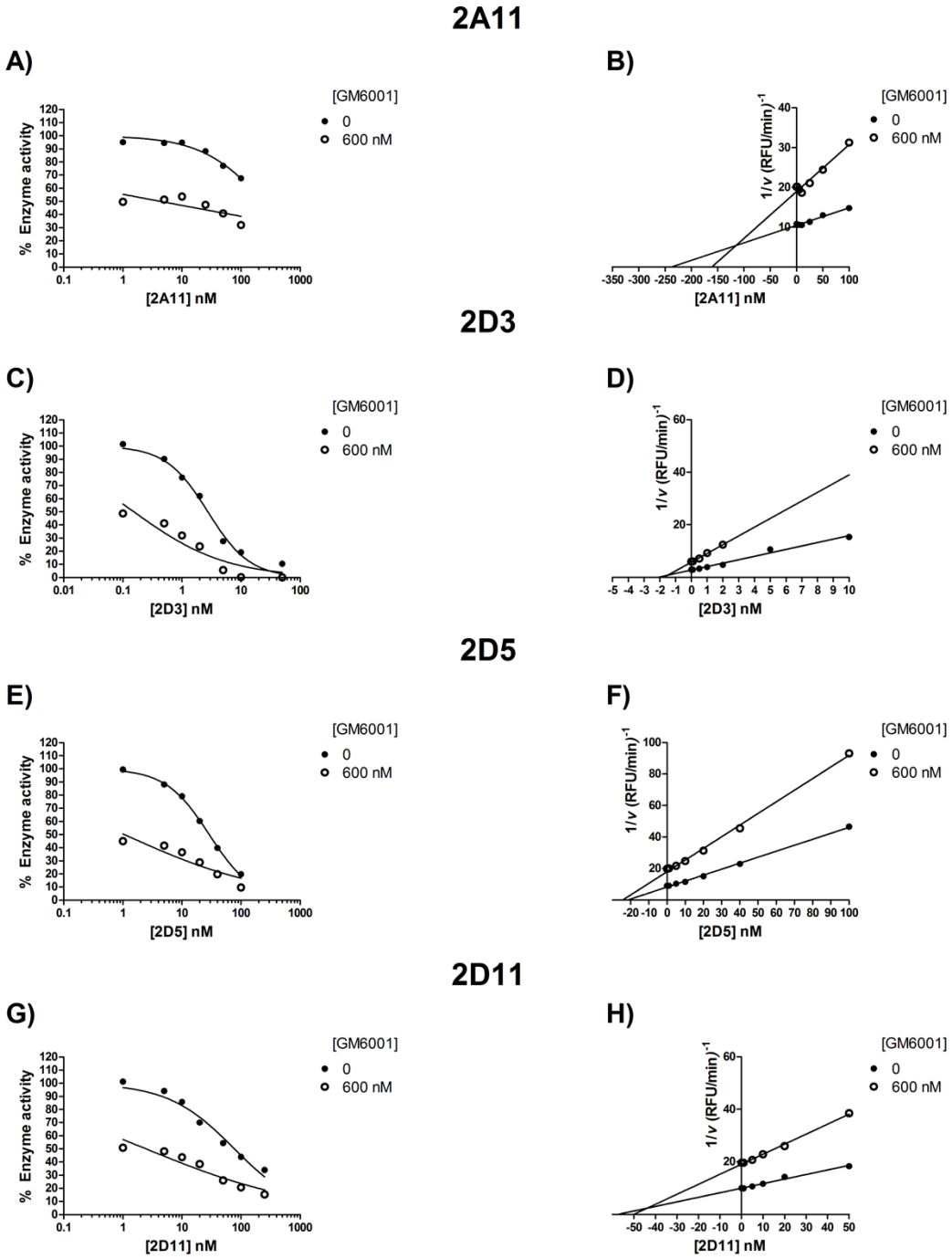

Figure 5.13: Effect of GM6001 on inhibitory potency of anti-ADAMTS-5 scFv-Fc antibodies. Dose-response (left) and Yonetani-Theorell plots (right) for ADAMTS-5 inhibition by 2A11 **(A, B)**, 2D3 **(C, D)**, 2D5 **(E, F)**, and 2D11 **(G, H)** scFv-Fc antibodies in the absence and presence of a fixed concentration (600 nM) of GM6001. Concentration of enzyme was 5 nM for all scFv-Fc antibodies except 2D3. For 2D3, 0.5 nM of enzyme was incubated with substrate for 18 h at 37°C before end-point reading.

Clone	$K_{i\ app}$ (nM)	+GM6001 $K_{i\ app}$ (nM)	Phage display selection
2A11	250 ± 50	140 ± 20	+/- GM6001
2D3	2.8 ± 0.2	1.6 ± 0.2	+ GM6001
2D5	30 ± 0.6	32 ± 0.5	+ GM6001
2D11	77 ± 10	70 ± 7	+ GM6001

Table 5.4: $K_{i\ app}$ values (nM) for inhibition of ADAMTS-5 by scFv-Fc antibodies in the presence and absence of GM6001 (600 nM). Data are $K_{i\ app}$ values of the mean data ± S.E. of the curve fit. In the presence of GM6001, the $K_{i\ app}$ value for the antibodies was measured by fixing as 100 % the activity from the control reaction containing enzyme and GM6001. The presence/absence of GM6001 during the respective phage display selection is reported.

Antibodies 2A11 and 2D3 showed a slight increased inhibitory potency (less than 2-fold) in the presence of GM6001 at a concentration corresponding to its $K_{i\ app}$ under these conditions, whereas no synergistic effect was observed in the case of 2D5 and 2D11. Thus, binding of these antibodies and GM6001 is mutually non-exclusive. Since GM6001 is known to bind to zinc (as well as S1' and other active site cleft sites), these antibodies most likely act via a non zinc-binding mechanism or do not share an epitope deep in the active site cleft. This can be explained on the basis of a noncompetitive/uncompetitive inhibition mode where inhibition of peptide cleavage still allows for GM6001 access to the active site cleft. Intriguingly, antibodies 2D3, 2D5 and 2D11 were all isolated from phage display selections performed in the presence of GM6001, whereas antibody 2A11 was isolated in multiple copies independently of the presence/absence of GM6001 **(Table 5.4)**. This underlies the potency and versatility of phage display conditions for isolation of antibodies with desired properties, in this case an allosteric mechanism of inhibition. Exosite antibody 2B9, which was isolated from phage display selection in the absence of GM6001, did not show any effect in this assay **(Figure 5.14)**. In fact, $K_{i\ app}$ values for inhibition of ADAMTS5-2 by GM6001 in the presence and absence of 2B9 were 510 ± 40 and 490 ± 34, respectively. In this case, 2B9 was used at a concentration equivalent to its K_D value, as measured by SPR **(Table 5.2)**. However, I cannot exclude that higher antibody concentrations may affect the inhibitory potency of GM6001 for ADAMTS5-2.

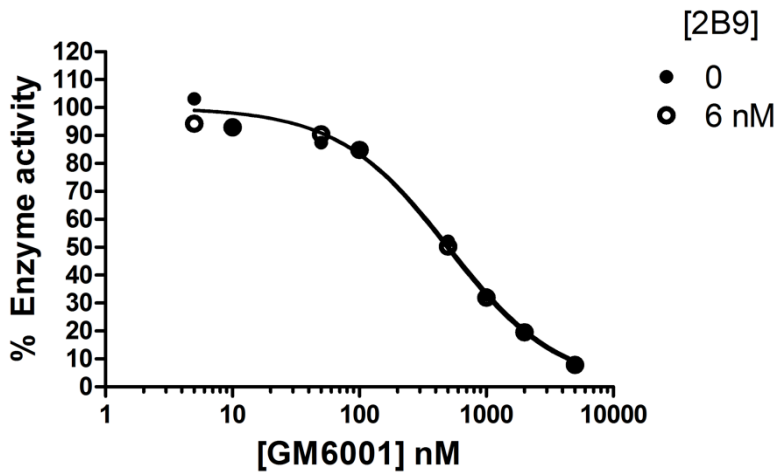

Figure 5.14: Dose-response for ADAMTS-5 inhibition by GM6001 in the absence and presence of a fixed concentration (6 nM) of 2B9 antibody. Concentration of enzyme was 5 nM.

5.7.2. Effect of heparin

Inhibition mechanisms determined with a peptide substrate not only suffer from the drawbacks discussed in **Section 5.6** but also may not correctly describe the mechanism of inhibition when the native (macromolecular) substrate is used. This is because potential interactions between the substrate and enzyme exosites are abolished. As discussed in **Section 1.3.2**, interactions between GAGs of aggrecan and ADAMTS-5 are important for aggrecan cleavage. To simulate the effect of GAGs on antibody activity, heparin was co-incubated with ADAMTS-5 and scFv-Fc antibodies prior to adding the QF substrate. The concentration of heparin was 50 μg/ml (assuming a molecular weight of 15 kDa, this corresponds to 3.33 μM). At this concentration, heparin did not inhibit cleavage of QF peptide by ADAMTS5-2 **(Figure 5.15)**. However, the $K_{i\ app}$ value for inhibition of ADAMTS-5 cleavage of an IGD substrate by heparin is 20 μg/ml (Troeberg et al., 2008).

Addition of heparin at 50 μg/ml did not produce any significant effect on the inhibitory potency of scFv-Fc antibodies 2D3, 2D5, 2D11 **(Figure 5.16 and Table 5.5)**. Moreover, combination of antibody 2B9 (which does not inhibit cleavage of QF peptide) with heparin did not result in any inhibition of ADAMTS-5 in this assay **(Figure 5.17)**.

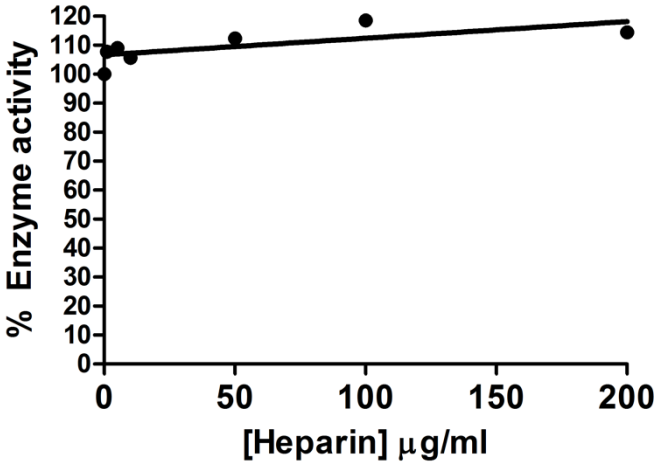

Figure 5.15: Effect of heparin on ADAMTS-5 cleavage of QF peptide. ADAMTS5-2 (5 nM) was incubated with different concentrations of heparin for 2 h and residual activity against Abz-TESE~SRGAIY-Dpa-KK (1 h, 37°C) was determined.

Clone	$K_{i\ app}$ (nM)	+Heparin $K_{i\ app}$ (nM)
2D3	1.7±0.2	1.4 ± 0.3
2D5	17 ± 1.5	14 ± 0.3
2D11	72 ± 14	80 ± 14

Table 5.5: $K_{i\ app}$ values (nM) for inhibition of ADAMTS-5 by scFv-Fc in the presence and absence of heparin (50 µg/ml). Data are $K_{i\ app}$ values of the mean data ± S.E. of the curve fit.

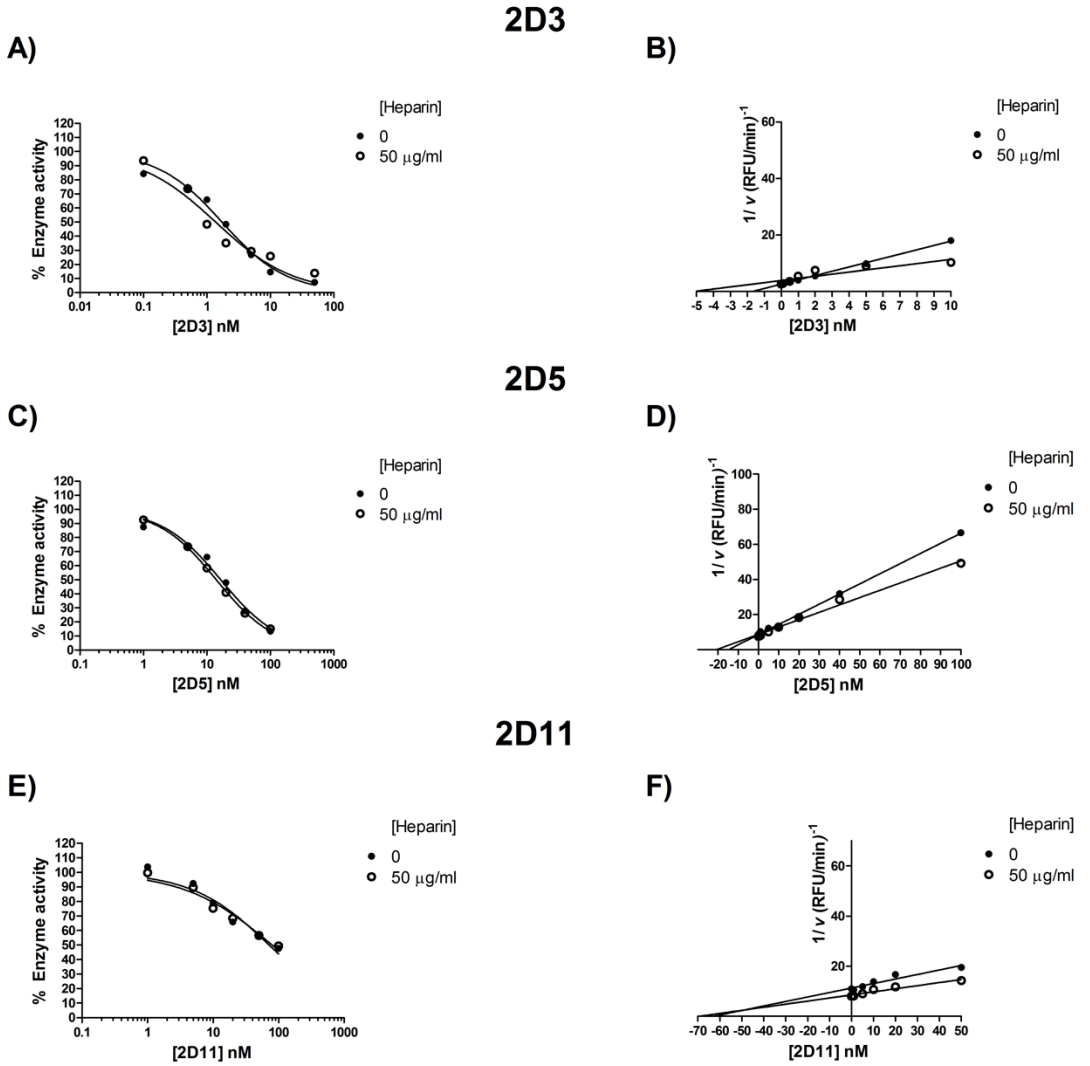

Figure 5.16: Heparin does not affect inhibitory potency of scFv-Fc antibodies on ADAMTS-5. Dose-response (left) and Yonetani-Theorell plots (right) for ADAMTS-5 inhibition by 2D3 (A, B), 2D5 (C, D), and 2D11 (E, F) scFv-Fc antibodies in the absence and presence of a fixed concentration (50 μg/ml) of heparin. Concentration of enzyme was 5 nM for all scFv-Fc antibodies except 2D3. For 2D3, 0.5 nM of enzyme was incubated with substrate for 18 h at 37°C before end-point reading.

A solid-phase binding assay was used to evaluate whether scFv-Fc antibodies were able to bind to heparin-bound ADAMTS-5. Heparin was coated onto multi-well plates (Mahoney et al., 2004) and subsequent binding of ADAMTS5-2 or ADAMTS5-5 was quantified using an antibody against their C-terminal FLAG. ADAMTS5-2 bound strongly to immobilised heparin, whereas binding was much reduced in the case of ADAMTS5-5 by deletion of Sp, CysR and TS-1 domains, as previously reported (Troeberg et al., 2012) **(Figure 5.18 A)**. The CysR domain of ADAMTS-5 is the primary site for interaction with the sulphated polysaccharide chains of aggrecan (Gendron et al., 2007). Approximately 40 nM ADAMTS5-5 were necessary to generate the same signal of 10 nM ADAMTS5-2 on this solid-phase ELISA **(Figure 5.18 B)**.

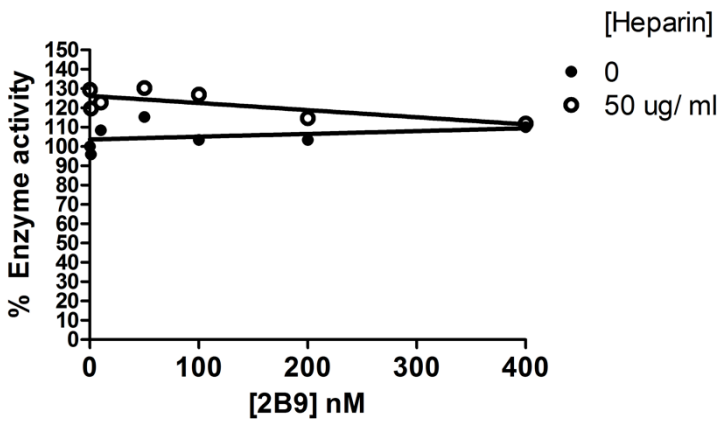

Figure 5.17: Combination of antibody 2B9 with heparin does not affect ADAMTS-5 cleavage of QF peptide. ADAMTS5-2 (5 nM) was incubated with different concentrations of 2B9 for 2 h in the absence and in the presence of a fixed concentration (50 µg/ml) of heparin and residual activity against Abz-TESE~SRGAIY-Dpa-KK (1 h, 37°C) was determined.

Binding of scFv-Fc antibodies to heparin-bound ADAMTS5-2 (10 nM) and ADAMTS5-5 (40 nM) was then quantified using an HRP-conjugated anti-human IgG antibody. Antibodies 2B9, 2D3, 2D5, and 2D11 were all able to bind to ADAMTS-5 under these conditions, confirming that heparin-binding sites on ADAMTS-5 do not overlap with the respective epitopes on the enzyme surface **(Figure 5.18 C-F)**. It is likely that other GAGs such as CS/KS chains which are attached on aggrecan would not affect binding of scFv-Fc antibodies to ADAMTS-5, although the effect of the aggrecan protein core on antibody binding has not been examined. Some differences between antibodies were remarkable. Antibodies 2D3 and 2D11 bound with essentially the same affinity to both ADAMTS5-2 and ADAMTS5-5, but antibody 2D5 bound to ADAMTS5-5 with a drastic decrease in affinity and antibody 2B9 was essentially unable to bind to ADAMTS5-5. These data confirmed Biacore data where antibodies 2D3 and 2D11 recognised the Cat/Dis domains, 2B9 the Sp, and antibody 2D5 bound to ADAMTS5-5 with decreased affinity compared with ADAMTS5-2 **(Table 5.2)**.

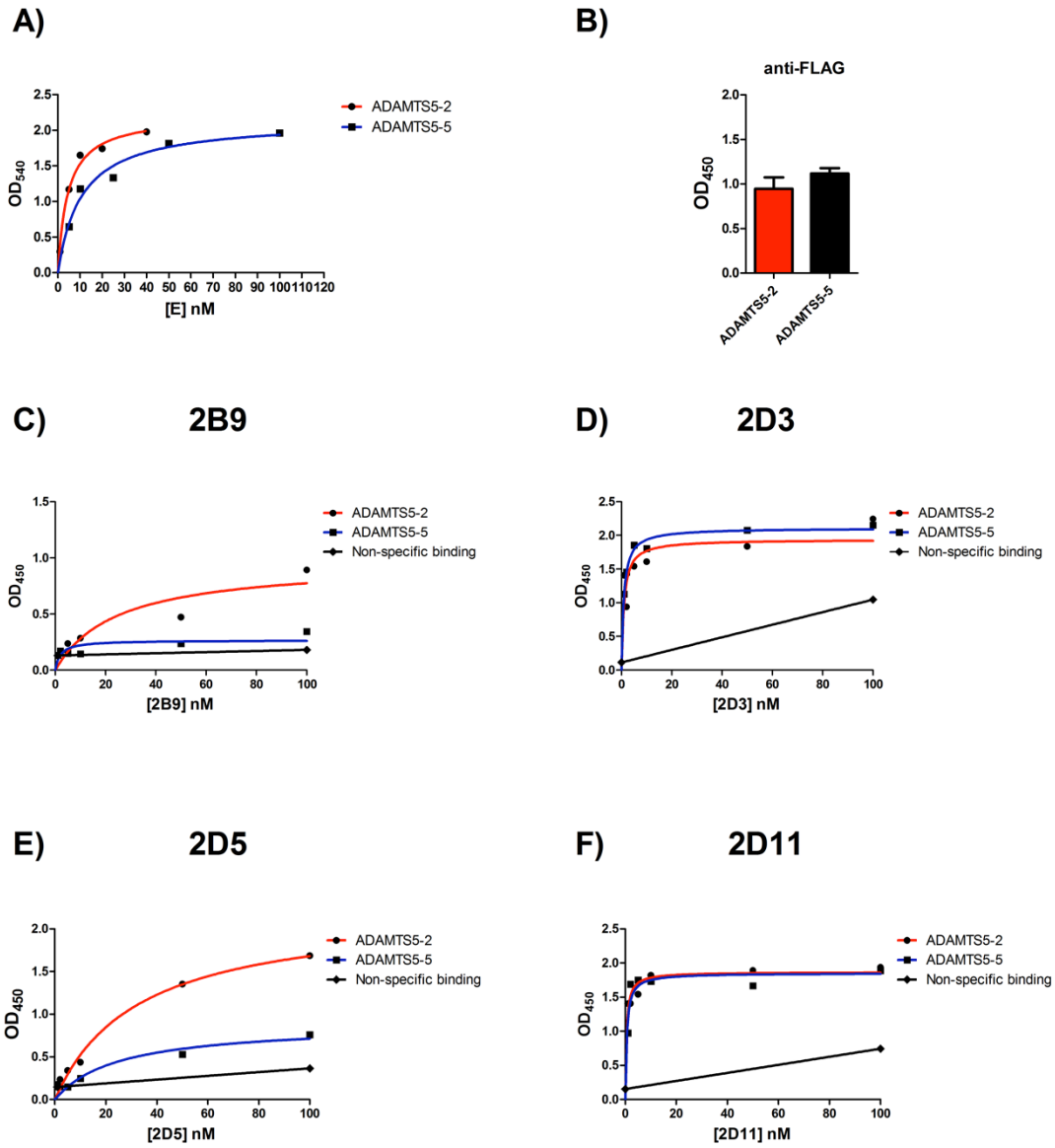

Figure 5.18: Binding of scFv-Fc antibodies to GAG-bound ADAMTS-5. A) Heparin (10 µg/ml) was immobilised on GAG-binding plates and subsequent binding of ADAMTS5-2 or ADAMTS5-5 was detected by anti-FLAG and HRP-conjugated anti-mouse antibody. **B)** 10 nM ADAMTS5-2 produced the same signal of 40 nM ADAMTS5-5. **C-F)** Binding of antibodies 2B9, 2D3, 2D5, and 2D11 to ADAMTS5-2 (10 nM), ADAMTS5-5 (40 nM) or heparin (non-specific binding) was detected by HRP-conjugated anti-human IgG. OD, optical density.

5.7.3. Effect of TIMP-3

TIMP-3 is an endogenous inhibitor of ADAMTS-5 and -4 (Gendron et al., 2003); we therefore investigated whether lead antibodies share an overlapping epitope with TIMP-3 (**Figure 5.19 and Table 5.6**). When antibodies were incubated in the presence of TIMP-3, the Yonetani-Theorell plot produced non-parallel lines of best fit for 2D5 and 2D11, indicating mutually non-exclusive binding by TIMP-3 and each of these antibodies, whereas for 2A11 and 2D3 the parallel lines indicate mutual exclusive binding with TIMP-3. In the case of 2D11, synergism was observed, with an increase in potency in the presence of TIMP-3 of about 2-fold.

Clone	$K_{i\ app}$ (nM)	+TIMP-3 $K_{i\ app}$ (nM)
2A11	210 ± 70	> 300
2D3	3.2 ±0.3	> 400
2D5	15 ± 0.3	11 ± 0.3
2D11	60 ± 10	35 ± 6

Table 5.6: $K_{i\ app}$ values (nM) for inhibition of ADAMTS-5 by scFv-Fc antibodies in the presence and absence of TIMP-3. Data are $K_{i\ app}$ values of the mean data ± S.E. of the curve fit. In the presence of TIMP-3, the $K_{i\ app}$ values were measured by fixing as 100 % the activity from the control reaction containing enzyme and TIMP-3.

In order to examine the effect on TIMP-3 potency, titrating concentrations of TIMP-3 were incubated in the presence of a fixed concentration of each antibody **(Figure 5.20 and Table 5.7)**. The $K_{i\ app}$ value for ADAMTS5-2 inhibition by TIMP-3 was in line with the published value of 0.72 ± 0.17 nM (Troeberg et al., 2009). In the presence of 2D3, an antagonist effect was observed, again indicating mutually exclusive binding; quite surprisingly, the same was observed also in the case of anti-Sp antibody 2B9. On the other hand, antibodies 2D5 and 2D11, at a concentration equivalent to their $K_{i\ app}$ value, enhanced inhibitory potency of TIMP-3. Accurate determinations of the improved $K_{i\ app}$ were not possible, as ADAMTS-5 concentrations below 0.5 nM cannot be reliably assayed with the currently available QF substrate.

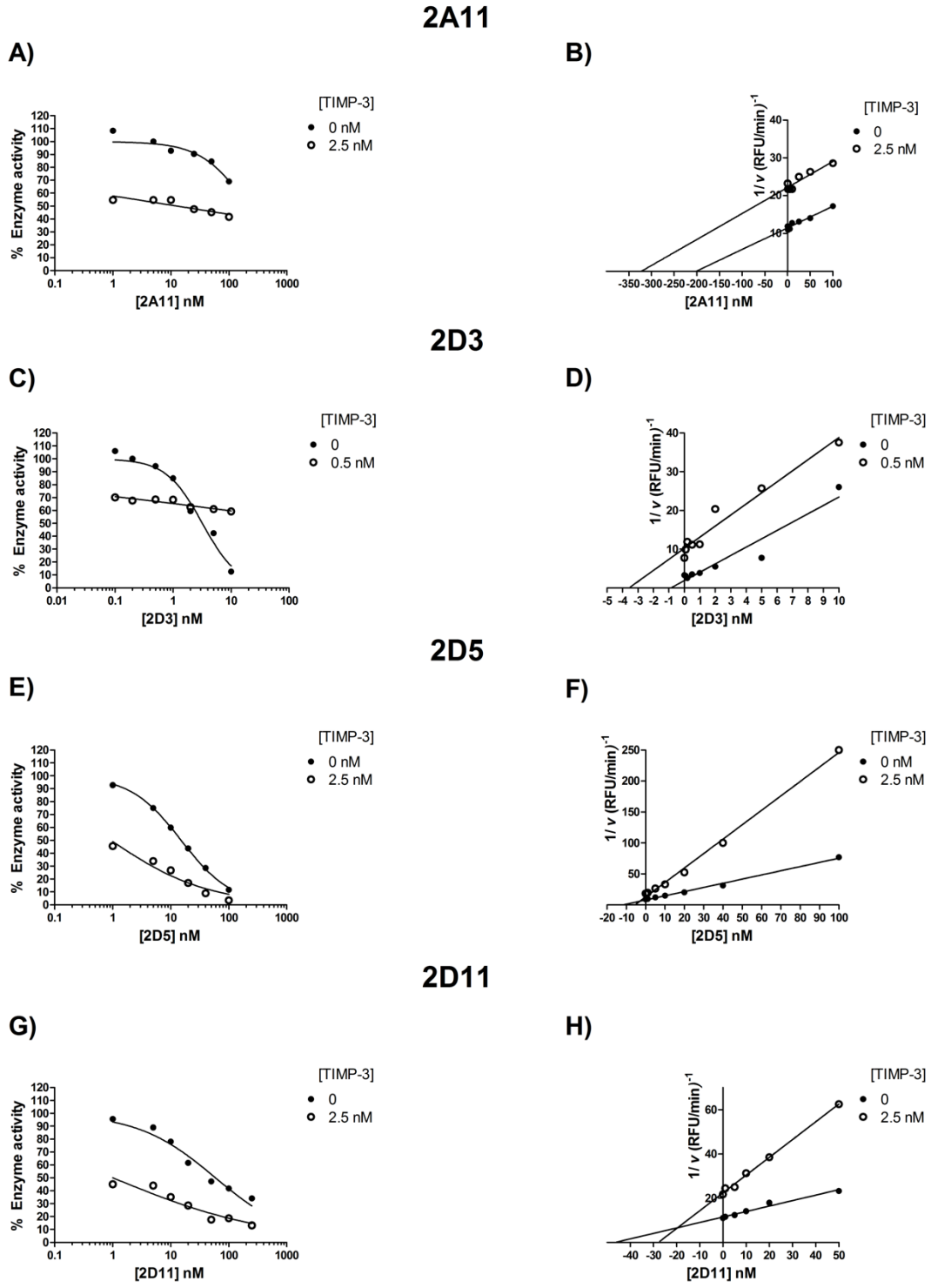

Figure 5.19: Dose-response (left) and Yonetani-Theorell plots (right) for ADAMTS-5 inhibition by 2A11 (A, B), 2D3 (C, D), 2D5 (E, F), and 2D11 (G, H) scFv-Fc antibodies in the absence and presence of a fixed concentration (2.5 nM) of TIMP-3 (5 nM ADAMTS5-2). Since 2D3 is a tight-binding inhibitor, 0.5 nM enzyme and 0.5 nM TIMP-3 were used and rates against Abz-TESE~SRGAIY-Dpa-KK (18 h, 37°C) were determined.

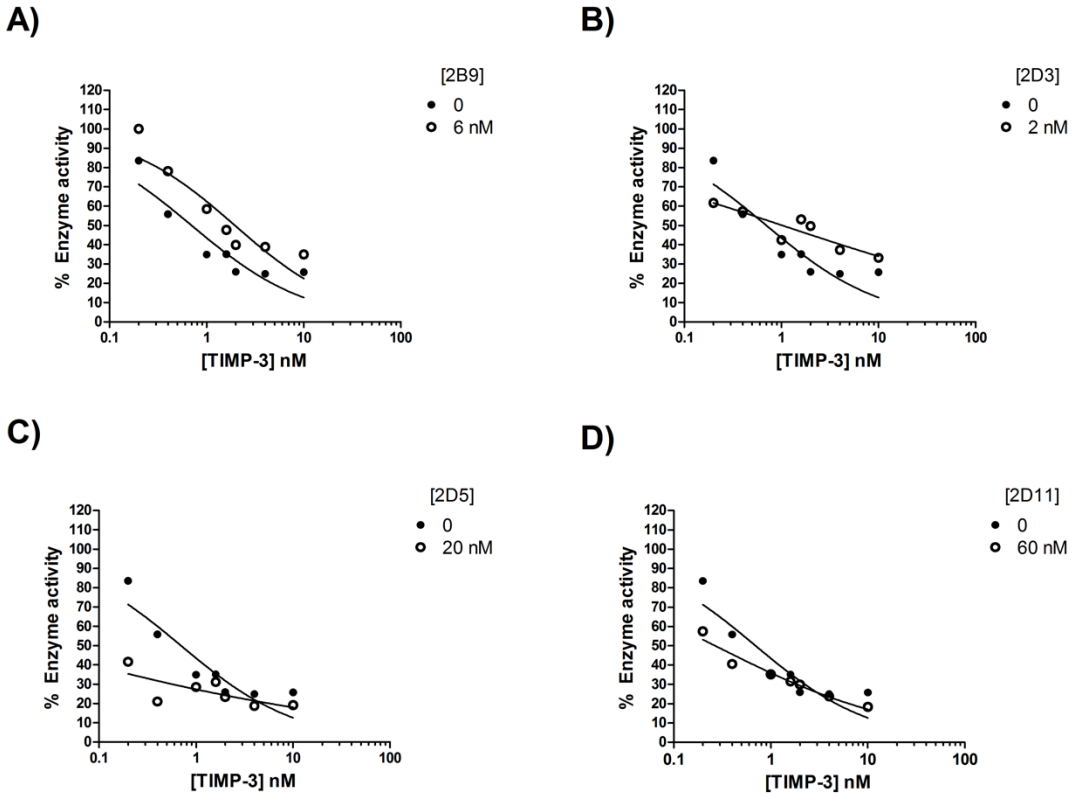

Figure 5.20: Effect of antibodies 2B9 (A, 6 nM), 2D3 (B, 2 nM), 2D5 (C, 20 nM), and 2D11 (D, 60 nM) on TIMP-3 inhibition of ADAMTS-5. ADAMTS5-2 (0.5 nM) was incubated with TIMP-3 (0.2-10 nM) and a fixed concentration of scFv-Fc antibodies and residual activity against Abz-TESE~SRGAIY-Dpa-KK was determined (18 h, 37°C). Note: at this antibody concentration residual activity in the absence of TIMP-3 is around 70%.

	$K_{i\ app}$ (nM)
TIMP-3	0.70 ± 0.16
+2B9	2.0 ± 0.4
+2D3	4.5 ± 1.5
+2D5	<0.4
+2D11	~0.3

Table 5.7: $K_{i\ app}$ values (nM) for inhibition of ADAMTS-5 by TIMP-3 in the presence and absence of scFv-Fc antibodies. The activity from the control reaction containing the enzyme and the fixed concentration of scFc-Fv (6 nM for 2B9, 2 nM for 2D3, 20 nM for 2D5 and 60 nM for 2D11) was fixed as 100 %.

To determine if scFv-Fc antibodies 2B9, 2D3, 2D5 and 2D11 were able to bind to ADAMTS-5 in the presence of TIMP-3, a co-immunoprecipitation experiment was performed **(Figure 5.21)**. scFv-Fc antibodies were bound to protein G-paramagnetic beads and successively incubated with ADAMTS5-2 in the presence and in the absence of TIMP-3 (1:1 enzyme/TIMP-3 ratio). Both ADAMTS-5 and ADAMTS-5/TIMP-3 complex were precipitated by 2D5 and 2D11 but not by an isotype scFv-Fc control. 2D3 was able to pull-down ADAMTS5-2 and ADAMTS5-

2/TIMP-3 complex, but also to a certain degree TIMP-3 alone. Since a faint band was detected also in the TIMP-3 alone control in the case of 2D5 by anti-TIMP-3 probing, the observed band is likely due to non-specific binding between antibody and TIMP-3. Unfortunately, the anti-Sp antibody 2B9 underwent degradation under these assays conditions **(Figure 5.21)** such that it was not possible to assess its ability to immunoprecipitate ADAMTS-5 or ADAMTS-5/TIMP-3 complex. The reasons for degradation are not known; I cannot exclude that a protease contamination occurred.

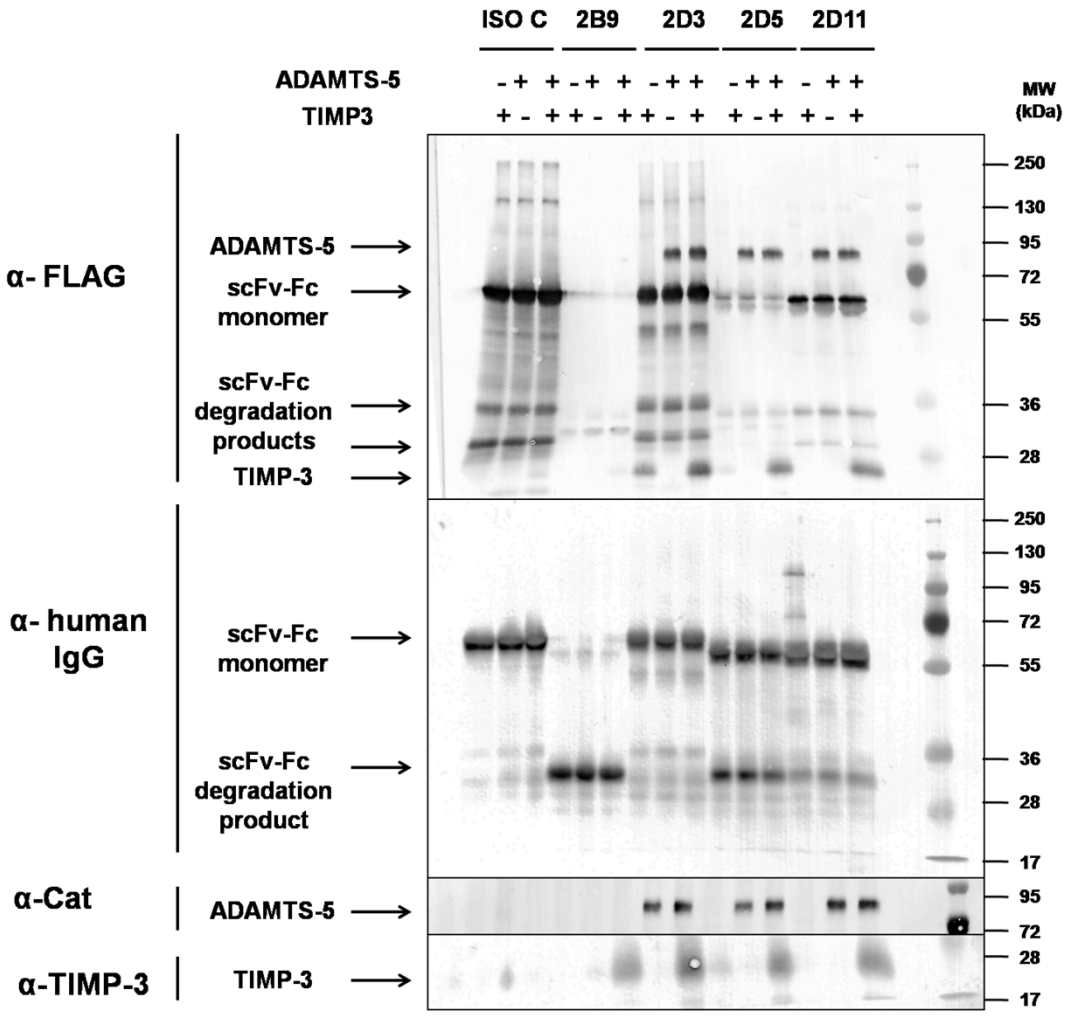

Figure 5.21: Co-immunoprecipitation of ADAMTS-5/TIMP-3 complex by anti-ADAMTS-5 scFv-Fc antibodies. Antibodies 2B9, 2D3, 2D5, 2D11 and an isotype scFv-Fc control (Iso C) were bound to protein G-coated paramagnetic beads and used to pull-down ADAMTS5-2 (100 nM) in the presence and absence of an equimolar concentration of TIMP-3 (100 nM). Samples were subjected to SDS-PAGE under reducing conditions and immunoblotting. Membranes were probed with anti-FLAG M2 mAb, anti-human IgG antibody, polyclonal rabbit-anti ADAMTS-5 Cat domain antibody or anti-TIMP-3 mAb. Arrows indicate protein bands.

5.7.4. Effect of antibody combination

If two lead scFv-Fc antibodies bind to different epitopes on ADAMTS-5, they will exhibit synergism (increase in inhibitory potency which should reflect an increase in affinity) when added simultaneously to the enzyme solution. This is particularly important in view of a potential

therapeutic application. To investigate if a combination of two anti-ADAMTS-5 scFv-Fc antibodies is more effective than a single antibody taken individually, double inhibitor studies were performed using the QF peptide substrate. 2B9 is the only antibody among the characterised leads which is not able to bind to ADAMTS-5 Cat/Dis domain; moreover, it does not inhibit QF peptide cleavage but inhibits the aggrecanase activity of ADAMTS-5. When used at a concentration near its K_D value (5 nM), 2B9 showed a synergistic effect with antibodies 2A11, 2D3, 2D5 and 2D11 **(Figure 5.22)**. The increase in inhibitory potency in the presence of 2B9 was ~ 2-fold for 2A11, 2D3 and 2D11 and ~ 3-fold for 2D5 **(Table 5.8)**.

Clone	$K_{i\ app}$ (nM)	+2B9 $K_{i\ app}$ (nM)
2A11	170 ± 22	97 ± 2
2D3	2.3 ± 0.3	1.2 ± 0.1
2D5	17 ± 0.6	5.8 ± 0.7
2D11	61 ± 11	28 ± 3

Table 5.8: $K_{i\ app}$ values (nM) for inhibition of ADAMTS-5 by scFv-Fc antibodies in the presence and absence of 2B9. Data are $K_{i\ app}$ values of the mean data ± S.E. of the curve fit. Note: 2B9 does not inhibit cleavage of QF peptide by ADAMTS-5.

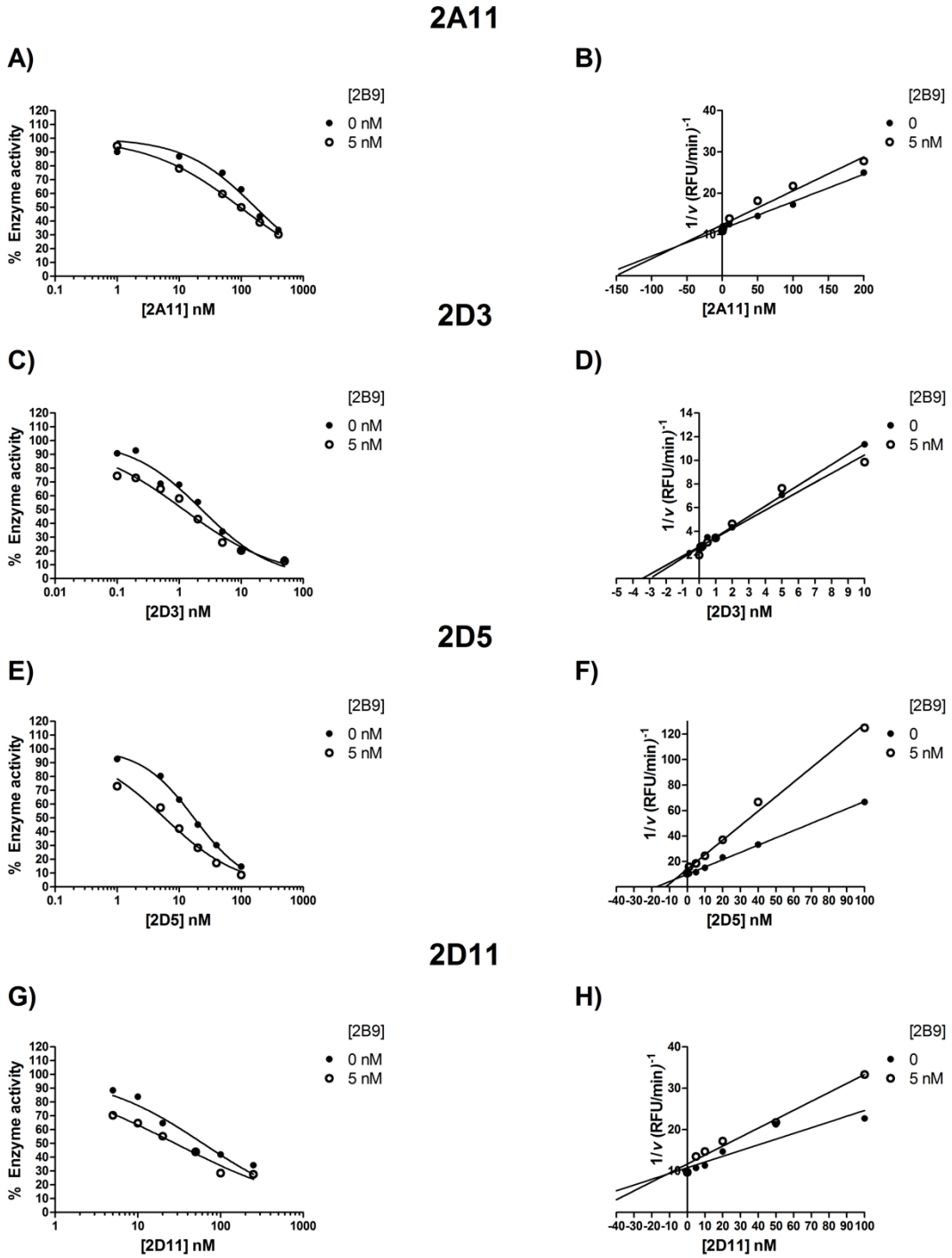

Figure 5.22: Dose-response (left) and Yonetani-Theorell plots (right) for ADAMTS-5 inhibition by 2A11 (A, B), 2D3 (C, D), 2D5 (E, F), and 2D11 (G, H) scFv-Fc antibodies in the absence and presence of a fixed concentration (5 nM) of antibody 2B9. Concentration of enzyme was 5 nM for all scFv-Fc antibodies except 2D3. For 2D3, 0.5 nM of enzyme was incubated with QF peptide substrate for 18 h at 37°C before end-point reading.

On the basis of the SPR data **(Table 5.2)**, antibodies 2D5 and 2D3 show a different ability to bind to the Cat/Dis domain, with 2D5 showing a preference for ADAMTS5-2 over ADAMTS5-5 and 2D3 binding with the same affinity to both enzyme forms. I therefore studied the effect that a combination of these two antibodies had on the reciprocal inhibitory potency **(Figure 5.23)**. The

Yonetani-Theorell plots produced parallel lines of best fit for these two antibodies each in the presence of a fixed concentration of the other, indicating mutually exclusive binding. The increase in $K_{i\ app}$ value for 2D3 was about 3-fold, whereas for 2D5 the increase of $K_{i\ app}$ value in the presence of 2D3 was modest due to the low concentration of 2D3 (corresponding to the $K_{i\ app}$ of 3 nM) relative to the enzyme concentration (5 nM) under the conditions used to test inhibitory activity of 2D5 **(Table 5.9)**.

Clone	$K_{i\ app}$ (nM)	+2D5 $K_{i\ app}$ (nM)	+2D3 $K_{i\ app}$ (nM)
2D3	1.7 ± 0.2	5.2 ± 1.2	-
2D5	16 ± 0.6	-	19 ± 0.8

Table 5.9: $K_{i\ app}$ values (nM) for inhibition of ADAMTS-5 by combination of 2D3 and 2D5 scFv-Fc antibodies. The activity from the control reaction containing the enzyme and the fixed concentration of scFc-Fv (20 nM for 2D5 and 3 nM for 2D3) was fixed as 100 %.

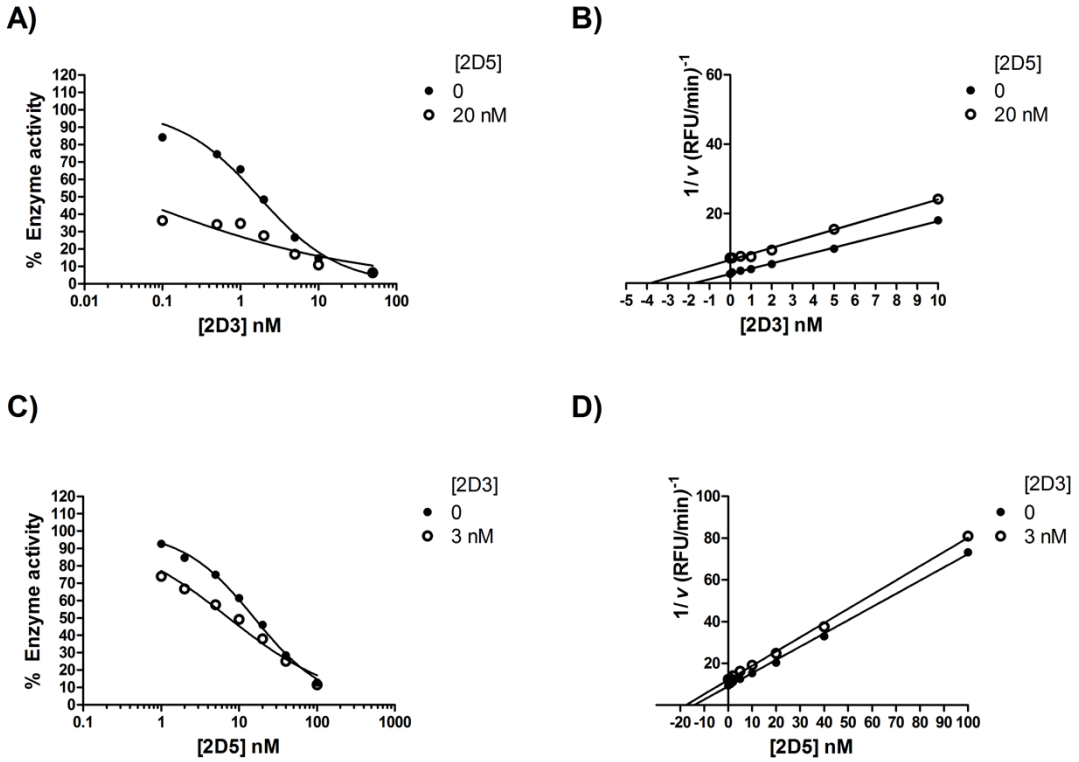

Figure 5.23: Dose-response (left) and Yonetani-Theorell plots (right) for ADAMTS-5 inhibition by 2D3(A,B) and 2D5 (C,D) scFv-Fc antibodies in the absence and presence of a fixed concentration of 2D5 (20 nM) and 2D3 (3 nM), respectively. Concentration of enzyme was 5 nM for 2D5. For 2D3, 0.5 nM of enzyme was incubated with QF peptide substrate for 18 h at 37°C before end-point reading.

5.8. Effect of scFv-Fc antibodies on aggrecan breakdown in cartilage explants treated with IL-1 and OSM

As was discussed in **Chapter 1**, aggrecanases are the main proteinases involved in cartilage degradation in stimulated cartilage explants (Sandy et al., 1991; Arner et al., 1998; Little et al., 1999). We therefore investigated the ability of ADAMTS-5 inhibitory antibodies 2B9, 2D3, 2D5, and 2D11 to inhibit stimulated aggrecanase activity in porcine and human articular cartilage explants. As controls, the non-inhibitory anti-ADAMTS-5 antibody 1B3 **(See Section 4.4.2)** and an isotype scFv-Fc antibody (directed against desmin) were used. Donor details for human explants are reported in **Table 5.10.**

Patient	Age	Sex	Pathology	OA	Explant source
N104	49	F	Spindle cell sarcoma Hip replacement	Moderate	Knee
N108			Data not available		Knee
N110	47	M	Chondrosarcoma	Absent	Knee

Table 5.10: Clinical data for knee explant donors.

Porcine and human articular cartilage explants were stimulated with IL-1α (10 ng/ml) and OSM (50 ng/ml) in the presence or absence of scFv-Fc antibodies (1μM) and N-TIMP-3 (0.1 μM) for 24 h and then the medium was analysed for the presence of GAGs and aggrecanase-generated aggrecan fragments by dimethylmethylene blue (DMMB) assay (Farndale et al., 1986).

Porcine articular explants treated with IL-1α/OSM alone showed approximately 2-fold increase in GAG release over controls after 24 h of stimulation **(Figure 5.24 A)**. In the case of human articular explants this increase was approximately 3-fold **(Figure 5.24 B)**.

The IL-1α-stimulated release from both porcine and human explants was inhibited by N-TIMP-3 to the basal level as previously reported (Gendron et al., 2003); however, a negative isotype control (anti-desmin scFv-Fc), as well as anti-ADAMTS-5 scFv-Fc antibodies 1B3, 2B9, 2D3, 2D5 and 2D11 were not effective. The basal level of GAG-release was not increased in the presence of scFv-Fc antibodies **(Figure 5.24)**.

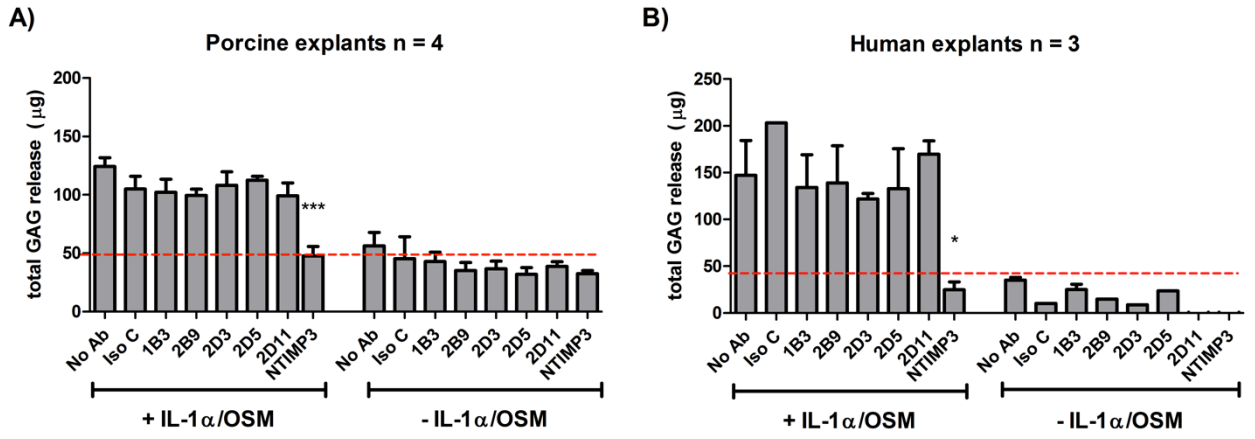

Figure 5.24: Inhibition of GAG release by scFv-Fc antibodies. Porcine **(A)** and human **(B)** articular cartilage explants were incubated with DMEM with or without 10 ng/ml IL-1α and 50 ng/ml OSM plus scFv-Fc antibodies (1 µM) or N-TIMP-3 (0.1 µM) for 24 h. The GAG content released into the media was measured using the DMMB assay. The results are from 4 (A) or 3 (B) separate experiments ± S.E.M. (three pieces of cartilage for each condition). *P<0.05; ***P < 0.001 as compared with the IL-1α/OSM treatment without antibody. Iso C, isotype control.

Conditioned media from these experiments were analysed by Western blot analysis using a mAb that recognises the aggrecanase-generated neoepitope ARGSV **(Figures 5.25 and 5.26)**. Although Western blot is not as sensitive as methods such as ELISA, the advantage with this technique is that it discriminates between different proteolytic fragments carrying the same epitope. In concordance with the GAG release data, there was an increase in the amount of aggrecanase-generated fragments released upon treatment with IL-1α/OSM from both porcine and human explants. In both cases, the release of aggrecanase-generated fragments was completely blocked by 0.1 µM N-TIMP-3. In porcine explants, the isotype antibody control showed approximately 50% inhibition of aggrecanase-generated fragments in porcine explants cultures. Although desmin is reported as a muscle marker, it is still possible that porcine chondrocytes express an antigen sharing homology with desmin and that this antigen is recognised by the anti-desmin antibody. Alternatively, we cannot rule out a non-specific effect mediated by the Fc portions of the antibodies in porcine explants. On the other hand, the anti-ADAMTS-5 non-inhibitory antibody 1B3, showed only a modest (approximately 25%) reduction in aggrecanase-generated fragments and was thus used as a control for porcine explants. Antibodies 2B9, 2D3 and 2D5, but not 2D11, showed a significant inhibition of aggrecanase-generated fragments compared with antibody 1B3 in porcine explants **(Figure 5.25)**. This efficacy is in contrast with the GAG release data **(Figure 5.24)** and can be explained on the basis of specific inhibition of ADAMTS-5.

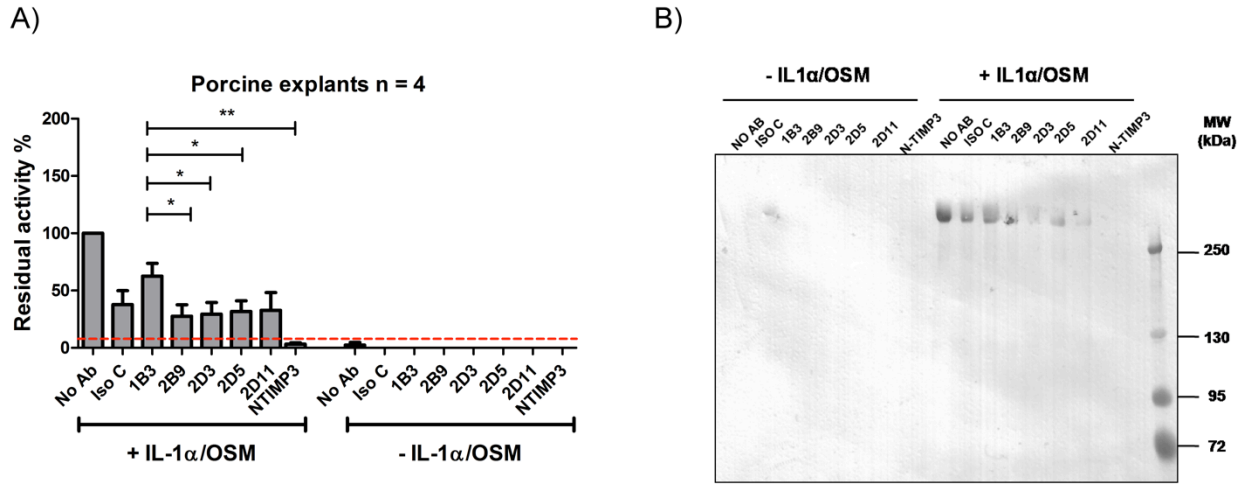

Figure 5.25: Analysis of aggrecan degradation in conditioned media from IL-1α/OSM-stimulated porcine articular cartilage. The conditioned media from porcine articular cartilage explants treated with IL-1α/OSM were deglycosylated and analysed by Western blotting with anti-ARGSV neoepitope antibody BC3. **A)** Densitometric analysis of Western blot. Intensity of anti-ARGSV reactive band is plotted as percentage of residual activity of untreated explants. *P<0.05; **P < 0.005 as compared with the IL-1α/OSM treatment with the control antibody 1B3. The results are from 4 separate experiments ± S.E.M. (three pieces of cartilage for each condition). **B)** A representative Western blot is shown.

In the conditioned medium from human samples **(Figure 5.26)**, two main ARGSV-cross reactive bands were observed, one at around 310 kDa, corresponding in size to the ^{393}ARGSV---SELE^{1564} fragment and a lower band at around 130-160 kDa corresponding to ARGSV-fragments produced by multiple cleavage in the CS-1 domain (Struglics et al., 2006). The presence of further anti-ARGSV-reactive fragments at low molecular weight is distinctive of human samples. Conditioned media from human knee cartilage showed a significant inhibition of the ^{393}ARGSV---SELE^{1564} aggrecanase-generated fragment after treatment with IL-1α/OSM in the presence of antibodies 2B9 and 2D3 (approximately 60% inhibition), whereas antibodies 1B3, 2D5 and isotype control had no effect. Surprisingly, antibody 2D11 showed a highly significant (approximately 2-fold) increase in the 310-kDa band **(Figure 5.26)**.

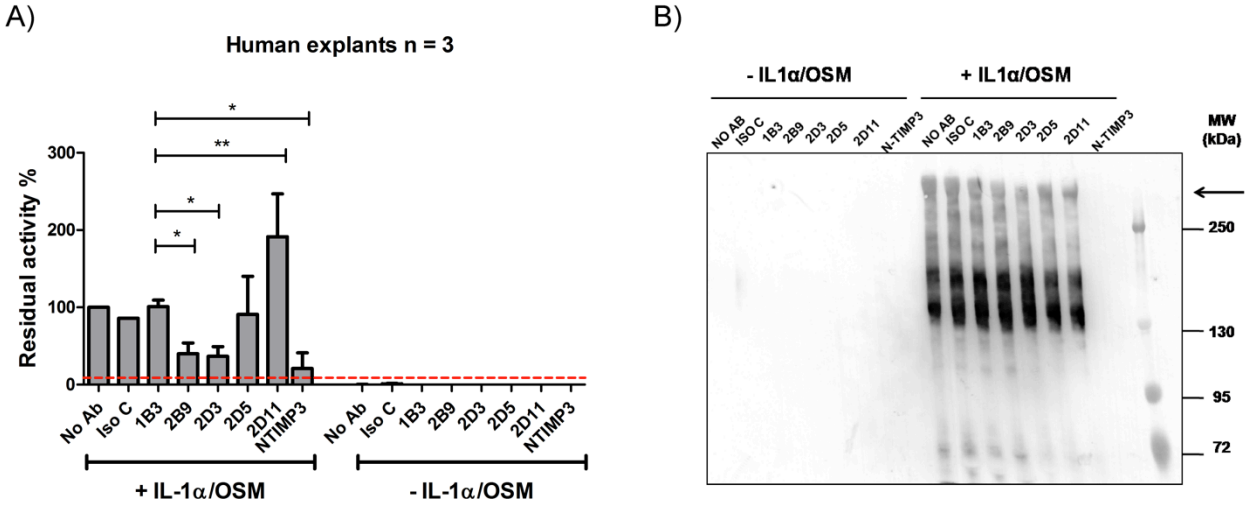

Figure 5.26 (pag 164): Analysis of aggrecan degradation in conditioned media from IL-1α/OSM-stimulated human articular cartilage. The conditioned media from human articular cartilage explants treated with IL-1α/OSM were deglycosylated and analysed by Western blotting with anti-ARGSV neoepitope antibody BC3. **A)** Densitometric analysis of Western blot. Intensity of anti-ARGSV reactive band is plotted as percentage of residual activity of untreated explants. *P<0.05; **P < 0.005 as compared with the IL-1α/OSM treatment with the control antibody 1B3. The results are from 3 separate experiments ± S.E.M. (three pieces of cartilage for each condition). **B)** A representative Western blot for one patient is shown.

5.9. Discussion

In this chapter, I characterised the inhibitory mechanisms and epitopes of scFv-Fc antibodies 2A11, 2B9, 2D3, and 2D11 and tested their efficacy in an *ex vivo* model of cartilage degradation. Antibodies 2D3, 2D5 and 2D11 inhibited ADAMTS-5 cleavage both of a QF peptide and bovine aggrecan. Notably, no inhibition of ADAMTS-4 or MMPs was observed**,** indicating that these antibodies are specific for ADAMTS-5 (**Table 5.1**). Antibody 2B9 was only able to inhibit the enzyme activity against aggrecan so we speculated that it might act as an exosite inhibitor.

SPR studies using different deletion mutants of ADAMTS-5 allowed us to map the specific domain(s) which constitute(s) the epitope of these antibodies. The absence of binding to ADAMTS-4 on SPR confirmed that these antibodies are truly specific for ADAMTS-5 **(Table 5.2)**. The putative domains of ADAMTS-5 recognised by anti-ADAMTS-5 lead antibodies are reported in **Figure 5.27**. Antibodies 2D3 and 2D11 recognised the Cat/Dis domain of ADAMTS-5; 2D5, although still recognising the Cat/Dis domain, showed a preference for ADAMTS5-2. For 2B9 the Sp domain is crucial for binding to ADAMTS-5 **(Table 5.2 and Figure 5.27)**. These data were essentially confirmed by Western blot analysis of ADAMTS-5 deletion forms where scFv-Fc antibodies were used as primary antibodies **(Figure 5.10)**. 2B9 was still able to recognise the ADAMTS5-3 and 5-4 on Western blots, suggesting further contacts with CysR and TS-1 domains. However, from the SPR data it is evident that binding to these forms of ADAMTS-5 is at least 100-fold less effective after removal of the Sp domain **(Table 5.2)**. 2B9 is therefore similar to CRB0017 mAb, developed by the Rottapharm group (Visintin et al., 2012). CRB0017 is specific for the Sp domain of ADAMTS-5 with a K_D value in the low nanomolar range; moreover, it inhibits proteolytic activity of the enzyme *in vitro* with a $K_{i\ app}$ value in the low nanomolar range (Visintin et al., 2012) and has been found protective in a murine model of spontaneous OA (Chiusaroli et al., 2013).

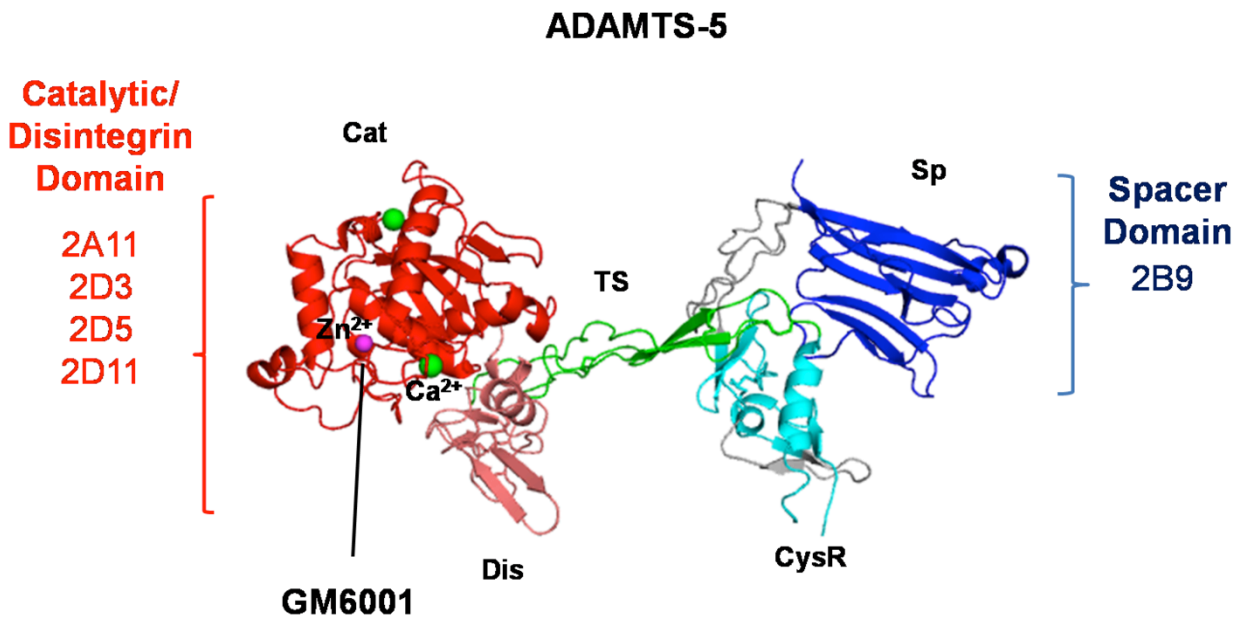

Figure 5.27: Schematic representation of domains recognised by anti-ADAMTS-5 antibodies. The figure shows crystal structures of ADAMTS-5 Cat (red)/ Dis (salmon) domains (pdb entry 2RJQ) aligned with the TS (green), Cys-R (sky blue) and Sp (blue) domains from crystal structure of ADAMTS-13 (pdb entry 3GHN). Main epitopes as well as catalytic zinc ion (pink) chelated by GM6001 and calcium ions (green) are outlined.

The ability of exosite antibody 2B9 to inhibit ADAMTS-5 cleavage at the $Glu^{392}\downarrow^{393}Ala$ site of bovine aggrecan suggests that this antibody exerts its inhibitory potency by impairing binding of ADAMTS-5 to the aggrecan molecule through its Sp domain. At least 32 residues at the N-terminal of the cleavage site (P residues of the substrate) and 13 residues at the C-terminal side (P' residues) are required for cleavage at the $Glu^{392}\downarrow^{393}Ala$ bond by aggrecanases (Hörber et al., 2000). Thus these sequences serve as further sites of interaction between the enzyme and its substrate. Unlike aggrecanases, MMPs require just 8 amino acid N-terminal and 8 amino acids C-terminal to the aggrecanase site to cleave efficiently at the $Glu^{392}\downarrow^{393}Ala$ bond (Horber et al., 2000). In the case of serine proteases, several works have suggested that interactions between substrate and enzyme far away from the active site may be important for catalysis by properly aligning the substrate in the active site cleft (Hedström, 2002). These remote interactions can propagate down the peptide chain, resulting in significant effects on the stabilisation of the transition state (Hedström, 2002). It may be possible that the same effect is produced by anti-ADAMTS-5 exosite antibodies such as 2B9. However it would be interesting to test whether 2B9 is able to inhibit cleavage in the CS-2 domain of aggrecan.

I was not able to unequivocally establish the mechanism of inhibition of QF peptide cleavage by varying the concentrations of substrate (**Figure 5.12**). One of the limitations with QF peptides is that the solubility of the substrate concentrations well above the K_m of the enzyme are

difficult to reach and the substrate auto-quenches. Moreover, modulation of enzyme activity is substrate-dependent, thus inhibition mechanisms determined with a peptide substrate may not correctly describe the mechanism of inhibition when the native (macromolecular) substrate is used and enzyme exosites are involved. In the case of several coagulation proteases, where exosites play a pivotal role in substrate recognition and specificity, inhibitors competitive with small peptide substrates appear noncompetitive with the native pro-enzyme substrates (Krishnaswamy et al., 2005). In the case of ADAMTS-5, deletion of the Sp or CysR domains severely affects aggrecanase activity both at the IGD and CS-2 regions of aggrecan and the Cat domain alone is devoid of aggrecanase activity, suggesting a pivotal role for exosites in binding and cleavage of aggrecan (Gendron et al., 2007). Wittwer et al. (2007) reported that a hydroxamic acid inhibitor of ADAMTS-4 showed competitive inhibition against a peptide substrate but noncompetitive inhibition against aggrecan. This observation was explained by the ability of peptide-competitive inhibitors to bind both free-enzyme and initial aggrecan-enzyme exosite complex; thus according to this model, interactions between the exosite(s) and aggrecan precede those between active site and aggrecan (Wittwer et al., 2007). Exosite inhibitors such as 2B9 may prevent the formation of the Michaelis complex by blocking the formation of the initial enzyme exosite-substrate complex. According to this model, these inhibitors should act as competitive with the native substrate. In my case, it was difficult with the current semi-quantitative aggrecan digestion assay used here to perform inhibition studies at increasing concentrations of aggrecan. As an alternative, competition with aggrecan could be assessed using recombinant aggrecan fragments, such as the gst-IGD substrate described by Lim et al. (2010).

I then chose to study the effect of GAGs such as heparin on the activity and binding of scFv-Fc antibodies. At 50 μg/ml heparin did not produce any significant effect on inhibition of ADAMTS-5 by these antibodies when the QF peptide was used as a substrate **(Table 5.5 and Figure 5.16)**; moreover, in a solid-phase ELISA, 2B9, 2D3, 2D5 and 2D11 all show saturating binding to ADAMTS-5 bound to heparin-coated wells, suggesting that the epitope recognised by these antibodies is not significantly disturbed by GAG binding **(Figure 5.18)**. These results therefore indicate that the cartilage environment may not affect the enzyme-antibody complexes. Nevertheless, the effects of co-factors such as syndecan-4 (Echtermeyer et al., 2009) and fibulin (Lee NV et al., 2005; McCulloch et al., 2009a), as well as competition with protein core (deglycosylated protein) of aggrecan should be assessed. For example, calcium pentosan polysulphate (CaPPS), a chemically-sulphated xylanopyranose from beechwood, increases the affinity of TIMP-3 for ADAMTS-4 and -5 by more than 100-fold, (Troeberg et al., 2008; Troeberg et al., 2012). Also Wayne et al. (2007) reported that interaction of full-length TIMP-3 with

ADAMTS-4 was enhanced by the presence of aggrecan through binding of GAGs of the substrate to TS and Sp domains of the enzyme. It is noteworthy that in this study the effect of aggrecan on ADAMTS-4 was analysed directly using a QF peptide substrate. This peptide had a K_m value around 10 μM and as little as 10 pM of ADAMTS-4 could be reliably used (Wayne et al., 2007). Unfortunately, in my case ADAMTS-5 has a K_m around 80 μM for its QF peptide substrate, and the minimum enzyme concentration to be used is 0.5 nM with 18 h digestion (Troeberg et al., 2012); on the other hand, this same enzyme concentration readily cleaves bovine aggrecan within 2 h **(See Section 3.3.)** so it is not possible to follow the effect of the simultaneous presence of the substrates on the antibody/enzyme complex.

In our effort to isolate antibodies specific for ADAMTS-5 we then wished to compare the inhibition mechanism of anti-ADAMTS-5 antibodies with that of broad-spectrum hydroxamate small molecule inhibitors such as GM6001. Dual inhibitor studies performed with GM6001 identified antibodies 2A11, 2D3, 2D5 and 2D11 as non-zinc chelating inhibitory antibodies. Zinc-chelating inhibitory antibodies have been reported before. For example, Sela-Passwell et al. (2011) reported the isolation of an anti-gelatinase (MMP-2/MMP-9) antibody SDS3 which was isolated by immunisation with a synthetic zinc-histidine complex mimicking the catalytic centre of MMPs. As expected, SDS3 bound to the catalytic zinc region of the active form of MMPs. The fact that the anti-ADAMTS-5 antibodies here described are not affected by (2D5, 2D11), or show a synergistic (i.e. non additive) effect (2A11, 2D3) with GM6001 **(Figure 5.13 and Table 5.4)**, can be explained by the fact that they were originally isolated from phage display selections where the active site of ADAMTS-5 was blocked with a 100-fold excess of this small molecule inhibitor. This is a proof of principle that a careful choice of conditions during phage display selections allows the isolation of antibodies with desired properties.

The next step was to investigate the effect of full-length TIMP-3 on inhibitory potency of anti-ADAMTS-5 inhibitory antibodies. Although the inhibitory potency of 2A11 and 2D3 was decreased by the presence of TIMP-3, 2D5 and, especially, 2D11, showed improved inhibitory potency in the presence of TIMP-3, suggesting non-overlapping binding sites **(Figures 5.19 and 5.20 and Tables 5.6 and 5.7)**. When concentration of scFv-Fc antibodies was kept constant, TIMP-3 showed decreased inhibitory potency in the presence of 2D3 but increased inhibitory potency in the presence of 2D5 and 2D11. These results were confirmed by co-immunoprecipitation experiments where 2D5 and 2D11 were able to pull-down both ADAMTS-5 and ADAMTS-5/TIMP-3 complexes **(Figure 5.21)**. By contrast, an isotype scFv-Fc control was not able to pull-down ADAMTS-5 nor ADAMTS-5/TIMP-3 complex.

The mechanism of inhibition of metalloproteinases by TIMPs is the bidentate coordination of the catalytic zinc ion by the N-terminal α-amino group and the carbonyl group of the first N-terminal residue (a cysteine), which displaces from the enzyme the water molecule needed for peptide bond hydrolysis (Brew and Nagase, 2010). In the complex between full-length TIMPs and the catalytic domains of MMPs, it emerges that C-terminal domains of TIMPs establish few contacts with the enzyme and these do not appear to make important contributions to complex formations since the N-terminal domains of TIMPs have high affinity for the enzyme (Gomis-Rüth et al., 1997; Fernandez-Catalan et al., 1998; Maskos et al., 2007). For example, the $K_{i\ app}$ value for ADAMTS5-2 inhibition by N-TIMP-3 is 0.35 nM, whereas the $K_{i\ app}$ value for full-length TIMP-3 is 0.72 nM (Troeberg et al., 2009). C-terminal domains may be involved in the competitive effect exerted by anti-Sp antibody 2B9 on TIMP-3/ADAMTS-5 complex **(Figure 5.20 and Table 5.7)**. On the other hand, another possible explanation for the reduced reactivity of TIMP-3 in the presence of 2B9 is that C-terminal domains of the enzyme affect the structure around the active site, favouring interactions with N-TIMP-3 (Troeberg et al., 2009). If these interactions are abolished by 2B9, TIMP-3 binding may be disrupted. A model showing ADAMTS-5 regions that are occupied by N-TIMP3 or full-length TIMP-3 includes the Dis domain (**Figure 5.28)**. These TIMP-3 contact regions are likely to be the epitopes for 2D3 and 2A11, but neither for 2D5 nor 2D11.

The effects of TIMP-3, GM6001, heparin, and combinations of antibody on inhibitory potency of each lead antibody were examined by double inhibition studies. When we examine the effects of protein inhibitors such as TIMP-3 and antibodies (not small molecule inhibitors) on a single enzyme, we do not expect that binding of any of these inhibitors would be independent because the effect of the binding of a single protein ligand can be transduced over the whole enzyme molecule. So, even if two proteins bind at different sites of the enzyme, their inhibitory effects are not independent since they may influence indirectly the binding of each other and/or they may alter the substrate affinity (Palatini, 1983). For example, two independently-bound inhibitors might facilitate the binding of each other, since the binding of one of them may increase the affinity of the other inhibitor for the enzyme. This would result in an increase in the relative inhibitory potency of the two inhibitors. By contrast, if two inhibitors are able to bind independently (for example one inhibitor binds to the active site and another one binds to an ancillary domain), it is possible that conformational changes in the enzyme molecule may preclude their simultaneous binding.

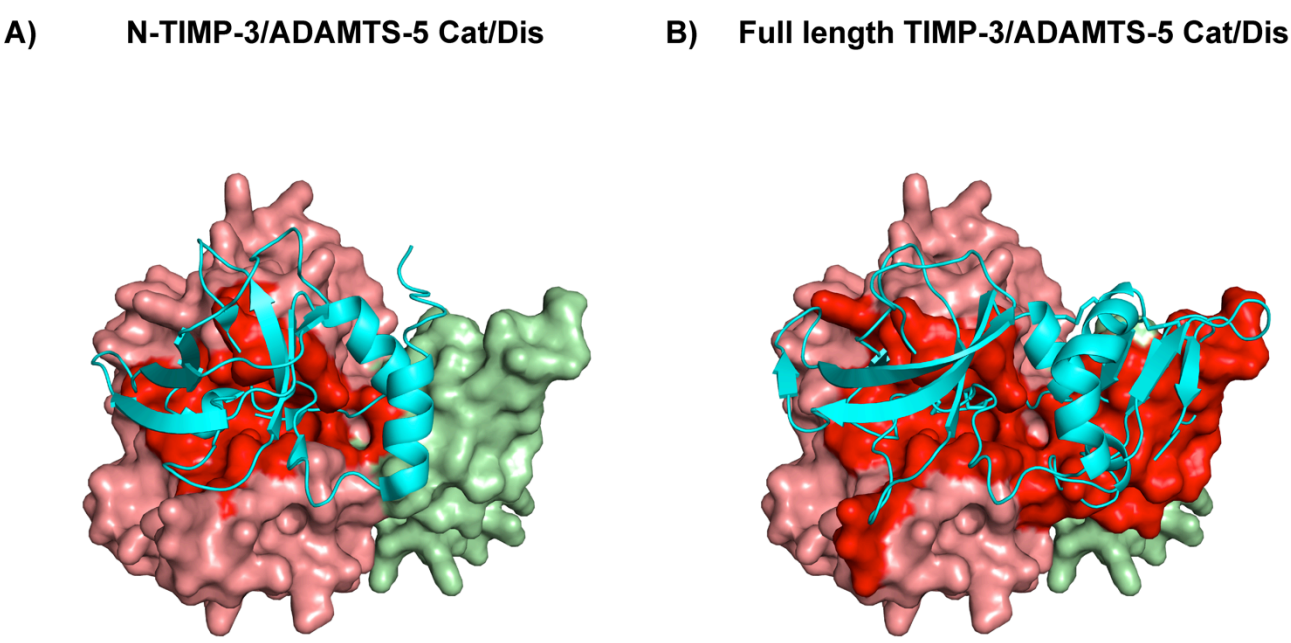

Figure 5.28: Models of interactions between ADAMTS-5 and TIMP-3. A) TACE/N-TIMP3 complex from TACE 3CKI was superimposed on Cat/Dis ADAMTS-5 structure 2RJQ and then residues within 4 angstrom were selected (red). **B)** ADAMTS5 structure 2RJQ was superimposed on TACE 3CKI and then on top of N-TIMP3 structure a model of full-length TIMP-3 realised from MMP-3/TIMP-1 complex (1UEA) was super-imposed. Purple, Cat domain; green, Dis domain.

Another possibility is that two inhibitors bind to the same site on the enzyme but their binding is directed to different forms (Fletcher et al., 1995). This may be the case if ADAMTS-5 exists as an ensemble of at least two isomers (Mosyak et al., 2008). Extensive inter-domain flexibility and conformational heterogeneity is a feature of MMPs (Bertini et al., 2005), ADAM/adamalysin/reprolysin families (Igarashi et al., 2007) and ADAMTSs (Akiyama et al., 2009). Antibodies 2D3, 2D5 and 2D11 were all able to co-immunoprecipitate ADAMTS-5/TIMP-3 complexes **(Figure 5.21)**. However, in order to correlate an increase/decrease in inhibitory potency of scFv-Fc antibodies in the presence of TIMP-3 with an increase/decrease in affinity between scFv-Fc antibodies and ADAMTS-5, SPR studies investigating the affinity of scFv-Fc antibodies for ADAMTS-5/TIMP-3 complex should be performed.

Model systems of cartilage degradation include IL-1α, retinoic acid or IL-1α/OSM–stimulated bovine nasal, porcine articular and human articular cartilage. In our study we decided to focus our efforts in examining the effects of scFv-Fc antibodies on the IL-1α/OSM-stimulated porcine and human articular cartilage on the basis of the availability of these samples. Each species responded in a different way to the stimulation by IL-1α/OSM. For example, we observed consistently a 2-fold increase in GAG release from porcine-explants after incubation with IL-1α/OSM, whereas in the case of human articular cartilage this increase was about 3-fold.

We did not find a correlation between detection of ARGSV fragments by Western blot and GAG release. Pratta et al. (2006) reported that there was no good correlation between the levels of ARGSV fragments (detected by sandwich ELISA) and the release of the total GAG levels in SF of individuals without joint diseases. It is still not known if ADAMTS-5 is the main aggrecanase in porcine and human cartilage. Treatment with OSM in combination with either IL-1α or TNF-α in human chondrocytes or cultured human cartilage explants led to a marked induction of *ADAMTS-4* gene expression and some induction of *ADAMTS-5*; siRNA-mediated knock down suggested that both enzymes are involved in stimulated aggrecan degradation (Song et al., 2007). OSM is a potent catabolic cytokine which is involved not only in release of aggrecanase-generated fragments but also link protein and HA degradation in bovine cartilage (Durigova et al., 2008a,b). In bovine cartilage explants, treatment for 2 days with IL-1β induces a dramatic up-regulation of *Adamts-4* gene expression and only a modest up-regulation of *Adamts-5*, although the mRNA levels of ADAMTS-5 are always higher than ADAMTS-4 (Durigova et al., 2011b). Another possible mechanism by which catabolic cytokines regulate aggrecan degradation is stimulation of C-terminal processing of aggrecanases (Patwari et al., 2005; Durigova et al., 2011b). In any case, under stimulated conditions both ADAMTS-5 and ADAMTS-4 contribute to aggrecan degradation, as detected by ARGSV-neoepitope antibodies.

N-TIMP-3 inhibits both ADAMTS-4 and ADAMTS-5, and hence is efficient in blocking GAG release **(Figure 5.24)** and aggrecan degradation **(Figures 5.25 and 5.26)** from porcine and human articular cartilage explants under stimulated conditions. On the other hand, anti-ADAMTS-5 inhibitory antibodies were not able to inhibit GAG release **(Figure 5.24)**. It is possible that this lack of efficacy is partly due to lower affinity of the antibodies. However, an aggrecanase-independent pathway for GAG-release has been observed in bovine and porcine explants after stimulation by IL-1α and retinoic acid (Gendron et al., 2003), so the cumulative GAG-release observed in the presence of IL-1 α/OSM may be due to ADAMTS-4 as well as other activities (for example hyaluronidases, Sztrolovics et al., 2002a,b).

Anti-ADAMTS-5 scFv-Fc antibodies 2D3 and 2B9 were able to inhibit aggrecan degradation (as measured by generation of ARGSV neoepitope) from both porcine and human articular cartilage explants. In the case of human explants, only a decrease in the intensity of the ^{393}ARGSV---SELE^{1564} band was observed, likely due to an excessive response of human chondrocytes to IL-1α/OSM stimulus **(Figure 5.26)**. It is noteworthy that studies with human OA cartilage explants described by GlaxoSmithKline in US Patent 2012/0095193 (Burden et al., 2012) followed spontaneous cartilage degradation for a 2-3 week period *ex vivo* in the absence of stimulation; this was possible due to sensitive methods (such as ELISA) used to detect ARGSV

neoepitope generation. Anti-ADAMTS-5 specific antibodies described in this patent produced a 70% inhibition of ARGSV neoepitope at the concentration of 670 nM (Burden et al., 2012). After removal of the treatment media, the effect on ARGSV generation lasted as long as 23 days. The results described in this patent provide evidence of the extended duration of the therapeutic effect of ADAMTS-5 inhibition in human OA cartilage and indicate a low turnover rate of ADAMTS-5 in diseased tissue, thus confirming an impairment of ADAMTS-5 endocytosis in OA cartilage (Yamamoto et al., 2013). ADAMTS-5 endocytosis is mediated by LRP-1 **(See Section 1.2.4.3)** and addition of receptor-associated protein (RAP) to porcine cartilage explants increases the basal level of aggrecan degradation, as well as ADAMTS-5-mediated aggrecan degradation (Yamamoto et al., 2013). Therefore, the ability of anti-ADAMTS-5 antibodies to inhibit aggrecan degradation in cartilage explants should be assessed under unstimulated conditions in the presence of RAP in order to exclude ADAMTS-4 interference with this system.

The specific inhibition of aggrecanase-generated fragments reported here is potentially beneficial in disease treatment. In particular, side effects such as MSS associated with broad-spectrum MMP inhibitors **(See Section 1.4.1)** should be abolished. In the case of antibody 2D11, an increase in aggrecan degradation was observed in all three human samples examined. Since the same phenomenon was not observed for porcine articular explants, more human samples needed to be analysed by this method.

Generally, aggrecanase inhibitors are much more potent in *in vitro* than in *ex vivo* systems. For example, in our study, the concentration of scFv-Fc antibodies used to test inhibitory effect on stimulated cartilage explants was 1 μM (i.e. from 20 to 500-fold higher than the $K_{i\ app}$). One reason for the observed decrease in potency may be competition with aggrecan. Since high levels of aggrecan are present in the cartilage matrix (>10 mg/ml, ~ 10 μM for nasal cartilage, Wittwer et al., 2007), when inhibitors are tested in explants cartilage systems their $K_{i\ app}$ will increase according to the Cheng and Prusoff equation (i.e. $K_i = K_{i\ app} /(1+ [S]/K_m)$) (Cheng and Prusoff, 1973). As discussed before, since the anti-ADAMTS-5 antibodies described here do not act through a zinc-chelating mechanism and therefore likely act through a noncompetitive/uncompetitive mechanism of inhibition, but the exact inhibitory mechanisms of these antibodies against aggrecan were not elucidated.

Other factors that may affect antibody performances in explants studies are antibody stability, ability to reach the target, isoelectric point (pI) and affinity for polyanionic components of the ECM, and epitope masking by interactions of ADAMTS-5 with ECM molecules. The pI values of the antibodies described here is very similar, ranging from 5.70 for 1B3 to 6.46 for 2B9, and these values should be compared with the basic pI of N-TIMP-3 (9.27) (Gendron et al., 2003). Few

studies have so far examined the permeability of this tissue to large macromolecules such as antibodies. It is still a matter of debate whether IgGs can penetrate the cartilage. Maroudas (1976) reported that variations in GAG content between different joints and between different zones of the same joint lead to large differences in the penetration of IgGs (~ 160 kDa), but with a partition coefficient of the same order of magnitude of serum albumin (~69 kDa). Anti-ADAMTS-5 antibodies described in US Patent 2012/0095193 (IgGs) are capable of penetrating mouse cartilage *in vivo* even when administered by a non-articular route of administration (intravenous, intramuscular, subcutaneous, oral, intranasal and intraperitoneal administration) (Burden et al., 2012). In the same patent, the ability of mAbs to penetrate human cartilage was tested on *ex vivo* tissues. Irrespective of target specificity, mAb penetration was observed to be a concentration and time-dependent process primarily originating from the synovial surface of the cartilage and proceeding to full thickness penetration within 3-4 days; an isotype control (non-specific for any cartilage target) failed to penetrate the cartilage (Burden et al., 2012). Also, *in vivo* assessment of cartilage penetration was performed using near-infrared (NIR) dye-labelled mAbs, administered intraperitoneally to mice that had undergone surgical DMM 6 weeks prior to the test. Again, within 4 days after systemic mAb administration, full-thickness cartilage penetration was observed for anti-ADAMTS-5 and anti-ADAMTS-4 mAbs, but no staining for an isotype control (Burden et al., 2012). This indicates that cartilage penetration by mAbs is antigen-specific. The anti-ADAMTS-5 mAb CRB0017 (IgG) is effective in delaying cartilage breakdown in STR/ort mice (which spontaneously develop age-related OA) when administered intra-articularly, although no quantitative bioanalytical methods have been used to assess cartilage penetration (Chiusaroli et al. 2013).

Penetration of scFv-Fc antibodies (~ 110 kDa) may thus be a combined result of molecular size, isoelectric point, and affinity for the target antigen. Immunohistochemistry will be needed to assess the extent and deepness of cartilage penetration by these lead antibodies. Taking into account the relevance of the *ex vivo* systems to the human disease and the observed efficacy, the data presented in this chapter strongly support further therapeutic validation of the anti-ADAMTS-5 antibodies described here. However, dose-response inhibition as well as cytotoxicity studies should be performed in order to establish conditions for *in vivo* treatment.

Chapter 6
General discussion and future prospects

6.1. Mechanisms of action of inhibitory antibodies

Developing selective and potent inhibitors of proteases is difficult because a target protease is frequently co-expressed with other similar proteases that differ only slightly in sequence, global fold and even substrate specificity. One example is the metallopeptidase clan MA that includes matrix metalloproteinases (family M10), astacins, ADAMs, ADAMTSs and snake venom metallopeptidases (family M12). More than 200 structures of metallopeptidases have been deposited in the Protein Data Bank so far. This huge complexity and similarity traditionally hampered the therapeutic development of small molecule inhibitors which generally targeted the conserved catalytic zinc ion of these families and therefore lacked selectivity (Coussens et al., 2002). Since the first studies showing protection of *Adamts-5* knock out mice from cartilage degradation (Glasson et al., 2005; Stanton et al., 2005), a lot of effort has been spent to develop small molecule inhibitors targeting this enzyme. Generally, these compounds contained a zinc-chelating group such as hydroxamate (Yao et al., 2001; Cappelli et al., 2010; Nuti et al., 2013), carboxylate (Shiozaki et al., 2001) or acylthiosemicarbazide (Maingot et al., 2013). Due to the paucity of structural informations, so far few examples of non-zinc chelating aggrecanase inhibitors have been reported (Ding, 2010; Deng et al., 2012). As discussed in **Section 1.4.1**, zinc-chelating small molecule inhibitors, although potent, are generally thought to be associated with MSS.

The antibody scaffold is an attractive alternative for the development of highly potent and selective inhibitors of metallopeptidases since it can immunologically distinguish between structurally closely related proteins. Phage display of antibody fragments is a well-established technology which, by exploring the huge diversity of natural antibody repertoire, has enabled the isolation of inhibitory antibodies against complex extracellular proteins (Hoogenboom, 2005). However, despite the ability of the antibody repertoire to generate specific binders against virtually all antigens, the number of antibodies acting as enzyme inhibitors is low. A possible explanation for this scarce representation lies in the surface topography of both enzyme active site and the antigen-binding site of antibodies. The active site of most enzymes is found usually in the largest cleft on the protein surface (Laskowski et al., 1996). In the case of ADAMTS-5, the catalytic site has the shape of a funnel that opens up at the zinc site at its widest point and then forms an L-shaped hydrophobic channel through the S1'pocket and out to solvent at its distal end (Shieh et al., 2008). On the other hand, the antigen-binding surface of conventional antibodies frequently forms a flat surface when interacting with other protein antigens (Webster et al., 1994). Large protruding flexible loops are not frequently observed at the antigen-binding site (Wu et al., 1993; Padlan, 1996). This may be due to the loss of degrees of freedom upon binding to the antigen. A consequence is that, unlike canonical inhibitors which present a convex surface and target the

protease cleft to inhibit the enzyme in a substrate-like manner (Laskowski and Kato, 1980), conventional antibodies may preferentially bind to protruding loops at the rim of the substrate-binding cleft with flat or concave paratopes (Wu et al., 2007).

One important exception is represented by heavy chain antibodies (hcAbs) from camels and sharks. The immune system of these species seems to possess an inherent propensity for forming enzyme-blocking antibodies. hcAbs are formed only by a single domain, designated VHH in camelids and VNAR (shark variable new antigen receptor) in sharks, and so lack a light chain. The CDR3 region of hcAbs possesses the ability to form long extensions that can fit into cavities of antigens such as the active sites of enzymes (De Genst et al., 2006). A serious disadvantage of the use of the hcAbs in therapy is their potential immunogenicity, which represents a major concern for repeated and long-term treatments. However, humanisation may help to limit immunogenicity.

For the most part, the inhibitory antibodies of proteases reported in the literature have been mAbs raised from hybridomas which act through two different mechanisms: active-site inhibition (where the antibody inserts a loop in a substrate-like manner into the active site and produces steric hindrance) (Farady et al., 2007) and allosteric inhibition (where the antibody occludes substrate binding or causes conformational changes of the enzyme) (Petersen et al., 2001, Matias-Roman et al., 2005; Xuan et al., 2006). Allostery is a basic principle of control of enzymatic activities based on the interaction of a protein or small molecule at a site distinct from an enzyme active centre. An advantage of antibodies over small molecules when an allosteric modulation is desired is their size. Proteins that interact with other proteins generally use contact surfaces (1500-3000 angströms) (Jones and Thornton, 1997) much larger than the average contact area between a small molecule and its protein target (1000 angströms) (Cheng et al., 2007).

Historically, allostery was initially thought to be restricted to oligomeric proteins. It is now widely recognised that the native states are ensembles of pre-existing populations; thus, an allosteric effector leads to an equilibrium shift of pre-existing conformational and dynamic states (Gunasekaran et al., 2004). According to this view, allostery is an intrinsic property of all dynamic proteins, including monomeric proteins (Gunasekaran et al., 2004). Enzymes can adopt several conformations, some of them catalytically active, with others being inactive. Equilibria exist between these different states, and these can be shifted upon reversible ligand binding or irreversible trapping at the allosteric binding sites to result in redistribution of the conformation ensembles (Volkman et al., 2001). For example, there are peptidic allosteric regulators that induce a switch from the ordered active protease conformation to the disordered zymogen-like conformation, thereby following a mechanism similar to that of the allosteric zymogen activators (Dennis et al., 2000).

Antibodies can behave as allosteric effectors, giving rise to kinetic effects such as activation, noncompetitive inhibition and/or hyperbolic (i.e. partial) inhibition of enzymes and receptors (Pollock, 1964; Saerens et al., 2004; Shapira and Arnon, 1967; Barlow et al., 2009; Oyen et al., 2011). A common mechanism by which allosteric activators increase k_{cat} is enhancing product release, which is a rate-determining step commonly observed in enzymes (Suzuki et al., 1969; Barlow et al., 2009). Most allosteric effectors appear preferentially to target native low-energy conformations such as those found in the zymogen or active protease structure since it is easier to shift the protein conformation equilibrium into a low-energy conformation than into high-energy structures.

Allosteric antibody inhibitors show peculiar inhibitory profiles where they cannot inhibit the hydrolysis of peptide substrates or have different levels of inhibition against different substrates (Petersen et al., 2001; Xuan et al., 2006). Usually, allosteric inhibitors act by restricting the conformational flexibility in the enzyme active site and blocking substrate binding (Desmyter et al., 1996; Goodey and Benkovic, 2008). Auto-antibodies (i.e. antibodies that recognise self rather than foreign proteins) are a class of antibodies which can act according to the latter mechanism and are implicated in immune diseases (Makita et al., 2007; Scheiflinger et al., 2003; Colwell et al., 1998). An example is provided by auto-antibodies which occur in patients diagnosed with thrombotic thrombocytopenic purpura (TTP) **(See Section 1.2.2)**. These auto-antibodies react with the non-catalytic ancillary domain of ADAMTS-13 and inhibit enzyme cleavage of von Willebrand factor (vWF) (Soejima et al., 2003). vWF acts by anchoring platelets at sites of injured vessel walls under high shear stress. The result of impaired vWF cleavage is the accumulation of unprocessed high molecular weight-vWF on endothelial vessel walls, thus provoking microvascular thrombus formation and consequent haemolytic anaemia, renal failure, neurological dysfunction and fever (Moake et al., 1982). Epitope mapping studies have shown that the CysR/Sp domains represent the major antigenic determinant for human anti-ADAMTS-13 antibodies (Soejima et al., 2003; Klaus et al., 2004; Luken et al., 2005). Residues within Y658-Y665 of ADAMTS-13 Sp domain that are targeted by auto-antibodies in TTP directly interact with a complementary exosite within the vWF A2 domain (Pos et al., 2010). These auto-antibodies thus block initial binding of ADAMTS-13 to vWF (Zheng et al., 2003). As discussed below, this mechanism likely occurs in the case of the anti-ADAMTS-5 Sp antibody 2B9.

Other than active-site inhibition and allosteric inhibition, another mechanism by which antibodies can inhibit protease function is by targeting zymogen activation as reported for the serine protease urokinase-type plasminogen activator (uPA) activity (Blouse et al., 2009). An anti-uPA mAb reported by Blouse et al. (2009) not only interferes with the cleavage of pro-uPA but also

stabilises the active two-chain enzyme in a non-catalytic conformation by restricting the conformation flexibility of the activation domain. Antibodies targeting protease multimerisation and subsequent activation have been reported for HIV-proteases (Rezacova et al., 2001), cysteine proteases (Puchi et al., 2006), and the serine protease beta tryptase (Fukuoka and Schwartz, 2006).

The ability of the antibodies to interfere with the biological activity of their target protein at a distance from the epitope could arise from the induced-fit (Schechter et al., 1971) or selection of distinct conformational states (Berger et al., 1999). In the context of antigen-antibody recognition, the expression "induced-fit" implies that the binding reaction induces conformational changes leading to a better complementarity between epitope and paratope. Ganesan et al. (2009) reported a phage display-derived antibody which, although being a competitive inhibitor of serine protease hepatocyte growth factor activator (HGFA), bound to an epitope distant from the active site and induced a conformational change which switched the enzyme to a non-competent state, thus actually acting as an allosteric inhibitor. Conformational changes can be detected by NMR relaxation dispersion techniques (Brüschweiler et al., 2009). However, large conformational changes in proteins upon complex formation with antibodies are rarely observed by X-ray crystallography (Sundberg and Mariuzza, 2002). An alternative way for antibodies to modulate protein function is by altering protein dynamics. The rates of amide hydrogen exchange in some proteins are reduced upon antibody binding for amides at considerable distances from the epitope and without any evident change in crystal structure (Williams et al., 1996; Dumoulin et al., 2003).

Conformational selection is an alternative mechanism which does not need conformational changes during the binding reactions. In this case the antibody selects those antigen molecules whose epitope is already in a fitting conformational state (Leder et al., 1995; Berger et al., 1999) or, in the reciprocal case, the antigen selects the antibody which happens to be in the complementary conformation (Foote and Milstein, 1994). Popovych et al. (2006) presented direct experimental evidence illustrating that allostery can be mediated solely by changes in protein dynamics without any conformational change. This absence of conformational change leads to a definition of allostery in pure thermodynamic terms: allostery can be controlled by enthalpy, by enthalpy and entropy, or solely by entropy (Tsai et al., 2008; Tsai et al., 2009). A free energy change without conformational change is defined as entropy-dominated (Tsai et al., 2008; Tsai et al., 2009).

An hydroxamate-based succinamide derivative, which showed significant inhibitory activity towards many MMPs, including MMP-2, MMP-8, MMP-9 and MMP-13, was proved to inhibit ADAMTS-5 by inducing a conformational change in the S1' loop of the active site (Shieh et al., 2011). However, this flexibility of ADAMTS-5 active site may lead to allosteric inhibition by anti-

ADAMTS-5 antibodies which is entropy dominated and that will not produce detectable conformational changes.

The work described so far confirms that solution-phase scFv phage display is a suitable method to identify and isolate potent and specific inhibitory antibodies of ADAMTS-5. Sequences of lead antibodies are reported in **Table 6.1**, together with sequences for anti-ADAMTS-5 antibodies described by GlaxoSmithKline (GSK) in USA Patent 2012/0095193 (Burden et al., 2012). Sequences of anti-ADAMTS-5 antibodies described here differ widely from each other and from those described in the US Patent.

Clone	Variable Heavy			Variable Light		
	CDR-1	CDR-2	CDR-3	CDR-1	CDR-2	CDR-3
MP2 A11	GYSFTSYWIS	RIDPSDSYTNYSPSFQG	GGDSSSLYDAFDI	TGTSSDVGGYNYVS	EGSKRPS	SSYTSTNSVV
MP2 B9	GFTFSSYAMS	AISGSGGSTYYADSVKG	DQTPLGGFYFDY	RASQSISSYLN	AASSLQS	QQSYSTPGT
MP2 D3	GGTFSSYAIS	GIIPIFGTANYAQKFQG	EGRLVVGATTDYYYYGMDV	RASQNINTYLN	KASSLES	QQYDNLPIT
MP2 D5	GFTFDDYAMH	GISWNSGSIGYADSVKG	ESSSWYLRYFDY	RASQSISSYLN	AASSLQS	QQSYSTPFT
MP2 D11	GFTFTDYYMS	YIDTGSGGTYTKYADSVKG	LWTLGGWYFDL	QASQDISNYLN	DASNLET	QQYDNLRLT
US Patent 20120095193	DAWMD	EIRNKANNHARHYAESVKG	TYYYGSSYGYCDV	RTSENIYSYLA	NAKTLAE	QHHYGTPWT
US Patent 20120095193	DAWMD	EIRHKANDHAIFYDESVKG	PFAY	KASQNVGTAVV	SASNRHT	QQYTSYPFT

Table 6.1: Sequences of lead antibodies and comparison with sequences described in US Patent 20120095193 (Burden et al., 2012).

The antibodies characterised here show different epitopes **(Table 6.2)**. Inhibitory potency of antibody 2A11 is affected by TIMP-3. However, the interaction with GM6001 is positive. NMR studies indicate that the binding mode between TIMPs and MMPs are similar to zinc-chelating MMP inhibitors. The N-terminal side-chains of TIMP-1 (Thr2) and TIMP-2 (Ser2) (Fernandez-Catalan et al., 1998) have both been shown to extend into the S1'pocket containing the catalytic zinc ion of MMP-3. Hydroxamate inhibitors such as GM6001 also target the catalytic zinc ion within the S1' pocket; however, the number of interactions established with enzyme subsites is considerably less. It is thus likely that 2A11 binds to the Cat/Dis domain of ADAMTS-5 without chelating the zinc ion. Competition with TIMP-3 may occur through overlapping contacts in the catalytic site cleft or in the Dis domain **(Figure 5.28)**.

Similar interactions with GM6001 and TIMP-3 are observed in the case of 2D3. Thus, binding of this antibody does not compete with small molecule inhibitors but competes with the macromolecular protein inhibitor TIMP-3 which has extended contact sites with the enzyme. 2D3 (like 2A11) acts therefore as an allosteric orthosteric inhibitor since it competes with the

endogenous ligand for access to the enzyme. Interestingly, 2D3 has a long (20 residues) heavy chain CDR3 loop, whereas 2A11, 2B9, 2D5 and 2D11 have smaller heavy chain CDR3 loops (11-13 residues) **(Table 6.1)**. The main chain conformations are determined not only by the primary amino acidic sequence but also by the length of the antigen-binding loop, with longer loops associated with active-site inhibition (De Genst et al., 2006).

Clone	$K_{i\ app}$ QF peptide (nM)	$K_{i\ app}$ Aggrecan (nM)	K_D (nM)	Epitope	Interaction with GM6001	Interaction with TIMP-3	Interaction with heparin	Interaction with 2B9
2A11	180	ni	94	Dis-Cat	+	-	0	+
2B9	ni	300	6.7	Sp	0	-	0	na
2D3	2.5	30	2.8	Dis-Cat	+	-	0	+
2D5	20	300	29	Dis-Cat	0	+	0	+
2D11	70	100	22	Dis-Cat	0	+	0	+

Table 6.2: Summary of characterisation of anti-ADAMTS-5 antibodies. Data for ADAMTS5-2 are reported. '+' indicates positive interaction, '- 'negative interaction and '0', null interaction in the QF peptide cleavage assay. Ni, not inhibiting, na, not applicable. K_D values were measured by SPR.

We can compare the epitopes of anti-ADAMTS-5 antibodies with those of the anti-ADAMTS-5 antibodies described by GSK in US Patent 2012/0095193 (Burden et al., 2012). GSK antibodies were isolated by hybridoma technology and bind simultaneously to both Cat and Dis domains. The Cat and Dis domains of ADAMTS-5 are separated by a connecting peptide that may give some flexibility between the domains and act to regulate the substrate localisation to the catalytic site. GSK anti-ADAMTS-5 antibodies likely lock the Cat and Dis domains, thus impairing the flexibility between these regions. It thus seems that the effect of antibody binding on ADAMTS-5 is entropy-dominated. It is possible that antibodies directed against the Cat/Dis domain of ADAMTS-5 such as 2A11 and 2D3 may bind at the interface between the Cat/Dis domain and follow a similar mechanism of inhibition.

A different mechanism may characterise inhibition of ADAMTS-5 by 2D5 and 2D11 scFv-Fc antibodies. Inhibitory potency of 2D5 is not affected by GM6001 and only slightly increased in the presence of TIMP-3 (an increase in inhibitory potency of TIMP-3 was observed in the presence of 2D5, see **Figure 5.20 and Table 5.7**). Also, the higher K_D shown for ADAMTS5-5 compared with ADAMTS5-2 confirms that crucial interactions with ancillary domains happen in this case. This behaviour recalls that of an anti-ADAM-17 cross-domain inhibitory antibody described by Tape et al. (2011). We can speculate that 2D5 binds to the back of the Cat/Dis domain of ADAMTS-5 opposite to the catalytic site cleft. Antibody 2D11 showed the most peculiar mechanism of inhibition. This antibody shows increased inhibitory potency in the presence of

TIMP-3 and binds to ADAMTS5-2 and ADAMTS5-5 with similar affinity. Again, a possibility is that 2D11 binds to the back of the enzyme. Synergism with TIMP-3 has not been previously reported with antibody inhibitors. For example, the cross-domain anti-ADAM17 inhibitory antibody D1(A12) shares a partially overlapping catalytic-cleft with TIMP-3 so it may simply block access of macromolecular substrate to the active site (Tape et al., 2011). Thus, 2D5 and 2D11 act as allosteric modulators which do not compete with endogenous ligands and therefore can exert their effect even if the active-site ligand (TIMP-3) is bound. Mechanistically, this may involve an undescribed mechanism of inhibition. *In vivo* synergism with TIMP-3 may represent a way to increase inhibitory potency and treatment efficacy, and to reduce therapeutic dose.

A totally different mechanism is exerted by anti-Sp antibody 2B9. It induces allosteric effects that are more detrimental to the cleavage of the macromolecular substrate (aggrecan) but not to the peptide substrate. A similar trend was observed with a Fab inhibitory antibody of the trypsin-like hepatocyte growth factor activator (HGFA) (Wu et al., 2007), although in our case no inhibition of peptide substrate cleavage was observed at all. Also, monoclonal antibodies mAb 5, mAb 16 and mAb394 which bind to the serine protease domain of uPA do not inhibit the peptidolytic activity of uPA (Petersen et al., 2001). However these antibodies block plasminogen activation. So the active site cleft is still accessible to small molecule synthetic substrate in the presence of bound monoclonal antibodies (Petersen et al., 2001). Therefore, the inhibitory effects observed with peptide substrates do not always reflect those observed with macromolecular substrates. This indicates that peptide substrates are inadequate surrogates of natural protein substrates, which require precise alignment of the scissile bond involving interactions with exosites (Gendron et al., 2007). Recently, an inhibitory antibody of ADAMTS-5 directed against the Sp domain, CRB0017, has been reported by Visintin et al. (2012). The mechanisms of 2B9 and CRB0017 can be compared to those of auto-antibodies present in patients with TTP, that mainly target the Sp domain of ADAMTS-13 and impair initial binding of the enzyme to the substrate (Zheng et al., 2003). Ability of 2B9 to inhibit only aggrecan cleavage with no effect in QF peptide cleavage, together with Biacore data, defined this antibody as a truly exosite antibody and may challenge the use of synthetic substrates during drug screening. In this instance, our use of both QF peptide and the physiological substrate aggrecan allowed the identification of both active-site directed and exosite-directed antibodies.

Potentially, antibodies that bind to the exosites of ADAMTSs are attractive as they could modulate enzyme activity for the natural substrates with high-specificity. In fact they either 1) mask scissile bonds on the substrate; 2) compete with the substrate for protease binding at exosites; 3) reduce the binding and cleavage of specific substrates while still allowing for proteolysis of other

substrates of the same enzyme. For example, anti-ADAMTS-5 Sp antibodies such as 2B9 may spare versicanase activity of ADAMTS-5 while still inhibiting aggrecanase activity. This is particularly important given the increasing evidence of ADAMTS-5 as a versicanase and the importance of this activity in vasculature since decreased cleavage of versican in arterial smooth muscle cells and pericardial cavities is involved in myxomatous valve disease (Dupuis et al., 2011) and development of aortic lesions (Didangelos et al., 2012).

In conclusion, we may hypothesise that binding of antibodies to the Cat/Dis domain of ADAMTS-5 finally distorts active site structure, resulting in a loss of binding affinity to substrate, products and possibly transition states; on the other hand, the effect on catalysis by anti-Sp antibody 2B9 may be mediated by blocking or hampering accessibility of macromolecular substrates. Ultimately, description of the exact mechanism of inhibition may require X-ray crystallography.

6.2. Therapeutic development of anti-ADAMTS-5 scFv-Fc antibodies

Owing to their human origin, scFv-Fc antibodies could go straight into therapeutic development as lead compounds, for example by reconstituting a full IgG or by fusion to another antibody to generate a bispecific antibody. However, efficacy, clearance and toxicity in mouse models of OA should be assessed.

Species cross-reactivity allows better assessment of therapeutic efficacy and toxicity in animal models. We have shown the ability of anti-ADAMTS-5 antibodies to inhibit the mouse orthologue. It is noteworthy that cross-reactive antibodies are often difficult to obtain by hybridoma methods owing to tolerance. In contrast, phage display libraries are unaffected by immune tolerance and antibodies targeting conserved sites across species have proved to be more the rule than the exception (Carter, 2006).

In view of a potential therapeutic application, we have also shown that scFv-Fc antibodies 2B9, 2D3, 2D5 and 2D11 inhibit the mouse version of ADAMTS-5 **(Table 5.1 and Figure 5.3)**. Altogether, these encouraging results suggest that a future line of research should focus on using animal models of OA such as the DMM model or the spontaneous OA model with STR/ort mice (Mason et al., 2001) to test the therapeutic efficacy of anti-ADAMTS-5 antibodies. However, the effect of anti-ADAMTS-5 scFv-Fc antibodies on cell viability of isolated chondrocytes needs to be assessed before further development.

Another argument which should be addressed for therapeutic development of anti-ADAMTS-5 antibodies is the antibody format. *In vivo* half-lives of about 2-3.5 h are reported for scFvs (Powers et al., 2001; Holliger and Hudson, 2005) but these increase up to 93 h for scFv-Fc fusions (Powers et al., 2001). The reason for this prolonged serum half-life lies in the increased size

of the scFv-Fc dimer (approximately 110 kDa *versus* 25 kDa for scFv), which is well above the renal cut-off (50 kDa) (Powers et al., 2001; Holliger and Hudson, 2005). Moreover, the Fc domain recruits cytotoxic effector functions through complement and/or through interactions with Fcγ receptors (Fc receptors for gamma globulins) and can provide long serum half-lives (>10 days) through interaction with the neonatal Fc receptor (FcRn). FcRn acts as a salvage receptor by binding to and transporting IgGs in intact form both within and across cells, and rescuing them from a default degradation pathway (Woof and Burton, 2004). A reason for the diminished *in vivo* half-life from IgGs to scFv-Fc fusions is that in the latter case the linker residues can be exposed and thereby result in increased protease degradation. In conclusion, although scFv-Fc fusions could be tested directly for *in vivo* efficacy, eventually they may need to be reformatted in the standard IgG format. However, reformatting into an IgG may lead to a decrease in affinity of the molecule due to lack of degrees of freedom. In fact, although the Fv shares similar antigen-binding properties as the Fab or IgGs, the relative orientation of the V_L and the V_H domains in the Fv is not necessarily the same as that found in the IgG, owing to the lack of the constant regions and the presence of the linker. As a consequence, all residues of the IgG variable/constant domain interface become solvent-exposed in scFv. In an analysis of 30 non-redundant Fab structures it was found that in the region of the Fv fragment that originally in the IgGs constitutes the variable/constant domain interface the frequency of exposed hydrophobic residues is much higher than in the rest of the Fv fragment surface (Nieba et al., 1997). It is very likely that the success of reformatting from scFv-Fc to IgG is largely paratope-dependent.

Another issue to address is affinity. The antigen-binding affinity of current antibody therapeutics ranges from a K_D of 0.08 nM to 32 nM (Carter, 2006). Average monovalent affinities of primary hits from phage display libraries are usually distributed in the double-digit nanomolar range, matching the monovalent affinities of animal-derived mAbs (Carter, 2006). Affinity of lead antibodies such as 2D3 and 2B9 falls into the low nanomolar range (K_D 2 nM and 6 nM, respectively). However, depending on their efficacy in mouse models, this affinity may need to be improved by affinity maturation. Antibodies such as 2B9, which are characterised by a relatively high dissociation rate constant **(See Section 5.4)**, are particularly amenable to improvements by affinity maturation. For example, cloning of the V_H domain into a phage display library consisting only of V_L domains (a process termed "light-chain shuffling") will generate an antigen-biased phage display library containing a large repertoire of alternative V_L domains in combination with the V_H domain of the candidate scFv which can be selected and re-screened for improved affinity (Marks et al., 1992). Light-chain shuffling is limited to antibodies whose V_H domains contribute significantly to define the paratope. Error-prone PCR may be used to introduce random mutations

throughout the variable domains. This method has minimal bias toward any specific class of substitutions and allows mutations in CDR and in scaffold regions (Hoogenboom, 2005).

It is noteworthy that for some applications, such as virus neutralisation (Wu et al., 2005) and tumour targeting (Rudnick and Adams, 2009), there is no strict correlation between affinity and efficacy above a certain threshold. Engineered high-affinity antibodies have been shown to not necessarily have superior tumour-targeting efficacy compared with low-affinity variants, but on the contrary, may display diminished penetration into solid tumours (Thurber et al., 2008; Rudnick et Adams, 2009).

As a comparison, anti-ADAMTS-5 antibodies deposited in the US Patent 2012/0095193 (Burden et al., 2012) show K_D values between 0.9 nM and 0.08 nM with the ability to block aggrecanase activity at $Glu^{392}\downarrow^{393}Ala$ (as measured by ELISA) in the range of 0.05-2.5 nM. Mice which received a single dose (0.5 mg) of anti-ADAMTS-5 antibodies 3 days prior to surgical DMM were protected against cartilage degradation, thus mimicking the protection exhibited by *Adamts-5* knock out mice (Burden et al., 2012; Glasson et al., 2005). Similarly, CRB0017 mAb, which binds to the Sp domain of ADAMTS-5 with affinity in the low nanomolar range, delays cartilage breakdown in STR/ort mice when administered intra-articularly, thus proving that exosite antibody inhibitors may be effective as therapeutic tools (Chiusaroli et al., 2013).

It would be interesting to test the effects of co-administration of two anti-ADAMTS-5 antibodies on the same mouse. An alternative to co-administration is represented by bispecific-antibodies. Bispecific antibodies are hybrid molecules that comprise two specificities. To increase the binding avidity to a target; bispecific antibodies have been constructed by combining two antibodies or their fragments directed against different epitopes on the same target (Cheong et al., 1990; Holliger et al., 1993). Frequently, the antigen-binding avidity of the bispecific molecule is shown to be 1 to 2 logs higher than its individual constituents (Cheong et al., 1990). This increased avidity is probably due to the fact that the bispecific antibody, although monovalent to each epitope, is in fact bivalent to its target since both of its epitopes are located within the same molecule, providing that these epitopes are not overlapping.

Methods described to produce bispecific antibodies involve hybrid hybridomas (Milstein and Cuello, 1983), minibodies (Hu et al., 1996), diabodies (Holliger et al., 1993), chelating recombinant antibodies (Neri et al., 1995) and bisFvs (Atwell et al., 1996). BisFvs are dimers of two scFvs with different specificities: each scFv has a short linker (5 aa) which prevents the pairing of V_H and V_L domains on the same molecule and favours the formation of non-covalent dimers (Atwell et al., 1996). Chelating recombinant antibodies are bispecific scFv composed by two scFvs specific for two non-overlapping epitopes on the same antigen molecule connected by a flexible

polypeptide linker (Neri et al., 1995). The production of bispecific IgGs by co-expressing two different antibodies is not very efficient as a result of unwanted pairings between the component heavy and light chains (Suresh et al., 1986). Engineering of the interaction interface in antibody variable and constant domains can provide an efficient alternative way to drive heterotypic pairing (Carter, 2001).

As an alternative to create bispecific IgGs, Bostrom and co-workers (2009) obtained dual specific antibodies derived from a monospecific antibody through mutations in the periphery of the antigen binding site in the light chain CDRs. An antigen-binding site is thus potentially able of interacting with two unrelated antigens with high affinity.

In our case we have shown that combination of an antibody directed against the Cat/Dis domains of ADAMTS-5 (such as 2D3) with the anti-Sp antibody 2B9 produces a greater inhibitory effect than the single antibody. Thus an alternative approach to increase efficacy of anti-ADAMTS-5 antibodies would be the creation of a bispecific anti-ADAMTS-5 antibody recognising different domains on the antigen. However, before undertaking the creation of such antibodies, other experiments are mandatory. For example, one antibody such as 2B9 can be chemically immobilised and the affinity for the ADAMTS-5/2D3 complex can be measured by SPR. In this way it would be possible to establish if 2B9 and 2D3 do not indeed share an overlapping epitope.

6.3. Other applications of anti-ADAMTS-5 antibodies

In this work we described the characterisation of 54 anti-ADAMTS-5 antibodies. These antibodies were screened not only for their inhibitory potential (**Section 4.4.2**) but also for their ability to bind to ADAMTS-5 in a semi-solid-phase ELISA **(Section 4.3.4)**. Although they were selected and screened against a native mature form of the enzyme, they were generally able to recognise ADAMTS-5 in SDS PAGE when the protein was not previously heat-denatured under non-reducing conditions **(Section 4.4.3)**. By blotting different deletion forms of ADAMTS-5 it was possible to assign each antibody to a specific domain of the enzyme. It is evident that the anti-ADAMTS-5 antibodies here described may provide a toolbox to deepen our knowledge of ADAMTS-5 biology and its functional role in OA setting. Usage of scFv-Fc antibodies for Western blotting and immunostaining has been previously shown (Moutel et al., 2009). We report here some applications of anti-ADAMTS-5 antibodies.

i) Effect on ADAMTS-5 endocytosis

Acquired TTP has been linked to severe deficiency of ADAMTS-13 activity caused by inhibitory auto-antibodies (Levy et al., 2001; Soejima et al., 2003). However, it has been reported that some of these antibodies found in patients with TTP failed to inhibit ADAMTS-13 activity, suggesting they may influence the half-life of the enzyme, thereby compromising the regulation of its activity *in vivo* (Scheiflinger et al., 2003; Shelat et al., 2006). These non-neutralising auto-antibodies may reduce the absolute amount of target at different anatomical sites by antibody-mediated clearance. ADAMTS-5 has been shown to be regulated by endocytosis and this process is mediated by exosites (Yamamoto et al., 2013). Specifically, since the TS-1 domain is necessary but the Sp domain increases the rate of clearance (Yamamoto et al., 2013), it will be interesting to investigate the effect of antibodies directed against specific ADAMTS-5 domains on endocytosis. Antibodies able to increase clearance of ADAMTS-5, even if they are not able to inhibit catalytic activity, may have a potential for therapeutic use in the OA setting.

ii) Extracellular localisation of ADAMTS-5

Our lab has shown the extracellular localisation of ADAMTS-5 in human chondrosarcoma HTB-94 cell line (Gendron et al., 2007). The CysR domain is critical for ADAMTS-5 binding to the cell surface and ECM. However, a limitation of this study was that recombinant ADAMTS-5 was used, due to the lack of sensitive and specific anti-ADAMTS-5 mAbs. It will be therefore interesting to test the ability of anti-ADAMTS-5 antibodies here described to detect endogenous ADAMTS-5. Moreover, due to the availability of antibodies directed specifically against different domains of ADAMTS-5, it would be possible to test which ADAMTS-5 form predominates in different cell lines or, eventually, in sections from *in vivo* tissues or in patients with degenerative cartilage pathologies such as OA or RA. The specificity of monoclonal anti-ADAMTS-5 antibodies should be tested by immunoprecipitation from lysates of *Adamts-5* knock out and wild-type cells.

iii) Resolution of ADAMTS-5 structure

To accurately describe the interactions between antibodies and ADAMTS-5 the antibody/enzyme complex could be structurally resolved by co-crystallisation, followed by X-ray crystallography. In protein crystallography, Fab and scFv antibody fragments that bind to their antigens with high affinity and specificity have been employed as crystallisation chaperones, thus permitting successful structure determination of several “difficult” protein targets (Iwata et al., 1995; Koide, 2009). Backbone flexibility and conformational heterogeneity are a feature of MMP

structures in general (Bertini et al., 2005) and of ADAMTS-5 in particular (Shieh et al., 2011), so it may be worth obtaining complexes between ADAMTS-5 and different antibodies. mAbs are able to discriminate between different conformations of the same antigen (Gao et al., 2009), thus it would be interesting to check if the anti-ADAMTS-5 antibodies reported here are directed against different conformations of ADAMTS-5. Crystallisation of Fab/ADAMTS-5 complex may identify allosteric regions which are currently not predicted by modelling and help to elucidate the mechanisms of ADAMTS-5 catalysis.

Chapter 7
References

Abbaszade I, Liu RQ, Yang F, Rosenfeld SA, Ross OH, Link JR, Ellis DM, Tortorella MD, Pratta MA, Hollis JM, Wynn R, Duke JL, George HJ, Hillman MC Jr, Murphy K, Wiswall BH, Copeland RA, Decicco CP, Bruckner R, Nagase H, Itoh Y, Newton RC, Magolda RL, Trzaskos JM, Burn TC, et al. (1999), Cloning and characterization of ADAMTS11, an aggrecanase from the ADAMTS family. J Biol Chem 274 (33):23443-50.

Abraham DJ, Varga J (2005), Scleroderma: from cell and molecular mechanisms to disease models. Trends Immunol. 26 (11):587-95.

Aggarwal S (2011), What's fueling the biotech engine--2010 to 2011. Nat Biotechnol. 8: 29 (12):1083-9.

Agrotis A, Kanellakis P, Kostolias G, Di Vitto G, Wei C, Hannan R, Jennings, G., and Bobik, A. (2004), Proliferation of neointimal smooth muscle cells after arterial injury: dependence on interactions between fibroblast growth factor receptor-2 and fibroblast growth factor-9. J. Biol. Chem. 279 (40):42221-9.

Ahmad R, Sylvester J, Ahmad M, Zafarullah M (2009), Adaptor proteins and Ras synergistically regulate IL-1-induced ADAMTS- 4 expression in human chondrocytes. J Immunol 182 (8):5081-7.

Ahram D, Sato TS, Kohilan A, Tayeh M, Chen S, Leal S, Al-Salem M, El-Shanti H (2009), A homozygous mutation in ADAMTSL4 causes autosomal-recessive isolated ectopia lentis. Am. J. Hum. Genet. 84 (2):274-8.

Aiyar A (2000), The use of CLUSTAL W and CLUSTAL X for multiple sequence alignment. Methods Mol. Biol. 132:221-41.

Akiyama M, Takeda S, Kokame K, Takagi J, Miyata T (2009), Crystal structures of the noncatalytic domains of ADAMTS13 reveal multiple discontinuous exosites for von Willebrand factor. Proc Natl Acad Sci U S A. 106 (46):19274-9.

Aldahmesh MA, Khan AO, Mohamed JY, Alkuraya H, Ahmed H, Bobis S, Al-Mesfer S, Alkuraya FS (2011), Identification of ADAMTS18 as a gene mutated in Knobloch syndrome. J. Med. Genet. 48 (9):597-601.

Apweiler R, Bairoch A, Wu CH, Barker WC, Boeckmann B, Ferro S, Gasteiger E, Huang H, Lopez R, Magrane M, Martin MJ, Natale DA, O'Donovan C, Redaschi N, Yeh LS (2004), UniProt: the Universal Protein knowledgebase. Nucleic Acids Res. 32 (Database issue):D115-9.

Argraves WS, McKeown-Longo PJ, and Goetinck PF (1981), Absence of proteoglycan core protein in the cartilage mutant nanomelia. FEBS Lett. 131 (2):265-8.

Arner EC, Hughes CE, Decicco CP, Caterson B, Tortorella MD (1998), Cytokine-induced cartilage proteoglycan degradation is mediated by aggrecanase. Osteoarthritis Cartilage. 6(3):214-28.

Aspberg A, Miura R, Bourdoulous S, Shimonaka M, Heinegard D, Schachner M, Ruoslahti E, Yamaguchi Y (1997), The C-type lectin domains of lecticans, a family of aggregating chondroitin sulfate proteoglycans, bind tenascin-R by protein-protein interactions independent of carbohydrate moiety. Proc Natl Acad Sci U S A 94 (19):10116-21.

Aspberg A, Adam S, Kostka G, Timpl R, Heineg (1999), Fibulin-1 is a ligand for the C-type lectin domains of aggrecan and versican. J Biol Chem 274 (29): 20444-9.

Atapattu L, Saha N, Llerena C, Vail ME, Scott AM, Nikolov DB, Lackmann M, Janes PW (2012), Antibodies binding the ADAM10 substrate recognition domain inhibit Eph function. J Cell Sci. 125 (Pt 24):6084-93.

Atwell JL, Pearce LA, Lah M, Gruen LC, Kortt AA, Hudson PJ (1996), Design and expression of a stable bispecific scFv dimer with affinity for both glycophorin and N9 neuraminidase. Mol Immunol. 33 (17-18):1301-12.

Bader HL, Ruhe AL, Wang LW, Wong AK, Walsh KF, Packer RA, Mitelman J, Robertson KR, O'Brien DP, Broman KW, Shelton GD, Apte SS, Neff MW (2010), An ADAMTSL2 founder mutation causes Musladin–Lueke Syndrome, a heritable disorder of beagle dogs, featuring stiff skin and joint contractures. PLoS One 5(9):e12817.

Bahudhanapati H, Zhang Y, Sidhu SS, Brew K (2011), Phage display of Tissue Inhibitor of Metalloproteinases-2 (TIMP-2): Identification of selective inhibitors of Collagenase-1 (MMP-1). J Biol Chem. 286 (36):31761-70.

Bannister D, Wilson A, Prowse L, Walsh M, Holgate R, Jermutus L, Wilkinson T (2006), Parallel, high-throughput purification of recombinant antibodies for in vivo cell assays. Biotechnol Bioeng 94 (5):931-7.

Barlow JN, Conrath K and Steyaert J (2009), Substrate-dependent modulation of enzyme activity by allosteric effector antibodies. Biochim. Biophys. Acta 1794 (8):1259-68.

Barry FP, Gaw JU, Young CN, Neame PJ (1992), Hyaluronan binding region of aggrecan from pig laryngeal cartilage. Amino acid sequence, analysis of N-linked oligosaccharides and location of the keratan sulphate. Biochem J 286 (Pt 3):761-9.

Bau B, Gebhard PM, Haag J, Knorr T, Bartnik E, Aigner T (2002), Relative messenger RNA expression profiling of collagenases and aggrecanases in human articular chondrocytes in vivo and in vitro. Arthritis Rheum 46 (10):2648-57.

Behera AK, Hildebrand E, Szafranski J, Hung HH, Grodzinsky AJ, Lafyatis R, Koch AE, Kalish, R, Perides G, Steere AC, Hu LT (2006), Role of aggrecanase 1 in Lyme arthritis. Arthritis Rheum 54 (10): 3319-29.

Bentley KJ; Gewert R; Harris WJ (1998), Differential efficiency of expression of humanized antibodies in transient transfected mammalian cells. Hybridoma 17 (6):559-67.

Berger C, Weber-Bornhauser S, Eggenberger J, Hanes J, Plückthun A, Bosshard HR (1999), Antigen recognition by conformational selection. FEBS Lett. 450 (1-2):149-53.

Bergeron F, Leduc R, Day R (2000), Subtilase-like pro-protein convertases: from molecular specificity to therapeutic applications. J Mol Endocrinol 24 (1):1-22.

Bertini I, Calderone V, Cosenza M, Fragai M, Lee YM, Luchinat C, Mangani S, Terni B, Turano P (2005), Conformational variability of matrix metalloproteinases: beyond a single 3D structure. Proc Natl Acad Sci U S A. 102 (15):5334-9.

Bevitt DJ, Mohamed J, Catterall JB, Li Z, Arris CE, Hiscott P, Sheridan C, Langton KP, Barker MD, Clarke MP, McKie N (2003), Expression of ADAMTS metalloproteinases in the retinal pigment epithelium derived cell line ARPE-19: transcriptional regulation by TNF alpha. Biochim Biophys Acta 1626 (1-3):83-91.

Bevitt DJ, Li Z, Barker MD, Clarke MP, McKie N (2005), Analysis of ADAMTS6 transcripts reveals complex alternative splicing and a potential role for the 5′ untranslated region in translational control. Gene 359:99-110.

Billinghurst RC, Wu W, Ionescu M, Reiner A, Daahlberg L, Chen J, van Wart H, and Poole AR (2000), Comparison of the degradation of type II collagen and proteoglycan in nasal and articular cartilages induced by interleukin-1 and the selective inhibition of type II collagen cleavage by collagenase. Arthritis Rheum. 43 (3):664-72.

Bird J, Montana JG, Wills RE, Baxter AD, Owen DA (1999) Selective matrix metalloproteinase (MMP) inhibitors having reduced side-effects. Chemical Abstracts 129:225751.

Birtalan S, Zhang Y, Fellouse FA, Shao L, Schaefer G, Sidhu SS (2008), The intrinsic contributions of tyrosine, serine, glycine and arginine to the affinity and specificity of antibodies. J Mol Biol. 377(5):1518-28.

Björklund M, Heikkilä P, Koivunen E (2004), Peptide inhibition of catalytic and noncatalytic activities of matrix metalloproteinase-9 blocks tumor cell migration and invasion. J Biol Chem. 279 (28):29589-97.

Blaney Davidson EN, Vitters EL, Mooren FM, Oliver N, Berg WB, van der Kraan PM (2006), Connective tissue growth factor/CCN2 overexpression in mouse synovial lining results in transient fibrosis and cartilage damage. Arthritis Rheum 54 (5):1653-61.

Blelloch R, Anna-Arriola SS, Gao D, Li Y, Hodgkin J, Kimble J (1999), The gon-1 gene is required for gonadal morphogenesis in Caenorhabditis elegans. Dev. Biol. 216 (1):382-93.

Blouse GE, Bøtkjaer KA, Deryugina E, Byszuk AA, Jensen JM, Mortensen KK, Quigley JP, Andreasen PA (2009), A novel mode of intervention with serine protease activity: targeting zymogen activation. J Biol Chem. 284 (7):4647-57.

Bode W, Gomis-Rüth FX, Stöcker W (1993), Astacins, serralysins, snake venom and matrix metalloproteinases exhibit identical zinc-binding environments (HEXXHXXGXXH and Met-turn) and topologies and should be grouped into a common family, the 'metzincins'. FEBS Lett. 331 (1-2):134-40.

Boeuf S, Graf F, Fischer J, Moradi B, Little CB, Richter W (2012), Regulation of aggrecanases from the ADAMTS family and aggrecan neoepitope formation during in vitro chondrogenesis of human mesenchymal stem cells. Eur Cell Mater. 23:320-32.

Bondeson J, Wainwright SD, Lauder S, Amos N, Hughes CE (2006), The role of synovial macrophages and macrophage-produced cytokines in driving aggrecanases, matrix metalloproteinases, and other destructive and inflammatory responses in osteoarthritis. Arthritis Res Ther 8 (6):R187.

Bondeson J, Lauder S, Wainwright S, Amos N, Evans A, Hughes C, Feldmann M, Caterson B (2007), Adenoviral gene transfer of the endogenous inhibitor I kappa B alpha into human osteoarthritis synovial fibroblasts demonstrates that several matrix metalloproteinases and aggrecanases are nuclear factor-kappa B-dependent. J Rheumatol 34 (3):523-33.

Bostrom J, Yu SF, Kan D, Appleton BA, Lee CV, Billeci K, Man W, Peale F, Ross S, Wiesmann C, Fuh G (2009), Variants of the antibody herceptin that interact with HER2 and VEGF at the antigen binding site. Science 323 (5921):1610-4.

Boussif O, Lezoualc HF, Zanta MA, Mergny MD, Scherman D, Demeneix B, Behr JP (1995), A versatile vector for gene and oligonucleotide transfer into cells in culture and in vivo: Polyethyleneimine. Proc Natl Acad Sci USA 92 (16):7297-301.

Brew K, Nagase H (2010), The tissue inhibitors of metalloproteinases (TIMPs): an ancient family with structural and functional diversity. Biochim Biophys Acta. 1803 (1):55-71.

Brewster M, Lewis EJ, Wilson KL, Greenham AK, Bottomley KMK (1998), Ro 32–3555, an orally active collagenase selective inhibitor prevents structural damage in the STR/ORT mouse model of osteoarthritis. Arthritis Rheum 41 (9):1639-44.

Brocker CN, Vasiliou V, Nebert DW (2009), Evolutionary divergence and functions of the ADAM and ADAMTS gene families. Hum Genomics 4 (1):43-55.

Brown HM, Dunning KR, Robker RL, Pritchard M, Russell DL (2006), Requirement for ADAMTS-1 in extracellular matrix remodeling during ovarian folliculogenesis and lymphangiogenesis. Dev. Biol. 300 (2):699-709.

Brown HM, Dunning KR, Robker RL, Boerboom D, Pritchard M, Lane M, Russell DL (2010), ADAMTS1 cleavage of versican mediates essential structural remodeling of the ovarian follicle and cumulus-oocyte matrix during ovulation in mice. Biol. Reprod. 83 (4): 549–57.

Brüschweiler S, Schanda P, Kloiber K, Brutscher B, Kontaxis G, Konrat R, Tollinger M (2009), Direct Observation of the Dynamic Process Underlying Allosteric Signal Transmission. J Am Chem Soc 131 (8):3063-8.

Burden MN, Hamblin PA, Larkin JD, White JR (2012), Polypeptides and methods of treatment. US Patent 2012/0095193 A1.

Büttner FH, Hughes CE, Margerie D, Lichte A, Tschesche H, Caterson B, Bartnik E (1998), Membrane type 1 matrix metalloproteinase (MT1-MMP) cleaves the recombinant aggrecan substrate rAgg1mut at the 'aggrecanase' and the MMP sites. Characterization of MT1-MMP catabolic activities on the interglobular domain of aggrecan. Biochem J. 333 (Pt 1):159-65.

Cappelli A, Nannicini C, Valenti S, Giuliani G, Anzini M, Mennuni L, Giordani A, Caselli G, Stasi LP, Makovec F, Giorgi G, Vomero S. (2010), Design, synthesis, and preliminary biological evaluation of pyrrolo[3,4-c]quinolin-1-one and oxoisoindoline derivatives as aggrecanase inhibitors, Chem. Med. Chem. 5 (5) 739-48.

Cardin AD, Weintraub HJ (1989), Molecular modeling of protein-glycosaminoglycan interactions. Arteriosclerosis 9 (1):21-32.

Carter P (2001), Bispecific human IgG by design. J. Immunol. Methods 248 (1-2):7-15.

Carter PJ (2006), Potent antibody therapeutics by design. Nat Rev Immunol 6 (5):343-57.

Chait A, Wight TN (2000), Interaction of native and modified low density lipoproteins with extracellular matrix. Curr. Opin. Lipidol. 11 (5): 457-63.

Chamberland A, Wang E, Jones AR, Collins-Racie LA, LaVallie ER, Huang Y, Liu L, Morris EA, Flannery CR, Yang Z (2009), Identification of a novel HtrA1-susceptible cleavage site in human aggrecan: evidence for the involvement of HtrA1 in aggrecan proteolysis in vivo. J Biol Chem. 284 (40): 27352-9.

Chapple SD, Crofts AM, Shadbolt SP, McCafferty J, Dyson MR (2006), Multiplexed expression and screening for recombinant protein production in mammalian cells. BMC Biotechnol. 6:49.

Chen L, Wu Y, Lee V, Kiani C, Adams ME, Yao Y, Yang BB (2002), The folded modules of aggrecan G3 domain exert two separable functions in glycosaminoglycan modification and product secretion. J Biol Chem 277 (4):2657-65.

Cheng YC, Prusoff WH (1973), Relationship between the inhibition constant (KI) and the concentration of inhibitor which causes 50 per cent inhibition (I50) of an enzymatic reaction. Biochem. Pharmacol. 22 (23):3099-108.

Cheng AC, Coleman RG, Smyth KT, Cao Q, Soulard P, Caffrey DR, Salzberg AC, Huang ES (2007), Structure-based maximal affinity model predicts small-molecule druggability. Nature Biotechnology 25 (1):71-5.

Cheong HS, Chang JS, Park JM, Byun SM (1990), Affinity enhancement of bispecific antibody against two different epitopes in the same antigen. Biochem Biophys Res Commun 173 (3):795-800.

Chia SL, Sawaji Y, Burleigh A, McLean C, Inglis J, Saklatvala J, Vincent T (2009), Fibroblast growth factor 2 is an intrinsic chondroprotective agent that suppresses ADAMTS-5 and delays cartilage degradation in murine osteoarthritis. Arthritis Rheum. 60 (7):2019-27.

Chiusaroli R, Visentini M, Galimberti C, Casseler C, Mennuni L, Covaceuszach S, Lanza M, Ugolini G, Caselli G, Rovati LC, Visintin M (2013), Targeting of ADAMTS-5's ancillary domain with the recombinant mAb CRB0017 ameliorates disease progression in a spontaneous murine model of osteoarthritis. Osteoarthritis Cartilage. doi:pii: S1063-4584(13)00919-9. 10.1016/j.joca.2013.08.015 [Epub ahead of print].

Chockalingam PS, Varadarajan U, Sheldon R, Fortier E, LaVallie ER, Morris EA, Yaworsky PJ, Majumdar MK (2007), Involvement of protein kinase Czeta in interleukin-1beta induction of ADAMTS-4 and type 2 nitric oxide synthase via NF-kappaB signaling in primary human osteoarthritic chondrocytes. Arthritis Rheum 56 (12):4074-83.

Christensen AE, Fiskerstrand T, Knappskog PM, Boman H, Rodahl E (2010), A novel ADAMTSL4 mutation in autosomal recessive ectopia lentis et pupillae. Invest Ophthalmol Vis Sci 51 (12):6369-73.

Clackson T, Hoogenboom.HR, Griffiths AD and Winter G (1991), Making antibody fragments using phage display libraries. Nature 352 (6336):624-28.

Clements KM, Price JS, Chambers MG, Visco DM, Poole AR, Mason R (2003), Gene deletion of either interleukin-1 beta, interleukin-1 beta-converting enzyme, inducible nitric oxide synthase, or stromelysin 1 accelerates the development of knee osteoarthritis in mice after surgical transection of the medial collateral ligament and partial medial meniscectomy. Arthritis Rheum. 48 (12):3452-63.

Close DR (2001), Matrix metalloproteinase inhibitors in rheumatic diseases. Ann Rheum Dis. 60 Suppl 3:iii62-7.

Colige A, Sieron A; Li S, Schwarze U, Petty E, Wertelecki W, Wilcox W, Krakow D, Cohn D, Reardon W, Byers P, Lapiere C, Prockop D, Nusgens B (1999), Human Ehlers-Danlos syndrome type VII C and bovine dermatosparaxis are caused by mutations in the procollagen I N-proteinase gene. Am. J. Hum. Genet. 65 (2):308-17.

Colige A, Ruggiero F, Vandenberghe I, Dubail J, Kesteloot F, Van Beeumen J, Beschin A, Brys L, Lapière CM, Nusgens B (2005), Domains and maturation processes that regulate the activity of ADAMTS-2, a metalloproteinase cleaving the aminopropeptide of fibrillar procollagens types I-III and V. J. Biol Chem. 280 (41):34397-408.

Collins-Racie LA, Flannery C, Zeng W, Corr M, Annis-Freeman B, Agostino MJ, Arai M, Di Blasio-Smith E, Dorner AJ, Georgiadis KE, Jin M, Tan XY, Morrison C, Lavallie ER (2004), ADAMTS-8 exhibits aggrecanase activity and is expressed in human articular cartilage. Matrix Biol. 23 (4):219-30.

Colwell NS, Blinder MA, Tsiang M, Gibbs CS, Bock PE, Tollefsen DM (1998), Allosteric effects of a monoclonal antibody against thrombin exosite II. Biochemistry 37 (43):15057-65.

Cortese R, Felici F, Galfre G, Luzzago A, Monaci P, Nicosia A (1994), Epitope discovery using peptide libraries displayed on phage. Trends Biotechnol 12 (7):262-7.

Coussens LM, Fingleton B, Matrisian LM (2002), Matrix metalloproteinase inhibitors and cancer: trials and tribulations. Science 295 (5564):2387-92.

Cross NA, Chandrasekharan S, Jokonya N, Fowles A, Hamdy FC, Buttle DJ, Eaton CL (2005), The expression and regulation of ADAMTS-1, -4, -5, -9, and -15, and TIMP-3 by TGF beta 1 in prostate cells: relevance to the accumulation of versican. Prostate 63 (3):269-75.

Cross AK, Haddock G, Stock CJ, Allan S, Surr J, Bunning RA, Buttle DJ, Woodroofe MN (2006), ADAMTS-1 and -4 are up-regulated following transient middle cerebral artery occlusion in the rat and their expression is modulated by TNF in cultured astrocytes. Brain Res 1088 (1):19-30.

Curtis CL, Hughes CE, Flannery CR, Little CB, Harwood JL, Caterson B (2000), n-3 fatty acids specifically modulate catabolic factors involved in articular cartilage degradation. J Biol Chem 275 (2):721-4.

Curtis CL, Rees SG, Little CB, Flannery CR, Hughes CE, Wilson C, Dent CM, Otterness IG, Harwood JL, Caterson B (2002), Pathologic indicators of degradation and inflammation in human osteoarthritic cartilage are abrogated by exposure to n-3 fatty acids. Arthritis Rheum 46 (6):1544-53.

Dagoneau N, Benoist-Lasselin C, Huber C, Faivre L, Mégarbané A, Alswaid A, Dollfus H, Alembik Y, Munnich A, Legeai-Mallet L, Cormier-Daire V (2004), ADAMTS10 mutations in autosomal recessive Weill Marchesani syndrome. Am. J. Hum. Genet. 75 (5):801-6.

De Genst E, Silence K, Decanniere K, Conrath K, Loris R, Kinne J, Muyldermans S, Wyns L (2006), Molecular basis for the preferential cleft recognition by dromedary heavy-chain antibodies. Proc Natl Acad Sci USA 103 (12):4586-91.

de Groot R, Bardhan A, Ramroop N, Lane DA, Crawley JT (2009), Essential role of the disintegrin-like domain in ADAMTS13 function. Blood 113 (22):5609-16.

de Kruif J, Terstappen L, Boel E, Logtenberg T (1995), Rapid selection of cell subpopulation-specific human monoclonal antibodies from a synthetic phage antibody library. Proc Natl Acad Sci U S A 92 (9):3938-42.

Demircan K, Gunduz E, Gunduz M, Beder LB, Hirohata S, Nagatsuka H, Cengiz B, Cilek MZ, Yamanaka N, Shimizu K, Ninomiya Y (2009), Increased mRNA expression of ADAMTS metalloproteinases in metastatic foci of head and neck cancer. Head Neck 31 (6):793-801.

Deng H, O'Keefe H, Davie CP, Lind KE, Acharya RA, Franklin GJ, Larkin J, Matico R, Neeb M, Thompson MM, Lohr T, Gross JW, Centrella PA, O'Donovan GK, Bedard KL, van Vloten K, Mataruse S, Skinner SR, Belyanskaya SL, Carpenter TY, Shearer TW, Clark MA, Cuozzo JW, Arico-Muendel CC, Morgan BA (2012), Discovery of Highly Potent and Selective Small Molecule ADAMTS-5 Inhibitors That Inhibit Human Cartilage Degradation via Encoded Library Technology (ELT). J Med Chem. 55 (16):7061-79.

Dennis MS, Eigenbrot C, Skelton NJ, Ultsch MH, Santell L, Dwyer MA, O'Connell MP, Lazarus RA (2000), Peptide exosite inhibitors of factor VIIa as anticoagulants. Nature 404 (6777):465-70.

Desmyter A, Transue TR, Ghahroudi MA, Dao Thi MH, Poortmans F, Hamers R, Muyldermans S, Wyns L (1996), Crystal structure of a camel single-domain VH antibody fragment in complex with lysozyme. Nat. Struct. Biol. 3 (9):803-11.

Devy L, Huang L, Naa L, Yanamandra N, Pieters H, Frans N, Chang E, Tao Q, Vanhove M, Lejeune A, van Gool R, Sexton DJ, Kuang G, Rank D, Hogan S, Pazmany C, Ma YL, Schoonbroodt S, Nixon AE, Ladner RC, Hoet R, Henderikx P, Tenhoor C, Rabbani SA, Valentino ML, Wood CR, Dransfield DT (2009), Selective inhibition of matrix metalloproteinase-14 blocks tumor growth, invasion, and angiogenesis. Cancer Res 69 (4):1517-26.

Dickinson SC, Vankemmelbeke MN, Buttle DJ, Rosenberg K, Heinegård D, Hollander AP (2003), Cleavage of cartilage oligomeric matrix protein (thrombospondin-5) by matrix metalloproteinases and a disintegrin and metalloproteinase with thrombospondin motifs. Matrix Biol. 22 (3):267-78.

Didangelos A, Mayr U, Monaco C, Mayr M (2012), Novel role of ADAMTS-5 protein in proteoglycan turnover and lipoprotein retention in atherosclerosis. J Biol Chem 287 (23):19341-5.

Ding L, Heying E, Nicholson N, Stroud NJ, Homandberg GA, Buckwalter JA, Guo D, Martin JA (2010), Mechanical impact induces cartilage degradation via mitogen activated protein kinases. Osteoarthritis Cartilage 18 (11):1509-17.

Ding Y, inventor, Praecis Pharmaceuticals, Inc., assignee (2010), Preparation of 2,4-diamino-1,3,5-triazine and 4,6-diamino-pyrimidine derivatives as aggrecanase inhibitors patent WO2010085246.

Ditzel HJ, Binley JM, Moore JP, Sodroski J, Sullivan N, Sawyer LSW, Hendry RM, Yang W, Barbas CF 3rd, Burton DR (1995), Neutralizing recombinant human antibodies to a conformational V2- and CD4-binding site-sensitive. epitope of HIV-1 gp120 isolated by using an epitope-masking procedure. J. Immunol. 154 (2):893-906

Dixon M, Webb EC, Thorne CJR, Tipton KF (1979), Enzymes. Longman Group, Third Edition.

Djouad F, Delorme B, Maurice M, Bony C, Apparailly F, Louis-Plence P, Canovas F, Charbord P, Noël D, Jorgensen C (2007), Microenvironmental changes during differentiation of mesenchymal stem cells towards chondrocytes. Arthritis Res Ther 9 (2):R33.

D'Mello F, Howard CR (2001), An improved selection procedure for the screening of phage display peptide libraries. J Immunol Methods 247 (1-2):191-203.

Doege KJ, Sasaki M, Kimura T, Yamada Y (1991), Complete coding sequence and deduced primary structure of the human cartilage large aggregating proteoglycan, aggrecan: Human-specific repeats, and additional alternatively spliced forms. J. Biol. Chem. 266 (2):894-902.

Doorbar J, Winter G (1994), Isolation of a peptide antagonist to the thrombin receptor using phage display. J Mol Biol 244 (4):361-9.

Dubail J, Kesteloot F, Deroanne C, Motte P, Lambert V, Rakic JM, Lapiere C, Nusgens B, Colige A (2010), ADAMTS-2 functions as anti-angiogenic and anti-tumoral molecule independently of its catalytic activity. Cell Mol Life Sci 67 (24):4213-32.

Dufield DR, Nemirovskiy OV, Jennings MG, Tortorella MD, Malfait AM, Mathews WR (2010), An immunoaffinity liquid chromatography-tandem mass spectrometry assay for detection of endogenous aggrecan fragments in biological fluids: Use as a biomarker for aggrecanase activity and cartilage degradation. Anal Biochem. 406 (2):113-23.

Dumoulin M, Conrath K, Van Meirhaeghe A, Meersman F, Heremans K, Frenken LG, Muyldermans S, Wyns L, Matagne A (2002), Single-domain antibody fragments with high conformational stability. Protein Sci. 11 (3):500-15.

Dumoulin M, Last AM, Desmyter A, Decanniere K, Canet D, Larsson G, Spencer A, Archer DB, Sasse J, Muyldermans S, Wyns L, Redfield C, Matagne A, Robinson CV, Dobson CM (2003), A camelid antibody fragment inhibits the formation of amyloid fibrils by human lysozyme. Nature 424 (6950):783–8.

Dunn JR, Panutsopulos D, Shaw MW, Heighway J, Dormer R, Salmo EN, Watson SG, Field JK, Liloglou T (2004), METH-2 silencing and promoter hypermethylation in NSCLC. Br. J. Cancer 91 (6):1149-54.

Dunn JR, Reed JE, du Plessis DG, Shaw EJ, Reeves P, Gee AL, Warnke P, Walker C (2006), Expression of ADAMTS-8, a secreted protease with antiangiogenic properties, is downregulated in brain tumours. Br. J. Cancer 94 (8):1186-93.

Dupuis LE, McCulloch DR, McGarity JD, Bahan A, Wessels A, Weber D, Diminich AM, Nelson CM, Apte SS, Kern CB (2011), Altered versican cleavage in ADAMTS5 deficient mice; A novel etiology of myxomatous valve disease. Dev Biol. 357 (1):152-64.

Durigova M, Roughley PJ, Mort JS (2008a) Mechanism of proteoglycan aggregate degradation in cartilage stimulated with oncostatin M. Osteoarthritis Cartilage 16 (1):98-104.

Durigova M, Soucy P, Fushimi K, Nagase H, Mort JS, Roughley PJ (2008b) Characterization of an ADAMTS-5-mediated cleavage site in aggrecan in OSM-stimulated bovine cartilage. Osteoarthritis Cartilage 16 (10):1245-52.

Durigova M, Nagase H, Mort JS, Roughley PJ (2011a), MMPs are less efficient than ADAMTS5 in cleaving aggrecan core protein. Matrix Biol. 30(2):145-53.

Durigova M, Troeberg L, Nagase H, Roughley PJ, Mort JS (2011b), Involvement of ADAMTS5 and hyaluronidase in aggrecan degradation and release from OSM-stimulated cartilage. Eur Cell Mater. 21:31-45.

Durocher Y, Perret S, Kamen A (2002), High-level and high-throughput recombinant protein production by transient transfection of suspension-growing human 293-EBNA1 cells. Nucleic Acids Res 30(2):E9.

Echtermeyer F, Bertrand J, Dreier R, Meinecke I, Neugebauer K, Fuerst M, Lee YJ, Song YW, Herzog C, Theilmeier G, Pap T (2009), Syndecan-4 regulates ADAMTS-5 activation and cartilage breakdown in osteoarthritis. Nat Med 15 (9):1072-6.

Ehlen, HWA, Sengle G, Klatt AR, Talke A, Müller S, Paulsson M, Wagener R (2009), Proteolytic processing causes extensive heterogeneity of tissue matrilin forms. J. Biol. Chem. 284 (32):21545–56.

El Hour M, Moncada-Pazos A, Blacher S, Masset A, Cal S, Berndt S, Detilleux J, Host L, Obaya AJ, Maillard C, Foidart JM, Ectors F, Noel A, Lopez-Otin C (2010), Higher sensitivity of Adamts12-deficient mice to tumor growth and angiogenesis. Oncogene 29 (20):3025-32.

Embry JJ, Knudson W (2003), G1 domain of aggrecan cointernalizes with hyaluronan via a CD44-mediated mechanism in bovine articular chondrocytes. Arthritis Rheum 48 (12):3431-41.

Enomoto H, Nelson CM, Somerville RP, Mielke K, Dixon LJ, Powell K, Apte SS (2010), Cooperation of two ADAMTS metalloproteases in closure of the mouse palate identifies a requirement for versican proteolysis in regulating palatal mesenchyme proliferation. Development 137 (23):4029-38.

Faivre L, Gorlin RJ, Wirtz MK, Godfrey M, Dagoneau N, Samples JR, Le Merrer M, Collod-Beroud G, Boileau C, Munnich A, Cormier-Daire V (2003), In frame fibrillin-1 gene deletion in autosomal dominant Weill-Marchesani syndrome. J Med Genet 40 (1):34-6.

Fajardo M, Di Cesare PE (2005), Disease-modifying therapies for osteoarthritis: current status. Drugs Aging 22 (2):141-61.

Farady CJ, Sun J, Darragh MR, Miller SM, Craik CS (2007), The mechanism of inhibition of antibody-based inhibitors of membrane-type serine protease 1 (MT-SP1). J Mol Biol. 369(4):1041-51.

Farndale RW, Buttle DJ, Barrett AJ (1986), Improved quantitation and discrimination of sulphated glycosaminoglycans by use of dimethylmethylene blue. Biochim. Biophys. Acta 883 (2):173-7.

Fernandes JC, Martel-Pelletier J, Pelletier JP (2002), The role of cytokines in osteoarthritis pathophysiology. Biorheology 39 (1-2):237-46.

Fernandez-Catalan C, Bode W, Huber R, Turk D, Calvete JJ, Lichte A, Tschesche H, Maskos K (1998), Crystal structure of the complex formed by the membrane type 1-matrix metalloproteinase with the tissue inhibitor of metalloproteinases- 2, the soluble progelatinase a receptor. EMBO J. 17 (17):5238-48.

Fletcher RS, Arion D, Borkow G, Wainberg MA, Dmitrenko GI, Parniak MA (1995) Synergistic inhibition of HIV-1 reverse transcriptase DNA polymerase activity and virus replication in vitro by combinations of carboxanilide nonnucleoside compounds. Biochemistry 34 (32):10106-12.

Filou S, Stylianou M, Triantaphyllidou IE, Papadas T, Mastronikolis NS, Goumas PD, Papachristou DJ, Ravazoula P, Skandalis SS, Vynios DH (2013), Expression and distribution of aggrecanases in human larynx: ADAMTS-5/aggrecanase-2 is the main aggrecanase in laryngeal carcinoma. Biochimie. 95(4):725-34.

Flannery CR, Lark MW, Sandy JD (1992), Identification of a stromelysin cleavage site within the interglobular domain of human aggrecan. Evidence for proteolysis at this site in vivo in human articular cartilage. J Biol Chem. 267 (2):1008-14.

Flannery CR, Zeng W, Corcoran C, Collins-Racie LA, Chockalingam PS, Hebert T, Mackie SA, McDonagh T, Crawford TK, Tomkinson KN, LaVallie ER, Morris EA (2002), Autocatalytic cleavage of ADAMTS-4 (aggrecanase-1) reveals multiple glycosaminoglycan-binding sites. J Biol Chem 277 (45):42775-80.

Foote J, Milstein C (1994), Conformational isomerism and the diversity of antibodies. Proc. Natl. Acad. Sci. USA 91 (22):10370-4.

Fosang AJ, Neame PJ, Last K, Hardingham TE, Murphy G, Hamilton JA (1992), The interglobular domain of cartilage aggrecan is cleaved by PUMP, gelatinases, and cathepsin B. J. Biol. Chem. 267 (27):19470-4.

Fosang AJ, Last K, Neame PJ, Hardingham TE, Murphy G, Hamilton JA (1993), Collagenase, plasmin and urokinase-type plasminogen activator cleave the aggrecan interglobular domain. Orthop. Trans. 17:848-9.

Fosang AJ, Last K, Maciewicz RA (1996), Aggrecan is degraded by matrix metalloproteinases in human arthritis. Evidence that matrix metalloproteinase and aggrecanase activities can be independent. J. Clin. Investig. 98 (10):2292-9.

Fosang AJ, Last K, Stanton H, Weeks DB, Campbell IK, Hardingham TE, Hembry RM (2000), Generation and novel distribution of matrix metalloproteinase-derived aggrecan fragments in porcine cartilage explants. J. Biol. Chem. 275 (42):33027-37.

Fransen M, McConnell S, Bell M (2002), Therapeutic exercise for people with osteoarthritis of the hip or knee. A systematic review. J. Rheumatol. 29 (8):1737-45.

Funck-Brentano T, Lin H, Hay E, Ah Kioon MD, Schiltz C, Hannouche D, Nizard R, Lioté F, Orcel P, de Vernejoul MC, Cohen-Solal ME (2012), Targeting bone alleviates osteoarthritis in osteopenic mice and modulates cartilage catabolism. PLoS One. 7(3):e33543.

Fukuoka Y, Schwartz LB (2006), The B12 antitryptase monoclonal antibody disrupts the tetrameric structure of heparin-stabilized beta-tryptase to form monomers that are inactive at neutral pH and active at acidic pH. J. Immunol. 176 (5):3165-72.

Fushimi K, Nakashima S, Banno Y, Akaike A, Takigawa M and Shimizu K (2004), Implication of prostaglandin E2 in TNF-α-induced release of m-calpain from HCS-2/8 chondrocytes. Inhibition of m-calpain release by NSAIDs. Osteoarthritis Cartilage 12 (11):895-903.

Fushimi K, Troeberg L, Nakamura H, Lim NH, and Nagase H (2008), Functional Differences of the Catalytic and Non-catalytic Domains in Human ADAMTS-4 and ADAMTS-5 in Aggrecanolytic Activity. J Biol Chem 283 (11):6706-16.

Ganesan R, Eigenbrot C, Wu Y, Liang WC, Shia S, Lipari MT, Kirchhofer D (2009), Unraveling the allosteric mechanism of serine protease inhibition by an antibody. Structure. 17 (12):1614-24.

Gao G, Westling J, Thompson VP, Howell TD, Gottschall PE, Sandy JD (2002), Activation of the proteolytic activity of ADAMTS4 (aggrecanase-1) by C- terminal truncation. J Biol Chem 277 (13): 11034-41.

Gao G, Plaas A, Thompson VP, Jin S, Zuo F, Sandy JD (2004), ADAMTS4 (aggrecanase-1) activation on the cell surface involves C-terminal cleavage by glycosylphosphatidyl inositol anchored membrane type 4-matrix metalloproteinase and binding of the activated proteinase to chondroitin sulfate and heparan sulfate on syndecan-1. J Biol Chem 279 (11):10042-51.

Gao W, Anderson PJ, Majerus EM, Tuley EA, Sadler JE (2006), Exosite interactions contribute to tension-induced cleavage of von Willebrand factor by the antithrombotic ADAMTS13 metalloprotease. Proc. Natl. Acad. Sci. USA. 103 (50):19099-104.

Gao W, Anderson PJ, Sadler JE (2008), Extensive contacts between ADAMTS13 exosites and von Willebrand factor domain A2 contribute to substrate specificity. Blood. 112 (5):1713-9.

Gao J, Sidhu SS, Wells JA (2009) Two-state selection of conformation-specific antibodies. Proc Natl Acad Sci USA 106 (9):3071-6.

Gao W, Zhu J, Westfield LA, Tuley EA, Anderson PJ, Sadler JE (2012), Rearranging exosites in noncatalytic domains can redirect the substrate specificity of ADAMTS proteases. J Biol Chem. 287 (32):26944-52.

Gary SC, Kelly GM, Hockfield S (1998), BEHAB/brevican: a brain-specific lectican implicated in gliomas and glial cell motility. Curr. Opin. Neurobiol. 8 (5):576-81.

Gendron C, Kashiwagi M, Hughes C, Caterson B and Nagase H (2003), TIMP-3 inhibits aggrecanase-mediated glycosaminoglycan release from cartilage explants stimulated by catabolic factors. FEBS Lett. 555 (3):431-6.

Gendron, C, Kashiwagi M, Lim NH, Enghild JJ, Thogersen IB, Hughes C, Caterson B, and Nagase H (2007), Proteolytic activities of Human ADAMTS-5. Comparative studies with ADAMTS-4. J Biol Chem. 282 (25):18294-306.

Georgiadis K, Crawford T, Tomkinson K, Shakey Q, Stahl M, Morris E, L. Collins-Racie, E. LaVallie (2002), ADAMTS-5 is autocatalytic at a E753-G754 site in the spacer domain. Trans Orthop Res Soc 48:167.

Gerhardt S, Hassall G, Hawtin P, McCall E, Flavell L, Minshull C, Hargreaves D, Ting A, Pauptit RA, Parker AE, Abbott WM (2007), Crystal structures of human ADAMTS-1 reveal a conserved catalytic domain and a disintegrin-like domain with a fold homologous to cysteine-rich domains. J Mol Biol. 373 (4):891-902.

Glasson SS, Askew R, Sheppard B, Carito BA, Blanchet T, Ma HL, Flannery CR, Kanki K, Wang E, Peluso D, Yang Z, Majumdar MK, Morris EA (2004), Characterization of and osteoarthritis susceptibility in ADAMTS-4-knockout mice. Arthritis Rheum 50 (8):2547-58.

Glasson SS, Askew R, Sheppard B, Carito B, Blanchet T, Ma HL, Flannery CR, Peluso D, Yang Z, Majumdar MK, and Morris EA (2005), Deletion of active ADAMTS5 prevents cartilage degradation in a murine model of osteoarthritis. Nature 434 (7033):644-8.

Gomis-Rüth FX, Maskos K, Betz M, Bergner A, Huber R, Suzuki K, Yoshida N, Nagase H, Brew K, Bourenkov GP, Bartunik H, Bode W (1997), Mechanism of inhibition of the human matrix metalloproteinase stromelysin-1 by TIMP-1. Nature 389 (6646):77-81.

Goodey NM, Benkovic SJ (2008), Allosteric regulation and catalysis emerge via a common route. Nat. Chem. Biol. 4 (8):474-82.

Goulas T, Arolas JL, Gomis-Rüth FX (2011), Structure, function and latency regulation of a bacterial enterotoxin potentially derived from a mammalian adamalysin/ADAM xenolog. Proc Natl Acad Sci U S A108 (5):1856-61.

Green NM (1963), Avidin. 1. The use of [14C]biotin for kinetic studies and for assay. Biochem J. 89 (3):585-591.

Grobelny D, Poncz L, Galardy RE (1992), Inhibition of human skin fibroblast collagenase, thermolysin, and Pseudomonas aeruginosa elastase by peptide hydroxamic acids. Biochemistry. 31 (31):7152-4.

Groma G, Grskovic I, Schael S, Ehlen HW, Wagener R, Fosang A, Aszodi A, Paulsson M, Brachvogel B, Zaucke F (2011), Matrilin-4 is processed by ADAMTS-5 in late Golgi vesicles present in growth plate chondrocytes of defined differentiation state. Matrix Biol 30 (4):275-80.

Gunasekaran K, Ma B, Nussinov R (2004), Is allostery an intrinsic property of all dynamic proteins? Proteins 57 (3):433-43.

Hadler N, Johnson A, Spitznagel J, Quinet R (1981), Protease inhibitors in inflammatory synovial effusions. Ann. Rheum. Dis. 40 (1):55-9.

Hagemeyer CE, von Zur Muhlen C, von Elverfeldt D, Peter K (2009), Single-chain antibodies as diagnostic tools and therapeutic agents. Thromb Haemost. 101 (6):1012-9.

Halasz K, Kassner A, Mörgelin M, Heinegård D (2007), COMP acts as a catalyst in collagen fibrillogenesis. J Biol Chem. 282(43):31166-73.

Hamel MG, Ajmo JM, Leonardo CC, Zuo F, Sandy JD, Gottschall PE (2008), Multimodal signaling by the ADAMTSs (a disintegrin and metalloproteinase with thrombospondin motifs) promotes neurite extension. Exp Neurol 210 (2):428-40.

Handley CJ, Tuck Mok M, Ilic MZ, Adcocks C, Buttle DJ, Robinson HC (2001), Cathepsin D cleaves aggrecan at unique sites within the interglobular domain and chondroitin sulfate attachment regions that are also cleaved when cartilage is maintained at acid pH. Matrix Biol. 20 (8):543-53.

Hardingham TE, Fosang AJ, Dudhia J (1992), in Articular Cartilage and Osteoarthritis (Kuettner KE, Schleyerbach R, Peyton JG, Hascall VC, eds) pp. 5-20, Raven Press, New York.

Hascall VC, Sajdera SW (1969), Protein-polysaccharide complex from bovine nasal cartilage. The function of glycoprotein in the formation of aggregates. J. Biol. Chem. 244 (9):2384-96.

Hashimoto G, Aoki T, Nakamura H, Tanzawa K, Okada Y (2001), Inhibition of ADAMTS4 (aggrecanase-1) by tissue inhibitors of metalloproteinases (TIMP-1, 2, 3 and 4). FEBS Lett 494 (3):192-5.

Hashimoto G, Shimoda M, Okada Y (2004), ADAMTS4 (aggrecanase-1) interaction with the C-terminal domain of fibronectin inhibits proteolysis of aggrecan. J Biol Chem 279 (31):32483-91.

Hattori N, Carrino DA, Lauer ME, Vasanji A, Wylie JD, Nelson CM, Apte SS (2011), Pericellular versican regulates the fibroblast-myofibroblast transition: a role for ADAMTS5 protease-mediated proteolysis. J Biol Chem. 286 (39):34298-310.

Hedström L (2002), Serine protease mechanism and specificity. Chem. Rev. 102 (12):4501-24.

Held-Feindt J, Paredes EB, Blömer U, Seidenbecher C, Stark AM, Mehdorn HM, Mentlein R (2006), Matrix-degrading proteases ADAMTS4 and ADAMTS5 (disintegrins and metalloproteinases with thrombospondin motifs 4 and 5) are expressed in human glioblastomas. Int. J. Cancer 118 (1):55-61.

Helmick CG, Felson DT, Lawrence RC, Gabriel S, Hirsch R, Kent Kwoh C, Liang MH, Maradit Kremers H, Mayes MD, Merkel PA, Pillemer SR, Reveille JD, Stone JH (2008), Estimates of the prevalence of arthritis and other rheumatic conditions in the United States. Part I. Arthritis Rheum. 58 (1):15-25.

Hendershot L, Bole D, Köhler G, Kearney JF (1987), Assembly and secretion of heavy chains that do not associate posttranslationally with immunoglobulin heavy chain-binding protein. J. Cell Biol. 104 (3):761-7.

Hills R, Mazzarella R, Fok K, Nemirovskiy O, Leone J, Zack MD, Arner EC, Viswanathan M, Abujoub A, Muruganandam A, Sexton DJ, Bassill GJ, Sato AK, Malfait AM, Tortorella MD (2007), Identification of an ADAMTS-4 cleavage motif using phage display leads to the development of fluorogenic peptide substrates and reveals matrilin-3 as a novel substrate. J. Biol. Chem. 282 (15):11101-9.

Hilschmann N, Craig LC (1965), Amino acid sequence studies with Bence-Jones proteins. Proc Natl Acad Sci U S A. 53(6):1403-9.

Hisanaga A, Morishita S, Suzuki K, Sasaki K, Koie M, Kohno T, Hattori M (2012), A disintegrin and metalloproteinase with thrombospondin motifs 4 (ADAMTS-4) cleaves Reelin in an isoform-dependent manner. FEBS Lett. 586 (19):3349-53.

Holliger P, Prospero T, Winter G (1993) "Diabodies:" small bivalent, and bispecific antibody fragments. Proc Natl Acad Sci U S A 90 (14):6444-8.

Holliger P, Hudson PJ (2005), Engineered antibody fragments and the rise of single domains. Nat Biotechnol. 23 (9):1126-36.

Holmbeck K, Bianco P, Caterina J, Yamada S, Kromer M, Kuznetsov SA, Mankani M, Robey PG, Poole AR, Pidoux I, Ward JM, Birkedal-Hansen H (1999), MT1-MMP-deficient mice develop dwarfism, osteopenia, arthritis, and connective tissue disease due to inadequate collagen turnover. Cell 99 (1):81-92.

Honda T, Kobayashi K, Mikoshiba K and Nakajima K (2011), Regulation of cortical neuron migration by the Reelin signaling pathway. Neurochem. Res. 36 (7):1270-9.

Hoogenboom HR (2005), Selecting and screening recombinant antibody libraries. Nat Biotechnol 23 (9):1105-16.

Hood JL, Brooks WH and Roszman TL (2004), Differential compartmentalization of the calpain/calpastatin network with the endoplasmic reticulum and Golgi apparatus. J. Biol. Chem. 279 (41):43126-35.

Hootman JM, Helmick CG (2006), Projections of US prevalence of arthritis and associated activity limitations. Arthritis Rheum 54 (1):226-9.

Hörber C, Buttner FH, Kern C, Schmiedeknecht G, Bartnik E (2000), Truncation of the amino-terminus of the recombinant aggrecan rAgg1mut leads to reduced cleavage at the aggrecanase site. Efficient aggrecanase catabolism may depend on multiple substrate interactions. Matrix Biol 19 (6):533-43.

Hsu YP, Staton CA, Cross N, Buttle DJ (2012), Anti-angiogenic properties of ADAMTS-4 in vitro. Int J Exp Pathol 93 (1):70-7.

Hu S, Shively L, Raubitschek A, Sherman M, Williams LE, Wong JY, Shively JE, Wu AM (1996), Minibody: A novel engineered anti-carcinoembryonic antigen antibody fragment (single-chain Fv-CH3) which exhibits rapid, high-level targeting of xenografts. Cancer Res. 56 (13):3055-61.

Hu LT, Eskildsen MA, Masgala C, Steere AC, Arner EC, Pratta MA, Grodzinsky AJ, Loening A, Perides G (2001), Host metalloproteinases in Lyme arthritis. Arthritis Rheum 44 (6):1401-10.

Hughes SE, Crossman D, Hall PA (1993), Expression of basic and acidic fibroblast growth factors and their receptor in normal and atherosclerotic human arteries. Cardiovasc. Res. 27 (7):1214-9.

Hughes CE, Caterson B, Fosang AJ, Roughley PJ, Mort JS (1995), Monoclonal antibodies that specifically recognize neoepitope sequences generated by 'aggrecanase' and matrix metalloproteinase cleavage of aggrecan: application to catabolism in situ and in vitro. Biochem. J. 305 (Pt 3):799-804.

Hughes CE, Büttner FH, Eidenmüller B, Caterson B and Bartnik E (1997), Utilization of a recombinant substrate rAgg1 to study the biochemical properties of aggrecanase in cell culture systems. J. Biol. Chem. 272 (32):20269-74.

Hurskainen TL, Hirohata S, Seldin MF, Apte SS (1999), ADAM-TS5, ADAM-TS6, and ADAM-TS7, novel members of a new family of zinc metalloproteases. General features and genomic distribution of the ADAM-TS family. J Biol Chem 274 (36):25555-63.

Hurt-Camejo E, Camejo G, Rosengren B, López F, Ahlström C, Fager G, Bondjers G (1992), Effect of arterial proteoglycans and glycosaminoglycans on low density lipoprotein oxidation and its uptake by human macrophages and arterial smooth muscle cells. Arterioscler Thromb 12 (5):569-83.

Igarashi T, Araki S, Mori H, Takeda S (2007), Crystal structures of catrocollastatin/VAP2B reveal a dynamic, modular architecture of ADAM/adamalysin/reprolysin family proteins. FEBS Lett. 581 (13):2416-22.

Ilic MZ, Robinson HC, and Handley CJ (1998), Characterization of aggrecan retained and lost from the extracellular matrix of articular cartilage. Involvement of carboxyl-terminal processing in the catabolism of aggrecan. J. Biol. Chem. 273 (28):17451-8.

Iozzo RV (1999), The biology of the small leucine-rich proteoglycans. Functional network of interactive proteins. J Biol Chem 274 (27):18843-6.

Iruela-Arispe ML, Carpizo D, Luque A (2003), ADAMTS1: a matrix metalloprotease with angioinhibitory properties. Ann N Y Acad Sci 995:183-90.

Isogai Z, Aspberg A, Keene DR, Ono RN, Reinhardt DP, and Sakai LY (2002), Versican interacts with fibrillin-1 and links extracellular microfibrils to other connective tissue networks. J. Biol. Chem. 277 (6):4565-72.

Itoh T, Matsuda H, Tanioka M, Kuwabara K, Itohara S, Suzuki RJ (2002), The role of matrix metalloproteinase-2 and matrix metalloproteinase-9 in antibody-induced arthritis. J Immunol. 169 (5):2643-7.

Iwata S, Ostermeier C, Ludwig B, Michel H (1995), Structure at 2.8 Å resolution of cytochrome c oxidase from Paracoccus denitrificans. Nature 376 (6542):660-9.

Jackson JR, Sathe G, Rosenberg M, Sweet R (1995), In vitro antibody maturation. Improvement of a high affinity, neutralizing antibody against IL-1 beta. J Immunol 154 (7):3310-9.

Jin H, Wang X, Ying J, Wong AH, Li H, Lee KY, Srivastava G, Chan AT, Yeo W, Ma BB, Putti TC, Lung ML, Shen ZY, Xu LY, Langford C, Tao Q (2007), Epigenetic identification of ADAMTS18 as a novel 16q23.1 tumor suppressor frequently silenced in esophageal, nasopharyngeal and multiple other carcinomas. Oncogene 26 (53):7490-8.

Jones S, Thornton JM (1997), Analysis of protein-protein interaction sites using surface patches. J. Mol. Biol. 272 (1):121-32.

Johnson G, Wu TT (2000), Kabat database and its applications: 30 years after the first variability plot. Nucleic Acids Res. 28 (1):214-8.

Jönsson-Rylander A, Nilsson T, Fritsche-Danielson R, Hammarström A, Behrendt M, Andersson J, Lindgren K, Andersson A,Wallbrandt P, Rosengren B, Brodin P, Thelin A, Westin A, Hurt-Camejo E, Lee- Søgaard C (2005), Role of ADAMTS-1 in atherosclerosis: Remodeling of carotid artery, immunohistochemistry, and proteolysis of Versican. Arterioscler Thromb Vasc Biol 25 (1):180-5.

Julenius K, Mølgaard A, Gupta R, and Brunak S (2005). Prediction, conservation analysis and structural characterization of mammalian mucin-type O-glycosylation sites. Glycobiology 15 (2):153-64.

Julenius K (2007), NetCGlyc 1.0: Prediction of mammalian C-mannosylation sites. Glycobiology, 17:868-76.

Jungers KA, Le Goff C, Somerville RP, and Apte SS (2005), Adamts9 is widely expressed during mouse embryo development. Gene Expr. Patterns 5 (5):609-17.

Karsdal MA, Madsen SH, Christiansen C, Henriksen K, Fosang AJ, Sondergaard BC (2008), Cartilage degradation is fully reversible in the presence of aggrecanase but not matrix metalloproteinase activity. Arthritis Res Ther. 10(3):R63.

Kashiwagi M, Tortorella M, Nagase H, Brew K (2001), TIMP-3 is a potent inhibitor of aggrecanase 1 (ADAM-TS4) and aggrecanase 2 (ADAM-TS5). J Biol Chem 276 (16):12501-4.

Kashiwagi M, Enghild JJ, Gendron C, Hughes C, Caterson B, Itoh Y, Nagase H (2004), Altered proteolytic activities of ADAMTS-4 expressed by C-terminal processing. J Biol Chem 279 (11):10109-19.

Kern CB, Wessels A, McGarity J, Dixon LJ, Alston E, Argraves WS, Geeting D, Nelson CM, Menick DR, Apte SS (2010), Reduced versican cleavage due to Adamts9 haploinsufficiency is associated with cardiac and aortic anomalies. Matrix Biol. 29 (4):304-16.

Kevorkian L, Young DA, Darrah C, Donell ST, Shepstone L, Porter S, Brockbank SM, Edwards DR, Parker AE, Clark IM (2004), Expression profiling of metalloproteinases and their inhibitors in cartilage. Arthritis Rheum 50 (1):131-41.

Kiani C, Chen L,Wu YJ, Yee AJ, Yang BB (2002), Structure and function of aggrecan. Cell Res. 12 (1):19-32.

Kim YH, Lee HC, Kim SY, Yeom YI, Ryu KJ, Min BH, Kim DH, Son HJ, Rhee PL, Kim JJ, Rhee JC, Kim HC, Chun HK, Grady WM, Kim YS (2011), Epigenomic analysis of aberrantly methylated genes in colorectal cancer identifies genes commonly affected by epigenetic alterations. Ann Surg Oncol 18 (8):2338-47.

Kimata K, Barrach H-J, Brown KS, Pennypacker JP (1981), Absence of proteoglycan core protein in cartilage from the cmd/cmd (cartilage matrix deficiency) mouse. J. Biol. Chem. 256 (13):6961-8.

Kirsch M, Zaman M, Meier D, Dübel S, Hust M (2005), Parameters affecting the display of antibodies on phage. J Immunol Meth 301 (1-2):173-85.

Klaus C, Plaimauer B, Studt JD, Dorner F, Lammle B, Mannucci PM, Scheiflinger F (2004), Epitope mapping of ADAMTS13 autoantibodies in acquired thrombotic thrombocytopenic purpura. Blood. 103 (12): 4514-9.

Klimpel KR, Molloy SS, Thomas G, Leppla SH (1992), Anthrax toxin protective antigen is activated by a cell surface protease with the sequence specificity and catalytic properties of furin. Proc. Natl. Acad. Sci. U. S. A. 89 (21):10277-81.

Knight CG, Willenbrock F, Murphy G (1992), A novel coumarin-labelled peptide for sensitive continuous assays of the matrix metalloproteinases. FEBS Lett. 296 (3):263-6.

Köhler G, Milstein C (1975), Continuous cultures of fused cells secreting antibody of predefined specificity. Nature 256 (5517):495-7.

Kohno S, Kohno T, Nakano Y, Suzuki K, Ishii M, Tagami H, Baba A, Hattori M (2009), Mechanism and significance of specific proteolytic cleavage of Reelin. Biochem. Biophys. Res. Commun. 380 (1):93-7.

Koide S (2009), Engineering of recombinant crystallization chaperones. Curr. Opin. Struct. Biol. 19 (4):449-57.

Koivunen E, Arap W, Valtanen H, Rainisalo A, Medina OP, Heikkilä P, Kantor C, Gahmberg CG, Salo T, Konttinen YT, Sorsa T, Ruoslahti E, Pasqualini R (1999), Tumor targeting with a selective gelatinase inhibitor. Nat Biotechnol. 17 (8):768-74.

Konttinen YT, Mandelin J, Li TF, Salo J, Lassus J, Liljeström M, Hukkanen M, Takagi M, Virtanen I, Santavirta S (2002), Acidic cysteine endoproteinase cathepsin K in the degeneration of the superficial articular hyaline cartilage in osteoarthritis. Arthritis Rheum. 46 (4):953-60.

Koo BH, Oh D, Chung SY, Kim NK, Park S, Jang Y, Chung KH (2002), Deficiency of von Willebrand factor-cleaving protease activity in the plasma of malignant patients. Thromb. Res. 105 (6):471-6.

Koo BH, Coe DM, Dixon LJ, Somerville RP, Nelson CM, Wang LW, Young ME, Lindner DJ, Apte SS (2010), ADAMTS9 is a cell-autonomously acting, anti-angiogenic metalloprotease expressed by microvascular endothelial cells. Am J Pathol 176 (3):1494-504.

Kost T, Condreay JP (1999), Recombinant baculoviruses as expression vectors for insect and mammalian cells. Current Opin Biotechnol 10 (5):428-33.

Kouzarides T (2000), Acetylation: a regulatory modification to rival phosphorylation? EMBO J. 19 (6):1176-9.

Kozaci LD, Buttle DJ, Hollander AP (1997), Degradation of type II collagen, but not proteoglycan, correlates with matrix metalloproteinase activity in cartilage explant cultures. Arthritis Rheum 40 (1):164-74.

Kramerova IA, Kawaguchi N, Fessler LI, Nelson RE, Chen Y, Kramerov AA, Kusche-Gullberg M, Kramer JM, Ackley BD, Sieron AL, Prockop DJ, Fessler JH (2000), Papilin in development; a pericellular protein with a homology to the ADAMTS metalloproteinases. Development 127 (24):5475-85.

Kretzschmar T, Zimmermann C, Geiser M (1995), Selection procedures for nonmatured phage antibodies: a quantitative comparison and optimization strategies. Anal Biochem 224 (1):413-9.

Krishnaswamy S (2005), Exosite-driven substrate specificity and function in coagulation. J. Thromb. Haemostasis 3 (1):54-67.

Krstic D, Rodriguez M, Knuesel I (2012), Regulated proteolytic processing of Reelin through interplay of tissue plasminogen activator (tPA), ADAMTS-4, ADAMTS-5, and their modulators. PLoS One. 7(10):e47793.

Kuchtey J, Olson LM, Rinkoski T, Mackay EO, Iverson TM, Gelatt KN, Haines JL, Kuchtey RW (2011), Mapping of the disease locus and identification of ADAMTS10 as a candidate gene in a canine model of primary open angle glaucoma. PLoS Genet. 7(2):e1001306.

Kumar S, Sharghi-Namini S, Rao N, Ge R (2012), ADAMTS5 functions as an anti-angiogenic and anti-tumorigenic protein independent of its proteoglycanase activity. Am J Pathol 181 (3):1056-68.

Kuno K, Kanada N, Nakashima E, Fujiki F, Ichimura F, Matsushima K (1997), Molecular cloning of a gene encoding a new type of metalloproteinase-disintegrin family protein with thrombospondin motifs as an inflammation associated gene. J Biol Chem 272 (1):556-62.

Kuno K, Matsushima K (1998), ADAMTS-1 protein anchors at the extracellular matrix through the thrombospondin type I motifs and its spacing region. J. Biol. Chem. 273 (22):13912-7.

Kuno K, Terashima Y, Matsushima K (1999), ADAMTS-1 is an active metalloproteinase associated with the extracellular matrix. J. Biol. Chem. 274 (26):18821-6.

Kutz WE, Wang LW, Bader HL, Majors AK, Iwata K, Traboulsi EI, Sakai LY, Keene DR, Apte SS (2011), ADAMTS10 protein interacts with fibrillin-1 and promotes its deposition in extracellular matrix of cultured fibroblasts. J. Biol. Chem. 286 (19):17156-67.

Kvist AJ, Johnson AE, Mörgelin M, Gustafsson E, Bengtsson E, Lindblom K, Aszódi A, Fässler R, Sasaki T, Timpl R, Aspberg A (2006), Chondroitin sulfate perlecan enhances collagen fibril formation. Implications for perlecan chondrodysplasias. J Biol Chem 281 (44):33127-39.

Laemmli UK (1970), Cleavage of structural proteins during the assembly of the head of bacteriophage T4. Nature 227 (5259):680-5.

Lambert de Rouvroit C, de Bergeyck V, Cortvrindt C, Bar I, Eeckhout Y, Goffinet AM (1999), Reelin, the extracellular matrix protein deficient in reeler mutant mice, is processed by a metalloproteinase. Exp Neurol. 156 (1):214-7.

Lang A, Horler D, Baici A (2000), The relative importance of cysteine peptidases in osteoarthritis. J Rheumatol 27 (8):1970-9.

Lark MW, Gordy JT, Weidner JR, Ayala J, Kimura JH, Williams HR, Mumford RA, Flannery CR, Carlson SS, Iwata M, et al (1995), Cell-mediated catabolism of aggrecan. Evidence that cleavage at the "aggrecanase" site (Glu373-Ala374) is a primary event in proteolysis of the interglobular domain. J Biol Chem. 270 (6):2550-6.

Lark MW, Bayne EK, Flanagan J, Harper CF, Hoerrner LA, Hutchinson NI, Singer II, Donatelli SA, Weidner JR, Williams HR, Mumford RA, Lohmander LS (1997), Aggrecan degradation in human cartilage. Evidence for both matrix metalloproteinase and aggrecanase activity in normal, osteoarthritic, and rheumatoid joints. J Clin Invest 100 (1):93-106.

Larsson S, Lohmander LS, Struglics A (2009), Synovial Fluid Level of Aggrecan ARGS Fragments Is a More Sensitive Marker of Joint Disease Than Glycosaminoglycan or Aggrecan Levels: A Cross-Sectional Study. Arthritis Res Ther 11 (3):R92.

Laskowski M Jr, Kato I (1980), Protein inhibitors of proteinases. Annu Rev Biochem. 49:593-626.

Laskowski RA, Luscombe NM, Swindells MB, Thornton JM (1996), Protein clefts in molecular recognition and function. Protein Sci. 5 (12):2438-52.

Lauer-Fields JL, Minond D, Sritharan T, Kashiwagi M, Nagase H, Fields GB (2007), Substrate conformation modulates aggrecanase (ADAMTS-4) affinity and sequence specificity. Suggestion of a common topological specificity for functionally diverse proteases. J Biol Chem. 282 (1):142-50.

Lawrence RC, Felson DT, Helmick CG, Arnold LM, Choi H, Deyo RA, Gabriel S, Hirsch R, Hochberg MC, Hunder GG, Jordan JM, Katz JN, Kremers HM, Wolfe F; National Arthritis Data Workgroup (2008), Estimates of the prevalence of arthritis and other rheumatic conditions in the United States. Part II. Arthritis Rheum. 58 (1):26-35.

Leder L, Berger C, Bornhauser S, Wendt H, Ackermann F, Jelesarov I, Bosshard HR (1995), Spectroscopic, calorimetric, and kinetic demonstration of conformational adaptation in peptide-antibody recognition. Biochemistry 34 (50):16509-18.

Lee JH, Fitzgerald JB, Dimicco MA, Grodzinsky AJ (2005), Mechanical injury of cartilage explants causes specific time-dependent changes in chondrocyte gene expression. Arthritis Rheum 52 (8):2386-95.

Lee NV, Rodriguez-Manzaneque JC, Thai SN, Twal WO, Luque A, Lyons KM, Argraves WS, Iruela-Arispe ML (2005), Fibulin-1 acts as a cofactor for the matrix metalloprotease ADAMTS-1. J Biol Chem 280 (41):34796-804.

Lee NV, Sato M, Annis DS, Loo JA, Wu L, Mosher DF, Iruela-Arispe ML (2006), ADAMTS1 mediates the release of antiangiogenic polypeptides from TSP1 and 2. EMBO J 25 (22):5270-83.

Le Goff C, Somerville RP, Kesteloot F, Powell K, Birk DE, Colige AC, Apte SS (2006), Regulation of procollagen amino-propeptide processing during mouse embryogenesis by specialization of homologous ADAMTS proteases: insights on collagen biosynthesis and dermatosparaxis. Development 133 (8):1587-96.

Le Goff C, Morice-Picard F, Dagoneau N, Wang LW, Perrot C, Crow YJ, Bauer F, Flori E, Prost-Squarcioni C, Krakow D, Ge G, Greenspan DS, Bonnet D, Le Merrer M, Munnich A, Apte SS, Cormier-Daire V (2008), ADAMTSL2 mutations in geleophysic dysplasia demonstrate a role for ADAMTS-like proteins in TGF-beta bioavailability regulation. Nat Genet. 40(9):1119-23.

Lerner RA, Benkovic SJ, Schultz PG (1991), At the cross-roads of chemistry and immunology: catalytic antibodies. Science 252 (5006):659-67.

Levy GG, Nichols WC, Lian EC, Foroud T, McClintick JN, McGee BM, Yang AY, Siemieniak DR, Stark KR, Gruppo R, Sarode R, Shurin SB, Chandrasekaran V, Stabler SP, Sabio H, Bouhassira EE, Upshaw JD Jr, Ginsburg D, Tsai HM (2001), Mutations in a member of the ADAMTS gene family cause thrombotic thrombocytopenic purpura. Nature 413 (6855):488-94.

Lewis EJ, Bishop J, Bottomley KM, Bradshaw D, Brewster M, Broadhurst MJ, Brown PA, Budd JM, Elliott L, Greenham AK, Johnson WH, Nixon JS, Rose F, Sutton B, Wilson K (1997), Ro 32–3555, an orally active collagenase inhibitor, prevents cartilage breakdown in vitro and in vivo. Br J Pharmacol 121 (3):540-6.

Li H, Schwartz NB, Vertel BM (1993), cDNA cloning of chick cartilage chondroitin sulfate (aggrecan) core protein and identification of a stop codon in the aggrecan gene associated with the chondrodystrophy, nanomelia. J. Biol. Chem. 268 (31):23504-11.

Li J, Anemaet W, Diaz MA, Buchanan S, Tortorella M, Malfait AM, Mikecz K, Sandy JD, Plaas A (2011), Knockout of ADAMTS5 does not eliminate cartilage aggrecanase activity but abrogates joint fibrosis and promotes cartilage aggrecan deposition in murine osteoarthritis models. J Orthop Res. 29 (4):516-22.

Lim NH, Kashiwagi M, Visse R, Jones J, Enghild JJ, Brew K, Nagase H (2010), Reactive-site mutants of N-TIMP-3 that selectively inhibit ADAMTS-4 and ADAMTS-5: biological and structural implications. Biochem J. 431 (1):113-22.

Lind GE, Kleivi K, Meling GI, Teixeira MR, Thiis-Evensen E, Rognum TO, Lothe RA (2006), ADAMTS1, CRABP1, and NR3C1 identified as epigenetically deregulated genes in colorectal tumorigenesis. Cell Oncol 28 (5-6):259-72.

Little CB, Flannery CR, Hughes CE, Mort JS, Roughley PJ, Dent C, Caterson B (1999), Aggrecanase versus matrix metalloproteinases in the catabolism of the interglobular domain of aggrecan in vitro. Biochem J. 344 (Pt 1):61-8.

Little CB, Hughes CE, Curtis CL, Jones SA, Caterson B, Flannery CR (2002a), Cyclosporin A inhibition of aggrecanase-mediated proteoglycan catabolism in articular cartilage. Arthritis Rheum 46 (1):124-9.

Little CB, Hughes CE, Curtis CL, Janusz MJ, Bohne R, Wang-Weigand S, Taiwo YO, Mitchell PG, Otterness IG, Flannery CR, Caterson B (2002b), Matrix metalloproteinases are involved in C-terminal and interglobular domain processing of cartilage aggrecan in late stage cartilage degradation. Matrix Biol. 21 (3):271-88.

Little CB, Mittaz L, Belluoccio D, Rogerson FM, Campbell IK, Meeker CT, Bateman JF, Pritchard MA, Fosang AJ (2005a), ADAMTS-1-knockout mice do not exhibit abnormalities in aggrecan turnover in vitro or in vivo. Arthritis Rheum.52 (5):1461-72.

Little CB, Meeker CT, Hembry RM, Sims NA, Lawlor KE, Golub SB, Last K, Fosang AJ (2005b), Matrix metalloproteinases are not essential for aggrecan turnover during normal skeletal growth and development. Mol Cell Biol 25 (8):3388-99.

Little CB, Meeker CT, Golub SB, Lawlor KE, Farmer PJ, Smith SM, Fosang AJ (2007), Blocking aggrecanase cleavage in the aggrecan interglobular domain abrogates cartilage erosion and promotes cartilage repair. J Clin Invest 117 (6):1627-36.

Liu CJ, Kong W, Ilalov K, Yu S, Xu K, Prazak L, Fajardo M, Sehgal B, Di Cesare PE (2006a), ADAMTS-7: a metalloproteinase that directly binds to and degrades cartilage oligomeric matrix protein. FASEB J. 20 (7):988-90

Liu CJ, Kong W, Xu K, Luan Y, Ilalov K, Sehgal B, Yu S, Howell RD, Di Cesare PE (2006b), ADAMTS-12 associates with and degrades cartilage oligomeric matrix protein. J. Biol. Chem. 281 (23):15800-8.

Liu YJ, Xu Y, Yu Q (2006), Full-length ADAMTS-1 and the ADAMTS-1 fragments display pro- and antimetastatic activity, respectively. Oncogene 25 (17): 2452-67.

Llamazares M, Cal S, Quesada V, Lopez-Otin C (2003), Identification and characterization of ADAMTS-20 defines a novel subfamily of metalloproteinases-disintegrins with multiple thrombospondin-1 repeats and a unique GON domain. J Biol Chem 278 (15):13382-9.

Llamazares M, Obaya AJ, Moncada-Pazos A, Heljasvaara R, Espada J, López-Otín C, Cal S (2007), The ADAMTS12 metalloproteinase exhibits anti-tumorigenic properties through modulation of the Ras-dependent ERK signalling pathway. Cell Sci. 120 (Pt 20):3544-52.

Llorente-Cortés V, Otero-Viñas M, Hurt-Camejo E, Martínez-González J, Badimon L (2002), Human coronary smooth muscle cells internalize versican-modified LDL through LDL receptorrelated protein and LDL receptors. Arterioscler Thromb Vasc Biol 22 (3):387-93.

Lo PH, Leung AC, Kwok CY, Cheung WS, Ko JM, Yang LC, Law S, Wang LD, Li J, Stanbridge EJ, Srivastava G, Tang JC, Tsao SW, Lung ML (2007), Identification of a tumor suppressive critical region mapping to 3p14.2 in esophageal squamous cell carcinoma and studies of a candidate tumor suppressor gene, ADAMTS9. Oncogene 26 (1):148-57.

Lo PH, Lung HL, Cheung AK, Apte SS, Chan KW, Kwong FM, Ko JM, Cheng Y, Law S, Srivastava G, Zabarovsky ER, Tsao SW, Tang JC, Stanbridge EJ, Lung ML (2010), Extracellular protease ADAMTS9 suppresses esophageal and nasopharyngeal carcinoma tumor formation by inhibiting angiogenesis. Cancer Res. 70 (13):5567-76.

Lohmander LS, Neame PJ, Sandy JD (1993), The structure of aggrecan fragments in human synovial fluid. Evidence that aggrecanase mediates cartilage degradation in inflammatory joint disease, joint injury, and osteoarthritis. Arthritis Rheum 36 (9):1214-22.

Lorenzo P, Bayliss MT, Heinegård D (2004), Altered patterns and synthesis of extracellular matrix macromolecules in early osteoarthritis. Matrix Biol. 23 (6):381-91.

Luan Y, Kong L, Howell DR, Ilalov K, Fajardo M, Bai XH, Di Cesare PE, Goldring MB, Abramson SB, Liu CJ (2008), Inhibition of ADAMTS-7 and ADAMTS-12 degradation of cartilage oligomeric matrix protein by alpha-2-macroglobulin. Osteoarthritis Cartilage 16 (11):1413-20.

Luken BM, Turenhout EA, Hulstein JJ, Van Mourik JA, Fijnheer R, Voorberg J (2005), The spacer domain of ADAMTS13 contains a major binding site for antibodies in patients with thrombotic thrombocytopenic purpura. Thromb Haemost. 93(2):267-74.

Lunder M, Bratkovic T, Kreft S, Strukelj B (2005), Peptide inhibitor of pancreatic lipase selected by phage display using different elution strategies. J Lipid Res 46 (7):1512-6.

Luque A, Carpizo DR, Iruela-Arispe ML (2003), ADAMTS1/METH1 inhibits endothelial cell proliferation by direct binding and sequestration of VEGF. J. Biol. Chem. 278 (26):23656-65.

Madsen SH, Sumer EU, Bay-Jensen AC, Sondergaard BC, Qvist P, Karsdal MA (2010), Aggrecanase- and matrix metalloproteinase-mediated aggrecan degradation is associated with different molecular characteristics of aggrecan and separated in time ex vivo. Biomarkers. 15 (3): 266-76.

Maehara H, Suzuki K, Sasaki T, Oshita H, Wada E, Inoue T, Shimizu K (2007), G1-G2 aggrecan product that can be generated by M-calpain on truncation at Ala709-Ala710 is present abundantly in human articular cartilage. J Biochem 141 (4):469-77.

Mahoney DJ, Whittle JD, Milner CM, Clark SJ, Mulloy B, Buttle DJ, Jones GC, Day AJ, Short RD (2004), A method for the non-covalent immobilization of heparin to surfaces. Anal. Biochem. 330 (1):123-9.

Maingot L, Elbakali J, Dumont J, Bosc D, Cousaert N, Urban A, Deglane G, Villoutreix B, Nagase H, Sperandio O, Leroux F, Deprez B, Deprez-Poulain R. (2013), Aggrecanase-2 inhibitors based on the acylthiosemicarbazide zinc-binding group. Eur J Med Chem. 69C:244-61 [Epub ahead of print].

Majumdar MK, Askew R, Schelling S, Stedman N, Blanchet T, Hopkins B, Morris EA, Glasson SS (2007), Double-knockout of ADAMTS-4 and ADAMTS-5 in mice results in physiologically normal animals and prevents the progression of osteoarthritis. Arthritis Rheum. 56 (11):3670-4.

Makihira S, Yan W, Murakami H, Furukawa M, Kawai T, Nikawa H, Yoshida E, Hamada T, Okada Y, Kato Y (2003), Thyroid hormone enhances aggrecanase-2/ADAM-TS5 expression and proteoglycan degradation in growth plate cartilage. Endocrinology 144 (6):2480-8.

Makita N, Sato J, Manaka K, Shoji Y, Oishi A, Hashimoto M, Fujita T, Iiri T (2007), An acquired hypocalciuric hypercalcemia autoantibody induces allosteric transition among human Ca-sensing receptor conformations. Proc. Natl Acad. Sci. USA 104 (13):5443-8.

Malfait AM, Liu RQ, Ijiri K, Komiya S, Tortorella MD (2002), Inhibition of ADAM-TS4 and ADAM-TS5 prevents aggrecan degradation in osteoarthritic cartilage. J Biol Chem. 277 (25):22201-8.

Malfait AM, Arner EC, Song RH, Alston JT, Markosyan S, Staten N, Yang Z, Griggs DW, Tortorella MD (2008), Proprotein convertase activation of aggrecanases in cartilage in situ. Arch Biochem Biophys 478 (1):43-51.

Malfait AM, Ritchie J, Gil AS, Austin JS, Hartke J, Qin W, Tortorella MD, Mogil JS (2010), ADAMTS-5 deficient mice do not develop mechanical allodynia associated with osteoarthritis following medial meniscal destabilization. Osteoarthritis Cartilage. 18 (4):572-80.

Marks JD, Griffiths AD, Malmqvist M, Clackson TP, Bye JM, Winter G (1992), By-passing immunization: building high affinity human antibodies by chain shuffling. Biotechnology (NY) 10 (7):779-83.

Maroudas A (1976), Transport of solutes through cartilage: permeability to large molecules. J Anat. 122 (Pt 2):335-47.

Martens E, Leyssen A, Van Aelst I, Fiten P, Piccard H, Hu J, Descamps FJ, Van den Steen PE, Proost P, Van Damme J, Liuzzi GM, Riccio P, Polverini E, Opdenakker G (2007), A monoclonal antibody inhibits gelatinase, B/MMP-9 by selective binding to part of the catalytic domain and not to the fibronectin or zinc binding domains. Biochim. Biophys. Acta 1770 (2):178-86.

Martin CD, Rojas G, Mitchell JN, Vincent KJ, Wu J, McCafferty J, Schofield DJ (2006), A simple vector system to improve performance and utilisation of recombinant antibodies. BMC Biotechnol. 6:46.

Maskos K, Lang R, Tschesche H, Bode W (2007), Flexibility and variability of TIMP binding: X-ray structure of the complex between collagenase-3/MMP-13 and TIMP-2. J. Mol. Biol. 366 (4):1222-31.

Mason RM, Chambers MG, Flannelly J, Gaffen JD, Dudhia J, Bayliss MT (2001), The STR/ort mouse and its use as a model of osteoarthritis. Osteoarthritis Cartilage. 9 (2):85-91.

Masui T, Hosotani R, Tsuji S, Miyamoto Y, Yasuda S, Ida J, Nakajima S, Kawaguchi M, Kobayashi H, Koizumi M, Toyoda E, Tulachan S, Arii S, Doi R, Imamura M (2001), Expression of METH-1 and METH-2 in pancreatic cancer. Clin. Cancer Res. 7 (11):3437-43.

Matias-Roman S, Galvez BG, Genis L, Yanez-Mo M, de la Rosa G, Sanchez-Mateos P, Sánchez-Madrid F, Arroyo AG (2005), Membrane type 1-matrix metalloproteinase is involved in migration of human monocytes and is regulated through their interaction with fibronectin or endothelium. Blood 105 (10):3956-64.

Matthews DJ, Wells JA (1993), Substrate phage: selection of protease substrates by monovalent phage display. Science 260 (5111):1113-7.

Matthews R, Gary S, Zerillo C, Pratta M, Solomon K, Arner E, Hockfield S (2000), Brain-enriched hyaluronan binding (BEHAB)/brevican cleavage in a glioma cell line is mediated by a disintegrin and metalloproteinase with thrombospondin motifs (ADAMTS) family member. J. Biol. Chem. 275 (30): 22695-703.

McCafferty J, Griffiths AD, Winter G, Chiswell DJ (1990), Phage antibodies: filamentous phage displaying antibody variable domains. Nature. 348 (6301):552-4.

McCulloch DR, Nelson CM, Dixon LJ, Silver DL, Wylie JD, Lindner V, Sasaki T, Cooley MA, Argraves WS, Apte SS (2009a) ADAMTS metalloproteases generate active versican fragments that regulate interdigital web regression. Dev Cell 17 (5):687-98.

McCulloch DR, Wylie JD, Longpre JM, Leduc R, Apte SS (2009b), 10mM glucosamine prevents activation of proADAMTS5 (aggrecanase-2) in transfected cells by interference with post-translational modification of furin. Osteoarthritis Cartilage 18 (3):455-63.

McCulloch DR, Le Goff C, Bhatt S, Dixon LJ, Sandy JD, Apte SS (2009c), Adamts5, the gene encoding a proteoglycan-degrading metalloprotease, is expressed by specific cell lineages during mouse embryonic development and in adult tissues. Gene Expr Patterns. 9(5):314-23.

Mead DA, Kemper B (1988) Chimeric single-stranded DNA phage-plasmid cloning vectors. Biotechnology 10:85-102.

Melching LI, Fisher WD, Lee ER, Mort JS, Roughley PJ (2006) The cleavage of biglycan by aggrecanases. Osteoarthritis Cartilage 14 (11):1147-54.

Mercuri FA, Doege KJ, Arner EC, Pratta MA, Last K, Fosang AJ (1999), Recombinant human aggrecan G1-G2 exhibits native binding properties and substrate specificity for matrix metalloproteinases and aggrecanase. J. Biol. Chem. 274 (45):32387-95.

Mills KH, Dunne A (2009) Immune modulation: IL-1, master mediator or initiator of inflammation. Nat Med 15 (12):1363-1364.

Mian IS, Bradwell AR, Olson AJ (1991), Structure, function and properties of antibody binding sites. J. Mol. Biol. 217 (1):133-51.

Milstein C, Cuello AC (1983), Hybrid hybridomas and their use in immunohistochemistry. Nature. 305 (5934):537-40.

Mimata Y, Kamataki A, Oikawa S, Murakami K, Uzuki M, Shimamura T, Sawai T (2012), Interleukin-6 upregulates expression of ADAMTS-4 in fibroblast-like synoviocytes from patients with rheumatoid arthritis. Int J Rheum Dis. 15 (1):36-44.

Mittaz L, Russell DL, Wilson T, Brasted M, Tkalcevic J, Salamonsen LA, Hertzog PJ, Pritchard MA (2004), Adamts-1 is essential for the development and function of the urogenital system. Biol Reprod. 70 (4):1096-105.

Miwa, Hazuki E, Thomas A Gerken, and Thomas M Hering (2006), Effects of covalently attached chondroitin sulfate on aggrecan cleavage by ADAMTS-4 and MMP-13. Matrix Biol 25 (8):534-45.

Miyaki S, Nakasa T, Otsuki S, Grogan SP, Higashiyama R, Inoue A, Kato Y, Sato T, Lotz MK, Asahara H (2009), MicroRNA- 140 is expressed in differentiated human articular chondrocytes and modulates interleukin-1 responses. Arthritis Rheum 60 (9):2723-30.

Miyaki S, Sato T, Inoue A, Otsuki S, Ito Y, Yokoyama S, Kato Y, Takemoto F, Nakasa T, Yamashita S, Takada S, Lotz MK, Ueno-Kudo H, Asahara H (2010), MicroRNA-140 plays dual roles in both cartilage development and homeostasis. Genes Dev 24 (11):1173-85.

Mizui Y, Yamazaki K, Kuboi Y, Sagane K, Tanaka I (2000), Characterization of 50-flanking region of human aggrecanase-1 (ADAMTS4) gene. Mol Biol Rep 27 (3):167-173.

Moake JL, Rudy CK, Troll JH, Weinstein MJ, Colannino NM, Azocar J, Seder RH, Hong SL, Deykin D (1982), Unusually large plasma factor VIII:von Willebrand factor multimers in chronic relapsing thrombotic thrombocytopenic purpura. N Engl J Med. 307 (23):1432-5.

Mok MT, Ilic MZ, Handley CJ, Robinso HC (1992), Cleavage of proteoglycan aggregate by leucocyte elastase. Arch. Biochem. Biophys. 292:442-7.

Mok SS, Masuda K, Hauselmann HJ, Aydelotte MB, Thonar EJ (1994), Aggrecan synthesized by mature bovine chondrocytes suspended in alginate. Identification of two distinct metabolic matrix pools. J Biol Chem 269 (52):33021-7.

Moncada-Pazos A, Obaya AJ, Fraga MF, Viloria CG, Capellá G, Gausachs M, Esteller M, López-Otín C, Cal S (2009), The ADAMTS12 metalloprotease gene is epigenetically silenced in tumor cells and transcriptionally activated in the stroma during progression of colon cancer. J Cell Sci 122 (Pt 16): 2906-13.

Morales TI, Hascall VC (1988), Correlated metabolism of proteoglycans and hyaluronic acid in bovine cartilage organ cultures. J Biol Chem. 263 (8):3632-8.

Morales J, Al-Sharif L, Khalil DS, Shinwari JM, Bavi P, Al-Mahrouqi RA, Al-Rajhi A, Alkuraya FS, Meyer BF, Al Tassan N (2009), Homozygous mutations in ADAMTS10 and ADAMTS17 cause lenticular myopia, ectopia lentis, glaucoma, spherophakia, and short stature. Am. J. Hum. Genet. 85 (5):558-68.

Moriguchi-Goto S, Yamashita A, Tamura N, Soejima K, Takahashi M, Nakagaki T, Goto S, Asada Y (2009), ADAMTS-13 attenuates thrombus formation on type I collagen surface and disrupted plaques under flow conditions. Atherosclerosis 203 (2):409-16.

Mort JS, Magny MC, Lee ER (1998), Cathepsin B: an alternative protease for the generation of an aggrecan 'metalloproteinase' cleavage neoepitope. Biochem J. 335 (Pt 3):491-4.

Mosyak L, Georgiadis K, Shane T, Svenson K, Hebert T, McDonagh T, Mackie S, Olland S, Lin L, Zhong X, Kriz R, Reifenberg EL, Collins-Racie LA, Corcoran C, Freeman B, Zollner R, Marvell T, Vera M, Sum PE, Lavallie ER, Stahl M, Somers W (2008), Crystal structures of the two major aggrecan degrading enzymes, ADAMTS4 and ADAMTS5. Protein Sci. 17(1):16-21.

Moulharat N, Lesur C, Thomas M, Rolland-Valognes G, Pastoureau P, Anract P, De Ceuninck F, Sabatini M (2004), Effects of transforming growth factor-beta on aggrecanase production and proteoglycan degradation by human chondrocytes in vitro. Osteoarthritis Cartilage 12 (4):296-305.

Moutel S, El Marjou A, Vielemeyer O, Nizak C, Benaroch P, Dübel S, Perez F (2009), A multi-Fc-species system for recombinant antibody production. BMC Biotechnol. 9:14.

Naito S, Shiomi T, Okada A Kimura T, Chijiiwa M, Fujita Y, Yatabe T, Komiya K, Enomoto H, Fujikawa K, Okada Y (2007) Expression of ADAMTS4 (aggrecanase-1) in human osteoarthritic cartilage. Pathol Int 57 (11):703-11.

Nakada M, Miyamori H, Kita D, Takahashi T, Yamashita J, Sato H, Miura R, Yamaguchi Y, Okada Y (2005), Human glioblastomas overexpress ADAMTS-5 that degrades brevican. Acta Neuropathol. 110 (3):239-46.

Neri D, Momo M, Prospero T, Winter G (1995), High-affinity antigen binding by chelating recombinant antibodies (CRAbs). J. Mol. Biol. 246 (3):367-73.

Nicholson AC, Malik SB, Logsdon JM Jr, Van Meir EG (2005), Functional evolution of ADAMTS genes: evidence from analyses of phylogeny and gene organization. BMC Evol Biol 5:11.

Nieba L, Honegger A, Krebber C, Plückthun A (1997), Disrupting the hydrophobic patches at the antibody variable/constant domain interface: improved in vivo folding and physical characterization of an engineered scFv fragment. Protein Eng 10 (4):435-44.

Nizak C, Monier S, del Nery E, Moutel S, Goud B, Perez F (2003), Recombinant antibodies to the small GTPase Rab6 as conformation sensors. Science 300 (5621):984-987.

Nuti E, Santamaria S, Casalini F, Yamamoto K, Marinelli L, La Pietra V, Novellino E, Orlandini E, Nencetti S, Marini AM, Salerno S, Taliani S, Da Settimo F, Nagase H, Rossello A. (2013), Arylsulfonamide inhibitors of aggrecanases as potential therapeutic agents for osteoarthritis: synthesis and biological evaluation. Eur J Med Chem. 62:379-94.

Ofran Y, Schlessinger A, Rost B (2008), Automated identification of complementarity determining regions (CDRs) reveals peculiar characteristics of CDRs and B cell epitopes. J Immunol. 181 (9):6230-5.

Oleksowicz L, Bhagwati N, DeLeon-Fernandez M (1999), Deficient activity of von Willebrand's factor-cleaving protease in patients with disseminated malignancies. Cancer Res. 59 (9):2244-50.

Oshita H, Sandy JD, Suzuki K, Akaike A, Bai Y, Sasaki T, Shimizu K (2004), Mature 1519 bovine articular cartilage contains abundant aggrecan that is C-terminally 1520 truncated at Ala719–Ala720, a site which is readily cleaved bym-calpain, Biochem. J. 382 (Pt 1):253-9.

Oyen D, Srinivasan V, Steyaert J, Barlow JN (2011), Constraining enzyme conformational change by an antibody leads to hyperbolic inhibition. J Mol Biol. 407(1):138-48.

Padlan EA (1996), X-ray crystallography of antibodies. Adv. Protein Chem. 49:57-133.

Paemen L, Martens E, Masure S, Opdenakker G (1995), Monoclonal antibodies specific for natural human neutrophil gelatinase B used for affinity purification, quantitation by two-site ELISA and inhibition of enzymatic activity. Eur. J. Biochem. 234 (3):759-65.

Page RDM (1996), TreeView: an application to display phylogenetic trees on personal computers. Comput. Appl. Biosci. 12 (4):357-8.

Palatini P (1983), The interaction between full and partial inhibitors acting on a single enzyme. A theoretical analysis. Mol. Pharmacol. 24 (1):30-41.

Pasqualini R, Ruoslahti E (1996), Organ targeting in vivo using phage display peptide libraries. Nature 380 (6572):364-6.

Patwari P, Gao G, Lee JH, Grodzinsky AJ, Sandy JD (2005), Analysis of ADAMTS4 and MT4-MMP indicates that both are involved in aggrecanolysis in interleukin-1-treated bovine cartilage. Osteoarthritis Cart 13 (4):269-77.

Pendley C, Schantz A, Wagner C (2003), Immunogenicity of therapeutic monoclonal antibodies. Curr. Opin. Mol. Ther. 5 (2):172-9.

Petersen HH, Hansen M, Schousboe SL, Andreasen PA (2001), Localization of epitopes for monoclonal antibodies to urokinase-type plasminogen activator: relationship between epitope localization and effects of antibodies on molecular interactions of the enzyme. Eur. J. Biochem. 268 (16):4430-9.

Piera-Velazquez S, Hawkins DF, Whitecavage MK, Colter DC, Stokes DG, Jimenez SA (2007), Regulation of the human SOX9 promoter by Sp1 and CREB. Exp Cell Res 313 (6):1069-79.

Plaas A, Osborn B, Yoshihara Y, Bai Y, Bloom T, Nelson F, Mikecz K, Sandy JD (2007), Aggrecanolysis in human osteoarthritis: confocal localization and biochemical characterization of ADAMTS5-hyaluronan complexes in articular cartilages. Osteoarthritis Cartilage 15 (7):719-34.

Pollock MR (1964), Stimulating and inhibiting antibodies for bacterial penicillinase. Immunology 7:707-23.

Pond MJ, Nuki G (1973) Experimentally induced osteoarthritis in the dog. Ann Rheum Dis 32 (4): 387-8.

Popovych N, Sun S, Ebright RH, Kalodimos CG (2006) Dynamically driven protein allostery. Nat Struct Mol Biol 13 (9):831-8.

Porter S, Scott SD, Sassoon EM, Williams MR, Jones JL, Girling AC, Ball RY, Edwards DR (2004), Dysregulated expression of adamalysin-thrombospondin genes in human breast carcinoma. Clin. Cancer Res. 10 (7): 2429-40.

Porter S, Clark IM, Kevorkian L, Edwards DR (2005), The ADAMTS metalloproteinases. Biochem. J. 386 (Pt 1):15-27.

Porter S, Span PN, Sweep FC, Tjan-Heijnen VC, Pennington CJ, Pedersen TX, Johnsen M, Lund LR, Rømer J, Edwards DR (2006), ADAMTS8 and ADAMTS15 expression predicts survival in human breast carcinoma. Int. J. Cancer 118 (5): 1241-7.

Pos W, Crawley JT, Fijnheer R, Voorberg J, Lane DA, Luken BM (2010), An autoantibody epitope comprising residues R660, Y661, and Y665 in the ADAMTS13 spacer domain identifies a binding site for the A2 domain of VWF. Blood. 115 (8):1640-9.

Powell AJ, CB Little, CE Hughes (2007), Low molecular weight isoforms of the aggrecanases are responsible for the cytokine-induced proteolysis of aggrecan in a porcine chondrocyte culture system. Arthritis Rheum. 56 (9):3010-19.

Powers DB, Amersdorfer P, Poul M, Nielsen UB, Shalaby MR, Adams GP, Weiner LM, Marks JD. (2001), Expression of single-chain Fv–Fc fusions in Pichia pastoris. J. Immunol. Methods 251 (1-2):123-35.

Pratta MA, Tortorella MD, Arner EC (2000), Age-related changes in aggrecan glycosylation affect cleavage by aggrecanase. J Biol Chem 275 (50): 39096-102.

Pratta MA, Yao W, Decicco C, Tortorella MD, Liu RQ, Copeland RA, Magolda R, Newton RC, Trzaskos JM, Arner EC (2003), Aggrecan protects cartilage collagen from proteolytic cleavage. J. Biol. Chem. 278 (46):45539-45.

Pratta MA, Su JL, Leesnitzer MA, Struglics A, Larsson S, Lohmander LS, Kumar S (2006), Development and characterization of a highly specific and sensitive sandwich ELISA for detection of aggrecanase-generated aggrecan fragments. Osteoarthritis Cartilage. 14(7):702-13.

Prelli F, Frangione B (1992), Franklin's disease: Igg2H chain mutant BUR. J. Immunol. 148 (3):949-52.

Puchi M, Quinones K, Concha C, Iribarren C, Bustos P, Morin V, Genevière AM, Imschenetzky M (2006), Microinjection of an antibody against the cysteine-protease involved in male chromatin remodeling blocks the development of sea urchin embryos at the initial cell cycle. J. Cell Biochem. 98 (2):335-42.

Puente XS, Sanchez LM, Overall CM, Lopez-Otin C (2003), Human and mouse proteases: A comparative genomic approach. Nat Rev Genet 4 (7):544-58.

Qureshi HY, Sylvester J, El Mabrouk M, Zafarullah M (2005), TGF-beta-induced expression of tissue inhibitor of metalloproteinases- 3 gene in chondrocytes is mediated by extracellular signal-regulated kinase pathway and Sp1 transcription factor. J Cell Physiol 203 (2):345-52.

Raj T, Kanellakis P, Pomilio G, Jennings G, Bobik A, Agrotis A (2006), Inhibition of fibroblast growth factor receptor signaling attenuates atherosclerosis in apolipoprotein E-deficient mice. Arterioscler. Thromb. Vasc. Biol. 26 (8):1845-51.

Rakonjac J, Model P (1998), Roles of pIII in filamentous phage assembly. J Mol Biol. 282 (1):25-41.

Rao C, Foernzler D, Loftus SK, Liu S, McPherson JD, Jungers KA, Apte SS, Pavan WJ, Beier DR (2003), A defect in a novel ADAMTS family member is the cause of the belted white-spotting mutation. Development 19(130):4665-72.

Rao N, Ke Z, Liu H, Ho CJ, Kumar S, Xiang W, Zhu Y, Ge R (2013), ADAMTS4 and its proteolytic fragments differentially affect melanoma growth and angiogenesis in mice. Int J Cancer. 133 (2):294-306.

Rawlings ND, Tolle DP, Barrett AJ (2004), Merops: the peptidase database. Nucl. Acids Res. 32: D160-4.

Rees SG, Flannery CR, Little CB, Hughes CE, Caterson B, Dent CM (2000), Catabolism of aggrecan, decorin and biglycan in tendon. Biochem J 350 (Pt 1):181-8.

Rees SG, Dent CM, Caterson B (2009), Metabolism of proteoglycans in tendon. Scand. J. Med. Sci. Sports 19:470-8.

Reiter Y, Brinkmann U, Lee B, Pastan I (1996), Engineering antibody Fv fragments for cancer detection and therapy: disulphide-stabilized Fv fragments. Nature Biotechol. 14 (10):1239-45.

Rezacova P, Lescar J, Brynda J, Fabry M, Horejsi M, Sedlacek J, Bentley GA (2001), Structural basis of HIV-1 and HIV-2 protease inhibition by a monoclonal antibody. Structure 9 (10):887-95.

Ricketts LM, Dlugosz M, Luther KB, Haltiwanger RS, Majerus EM (2007), O-fucosylation is required for ADAMTS13 secretion. J Biol Chem 282 (23):17014-23.

Rittenhouse E, Dunn LC, Cookingham J, Calo C, Spiegelman M, Dooher GB, Bennett D (1978), Cartilage matrix deficiency (cmd), a new autosomal recessive lethal mutation in the mouse. J. Embryol. Exp. Morphol. 43:71-84.

Roach HI, Yamada N, Cheung KS, Tilley S, Clarke NM, Oreffo RO, Kokubun S, Bronner F (2005), Association between the abnormal expression of matrix-degrading enzymes by human osteoarthritic chondrocytes and demethylation of specific CpG sites in the promoter regions. Arthritis Rheum 52 (10):3110-24.

Roberts BL, Markland W, Ley AC, Kent RB, White DW, Guterman SK, Ladner RC (1992), Directed evolution of a protein: selection of potent neutrophil elastase inhibitors displayed on M13 fusion phage. Proc Natl Acad Sci U S A. 89 (6):2429-33.

Rocks N, Paulissen G, Quesada Calvo F, Polette M, Gueders M, Munaut C, Foidart JM, Noel A, Birembaut P, Cataldo D (2006), Expression of a disintegrin and metalloprotease (ADAM and ADAMTS) enzymes in human nonsmall-cell lung carcinomas (NSCLC). Br. J. Cancer 94 (5):724-30.

Roddy EW, Zhang W, Doherty M (2005), Aerobic walking or strengthening exercise for osteoarthritis of the knee? A systematic review. Ann. Rheum. Dis. 64 (4):544-48.

Rodriguez-Manzaneque JC, Milchanowski AB, Dufour EK, Leduc R, Iruela-Arispe ML (2000), Characterization of METH-1/ADAMTS1 processing reveals two distinct active forms. J. Biol. Chem. 275 (43):33471-9.

Rodriguez-Manzaneque J, Westling J, Thai S, Luque A, Knauper V, Murphy G, Sandy J, Iruela-Arispe M (2002), ADAMTS1 cleaves aggrecan at multiple sites and is differentially inhibited by metalloproteinase inhibitors. Biochem. Biophys. Res. Commun. 293 (1):501-8.

Rogerson FM, Stanton H, East CJ, Golub SB, Tutolo L, Farmer PJ, Farmer PJ, Fosang AJ (2008), Evidence of a novel aggrecan-degrading activity in cartilage: studies of mice deficient in both ADAMTS-4 and ADAMTS-5. Arthritis Rheum 58 (6):1664-73.

Roman-Gomez J, Jimenez-Velasco A, Agirre X, Prosper F, Heiniger A, Torres A (2005), Lack of CpG island methylator phenotype defines a clinical subtype of T-cell acute lymphoblastic leukemia associated with good prognosis. J Clin Oncol 23 (28):7043-9.

Roughley PJ, White RJ, Poole AR (1985), Identification of a hyaluronic acid-binding protein that interferes with the preparation of high-buoyant density proteoglycan aggregates from adult human articular cartilage. Biochem. J. 231 (1):129-38.

Roughley PJ, Barnett J, Zuo F, Mort JS (2003). Variations in aggrecan structure modulate its susceptibility to aggrecanases. Biochem J 375 (Pt 1):183-9.

Rudnick SI, Adams GP (2009), Affinity and avidity in antibody-based tumor targeting. Cancer Biother Radiopharm 24 (2):155-61.

Russell DL, Doyle KM, Ochsner SA, Sandy JD, Richards JS (2003), Processing and localization of ADAMTS-1 and proteolytic cleavage of versican during cumulus matrix expansion and ovulation. J. Biol. Chem. 278 (43):42330-9.

Saerens D, Kinne J, Bosmans E, Wernery U, Muyldermans S, Conrath K (2004), Single domain antibodies derived from dromedary lymph node and peripheral lymphocytes sensing conformational variants of prostrate-specific antigen. J. Biol. Chem. 279 (50):51965-72.

Saghatelian A, Jessani N, Joseph A, Humphrey M, Cravatt BF (2004), Activity-based probes for the proteomic profiling of metalloproteases. Proc. Natl. Acad. Sci. USA 101 (27):10000-5.

Salter RC, Ashlin TG, Kwan AP, Ramji DP (2010), ADAMTS proteases: key roles in atherosclerosis? J Mol Med. 88 (12):1203-11.

Sandy JD, Neame PJ, Boynton RE, Flannery CR (1991), Catabolism of aggrecan in cartilage explants. Identification of a major cleavage site within the interglobular domain. J. Biol. Chem. 266 (14):8683-5.

Sandy JD, Gamett D, Thompson V, Verscharen C (1998), Chondrocyte-mediated catabolism of aggrecan: aggrecanase-dependent cleavage induced by interleukin-1 or retinoic acid can be inhibited by glucosamine. Biochem J 335 (Pt 1):59-66.

Sandy JD, Thompson V, Verscharen C, Gamett D (1999), Chondrocyte-mediated catabolism of aggrecan: evidence for a glycosylphosphatidylinositol-linked protein in the aggrecanase response to interleukin-1 or retinoic acid. Arch Biochem Biophys 367 (2):258-64.

Sandy JD, Thompson V, Doege K, Verscharen C (2000), The intermediates of aggrecanase-dependent cleavage of aggrecan in rat chondrosarcoma cells treated with interleukin-1. Biochem. J. 351 (Pt 1):161-6.

Sandy JD, Verscharen C (2001), Analysis of aggrecan in human knee cartilage and synovial fluid indicates that aggrecanase (ADAMTS) activity is responsible for the catabolic turnover and loss of whole aggrecan whereas other protease activity is required for C-terminal processing in vivo. Biochem J 358 (Pt 3):615-26.

Sandy J, Westling J, Kenagy R, Iruela-Arispe M, Verscharen C, Rodriguez-Mazaneque J, Zimmermann D, Lemire J, Fischer J, Wight T, Clowes A (2001), Versican V1 proteolysis in human aorta in vivo occurs at the Glu441-Ala442 bond, a site that is cleaved by recombinant ADAMTS-1 and ADAMTS-4. J. Biol. Chem. 276 (16):13372-8.

Sanz I (1991), Multiple mechanisms participate in the generation of diversity of human H chain CDR3 regions. J Immunol 147 (5):1720-9.

Satoh K, Suzuki N, Yokota H (2000), ADAMTS-4 (a disintegrin and metalloproteinase with thrombospondin motifs) is transcriptionally induced in beta-amyloid treated rat astrocytes. Neurosci Lett 289 (3):177-80.

Sawaji Y, Hynes J, Vincent T, Saklatvala J (2008), Fibroblast growth factor 2 inhibits induction of aggrecanase activity in human articular cartilage. Arthritis Rheum 58 (11):3498-509.

Scheiflinger F, Knöbl P, Trattner B, Plaimauer B, Mohr G, Dockal M, Dorner F, Rieger M (2003), Nonneutralizing IgM and IgG antibodies to von Willebrand factor-cleaving protease (ADAMTS-13) in a patient with thrombotic thrombocytopenic purpura. Blood 102 (9):3241-3.

Schechter I, Berger A (1967), On the size of the active site in proteases. Biochem. Biophys. Res. Commun. 27 (2):157-62.

Schechter B, Conway-Jacobs A, Sela M (1971), Conformational changes in a synthetic antigen induced by specific antibodies. Eur. J. Biochem. 20 (3):321-4.

Schett G, Hayer S, Tohidast-Akrad M, Schmid BJ, Lang S, Türk B, Kainberger F, Haralambous S, Kollias G, Newby AC, Xu Q, Steiner G, Smolen J (2001), Adenovirus-based overexpression of

tissue inhibitor of metalloproteinases 1 reduces tissue damage in the joints of tumor necrosis factor alpha transgenic mice. Arthritis Rheum 44 (12):2888-98.

Schofield DJ, Pope AR, Clementel V, Buckell J, Chapple SDj, Clarke KF, Conquer JS, Crofts AM, Crowther SR, Dyson MR, Flack G, Griffin GJ, Hooks Y, Howat WJ, Kolb-Kokocinski A, Kunze S, Martin CD, Maslen GL, Mitchell JN, O'Sullivan M, Perera RL, Roake W, Shadbolt SP, Vincent KJ, Warford A, Wilson WE, Xie J, Young JL, McCafferty J (2007), Application of phage display to high throughput antibody generation and characterization. Genome Biol. 8 (11):R254.

Sela-Passwell N, Kikkeri R, Dym O, Rozenberg H, Margalit R, Arad-Yellin R, Eisenstein M, Brenner O, Shoham T, Danon T, Shanzer A, Sagi I (2011), Antibodies targeting the catalytic zinc complex of activated matrix metalloproteinases show therapeutic potential. Nat Med. 18 (1):143-7.

Shapira E, Arnon R (1967), The mechanism of inhibition of papain by its specific antibodies. Biochemistry 6 (12):3951-6.

Sharghi-Namini S, Fan H, Sulochana KN, Potturi P, Xiang W, Chong YS, Wang Z, Yang H, Ge R (2008), The first but not the second thrombospondin type 1 repeat of ADAMTS5 functions as an angiogenesis inhibitor. Biochem Biophys Res Commun 371 (2):215-9.

Shelat SG, Smith P, Ai J, Zheng XL (2006), Inhibitory autoantibodies againstADAMTS-13 in patients with thrombotic thrombocytopenic purpura bindADAMTS-13protease and may accelerate its clearance in vivo. J Thromb Haemost. 4 (8):1707-17.

Shevchenko A, Wilm M, Vorm O, Mann M (1996), Mass spectrometric sequencing of proteins silver-stained polyacrylamide gels. Anal Chem 68 (5):850-8.

Shieh HS, Mathis KJ, Williams JM, Hills RL, Wiese JF, Benson TE, Kiefer JR, Marino MH, Carroll JN, Leone JW, Malfait AM, Arner EC, Tortorella MD, Tomasselli A (2008), High resolution crystal structure of the catalytic domain of ADAMTS-5 (aggrecanase-2). J Biol Chem. 283 (3):1501-7.

Shieh HS, Tomasselli AG, Mathis KJ, Schnute ME, Woodard SS, Caspers N, Williams JM, Kiefer JR, Munie G, Wittwer A, Malfait AM, Tortorella MD (2011), Structure analysis reveals the flexibility of the ADAMTS-5 active site. Protein Sci. 20 (4):735-44.

Shiozaki M, Maeda K, Miura T, Kotoku M, Yamasaki T, Matsuda I, Aoki K, Yasue K, Imai H, Ubukata M, Suma A, Yokota M, Hotta T, Tanaka M, Hase Y, Haas J, Fryer AM, Laird ER, Littmann NM, Andrews SW, Josey JA, Mimura T, Shinozaki Y, Yoshiuchi H, Inaba T (2011), Discovery of (1S,2R,3R)-2,3-Dimethyl-2-phenyl-1-sulfamidocyclopropanecarboxylates: Novel and Highly Selective Aggrecanase Inhibitors. J Med Chem. 54 (8):2839-63.

Silver DL, Hou L, Somerville R, Young ME, Apte SS, Pavan WJ (2008), The secreted metalloprotease ADAMTS20 is required for melanoblast survival. PLoS Genet. 4 (2):e1000003.

Silver J, Miller JH (2004), Regeneration beyond the glial scar. Nat Rev Neurosci 5 (2):146-56.

Sjöblom T, Jones S, Wood LD, Parsons DW, Lin J, Barber TD, Mandelker D, Leary RJ, Ptak J, Silliman N, Szabo S, Buckhaults P, Farrell C, Meeh P, Markowitz SD, Willis J, Dawson D, Willson JK, Gazdar AF, Hartigan J, Wu L, Liu C, Parmigiani G, Park BH, Bachman KE, Papadopoulos N, Vogelstein B, Kinzler KW, Velculescu VE (2006), The consensus coding sequences of human breast and colorectal cancers. Science 314 (5797):268-74.

Skalén K, Gustafsson M, Rydberg EK, Hultén LM, Wiklund O, Innerarity TL, Borén J (2002), Subendothelial retention of atherogenic lipoproteins in early atherosclerosis. Nature 417 (6890):750-4.

Skandalis SS, Theocharis AD, Vynios DH, Theocharis DA, Papageorgakopoulou N (2004a), Proteoglycans in human laryngeal cartilage. Identification of proteoglycan types in successive cartilage extracts with particular reference to aggregating proteoglycans. Biochimie 86 (3):221-9.

Skandalis SS, Theocharis AD, Theocharis DA, Papadas TH, Vynios DH, Papageorgakopoulou N (2004b), Matrix proteoglycans are markedly affected in advanced laryngeal squamous cell carcinoma. Biochim. Biophys. Acta 1689 (2):152-61.

Skerra A, Pfitzinger I, Plückthun A (1991), The functional expression of antibody Fv fragments in Escherichia coli: improved vectors and a generally applicable purification technique. Biotechnology 9 (3):273-8.

Smith GP, Petrenko VA (1997), Phage Display. Chem Rev. 97 (2):391-410.

Soejima K, Mimura N, Hirashima M, Maeda H, Hamamoto T, Nakagaki T, Nozaki C (2001), A novel human metalloprotease synthesized in the liver and secreted into the blood: possibly, the von Willebrand factor-cleaving protease? J. Biochem. 130 (4):475-80.

Soejima K, Matsumoto M, Kokame K, Yagi H, Ishizashi H, Maeda H, Nozaki C, Miyata T, Fujiomura Y, Nakagaki T (2003), ADAMTS-13 cysteine-rich/spacer domains are functionally essential for von Willebrand factor cleavage. Blood 102 (9):3232-37.

Somerville RP, Longpre´ JM, Jungers KA, Engle JM, Ross M, Evanko S, Wight TN, Leduc R, and Apte SS (2003a), Aggrecanase and metalloproteinase-specific aggrecan neo-epitopes are induced in the articular cartilage of mice with collagen II-induced arthritis. J. Biol. Chem. 278 (11):9503-13.

Somerville RPT, Longpre JM, Jungers KA, Engle JM, Ross M, Evanko S, Wight TN, Leduc R, Apte SS (2003b), Characterization of ADAMTS-9 and ADAMTS-20 as a distinct ADAMTS subfamily related to Caenorhabditis elegans GON-1. J. Biol. Chem. 278 (2003):9503-13.

Somerville RP, Longpré JM, Apel ED, Lewis RM, Wang LW, Sanes JR, Leduc R, Apte SS (2004), ADAMTS7B, the full-length product of the ADAMTS7 gene, is a chondroitin sulfate proteoglycan containing a mucin domain. J Biol Chem. 279 (34):35159-75.

Song RH, Tortorella MD, Malfait AM, Alston JT, Yang Z, Arner EC, Griggs DW (2007), Aggrecan degradation in human articular cartilage explants is mediated by both ADAMTS-4 and ADAMTS-5. Arthritis Rheum. 56 (2):575-85.

Spicer AP, Joo A, Bowling RA Jr. (2003), A hyaluronan binding link protein gene family whose members are physically linked adjacent to chondroitin sulfate proteoglycan core protein genes: the missing links. J. Biol. Chem. 278 (23):21083-91.

Stankunas K, Hang CT, Tsun ZY, Chen H, Lee NV, Wu JI, Shang C, Bayle JH, Shou W, Iruela-Arispe ML, Chang CP (2008), Endocardial Brg1 represses ADAMTS1 to maintain the microenvironment for myocardial morphogenesis. Dev. Cell 14 (2):298-311.

Stanton H, Rogerson FM, East CJ, Golub SB, Lawlor KE, Meeker CT, Little CB, Last K, Farmer PJ, Campbell IK, Fourie AM, Fosang AJ (2005), ADAMTS-5 is the major aggrecanase in mouse cartilage in vivo and in vitro. Nature 434 (7033):648-52.

Stokes A, Joutsa J, Ala-aho R, Pitchers M, Pennington CJ, Martin C, Premachandra DJ, Okada Y, Peltonen J, Grénman R, James HA, Edwards DR, Kähäri VM (2010), Expression profiles and clinical correlations of degradome components in the tumor microenvironment of head and neck squamous cell carcinoma. Clin Cancer Res 16 (7):2022-35.

Stradner MH, Hermann J, Angerer H, Setznagl D, Sunk I-, Windhager R, Graninger WB (2008), Spingosine-1-phosphate stimulates proliferation and counteracts interleukin- 1 induced nitric oxide formation in articular chondrocytes. Osteoarthritis Cartilage 16 (3):305-11.

Struglics A, Larsson S, Pratta M, Kumar S, Lark M, Lohmander L (2006), Human osteoarthritis synovial fluid and joint cartilage contain both aggrecanase and matrix metalloproteinase generated aggrecan fragments. Osteoarthritis Cartilage 14 (2):101-13.

Struglics A, Larsson S, Hansson M, Lohmander LS (2009), Western Blot Quantification of Aggrecan Fragments in Human Synovial Fluid Indicates Differences in Fragment Patterns between Joint Diseases. Osteoarthritis and Cartilage 17 (4):497-506.

Struglics A, Hansson M (2010), Calpain is involved in C-terminal truncation of human aggrecan, Biochem. J. 430 (3):531-38.

Struglics A, Larsson S (2010), A comparison of different purification methods of aggrecan fragments from human articular cartilage and synovial fluid. Matrix Biol. 29 (1):74-83.

Struglics A, Hansson M, Lohmander LS (2011), Human aggrecanase generated synovial fluid fragment levels are elevated directly after knee injuries due to proteolysis both in the inter globular and chondroitin sulfate domains. Osteoarthritis Cartilage. 19 (8):1047-57.

Struglics A, Hansson M (2012), MMP proteolysis of the human extracellular matrix protein aggrecan is mainly a process of normal turnover. Biochem J. 446 (2):213-23.

Studier FW (2005), Protein production by auto-induction in high density shaking cultures. Protein Exp Purif 41 (1):207-34.

Stupka N, Kintakas C, White JD, Fraser FW, Hanciu M, Aramaki-Hattori N, Martin S, Coles C, Collier F, Ward AC, Apte SS, McCulloch DR (2013), Versican Processing by a Disintegrin-like and Metalloproteinase Domain with Thrombospondin-1 Repeats Proteinases-5 and -15 Facilitates Myoblast Fusion. J Biol Chem. 288 (3):1907-17.

Sun HB (2010), Mechanical loading, cartilage degradation, and arthritis. Ann. N. Y. Acad. Sci. 1211:37-50.

Sun J, Pons J, Craik CS (2003), Potent and selective inhibition of membrane-type serine protease 1 by human single-chain antibodies. Biochemistry. 42(4):892-900.

Sundberg EJ, Mariuzza RA (2002), Molecular recognition in antibody–antigen complexes. Adv Protein Chem. 61:119-60.

Suresh MR, Cuello AC, Milstein C (1986), Bispecific monoclonal antibodies from hybrid hydridomas. Methods Enzymol: 121:210-28.

Suzuki T, Pelichova H, Cinader B (1969), Enzyme activation by antibody. I. Fractionation of immune sera in search for an enzyme activating antibody. J. Immunol. 103 (6):1366-76.

Suzuki K, Shimizu K, Hamamoto T, Nakagawa Y, Hamakubo T, Yamamuro T (1990), Biochemical demonstration of calpains and calpastatin in osteoarthritic synovial fluid. Arthritis Rheum. 33 (5):728-32.

Swaroop M, Moussalli M, Pipe SW, Kaufman RJ (1997), Mutagenesis of a potential immunoglobulin-binding protein binding site enhances secretion of coagulation factor VIII. J. Biol. Chem. 272 (39): 24121-4.

Swearingen CA, Carpenter JW, Siegel R, Brittain IJ, Dotzlaf J, Durham TB, Toth JL, Laska DA, Marimuthu J, Liu C, Brown DP, Carter QL, Wiley MR, Duffin KL, Mitchell PG, Thirunavukkarasu K (2010), Development of a novel clinical biomarker assay to detect and quantify aggrecanase-generated aggrecan fragments in human synovial fluid, serum and urine. Osteoarthritis Cartilage. 18 (9):1150-8.

Sylvester J, Ahmad R, Zafarullah M (2013), Role of Sp1 transcription factor in Interleukin-1-induced ADAMTS-4 (aggrecanase-1) gene expression in human articular chondrocytes. Rheumatol Int. 33 (2):517-22.

Szomor Z, Shimizu K, Fujimori Y, Yamamoto S, Yamamuro T (1995), Appearance of calpain correlates with arthritis and cartilage destruction in collagen induced arthritic knee joints of mice. Ann. Rheum. Dis. 54 (6):477-83.

Szomor Z, Shimizu K, Yamamoto S, Yasuda T, Ishikawa H, Nakamura T (1999), Externalization of calpain (calcium-dependent neutral cysteine proteinase) in human arthritic cartilage. Clin. Exp. Rheumatol. 17 (5):569-74.

Sztrolovics R, Alini M, Roughley PJ, Mort JS (1997), Aggrecan degradation in human intervertebral disc and articular cartilage. Biochem J. 326 (Pt 1):235-41.

Sztrolovics R, White RJ, Roughley PJ, Mort JS (2002a), The mechanism of aggrecan release from cartilage differs with tissue origin and the agent used to stimulate catabolism. Biochem. J. 362 (Pt 2): 465-72.

Sztrolovics R, Recklies AD, Roughley PJ, Mort JS (2002b), Hyaluronate degradation as an alternative mechanism for proteoglycan release from cartilage during interleukin-1beta-stimulated catabolism. Biochem. J. 362 (Pt 2):473-9.

Tape CJ, Willems SH, Dombernowsky SL, Stanley PL, Fogarasi M, Ouwehand W, McCafferty J, Murphy G (2011), Cross-domain inhibition of TACE ectodomain. Proc Natl Acad Sci U S A. 108 (14):5578-83.

Tauchi R, Imagama S, Natori T, Ohgomori T, Muramoto A, Shinjo R, Matsuyama Y, Ishiguro N, Kadomatsu K (2012), The endogenous proteoglycan-degrading enzyme ADAMTS-4 promotes functional recovery after spinal cord injury. J Neuroinflammation 9:53.

Tetsunaga T, Nishida K, Furumatsu T, Naruse K, Hirohata S, Yoshida A, Saito T, Ozaki T (2011), Regulation of mechanical stress-induced MMP-13 and ADAMTS-5 expression by RUNX-2 transcriptional factor in SW1353 chondrocyte-like cells. Osteoarthritis Cartilage. 19 (2):222-32.

Thirunavukkarasu K, Pei Y, Moore TL, Wang H, Yu XP, Geiser AG, Chandrasekhar S (2006), Regulation of the human ADAMTS-4 promoter by transcription factors and cytokines. Biochem Biophys Res Commun 345 (1):197-204.

Thirunavukkarasu K, Pei Y, Wei T (2007), Characterization of the human ADAMTS-5 (aggrecanase-2) gene promoter. Mol Biol Rep 34 (4):225-31.

Thomas G (2002), Furin at the cutting edge: from protein traffic to embryogenesis and disease. Nat Rev Mol Cell Biol 3 (10):753-66.

Thurber GM, Schmidt MM, Wittrup KD (2008), Antibody tumor penetration: transport opposed by systemic and antigen-mediated clearance. Adv Drug Deliv Rev 60 (12):1421-34.

Tierney GM, Griffin NR, Stuart RC, Kasem H, Lynch KP, Lury JT, Brown PD, Millar AW, Steele RJ, Parsons SL (1999), A pilot study of the safety and effects of the matrix metalloproteinase inhibitor marimastat in gastric cancer. Eur J Cancer 35 (4):563-8.

Tortorella MD, Burn TC, Pratta MA, Abbaszade I, Hollis JM, Liu R, Rosenfeld SA, Copeland RA, Decicco CP, Wynn R, Rockwell A, Yang F, Duke JL, Solomon K, George H, Bruckner R, Nagase H, Itoh Y, Ellis DM, Ross H, Wiswall BH, Murphy K, Hillman MC Jr, Hollis GF, Newton RC, Magolda RL, Trzaskos JM, Arner EC (1999), Purification and cloning of aggrecanase-1: a member of the ADAMTS family of proteins. Science 284 (5420):1664-6.

Tortorella MD, Pratta M, Liu RQ, Austin J, Ross OH, Abbaszade I, Burn T, Arner E (2000a), Sites of aggrecan cleavage by recombinant human aggrecanase-1 (ADAMTS-4). J Biol Chem 275 (24):18566-73.

Tortorella M, Pratta M, Liu RQ, Abbaszade I, Ross H, Burn T, Arner E (2000b), The thrombospondin motif of aggrecanase-1 (ADAMTS-4) is critical for aggrecan substrate recognition and cleavage. J Biol Chem. 275 (33):25791-7.

Tortorella MD, Malfait AM, Deccico C, Arner E (2001), The role of ADAM-TS4 (aggrecanase-1) and ADAM-TS5 (aggrecanase-2) in a model of cartilage degradation. Osteoarthritis Cartilage. 9 (6):539-52.

Tortorella MD, Liu RQ, Burn T, Newton RC, Arner E (2002), Characterization of human aggrecanase 2 (ADAMTS5): substrate specificity studies and comparison with aggrecanase 1 (ADAM-TS4). Matrix Biol 21 (6):499-511.

Tortorella MD, Arner EC, Hills R, Easton A, Korte-Sarfaty J, Fok K, Wittwer AJ, Liu RQ, Malfait AM (2004), Alpha2-macroglobulin is a novel substrate for ADAMTS-4 and ADAMTS-5 and represents an endogenous inhibitor of these enzymes. J Biol Chem 279 (17):17554-61.

Tortorella MD, Arner EC, Hills R, Gormley J, Fok K, Pegg L, Munie G, Malfait AM (2005), ADAMTS-4 (aggrecanase-1): N-terminal activation mechanisms. Arch Biochem Biophys 444 (1):34-44.

Tracy RP, Currie RM, Kyle RA, Young DS (1982), Two-dimensional gel electrophoresis of serum specimens from patients with monoclonal gammopathies. Clin Chem. 28 (4 Pt 2):900-7.

Troeberg L, Fushimi K, Khokha R, Emonard H, Ghosh P, Nagase H (2008), Calcium pentosan polysulfate is a multifaceted exosite inhibitor of aggrecanases. FASEB J. 22 (10):3515-24.

Troeberg L, Fushimi K, Scilabra SD, Nakamura H, Dive V, Thøgersen IB, Enghild JJ, Nagase H (2009), The C-terminal domains of ADAMTS-4 and ADAMTS-5 promote association with N-TIMP-3. Matrix Biol. 28 (8):463-9.

Troeberg L, Mulloy B, Ghosh P, Lee MH, Murphy G, Nagase H (2012), Pentosan polysulfate increases affinity between ADAMTS-5 and TIMP-3 through formation of an electrostatically driven trimolecular complex. Biochem J. 443 (1):307-15.

Tsai CJ, del Sol A, Nussinov R (2008), Allostery: absence of a change in shape does not imply that allostery is not at play. J Mol Biol 378 (1):1-11.

Tsai CJ, Del Sol A, Nussinov R (2009), Protein allostery, signal transmission and dynamics: a classification scheme of allosteric mechanisms. Mol Biosyst 5 (3):207-16.

Tselepis C, Kwan AP, Thornton D, and J Sheehan (2000), The biochemical characterization of aggrecan from normal and tibial-dyschondroplastic chicken growth-plate cartilage. Biochem. J. 351 (Pt 2):517-25.

Tuddenham L, Wheeler G, Ntounia-Fousara S, Waters J, Hajihosseini MK, Clark I, Dalmay T (2006), The cartilage specific microRNA-140 targets histone deacetylase 4 in mouse cells. FEBS Lett 580 (17):4214-17.

Utsunomiya-Tate N, Kubo K, Tate S, Kainosho M, Katayama E, Nakajima K, Mikoshiba K (2000), Reelin molecules assemble together to form a large protein complex, which is inhibited by the function-blocking CR-50 antibody. Proc Natl Acad Sci U S A. 97 (17):9729-34.

van der Laan WH, Quax PH, Seemayer CA, Huisman LG, Pieterman EJ, Grimbergen JM, Verheijen JH, Breedveld FC, Gay RE, Gay S, Huizinga TW, Pap T (2003), Cartilage degradation and invasion by rheumatoid synovial fibroblasts is inhibited by gene transfer of TIMP-1 and TIMP-3. Gene Ther 10 (3):234-42.

Vankemmelbeke MN, Holen I, Wilson AG, Ilic MZ, Handley CJ, Kelner GS, Clark M, Liu C, Maki RA, Burnett D, Buttle DJ (2001), Expression and activity of ADAMTS-5 in synovium. Eur J Biochem. 268 (5):1259-68.

van Lent PL, Grevers LC, Blom AB, Arntz OJ, van de Loo FA, van der Kraan P, Abdollahi-Roodsaz S, Srikrishna G, Freeze H, Sloetjes A, Nacken W, Vogl T, Roth J, van den Berg WB (2008), Stimulation of chondrocyte-mediated cartilage destruction by S100A8 in experimental murine arthritis. Arthritis Rheum 58 (12):3776-87.

van Meurs JB, van Lent PL, Holthuysen AE, Singer II, Bayne EK, van den Berg WB (1999a), Kinetics of aggrecanase- and metalloproteinase-induced neoepitopes in various stages of cartilage destruction in murine arthritis. Arthritis Rheum. 42(6):1128-39.

van Meurs J, van Lent P, Stoop R, Holthuysen A, Singer I, Bayne E, Mudgett J, Poole R, Billinghurst C, van der Kraan P, Buma P, van den Berg W (1999b), Cleavage of aggrecan at the Asn341-Phe342 site coincides with the initiation of collagen damage in murine antigen-induced arthritis: a pivotal role for stromelysin 1 in matrix metalloproteinase activity. Arthritis Rheum. 42 (10):2074-84.

Van Wart HE, Birkedal-Hansen H (1990), The cysteine switch: a principle of regulation of metalloproteinase activity with potential applicability to the entire matrix metalloproteinase gene family. Proc Natl Acad Sci U S A. 87 (14):5578-82.

Vaughan TJ, Williams AJ, Pritchard K, Osbourn JK, Pope AR, Earnshaw JC (1996), Human antibodies with sub-nanomolar affinities isolated from a large non-immunized phage display library. Nat Biotechnol 14 (3):309-14.

Vazquez F, Hastings G, Ortega M, Lane T, Oikemus S, Lombardo M, Iruela-Arispe M (1999), METH-1, a human ortholog of ADAMTS-1, and METH-2 are members of a new family of proteins with angio-inhibitory activity. J. Biol. Chem. 274 (33):23349-57.

Velasco J, Li J, DiPietro L, Stepp MA, Sandy JD, Plaas A (2011), ADAMTS5 ablation blocks murine dermal repair through CD44-mediated aggrecan accumulation and a switch in TGFb1 signaling from ALK5 to ALK1. J Biol Chem 286 (29):26016-27.

Vertel BM, Grier BL, Li H, Schwartz NB (1994), The chondrodystrophy, nanomelia: biosynthesis and processing of the defective aggrecan precursor. Biochem. J. 301 (Pt 1):211-6.

Vertel BM, Ratcliffe A (2000), Aggrecan. In Proteoglycans: Structure, biology and molecular interactions. (ed. R.V. Iozzo), pp. 343–377. Marcel Dekker, New York.

Viapiano MS, Matthews RT (2006), From barriers to bridges: chondroitin sulfate pro- teoglycans in neuropathology. Trends Mol. Med. 12 (10):488-96.

Viapiano MS, Hockfield S, Matthews RT (2008), BEHAB/brevican requires ADAMTS mediated proteolytic cleavage to promote glioma invasion. J. Neurooncol. 88 (3):261-72.

Viloria CG, Obaya AJ, Moncada-Pazos A, Llamazares M, Astudillo A, Capellá G, Cal S, López-Otín C (2009), Genetic inactivation of ADAMTS15 metalloprotease in human colorectal cancer. Cancer Res 69 (11):4926‑34.

Visintin M, Caselli G, Chiusaroli R, Rovati LC (2012), Anti-ADAMTS-5 antibody, derivatives and uses thereof. EP 12,164,107, filed April 13, 2012.

Volkman BF, Lipson D, Wemmer DE, Kern D (2001), Two-state allosteric behavior in a single-domain signaling protein. Science 291 (5512):2429-33.

Wågsäter D, Bjork H, Zhu C, Bjorkegren J, Valen G, Hamsten A, Eriksson P (2008), ADAMTS-4 and -8 are inflammatory regulated enzymes expressed in macrophage-rich areas of human atherosclerotic plaques. Atherosclerosis 196 (2):514-22.

Wainwright SD, Bondeson J, Hughes CE (2006), An alternative spliced transcript of ADAMTS4 is present in human synovium from OA patients. Matrix Biol. 25 (5):317-20.

Wainwright SD, Bondeson J, Caterson B, Hughes CE (2013), ADAMTS4_v1 is a splice variant of ADAMTS4 that is expressed as a protein in human synovium and cleaves aggrecan at the interglobular domain. Arthritis Rheum. [Epub ahead of print].

Wang P, Tortorella M, England K, Malfait AM, Thomas G, Arner EC, Pei D (2004), Proprotein convertase furin interacts with and cleaves pro-ADAMTS4 (aggrecanase-1) in the trans-Golgi network. J. Biol. Chem. 279 (15):15434-40.

Wang WM, Ge G, Lim NH, Nagase H, Greenspan DS (2006), TIMP-3 inhibits the procollagen N-proteinase ADAMTS-2. Biochem. J. 398 (3):515-9.

Wang LW, Leonhard-Melief C, Haltiwanger RS, Apte SS (2009), Post-translational modification of thrombospondin type-1 repeats in ADAMTS-like 1/punctin-1 by C-mannosylation of tryptophan. J Biol Chem 284 (44):30004-15.

Wang J, Markova D, Anderson DG, Zheng Z, Shapiro IM, Risbud MV (2011), TNF-α and IL-1β promote a disintegrin-like and metalloprotease with thrombospondin type I motif-5-mediated aggrecan degradation through syndecan-4 in intervertebral disc. J Biol Chem. 286 (46):39738-49.

Watanabe H, Kimata K, Line S, Strong D, Gao LY, Kozak CA, Yamada Y (1994), Mouse cartilage matrix deficiency (cmd) caused by a 7 bp deletion in the aggrecan gene. Nat. Genet. 7 (2):154-7.

Watanabe H, Cheung SC, Itano N, Kimata K, Yamada Y (1997), Identification of hyaluronan-binding domains of aggrecan. J Biol Chem 272 (44):28057-65.

Wayne GJ, Deng SJ, Amour A, Borman S, Matico R, Carter HL, Murphy G (2007), TIMP-3 inhibition of ADAMTS-4 (Aggrecanase-1) is modulated by interactions between aggrecan and the C-terminal domain of ADAMTS-4. J Biol Chem 282 (29):20991-8.

Webster DM, Pedersen J, Staunton D, Jones A, Rees AR (1994), Antibody-combining sites. Extending the natural limits. Appl Biochem Biotechnol. 47 (2-3):119-32; discussion 132-4.

Wei X, Prickett TD, Viloria CG, Molinolo A, Lin JC, Cardenas-Navia I, Cruz P, NISC Comparative Sequencing Program, Rosenberg SA, Davies MA, Gershenwald JE, López-Otín C, Samuels Y (2010), Mutational and functional analysis reveals ADAMTS18 metalloproteinase as a novel driver in melanoma. Mol Cancer Res. 8 (11):1513-25.

Weisser NE, Hall JC (2009), Applications of single-chain variable fragment antibodies in therapeutics and diagnostics. Biotechnol Adv. 27 (4):502-20.

Westling J, Fosang A, Last K, Thompson V, Tomkinson K, Hebert T, McDonagh T, Collins-Racie L, LaVallie E, Morris EA, Sandy JD (2002), ADAMTS4 cleaves at the aggrecanase site (Glu373-Ala374) and secondarily at the matrix metalloproteinase site (Asn341-Phe342) in the aggrecan interglobular domain. J. Biol. Chem. 277 (18):16059-66.

Westling J, Gottschall PE, Thompson VP, Cockburn A, Perides G, Zimmermann DR, Sandy JD (2004), ADAMTS4 (aggrecanase-1) cleaves human brain versican V2 at Glu405-Gln406 to generate glial hyaluronate binding protein. Biochem J. 377(Pt 3):787-95.

Whittaker M, Floyd CD, Brown P, Gearing AJ (1999), Design and therapeutic application of matrix metalloproteinase inhibitors. Chem Rev. 99 (9):2735-76.

Wiberg C, Hedbom E, Khairullina A, Lamande SR, Oldberg A, Timpl R, Morgelin M, Heinegard D (2001), Biglycan and decorin bind close to the n-terminal region of the collagen VI triple helix. J Biol Chem 276 (22):18947-52.

Wiberg C, Heinegard D, Wenglen C, Timpl R, Morgelin M (2002), Biglycan organizes collagen VI into hexagonal-like networks resembling tissue structures. J Biol Chem 277 (51):49120-6.

Wight TN (2002), Versican: a versatile extracellular matrix proteoglycan in cell biology. Curr. Opin. Cell Biol. 14 (5):617-23.

Wikstrom B, Engfeldt B, Heinegard D, Hjerpe A (1985), Proteoglycans and glycosaminoglycans in cartilage from the brachymorphic (bm/bm) mouse. Coll. Relat. Res. 5 (2):193-204.

Wikstrom B, Wallace ME, Hjerpe A, Engfeldt B (1987), Chubby: a new autosomal recessive skeletal mutation producing dwarfism in the mouse. J. Hered. 78 (1):8-14.

Williams Jr DC, Benjamin DC, Poljak RJ, Rule GS (1996), Global changes in amide hydrogen exchange rates for a protein antigen in complex with three different antibodies. J. Mol. Biol. 257 (4):866-76.

Wittwer AJ, Hills RL, Keith RH, Munie GE, Arner EC, Anglin CP, Malfait AM, Tortorella MD. (2007), Substrate-dependent inhibition kinetics of an active site-directed inhibitor of ADAMTS-4 (Aggrecanase 1). Biochemistry. 46 (21):6393-401.

Wojtowicz-Praga S, Torri J, Johnson M, Steen V, Marshall J, Ness E, Dickson R, Sale M, Rasmussen HS, Chiodo TA, Hawkins MJ (1998), Phase I trial of marimastat, a novel matrix metalloproteinase inhibitor, administered orally to patients with advanced lung cancer. J Clin Oncol 16 (6):2150-6.

Wood LD, Parsons DW, Jones S, Lin J, Sjöblom T, Leary RJ, Shen D, Boca SM, Barber T, Ptak J, Silliman N, Szabo S, Dezso Z, Ustyanksky V, Nikolskaya T, Nikolsky Y, Karchin R, Wilson PA, Kaminker JS, Zhang Z, Croshaw R, Willis J, Dawson D, Shipitsin M, Willson JK, Sukumar S, Polyak K, Park BH, Pethiyagoda CL, Pant PV, Ballinger DG, Sparks AB, Hartigan J, Smith DR, Suh E, Papadopoulos N, Buckhaults P, Markowitz SD, Parmigiani G, Kinzler KW, Velculescu VE, Vogelstein B (2007), The genomic landscapes of human breast and colorectal cancers. Science 318 (5853):1108-13.

Woof JM, Burton DR (2004), Human antibody-Fc receptor interactions illuminated by crystal structures. Nat. Rev. Immunol. 4 (2):89-99.

Wu TT, Johnson G, Kabat EA (1993), Length distribution of CDR H3 in antibodies. Proteins: Struct. Funct. Genet. 16 (1):1-7.

Wu H, Pfarr DS, Tang Y, An LL, Patel NK, Watkins JD, Huse WD, Kiener PA, Young JF (2005), Ultra-potent antibodies against Respiratory Syncytial Virus: effects of binding kinetics and binding valency on viral neutralization. J. Mol. Biol. 350 (1):126-44.

Wu Y, Eigenbrot C, Liang WC, Stawicki S, Shia S, Fan B, Ganesan R, Lipari MT, Kirchhofer D (2007), Structural insight into distinct mechanisms of protease inhibition by antibodies. Proc Natl Acad Sci U S A. 104 (50):19784-9.

Wyckoff M, Rodbard D, Chrambach A (1977), Polyacrylamide gel electrophoresis in sodium dodecyl sulfate-containing buffers using multiphasic buffer systems: properties of the stack, valid Rf- measurement, and optimized procedure. Anal Biochem 78 (2):459-82.

Wylie JD, Ho JC, Singh S, McCulloch DR, Apte SS (2012), Adamts5 (aggrecanase-2) is widely expressed in the mouse musculoskeletal system and is induced in specific regions of knee joint explants by inflammatory cytokines. J Orthop Res. 30 (2):226-33.

Xu JL, Davis MM (2000), Diversity in the CDR3 region of VH is sufficient for most antibody specificities. Immunity 13 (1):37-45.

Xuan JA, Schneider D, Toy P, Lin R, Newton A, Zhu, Y Finster S, Vogel D, Mintzer B, Dinter H, Light D, Parry R, Polokoff M, Whitlow M, Wu Q, Parry G (2006), Antibodies neutralizing hepsin protease activity do not impact cell growth but inhibit invasion of prostate and ovarian tumor cells in culture. Cancer Res. 66 (7):3611-9.

Yamada H, Watanabe K, Shimonaka M, Yamasaki M, Yamaguchi Y (1995), cDNA cloning and the identification of an aggrecanase-like cleavage site in rat brevican. Biochem. Biophys. Res. Commun. 216 (3):957-63.

Yamamoto S, Shimizu K, Shimizu K, Suzuki K, Nakagawa Y, Yamamuro T (1992), Calcium-dependent cysteine proteinase (calpain) in human arthritic synovial joints. Arthritis Rheum. 35 (11):1309-17.

Yamamoto K, Troeberg L, Scilabra SD, Pelosi M, Murphy CL, Strickland DK, Nagase H (2013), LRP-1-mediated endocytosis regulates extracellular activity of ADAMTS5 in articular cartilage. FASEB J. 27 (2):511-21.

Yamanishi Y, Boyle DL, Clark M, Maki RA, Tortorella MD, Arner EC, Firestein GS (2002), Expression and regulation of aggrecanase in arthritis: the role of TGF-beta. J Immunol 168 (3):1405-12.

Yang XD, Jia XC, Corvalan JR, Wang P, Davis CG, Jakibovits A (1999), Eradication of established tumors by a fully human monoclonal antibody to the epidermal growth factor receptor without concomitant chemotherapy. Cancer Res 59 (6):1236-43.

Yao W, Wasserman ZR, Chao M, Reddy G, Shi E, Liu RQ, Covington MB, Arner EC, Pratta MA, Tortorella M, Magolda RL, Newton R, Qian M, Ribadeneira MD, Christ D, Wexler RR, Decicco CP (2001) Design and synthesis of a series of (2r)-n(4)-hydroxy-2-(3-hydroxybenzyl)-n(1)-[(1s,2r)-2-hydroxy-2,3-dihydro-1h-inden-1-yl]butanediamide derivatives as potent, selective, and orally bioavailable aggrecanase inhibitors. J Med Chem 44 (21):3347-50.

Yonetani T, Theorell H (1964), Studies on liver alcohol hydrogenase complexes. 3. Multiple inhibition kinetics in the presence of two competitive inhibitors. Arch. Biochem. Biophys. 106:243-51.

Yoon H, Song JM, Ryu CJ, Kim YG, Lee EK, Kang S, Kim SJ (2012), An efficient strategy for cell-based antibody library selection using an integrated vector system. BMC Biotechnol. 12:62.

Yorimitsu M, Nishida K, Shimizu A, Doi H, Miyazawa S, Komiyama T, Nasu Y, Yoshida A, Watanabe S, Ozaki T (2008), Intra-articular injection of interleukin-4 decreases nitric oxide production by chondrocytes and ameliorates subsequent destruction of cartilage in instability-induced osteoarthritis in rat knee joints. Osteoarthritis Cartilage 16 (7):764-71.

Young DA, Lakey RL, Pennington CJ, Jones D, Kevorkian L, Edwards DR, Cawston TE, Clark IM (2005) Histone deacetylase inhibitors modulate metalloproteinase gene expression in chondrocytes and block cartilage resorption. Arthritis Res Ther. 7(3):R503-12.

Yu WH, Yu S, Meng Q, Brew K, Woessner JF Jr (2000), TIMP-3 binds to sulfated glycosaminoglycans of the extracellular matrix. J Biol Chem 275 (40):31226-32.

Yu H, Dong X, Sun Y (2004), An alternating elution strategy for screening high affinity peptides from a phage display library. Biochem Eng J 18:169-75.

Yuan W, Matthews RT, Sandy JD, Gottschall PE (2002), Association between protease-specific proteolytic cleavage of brevican and synaptic loss in the dentate gyrus of kainate-treated rats. Neuroscience: 114 (4):1091-101.

Zemlin M, Klinger M, Link J, Zemlin C, Bauer K, Engler JA, Schroeder HW Jr, Kirkham PM (2003), Expressed murine and human CDR-H3 intervals of equal length exhibit distinct repertoires that differ in their amino acid composition and predicted range of structures. J. Mol. Biol. 334 (4):733-49.

Zeng W, Corcoran C, Collins-Racie LA, Lavallie ER, Morris EA, Flannery CR (2006) Glycosaminoglycan-binding properties and aggrecanase activities of truncated ADAMTSs: comparative analyses with ADAMTS-5, -9, -16 and -18. Biochim Biophys Acta 1760 (3):517-24.

Zhang W, Moskowitz RW, Nuki G, Abramson S, Altman RD, Arden N, Bierma-Zeinstra S, Brandt KD, Croft P, Doherty M, Dougados M, Hochberg M, Hunter DJ, Kwoh K, Lohmander LS, Tugwell P (2008), OARSI recommendations for the management of hip and knee osteoarthritis, Part II: OARSI evidence-based, expert consensus guidelines. Osteoarthritis Cartilage 16 (2):137-162.

Zhang Y, Jordan JM (2010), Epidemiology of osteoarthritis. Clin Geriatr Med. 26 (3):355-69.

Zhao CQ, Zhang YH, Jiang SD, Li H, Jiang LS, Dai LY (2011), ADAMTS-5 and intervertebral disc degeneration: the results of tissue immunohistochemistry and in vitro cell culture. J. Orthop. Res. 29 (5):718-25.

Zhen EY, Brittain IJ, Laska DA, Mitchell PG, Sumer EU, Karsdal MA, Duffin KL (2008), Characterization of metalloprotease cleavage products of human articular cartilage. Arthritis Rheum. 58 (8):2420-31.

Zheng X, Chung D, Takayama TK, Majerus EM, Sadler JE, Fujikawa K (2001), Structure of von Willebrand factor-cleaving protease (ADAMTS13), a metalloprotease involved in thrombotic thrombocytopenic purpura. J. Biol. Chem. 276 (44):41059-63.

Zheng X, Nishio K, Majerus EM, Sadler JE (2003), Cleavage of von Willebrand factor requires the spacer domain of the metalloprotease ADAMTS13. J Biol Chem. 278 (32):30136-141.

Zimmerman TS, Ruggeri ZM (1987), Von Willebrand disease. Hum Pathol. 18 (2):140-152.